Theoretical and phenomenological aspects of vector boson production

Werthenbach, Anja

Theoretical and Phenomenological Aspects of Vector Boson Production

A thesis presented for the degree of
Doctor of Philosophy
by

Anja Werthenbach

September 2000

Centre for Particle Theory
University of Durham

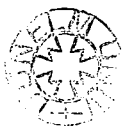

To Mum and Dad

Acknowledgements

It is my pleasure to express my gratitude towards Prof. W. J. Stirling not only for his excellent supervision, his intuition for relevant projects, his patience with my ignorance of `fortran`-programming and all his support on countless request to participate in some summer-school/conference or other, but also giving me the freedom to collaborate with other members of the group.

Naturally I am most grateful to Dr. Wim Beenakker who took the burden of collaborating with me. Countless hours spent at the white-board developing and disregarding some concept or other. He shared my enthusiasm (which I naturally exhibited on any minor sub-result), encouraged me on those long dark days of being lost in the middle of this horrible two-loop calculation, guided me through new techniques and concepts and eventually shared my sense of humor (or should I say put up with it?). Finally, I can't thank him enough for his most careful proof-reading of this very thesis. Thanks, Wim! So, so much!

Also my thanks to my dear office mates and friends Jeppe R. Andersen and Michael Davies for transforming the office into a cosy place where we not only shared our worries and excitement about physics, but uncountable hours of valuable friendship. My many apologies to them for disturbing them far beyond any reasonable scale by those countless white-board-sessions. My thanks also to Luc Bourhis for being a dear friend and a unique company to share every movie which made it to Durham.

More thanks to Jeppe and Stephen Burby for never getting tired of fixing my computer and sharing all their knowledge about `emacs` and friends with me.

Also thanks to the rest of the CPT group for providing such an excellent working environment.

Also my deepest gratitude towards my parents who never failed encouraging and supporting me in every possible way. Also to my brother for cheering me up in his very unique way. Even more so lots (and lots) of thanks to my unique friend Ferdinand Gertzen for all his understanding and for taking me away from my work ever so often for me to return full of energy.

Finally acknowledgements go to the DAAD (German Academic Exchange Service) for full financial support.

Abstract

The production of three gauge bosons in high-energy collisions – in particular in view of a next-linear collider with center of mass energies in the TeV range – offers an unique opportunity to probe the Standard Model (SM) of today's particle physics. In this thesis we pay particular attention to the electroweak sector of the theory. We investigate the gauge structure (*i. e.* possible deviations from the SM predictions of gauge boson self-interactions manifest *e. g.* in anomalous quartic gauge boson couplings and Radiation zeros) as well as electroweak radiative corrections in order to improve theoretical predictions for SM processes.
Quartic gauge boson couplings can be regarded as a direct window on the sector of electroweak symmetry breaking. We have studied the impact of three such anomalous couplings on the processes $e^+e^- \to WW\gamma$, $ZZ\gamma$ and $Z\gamma\gamma$ at LEP2 and a future linear collider.
In certain high-energy scattering processes involving charged particles and the emission of one or more photons, the scattering amplitude vanishes for particular configurations of the final state particles. The fact that gauge symmetry is a vital ingredient for the cancellation to occur means that radiation zeros can be used to probe physics beyond the standard model. For example anomalous electroweak gauge boson couplings destroy the delicate cancellation necessary for the zero to occur. We have studied the process $q\bar{q} \to WW\gamma$.
To match the expected experimental precision at future linear colliders, improved theoretical predictions beyond next-to-leading order are required. By choosing an appropriate gauge, we have developed a formalism to calculate such corrections for arbitrary electroweak processes. As an example we consider here the processes $e^+e^- \to f\bar{f}$ and $e^+e^- \to W_T^+W_T^-$, $W_L^+W_L^-$ and study the perturbative structure of the electroweak Sudakov logarithms by means of an explicit two-loop calculation. In this way we investigate how the Standard Model, with its mass gap between the photon and Z boson in the neutral sector, compares to unbroken theories like QED and QCD. We observe that the two-loop corrections are consistent with an exponentiation of the one-loop corrections. In this sense the Standard Model behaves like an unbroken theory at high energies.

Declaration

I declare that I have previously submitted no material in this thesis for a degree at this or any other university.

The research presented in this thesis has been carried out in collaboration with Prof. W. J. Stirling and Dr. W. Beenakker.

List of Publications

[1] SUDAKOV LOGARITHMS IN ELECTROWEAK PROCESSES, Wim Beenakker and Anja Werthenbach, Presented at *The XXXVth Rencontres de Moriond, Electroweak Interactions and Unified Theories* Les Arcs, France, 11-18March, 2000; to appear in the proceedings.

[2] ELECTROWEAK SUDAKOV LOGARITHMS IN THE COULOMB GAUGE., Wim Beenakker and Anja Werthenbach, Presented by W. B. at *Zeuthen Workshop on Elementary Particle Theory: Loops and Legs in Quantum Field Theory*, Koenigstein-Weissig, Germany, 9-14 Apr 2000; Published in *Nucl. Phys. Proc. Suppl.* **89**:88-93, 2000.

[3] NEW INSIGHTS INTO THE PERTURBATIVE STRUCTURE OF ELECTROWEAK SUDAKOV LOGARITHMS, Wim Beenakker and Anja Werthenbach, DTP-00-18, *Phys. Lett.* **B489**:148-156,2000.

[4] ANOMALOUS TRIPLE AND QUARTIC GAUGE BOSON COUPLINGS, P. J. Dervan, A. Signer,W. J. Stirling and A. Werthenbach. Presented at the *UK Phenomenology Workshop on Collider Physics*, Durham, UK, 19 -24 Sept. 1999, Published in *J. Phys.* **G26**:607-615, 2000.

[5] ANOMALOUS QUARTIC COUPLINGS, W. J. Stirling and Anja Werthenbach. Talk given at the Nato Advanced Study Institute, *Particle Physics: Ideas and Recent Development*, Cargese, France, 26 July - 7 Aug. 1999, Kluwer Academic Publishers, J. J. Aubert, R. Gastmans and J. M. Gerard (editors), p. 55-64.

[6] RADIATION ZEROS AS AN OBSERVABLE TO TEST PHYSICS BEYOND THE STANDARD MODEL, Anja Werthenbach. Talk given at International School of Subnuclear Physics: 36th Course: *From the Planck Length to the Hubble Radius*, Erice, Italy, 29 Aug - 7 Sep 1998, World Scientific, A. Zichichi (editor), p. 664-672.

[7] ANOMALOUS QUARTIC COUPLINGS IN $\nu\bar{\nu}\gamma\gamma$ PRODUCTION VIA WW FUSION AT LEP2, W. James Stirling and Anja Werthenbach, DTP-99-62, *Phys. Lett.* **B466**:369-374, 1999.

[8] RADIATION ZEROS IN $WW\gamma$ PRODUCTION AT HIGH ENERGY COLLIDERS, W. J. Stirling and Anja Werthenbach, DTP-99-42, *Eur. Phys. J.* **C12**:441-450, 2000.

[9] ANOMALOUS QUARTIC COUPLINGS IN $WW\gamma$,$ZZ\gamma$ AND $Z\gamma\gamma$ PRODUCTION AT PRESENT AND FUTURE e^+e^- COLLIDERS, W. J. Stirling and Anja Werthenbach, DTP-99-30, *Eur. Phys. J.* **C14**:103-110, 2000.

[10] ANGULAR DISTRIBUTION OF DECAY LEPTONS FROM $e^+e^- \to W^+W^-$ AT THRESHOLD, Anja Werthenbach and L.M. Sehgal, PITHA-98-38, *Phys. Lett.* **B458**:383-388, 1999.

[11] ENERGY SPECTRUM OF LEPTONS FROM $e^+e^- \to W^+W^-$ IN THE PRESENCE OF STRONG $W_L^+W_L^-$ INTERACTION, Anja Werthenbach and L.M. Sehgal, PITHA-97-02,*Phys. Lett.* **B402**:189-194, 1997.

Contents

Chapter 1

Introduction

1.1 A brief History of Particle Physics

Quantum field theory has emerged as the most successful physical framework describing the subatomic world. Both its computational power and its conceptual scope are remarkable. The undeniable successes of quantum field theory, however, were certainly not apparent in 1928 when P. A. M. Dirac [1] wrote the first pioneering paper combining quantum mechanics with the classical theory of radiation. The early success of Quantum Electrodynamics (QED) was however premature: it only presented the lowest order corrections to classical physics. Higher order corrections in QED necessarily led to divergent integrals [2].

Over the decades many of the world's finest physicists literally brushed these divergent quantities under the rug by manipulating infinite quantities as if they were small. This clever sleight-of-hand was called renormalization theory, because the divergent integrals were absorbed into an infinite rescaling of the couplings constants and masses of the theory. Finally, in 1949, Tomonaga, Schwinger and Feynman [3] penetrated this thicket of infinities and demonstrated how to extract meaningful physical information from QED, for which they received the Nobel Prize in 1965. The experimental success of such a renormalizable theory followed with the measurement of the anomalous magnetic moment of the electron and the Lamb shift.

In the early 1960's particle physicists described nature in terms of four different forces, namely the electromagnetic, the weak and the strong forces as well as gravity, all characterized by very different strengths of the couplings.

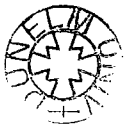

Guided by the renormalizable quantum field theoretical description of the electromagnetic force and the experimental evidence for massive weak currents, the weak force was predicted to be mediated by three massive gauge bosons W^+, W^- and Z, limiting the range of the weak forces due to the exchange of massive particles. Since the W bosons carry electric charge they must couple to the photon (the mediator of the electromagnetic force) implying a gauge theory that unifies the weak and the electromagnetic force [4]. The crucial ingredient being here that the unified gauge group $SU(2)_L \times U(1)_Y$ is spontaneously broken, i. e. the Lagrangian obeys a local gauge symmetry but the vacuum state explicitly breaks this symmetry. Three of the four gauge bosons then acquire a mass via the so-called Higgs mechanism, where the unphysical degrees of freedom in the form of massless goldstone bosons are 'eaten' by the longitudinal components of the massive gauge bosons. A direct mass term for the gauge bosons would spoil gauge invariance of the Lagrangian. Hence only particles (matter as well as gauge) interacting with the Higgs field can acquire a mass at all. The theoretical breakthrough for the standard model (SM) of electroweak interactions was the proof that this broken gauge theory is still a renormalizable quantum theory, i. e. the predictive power of the theory is preserved beyond lowest order in the perturbative expansion in the electromagnetic coupling α. In 1999 G. 't Hooft and M. Veltman received the Nobel prize for proving the SM to be a renormalizable theory [5].
However the Higgs particle H, predicted by the Higgs mechanism, remains the one fundamental particle yet to be discovered in the SM. Hence one of the most urgent questions asked by today's particle physicists is the question of the origin of electroweak symmetry breaking.

1.2 The Standard Model of Electroweak Interactions[1]

The Standard Model of electroweak interactions [4] is based on the gauge group $\mathrm{SU}(2)_L \times \mathrm{U}(1)_Y$, where the generators of $\mathrm{SU}(2)_L$ correspond to the three components of weak isospin I_i and the $\mathrm{U}(1)_Y$ generator to the weak hypercharge Y. These are related to the electric charge generator by $Q = I_3 + Y/2$. The Lagrangian describing the electroweak interactions

[1] This section follows closely the introductory pages of Ref. [6].

is

$$\begin{aligned}\mathcal{L}_{SM} &= -\frac{1}{4}B_{\mu\nu}B^{\mu\nu} - \frac{1}{4}\mathbf{W}_{\mu\nu}\mathbf{W}^{\mu\nu} + i\bar{\psi}_j\gamma^\mu D_\mu\psi_j + (D_\mu\phi)(D^\mu\phi)^\dagger - \mu^2\phi^\dagger\phi - \lambda(\phi^\dagger\phi)^2 \\ &+ \left[\lambda_{e_k}\bar{L}_{L_k}\phi\, e_{R_k} + \lambda_{u_{jk}}\bar{Q}_{L_j}\tilde{\phi}\, u_{R_k} + \lambda_{d_{jk}}\bar{Q}_{L_j}\phi\, d_{R_k} + h.\ c.\right], \qquad (1.1)\end{aligned}$$

with ϕ being the Higgs field defined later and the field strength tensors

$$\begin{aligned}B_{\mu\nu} &= \partial_\mu B_\nu - \partial_\nu B_\mu \\ \mathbf{W}_{\mu\nu} &= \partial_\mu \mathbf{W}_\nu - \partial_\nu \mathbf{W}_\mu + g\mathbf{W}_\mu \times \mathbf{W}_\nu \qquad (1.2)\end{aligned}$$

with

$$\mathbf{W}_\mu = \begin{pmatrix} W_{1\,\mu} \\ W_{2\,\mu} \\ W_{3\,\mu} \end{pmatrix} \qquad (1.3)$$

for the abelian gauge field B associated with $U(1)_Y$ and the three non-abelian fields W_i of $SU(2)_L$, respectively. The covariant derivative is

$$D_\mu = \partial_\mu + ig\,\mathbf{I}\cdot\mathbf{W}_\mu - ig'\frac{Y}{2}B_\mu \qquad (1.4)$$

with g, g' being the $SU(2)_L, U(1)_Y$ coupling strength, respectively. The $SU(2)$ generators obey the usual relation $[I_i, I_j] = i\epsilon_{ijk}I_k$ and are related to the Pauli spin matrices by $I_i = \tau_i/2$. This Lagrangian is invariant under the infinitesimal local gauge transformation for $SU(2)_L$ and $U(1)_Y$ independently. Being in the adjoint representation, the $SU(2)_L$ massless gauge fields form a weak isospin triplet with the charged fields being defined by $W^\pm_\mu = \frac{1}{\sqrt{2}}(W_{1\,\mu} \mp i\,W_{2\,\mu})$. The neutral component $W_{3\,\mu}$ mixes with the abelian gauge field to form the physical states (after diagonalizing the gauge boson mass matrix)

$$\begin{aligned}Z_\mu &= W_{3\,\mu}\cos\theta_{\rm w} + B_\mu \sin\theta_{\rm w}, \\ A_\mu &= -W_{3\,\mu}\sin\theta_{\rm w} + B_\mu\cos\theta_{\rm w}\,, \qquad (1.5)\end{aligned}$$

with $\tan\theta_{\rm w} = g'/g$, $\theta_{\rm w}$ is the weak mixing angle.

To generate the left-handed structure of the weak charged current interactions, the $SU(2)$ symmetry is applied to left-handed fermion fields only. The fermion fields are thus given by

$$\psi_L: \quad L_{L_k} = \frac{1}{2}(\mathbf{1}-\gamma_5)\begin{pmatrix}\nu_k \\ e_k\end{pmatrix}, \quad Q_{L_k} = \frac{1}{2}(\mathbf{1}-\gamma_5)\begin{pmatrix}u_k \\ d_k\end{pmatrix}, \qquad (1.6)$$

for the $SU(2)_L$ left-handed leptonic and quark doublets and

$$\psi_R: \quad e_{R_k} = \frac{1}{2}(\mathbf{1}+\gamma_5)\, e_k\,, \quad u_{R_k} = \frac{1}{2}(\mathbf{1}+\gamma_5)\, u_k\,, \quad d_{R_k} = \frac{1}{2}(\mathbf{1}+\gamma_5)\, d_k\,, \tag{1.7}$$

for the right-handed singlets, with $k = 1\ldots3$ being a generation index. The original convention is that right handed neutrinos are not introduced. However in the light of the recent Superkamiokande results [7] right-handed neutrinos might be introduced to accommodate a Dirac mass term for neutrinos. The λ_i in (1.1) are the Yukawa couplings of the quarks and leptons.

Masses for non-abelian gauge fields and fermions are generated by the Higgs mechanism [8] via spontaneous symmetry breaking which preserves the renormalizability of the theory [5]. The Higgs fields are complex scalar iso-doublets (ϕ^+, $\frac{1}{\sqrt{2}}[v+H(x)+i\chi(x)]$) with electroweak interactions described in (1.1). For the choice of $\mu^2 < 0$, the ground state of the theory is obtained when the neutral member of the Higgs doublet acquires a vacuum expectation value

$$\langle\phi\rangle = \begin{pmatrix} 0 \\ v/\sqrt{2} \end{pmatrix}, \tag{1.8}$$

with $v^2 = -\mu^2/\lambda$. This non-vanishing vacuum expectation value selects a preferred direction in $SU(2)_L \times U(1)_Y$ space and spontaneously breaks the theory, leaving the $U(1)_{em}$ subgroup intact. The remaining degrees of freedom, *i. e.* the Goldstone bosons, are gauged away from the scalar sector, but essentially reappear in the gauge sector, providing the longitudinal modes for the W and Z bosons. The various masses are given by

$$M_W = \frac{1}{2}gv\,, \quad M_Z = \frac{v}{2}\sqrt{g^2+g'^2}\,, \quad M_H = v\sqrt{2\lambda}\,, \quad m_f = -\lambda_f\frac{v}{\sqrt{2}}\,. \tag{1.9}$$

In order to obtain QED, the massless A_μ is identified with the photon and $e = g\sin\theta_{\rm w}$.

1.3 Relevant SM Cross sections

In the following section we are going to review some standard model cross sections, such as $e^+e^- \to W^+W^-, ZZ, Z\gamma, W^+W^-\gamma, ZZ\gamma$ and $Z\gamma\gamma$. For the simple example of $e^+e^- \to W^+W^-$ we are going to apply the spinor technique [9] which simplifies in particular the contraction of strings of γ – matrices.

1.3.1 Vector boson pair production: $e^+e^- \to W^+W^-, ZZ, Z\gamma$

One of the most celebrated discoveries at the $p\bar{p}$ collider at CERN was the discovery of the predicted weak particles [10]. From LEP2 data we witness the agreement between theory and experiment at the precision of 1%, at the level of testing higher order perturbation theory. For almost two decades the process $e^+e^- \to W^+W^-$ has been (and still is) of major theoretical interest [11]. Providing the simplest direct test of the triple gauge boson couplings $W^+W^-\gamma$ and W^+W^-Z its measurement has been awaited with great anticipation. The cross section has been measured [12] and found to be in excellent agreement with the theoretical predictions; taking next-to-leading order radiative corrections [13, 14, 15] into account. The process can be illustrated by the following Feynman diagrams [2].

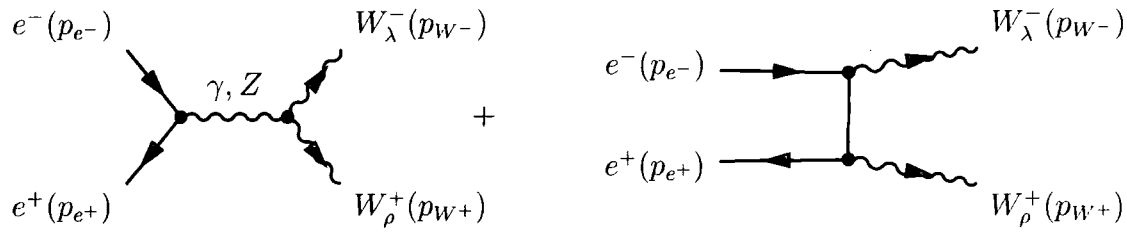

Figure 1.1: Feynman diagrams illustrating the process $e^+e^- \to W^+W^-$.

Making use of the conventions and Feynman rules in Appendix A and B the polarized (say here left handed) matrix element for s- and t-channel diagrams can in the unitary gauge be written as

$$
\begin{aligned}
i\mathcal{M}_s^\gamma &= \bar{u}_-(p_{e^+})\,(ie)\,\gamma^\mu\,u_-(p_{e^-})\left(-i\frac{g_{\mu\nu}}{p^2+i\epsilon}\right)\epsilon^*_\lambda(p_{W^-})\,\epsilon^*_\rho(p_{W^+}) \\
&\quad (-ie)\,[g^{\nu\rho}\,(p+p_{W^+})^\lambda + g^{\rho\lambda}\,(-p_{W^+}+p_{W^-})^\nu + g^{\lambda\nu}\,(-p_{W^-}-p)^\rho] \qquad (1.10)\\
i\mathcal{M}_s^Z &= \bar{u}_-(p_{e^+})\;(ie(v_{e^-}+a_{e^-}))\;\gamma^\mu\,u_-(p_{e^-})\left(-i\frac{g_{\mu\nu}-(p_\mu p_\nu)/M_Z^2}{p^2-M_Z^2+i\epsilon}\right)\epsilon^*_\lambda(p_{W^-})\,\epsilon^*_\rho(p_{W^+}) \\
&\quad \left(\frac{ie\cos\theta_w}{\sin\theta_w}\right)[g^{\nu\rho}\,(p+p_{W^+})^\lambda + g^{\rho\lambda}\,(-p_{W^+}+p_{W^+})^\nu + g^{\lambda\nu}\,(-p_{W^-}-p)^\rho] \qquad (1.11)\\
i\mathcal{M}_t &= \bar{u}_-(p_{e^+})\,(i\frac{g}{\sqrt{2}})\,\gamma^\rho\,\epsilon^*_\rho(p_{W^+})\left(i\,\frac{(\not{p}_{e^-}-\not{p}_{W^-})}{(p_{e^-}-p_{W^-})^2}\right)(i\frac{g}{\sqrt{2}})\gamma^\lambda\,\epsilon^*_\lambda(p_{W^-})\,u_-(p_{e^-})\,, \qquad (1.12)
\end{aligned}
$$

[2] The diagrams are drawn with help of the feynmp style file based on [16].

with $p_{e^-}, p_{e^+}, p_{W^+}$ and p_{W^-} the momentum of the e^-, e^+, W^+ and W^- respectively and $p = p_{e^+} + p_{e^-}$. We have neglected the fermion mass here.
To further simplify the calculation the following identities are useful

$$\bar{u}_{\lambda_1}(p_1)\,\Gamma\,u_{\lambda_2}(p_2) = \lambda_1\lambda_2\,\bar{u}_{-\lambda_2}(p_2)\,\Gamma^R\,u_{-\lambda_1}(p_1) \tag{1.13a}$$

$$[\bar{u}_\lambda(p_1)\,\gamma^\mu\,u_\lambda(p_2)]\,\gamma_\mu = 2\,u_\lambda(p_2)\,\bar{u}_\lambda(p_1) + 2\,u_{-\lambda}(p_1)\,\bar{u}_{-\lambda}(p_2) \tag{1.13b}$$

$$\bar{u}_+(p_1)\,u_-(p_2) \equiv s(p_1,p_2) = -s(p_2,p_1) \tag{1.13c}$$

$$\bar{u}_-(p_1)\,u_+(p_2) \equiv t(p_1,p_2) = -t(p_2,p_1) \tag{1.13d}$$

$$s(p,p) = 0 \quad , \quad t(p,p) = 0 \tag{1.13e}$$

where Γ is any string of γ matrices and Γ^R is the same string with reversed order of the matrices.
Furthermore the polarization vectors of massive particles are rewritten as

$$\epsilon^*_\rho(p_{W^+}) = \bar{u}_-(r_4)\,\gamma_\rho\,u_-(r_3) \tag{1.14}$$

$$\epsilon^*_\lambda(p_{W^-}) = \bar{u}_-(r_1)\,\gamma_\lambda\,u_-(r_2)\,, \tag{1.15}$$

where $r_3 + r_4 = p_{W^+}$ and $r_3^2 = 0 = r_4^2$, and $r_1 + r_2 = p_{W^-}$ and $r_1^2 = 0 = r_2^2$. Note here that for all practical purposes the spinor products have to be normalized by the mass of the particle and a phase space factor of $\sqrt{2/3}$.
In the case of massless bosons the polarization vector can be written as

$$\begin{aligned}\epsilon^{+*}_\kappa(k) &= \frac{1}{\sqrt{4\,p_0\cdot k}}\,\bar{u}_+(k)\,\gamma_\kappa\,u_+(p_0)\\ \epsilon^{-*}_\kappa(k) &= \frac{1}{\sqrt{4\,p_0\cdot k}}\,\bar{u}_-(k)\,\gamma_\kappa\,u_-(p_0)\end{aligned} \tag{1.16}$$

the photon polarization being either *plus* or *minus* respectively. Here p_0 can be chosen as any of the lightlike incoming vectors. Throughout the calculation we make use of the identity $\not{p} \equiv u_+(p)\bar{u}_+(p) + u_-(p)\bar{u}_-(p)$.

The matrix elements can then be further calculated

$$\begin{aligned}
\mathcal{M}_s^\gamma + \mathcal{M}_s^Z &= 4\,e^2 \left(-\frac{1}{p^2} + \frac{\cos\theta_w}{\sin\theta_w} (v_e + a_e) \frac{1}{p^2 - M_Z^2} \right) \\
&\quad \Big[t(p_{e^+}, r_4)\, s(r_3, p_{e^-})\, (t(r_1, r_4)\, s(r_4, r_2) + t(r_1, r_3)\, s(r_3, r_2)) \\
&\quad - t(p_{e^+}, r_1)\, s(r_2, p_{e^-})\, (t(r_4, r_2)\, s(r_2, r_3) + t(r_4, r_1)\, s(r_1, r_3)) \\
&\quad - t(r_4, r_1)\, s(r_2, r_3)\, (t(p_{e^+}, r_4)\, s(r_4, p_{e^-}) + t(p_{e^+}, r_3)\, s(r_3, p_{e^-})) \Big] \\
\mathcal{M}_t &= -2\,g^2 \frac{1}{(p_{e^-} - p_{W^-})^2} \\
&\quad t(p_{e^+}, r_4)\, (s(r_3, p_{e^-})\, t(p_{e^-}, r_1) - s(r_3, r_2)\, t(r_2, r_1))\, s(r_2, p_{e^-})\,. \qquad (1.17)
\end{aligned}$$

Writing the matrix element in this form is particularly suitable for numerical calculations. For any given set of four vectors $(p^\mu_{e^-}, \ldots, p^\mu_{W^-})$ the numerical value of any $s(p_i, p_j)$ (and by complex conjugation $t(p_i, p_j)$) can be calculated using a minimum of computational power. To calculate, for instance, the total cross section of this process, the phase space can be generated using RAMBO [17].

The processes $e^+e^- \to ZZ$, $Z\gamma$ are of far less theoretical interest since at leading order no boson self interactions are involved. In the SM, triple gauge boson vertices involve two charged particles (see (1.2). Hence neutral t and u-channel currents are sufficient to describe those processes diagrammatically.

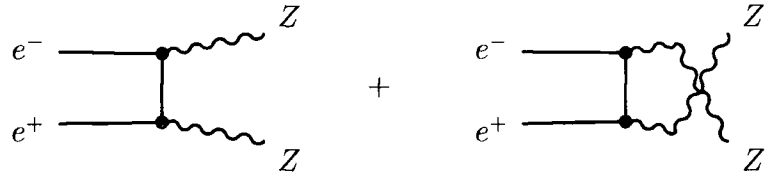

Figure 1.2: Feynman diagrams illustrating the process $e^+e^- \to ZZ$.

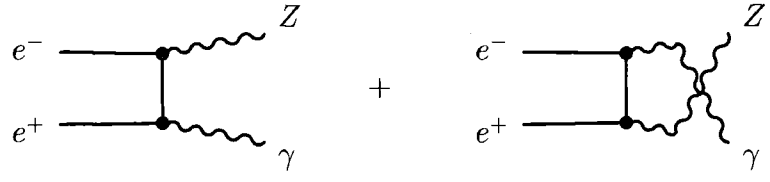

Figure 1.3: Feynman diagrams illustrating the process $e^+e^- \to Z\gamma$.

1.3.2 Triple gauge boson production: $f\bar{f} \to W^+W^-\gamma$, $e^+e^- \to ZZ\gamma$, $Z\gamma\gamma$

The process $f\bar{f} \to W^+W^-\gamma$ is one of the key processes in this thesis. Anomalous quartic couplings (Chapter 2, $f\,\bar{f} = e^-\,e^+$) as well as radiation zeros (Chapter 3, $f\,\bar{f} = q\,\bar{q}$) will be studied using this process. Naturally the total cross section for a three particle final state (in particular since two out of three particles are massive) is one order of magnitude smaller than the corresponding two particle W^+W^-cross section.

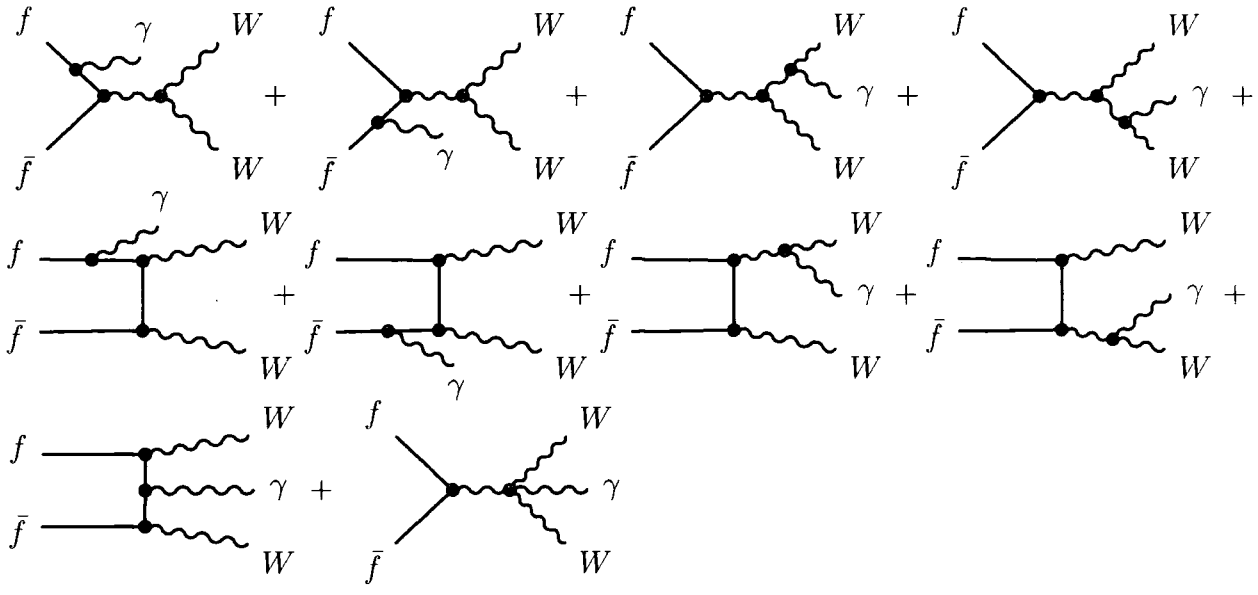

Figure 1.4: Feynman diagrams illustrating the process $f\,\bar{f} \to W^+W^-\gamma$.

Note that this process is built on the W^+W^-pair production topologies, where a photon is attached at each external leg (in particular the radiation off the W bosons, which is a unique feature of the charged bosons), at the particle exchanged in the t-channel (for $f\bar{f} = q\bar{q}$ where the exchanged particle is a quark; for $f\bar{f} = e^+e^-$ the exchanged particle in the t-channel is a neutrino with no coupling to the photon) and at the three boson vertex.

This last diagram illustrates the first appearance of quartic couplings within the SM, arising naturally from the kinetic term of the $SU(2)$ triplet in the Lagrangian (1.1). Just as in Fig. 1.1 the s-channel diagrams stand for both photon and Z exchange, and hence the last diagram has to be understood as involving $W^+W^-\gamma\gamma$ as well as $W^+W^-Z\gamma$ couplings. The

matrix elements can be found in Appendix C. Again the spinor technique has been used to prepare the matrix element for numerical calculation purposes.

The process $e^+e^- \to ZZ\gamma$ can again be illustrated as the lowest order process $e^+e^- \to ZZ$ where a photon is emitted wherever possible. Note also that in the SM no four boson vertex involving three (or more) neutral particles is realized. Again the matrix element can be found in Appendix C.

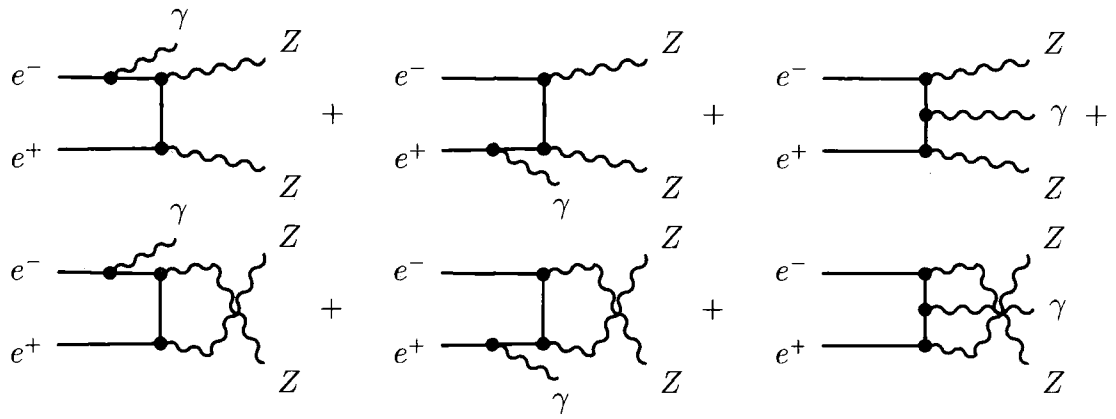

Figure 1.5: Feynman diagrams illustrating the process $e^+e^- \to ZZ\gamma$.

The process $e^+e^- \to Z\gamma\gamma$ can be calculated just as $e^+e^- \to ZZ\gamma$, where one of the Z bosons is exchanged by a photon. Hence the overall coupling will change, whereas the topological structure remains the same. Note here that using the spinor technique both possible polarizations of the photon have to be considered.

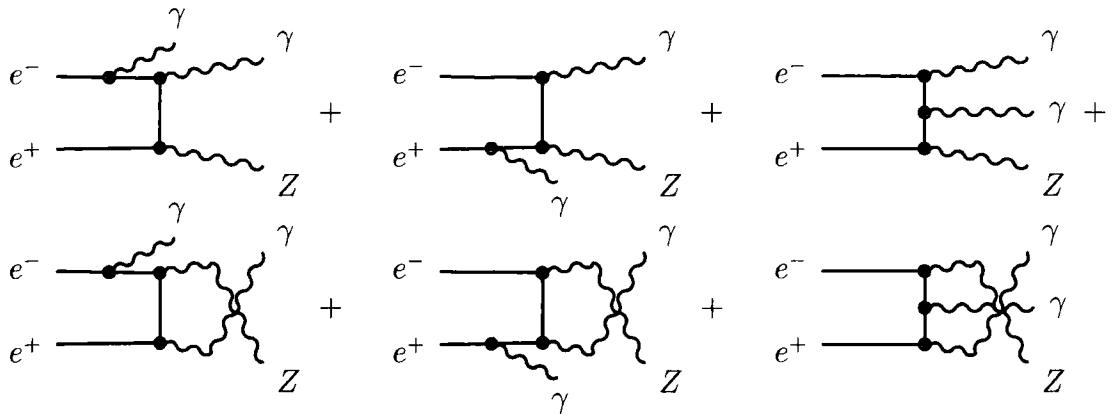

Figure 1.6: Feynman diagrams illustrating the process $e^+e^- \to Z\gamma\gamma$.

For all those processes Monte Carlo generators are available upon request.
Finally in Fig. 1.7 the total integrated cross section for all the above processes is displayed for a range of centre of mass energies. Wherever a photon is involved the following cuts have been used

$$E_\gamma > 20 \text{ GeV} \qquad , |\eta| = |\frac{1}{2} \log \frac{1+\cos\theta_\gamma}{1-\cos\theta_\gamma}| < 2 \tag{1.18}$$

with E_γ and θ_γ the photon energy and the angle between the photon and the beam axis respectively. These cuts are implemented to avoid infrared and collinear singularities respectively. Infrared and collinear divergences arise due to $1/(p_i \cdot p_\gamma) \sim [1/E_\gamma]\ [1/(1-\cos\theta_\gamma)]$ terms in the matrix element, originating from fermion or boson propagators with momentum shifted by $\mp p_\gamma$ with respect to the initial or final state particle-momentum respectively.

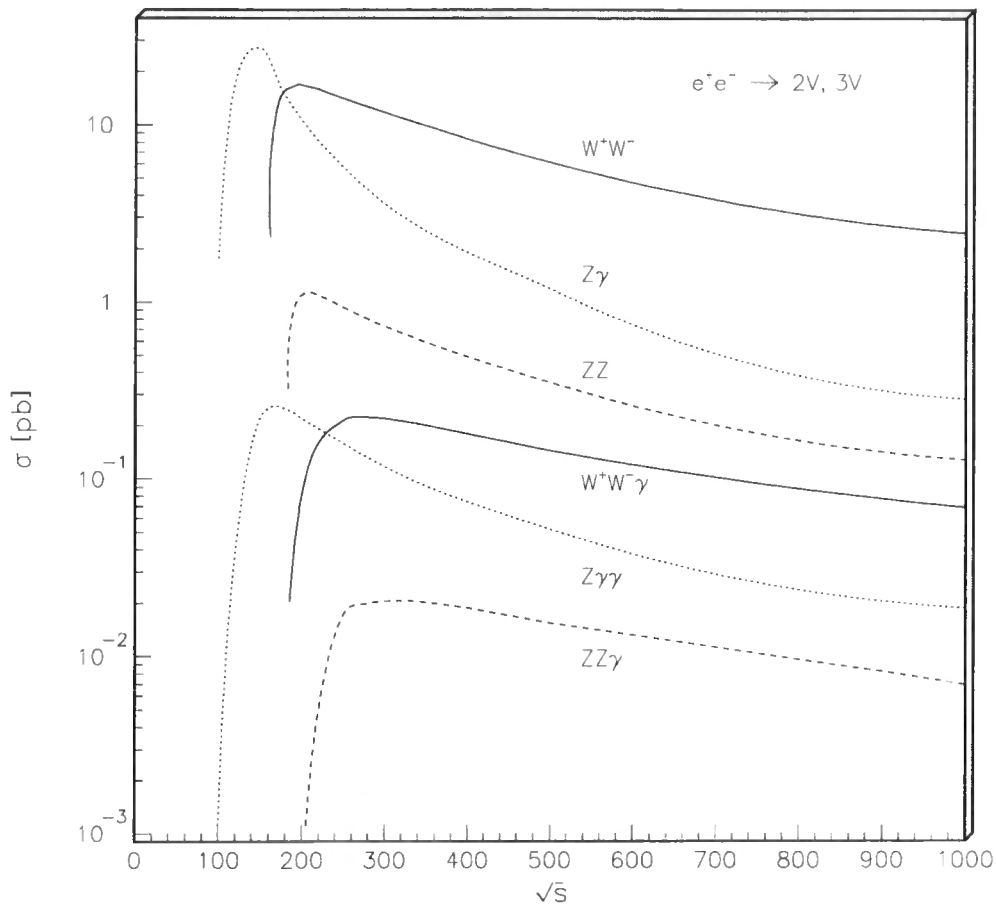

Figure 1.7: Total integrated SM cross section for $e^+e^- \to W^+W^-$, ZZ, $Z\gamma$, $W^+W^-\gamma$, $ZZ\gamma$, $Z\gamma\gamma$ (in pb) as a function of $\sqrt{s}$ (in GeV) .

For convenience (and perhaps easy comparison with other event generators) the numerical values for the total cross section of all processes are given in Table 1.1 for the two most relevant center of mass energies, the maximal expected LEP2 energy ($\sqrt{s} = 200$ GeV) and the generic energy of a future linear collider ($\sqrt{s} = 500$ GeV), using the cuts introduced in (1.18). Note that this means for on-shell Z bosons that the threshold for $ZZ\gamma$ production

is $\sqrt{s} = 202.38$ GeV and hence the given value for this process is in fact for $\sqrt{s} = 205$ GeV.

process	$\sqrt{s} = 200$ GeV	$\sqrt{s} = 500$ GeV
W^+W^-	16.65 pb	6.12 pb
ZZ	1.11 pb	0.35 pb
$Z\gamma$	10.44 pb	1.18 pb
$W^+W^-\gamma$	84.77 fb	144.92 fb
$ZZ\gamma$	1.11 fb	15.39 fb
$Z\gamma\gamma$	218.23 fb	51.82 fb

Table 1.1: Numerical values of the total cross section for the processes $e^+e^- \to 2V, 3V$ for the two generic center of mass energies $\sqrt{s} = 200$ GeV and $\sqrt{s} = 500$ GeV.

Now that we have presented the SM cross sections for triple gauge boson production we are going to investigate, in the next two chapters, how those processes can be used to study physics beyond the SM. In particular we are going to study the impact of anomalous quartic couplings on the processes $e^+e^- \to W^+W^-\gamma$, $ZZ\gamma$ and $Z\gamma\gamma$ to be measured at a next linear collider or LEP2 [18, 19]. We further study the presence of radiation zeros in the process $q\bar{q} \to W^+W^-\gamma$ to be investigated at a hadron collider [20]. In the last chapter we study a class of dominant electroweak radiative corrections to $e^+e^- \to W^+W^-$. We like to point out here that our method of calculating those electroweak radiative corrections is not process dependent, and is in principle applicable to any electroweak process [21, 22]. So far the analysis is not completed in the neutral gauge boson sector, *i. e.* for photons or Z bosons in the final state, but it will be soon [23].

Chapter 2

Anomalous Quartic Couplings

2.1 Introduction

In the Standard Model (SM), the couplings of the gauge bosons and fermions are tightly constrained by the requirements of gauge symmetry (see (1.1)). In the electroweak sector, for example, this leads to trilinear VVV and quartic $VVVV$ interactions between the gauge bosons $V = \gamma, Z, W^{\pm}$ with completely specified couplings. Electroweak symmetry breaking via the Higgs mechanism gives rise to additional Higgs – gauge boson interactions, again with specified couplings.

The trilinear and quartic gauge boson couplings probe different aspects of the weak interactions. The trilinear couplings directly test the non-Abelian gauge structure, and possible deviations from the SM couplings have been extensively studied in the literature, see for example [11, 24] and references therein. Experimental bounds have also been obtained [25, 26]. In contrast, the quartic couplings can be regarded as a more direct window on electroweak symmetry breaking, in particular to the scalar sector of the theory (see for example [27]) or, more generally, on new physics which couples to electroweak bosons.

In this respect it is quite possible that the quartic couplings deviate from their SM values while the triple gauge vertices do not. For example, if the mechanism for electroweak symmetry breaking does not reveal itself through the discovery of new particles such as the Higgs boson, supersymmetric particles or technipions, it is possible that anomalous quartic couplings could provide the first evidence of new physics in this sector of the electroweak

theory [27].

High-energy colliders provide the natural environment for studying anomalous quartic couplings. The paradigm process is $f\bar{f} \to VVV$, with $f = e$ (e^+e^- colliders) or $f = q$ (hadron-hadron colliders), where one of the Feynman diagrams corresponds to $f\bar{f} \to V^* \to VVV$. In this context, one may consider the quartic-coupling diagram(s) as the signal, and the remaining diagrams as constituting the background. The sensitivity of a given process to anomalous quartic couplings depends on the relative importance of these two types of contribution, as we shall see.

In this study we shall focus on e^+e^- collisions, and quantify the dependence of various $e^+e^- \to VVV$ cross sections on the anomalous couplings. We shall consider in particular $\sqrt{s} = 200$ and 500 GeV, corresponding to LEP2 and a future linear collider (LC) respectively. For obvious kinematic reasons, processes where at least one of the gauge bosons is a photon have the largest cross sections. Indeed, VVV production with $V = Z, W^\pm$ are kinematically forbidden at 200 GeV and suppressed at 500 GeV. We therefore consider $W^+W^-\gamma$, $ZZ\gamma$ and $Z\gamma\gamma$ production. Each of these contains at least one type of quartic interaction.[1]

There have been several studies of this type reported in the literature [28, 29]. Our aim is partly to complete as well as update these, and partly to assess the relative merits of the above-mentioned processes in providing information on the anomalous couplings. Note that our primary interest is in the so-called 'genuine' anomalous quartic couplings, i.e. those which give no contribution to the trilinear vertices.

In the following section we review the various types of anomalous quartic coupling that might be expected in extensions of the SM. In Section 2.3 we present numerical studies illustrating the impact of the anomalous couplings on various VVV cross sections. Finally in Section 2.4 we present our conclusions.

[1] We ignore the process $e^+e^- \to \gamma\gamma\gamma$ which involves no trilinear or quartic interactions.

2.2 Anomalous gauge boson couplings

The lowest dimension operators which lead to genuine quartic couplings where at least one photon is involved are of dimension 6 [28].

A dimension 4 operator is not realised since a custodial $SU(2)$ symmetry is required to keep the ρ parameter, $\rho = M_W^2/(M_Z^2 \cos^2\theta_w)$, close to its measured SM value of 1. As a result, the allowed the 4-dimensional operator

$$\mathcal{L}_4 = -\frac{1}{4} g^2 (\overrightarrow{W_\mu} \times \overrightarrow{W_\nu}) (\overrightarrow{W^\mu} \times \overrightarrow{W^\nu}) \tag{2.1}$$

with

$$\overrightarrow{W_\mu} = \begin{pmatrix} \frac{1}{\sqrt{2}}(W_\mu^+ + W_\mu^-) \\ \frac{i}{\sqrt{2}}(W_\mu^+ - W_\mu^-) \\ W_\mu^3 + \frac{g'}{g} B_\mu \end{pmatrix} \tag{2.2}$$

and

$$\begin{aligned} W_\mu^3 + \frac{g'}{g} B_\mu &= \cos\theta_w Z_\mu - \sin\theta_w A_\mu + \frac{e}{\cos\theta_w} \frac{\sin\theta_w}{e} (\sin\theta_w Z_\mu + \cos\theta_w A_\mu) \\ &= \frac{Z_\mu}{\cos\theta_w} , \end{aligned} \tag{2.3}$$

does not involve the photon field A_μ.

The anomalous quadrupole moment operator [28]

$$\widetilde{\mathcal{L}_4} = -ie \frac{\lambda_\gamma}{M_W^2} F^{\mu\nu} W_{\mu\alpha}^\dagger W^\alpha{}_\nu \tag{2.4}$$

with

$$\begin{aligned} F_{\mu\nu} &= \partial_\mu A_\nu - \partial_\nu A_\mu \\ \mathbf{W}_{\mu\nu} &= \partial_\mu \mathbf{W}_\nu - \partial_\nu \mathbf{W}_\mu + g \mathbf{W}_\mu \times \mathbf{W}_\nu \end{aligned} \tag{2.5}$$

and

$$\mathbf{W}_\mu = \begin{pmatrix} \frac{1}{\sqrt{2}}(W_\mu^+ + W_\mu^-) \\ \frac{i}{\sqrt{2}}(W_\mu^+ - W_\mu^-) \\ \cos\theta_w Z_\mu - \sin\theta_w A_\mu \end{pmatrix} , \tag{2.6}$$

generates trilinear couplings in addition to quartic ones and is therefore not 'genuine'. In Section 2.4 we will briefly discuss the impact of possible non-zero anomalous trilinear couplings on our analysis.

Assuming for simplicity invariance under the discrete symmetries $\mathcal{C}$ (charge conjugation) and $\mathcal{P}$ (parity) with

$$\begin{array}{ll} \mathcal{C}\, W_\mu\, \mathcal{C}^{-1} := W_\mu^\dagger & \\ \mathcal{C}\, Z_\mu\, \mathcal{C}^{-1} := Z_\mu^\dagger & \end{array} \quad \text{and} \quad \begin{array}{l} \mathcal{P}\, W_\mu(\mathbf{x},t)\, \mathcal{P}^{-1} := W^\mu(-\mathbf{x},t) \\ \mathcal{P}\, Z_\mu(\mathbf{x},t)\, \mathcal{P}^{-1} := Z^\mu(-\mathbf{x},t) \end{array} \tag{2.7}$$

we are left with several 6-dimensional operators. First the neutral and the charged Lagrangians, both giving anomalous contributions to the $VV\gamma\gamma$ vertex, with VV either being W^+W^- or ZZ:

$$\begin{aligned} \mathcal{L}_0 &= -\frac{e^2}{16\Lambda^2}\, a_0\, F^{\mu\nu}\, F_{\mu\nu}\, \overrightarrow{W^\alpha} \cdot \overrightarrow{W_\alpha} \\ &\to -\frac{e^2}{16\Lambda^2}\, a_0 \left[-2(p_1 \cdot p_2)(A \cdot A) + 2(p_1 \cdot A(p_2))(p_2 \cdot A(p_1)) \right] \\ &\qquad \times \left[2(W^+ \cdot W^-) + (Z \cdot Z)/\cos^2\theta_w \right] \quad , \end{aligned} \tag{2.8}$$

$$\begin{aligned} \mathcal{L}_c &= -\frac{e^2}{16\Lambda^2}\, a_c\, F^{\mu\alpha}\, F_{\mu\beta}\, \overrightarrow{W^\beta} \cdot \overrightarrow{W_\alpha} \\ &\to -\frac{e^2}{16\Lambda^2}\, a_c \left[-(p_1 \cdot p_2)\, A^\alpha A_\beta + (p_1 \cdot A(p_2))\, A^\alpha(p_1) p_{2\beta} \right. \\ &\qquad \left. + (p_2 \cdot A(p_1))\, p_1^\alpha A_\beta(p_2) - (A \cdot A)\, p_1^\alpha p_{2\beta} \right] \\ &\qquad \times \left[W_\alpha^- W^{+\beta} + W_\alpha^+ W^{-\beta} + Z_\alpha Z^\beta/\cos^2\theta_w \right] . \end{aligned} \tag{2.9}$$

where p_1 and p_2 are the photon momenta, Λ is the scale parameter of new physics, to which we come back soon.

Since we are interested in the anomalous $VV\gamma\gamma$ contribution we pick up the corresponding part of the Lagrangian. To obtain the Feynman rules for the corresponding vertex (in agreement with [30]) we have to multiply by 2 for the two identical photons (as well as for the Zs in the case of $VV = ZZ$) and by i for convention.

Finally, an anomalous $WWZ\gamma$ vertex is for instance obtained from the Lagrangian [30]

$$\begin{aligned}
\mathcal{L}_n &= i\frac{e^2}{16\Lambda^2}\, a_n \epsilon_{ijk} W^{(i)}_{\mu\alpha} W^{(j)}_{\nu} W^{(k)\alpha} F^{\mu\nu} \\
&\rightarrow -\frac{e^2}{16\Lambda^2 \cos\theta_w}\, a_n \left(p^\nu A^\mu - p^\mu A^\nu\right) \\
&\quad \times \left(-W^-_\nu p^+_\mu \left(Z \cdot W^+\right) + W^+_\nu p^-_\mu \left(Z \cdot W^-\right) + Z_\nu p^+_\mu \left(W^+ \cdot W^-\right)\right. \\
&\quad -Z_\nu p^-_\mu \left(W^+ \cdot W^-\right) + W^-_\nu W^+_\mu \left(p^+ \cdot Z\right) - W^+_\nu W^-_\mu \left(p^- \cdot Z\right) \\
&\quad -Z_\nu W^+_\mu \left(p^+ \cdot W^-\right) + Z_\nu W^-_\mu \left(p^- \cdot W^+\right) - W^+_\nu p^0_\mu \left(Z \cdot W^-\right) \\
&\quad \left. +W^-_\nu p^0_\mu \left(Z \cdot W^+\right) - W^-_\nu Z_\mu \left(p^0 \cdot W^+\right) + W^+_\nu Z_\mu \left(p^0 \cdot W^-\right)\right) \qquad (2.10)
\end{aligned}$$

where $W^{(j)}_\nu$ are the components of the vector (2.2), p, p^+, p^- and p^0 are the momenta of the photon, the W^+, the W^- and the Z respectively, and

$$\overrightarrow{W}_{\mu\nu} = \partial_\mu \overrightarrow{W}_\nu - \partial_\nu \overrightarrow{W}_\mu + g\, \overrightarrow{W}_\mu \times \overrightarrow{W}_\nu \ . \qquad (2.11)$$

Note that we have only used the terms leading to four point interactions, *i. e.* the first two terms of (2.11).

Note here that the choice for this anomalous Lagrangian is not completely unique and other authors have chosen to take another parametrisation [31] assuming

$$\begin{aligned}
\mathcal{C} W_\mu \mathcal{C}^{-1} &:= -W^\dagger_\mu \\
\mathcal{C} Z_\mu \mathcal{C}^{-1} &:= -Z^\dagger_\mu \, . \qquad (2.12)
\end{aligned}$$

Imposing invariance under *this* definition of the charge operation can lead to five independent anomalous couplings.

It follows from the Feynman rules that any anomalous contribution is *linear* in the photon energy E_γ. This means that it is the hard tail of the photon energy distribution that is most affected by the anomalous contributions, but unfortunately the cross sections here are very small. In the following numerical studies we will impose a lower energy photon cut of $E^{\min}_\gamma = 20$ GeV. Moreover, since there is no anomalous contribution for initial state photon radiation, the effects are largest for centrally-produced photons. We therefore impose an additional cut of $|\eta_\gamma| < 2$.[2]

[2]Obviously in practice these cuts will also be tuned to the detector capabilities.

To illustrate the above we give here, as an example, the photon energy distribution for the process $e^+e^- \to W^+W^-\gamma$ in the SM and for various values of the anomalous parameter a_0 at $\sqrt{s} = 500$ GeV.

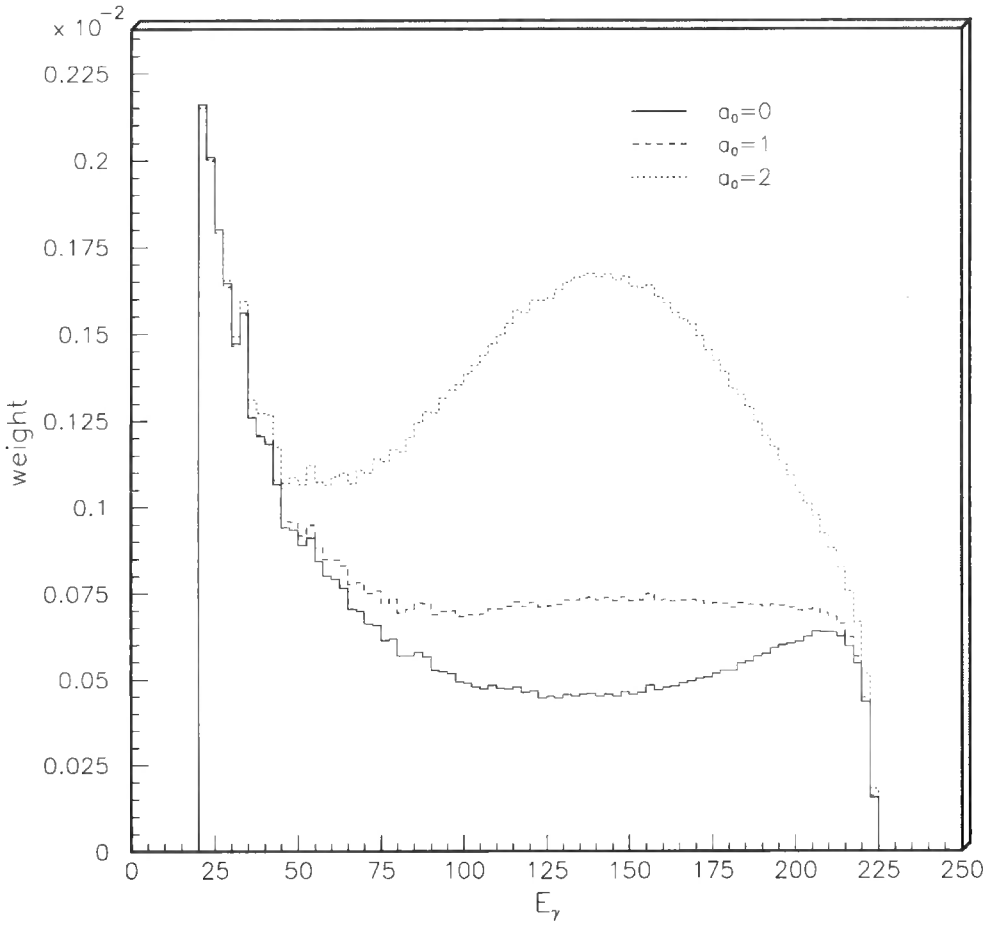

Figure 2.1: Photon energy distribution for the process $e^+e^- \to W^+W^-\gamma$ in the SM and for various values of the anomalous parameter a_0 ($\Lambda = M_W$) at $\sqrt{s} = 500$ GeV.

A further consideration concerns the effects of beam polarisation. One of the 'background'

(i.e. non-anomalous) diagrams for $e^+e^- \to W^+W^-\gamma$ production is where all three gauge bosons are attached to the electron line. Such contributions can be suppressed by an appropriate choice of beam polarisation (i.e. right-handed electrons) thus enhancing the anomalous signal. We will illustrate this below.

Finally, the anomalous parameter Λ that appears in all the above anomalous contributions has to be fixed. In practice, Λ can only be meaningfully specified in the context of a specific model for the new physics giving rise to the quartic couplings. One example is an excited W scenario $W^+\gamma \to W^* \to W^+\gamma$, where we would expect $\Lambda \sim M_{W^*}$ and a_i to be related to the decay width for $W^* \to W + \gamma$. However, in order to make our analysis independent of any such model, we choose to fix Λ at a reference value of M_W, following the conventions adopted in the literature. Any other choice of Λ (e.g. $\Lambda = 1$ TeV) results in a trivial rescaling of the anomalous parameters a_0, a_c and a_n.

2.3 Numerical studies

In this section we study the dependence of the cross sections on the three anomalous couplings defined in Section 2.2. As already stated, we apply a cut on the photon energy $E_\gamma > 20$ GeV to take care of the infrared singularity, and a cut on the photon rapidity $|\eta_\gamma| < 2$ to avoid collinear singularities. We do not include any branching ratios or acceptance cuts on the decay products of the produced $W^\pm$ and Z bosons, since we assume that at e^+e^- colliders the efficiency for detecting these is high.

2.3.1 Vector Boson Production

We first consider the SM cross sections for the processes of interest, i.e. with all anomalous couplings set to zero. Figure 2.2 shows the collider energy dependence of the $e^+e^- \to W^+W^-\gamma$, $e^+e^- \to ZZ\gamma$ and $e^+e^- \to Z\gamma\gamma$ cross sections.[3]

[3]Note that although these cross sections have appeared before in the literature, we are unable to reproduce the results for $\sigma(Z\gamma\gamma)$ given in Figure 2 of Ref. [32]. To cross check our results we used MADGRAPH [33].

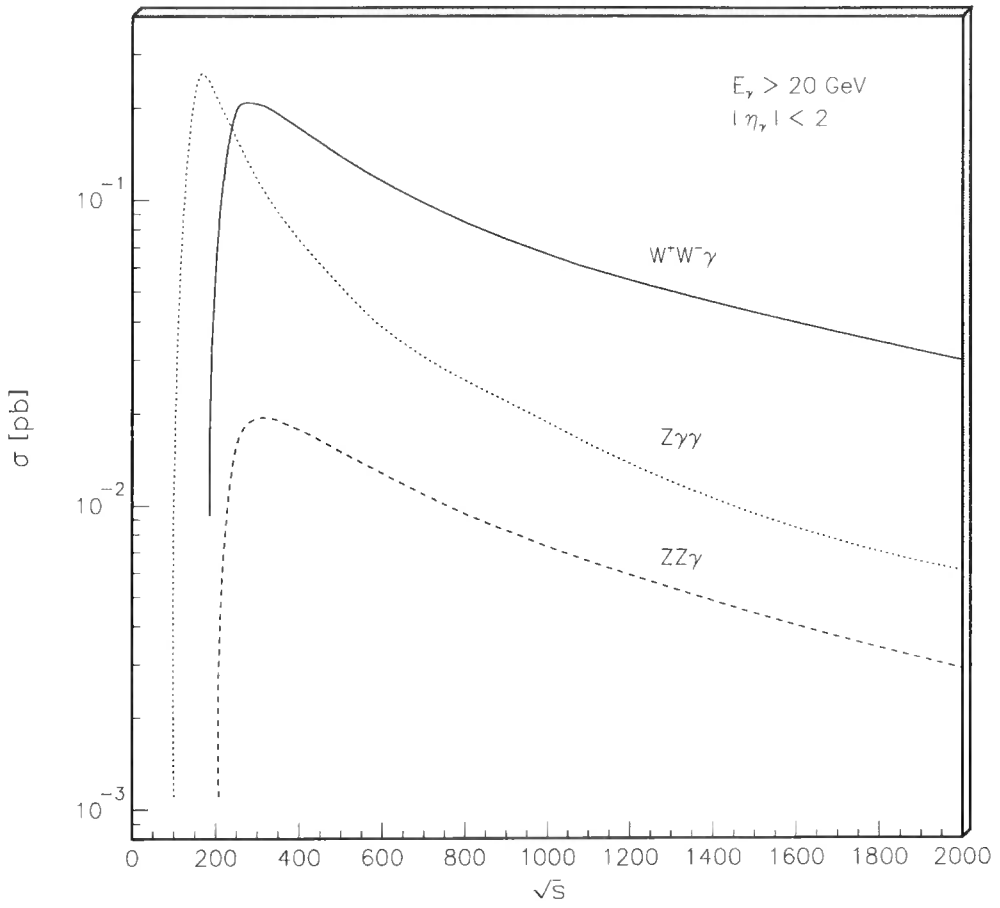

Figure 2.2: Total SM cross sections for $e^+e^- \to W^+W^-\gamma$, $ZZ\gamma$, $Z\gamma\gamma$ (in pb) as a function of $\sqrt{s}$ (in GeV).

Next we study the influence of each of the three anomalous parameters a_0, a_c and a_n separately in order to gauge the impact of each on the cross section. Note that $\sigma(W^+W^-\gamma)$ depends on all three parameters, while $\sigma(ZZ\gamma)$ and $\sigma(Z\gamma\gamma)$ depend only on a_0 and a_c. Figure 2.3 shows the dependence of the three total cross sections of Figure 2.2 at $\sqrt{s} =$ 500 GeV on the anomalous parameters. In each case the cross section is normalised to its

SM value, and the cuts are the same as in Figure 2.2.

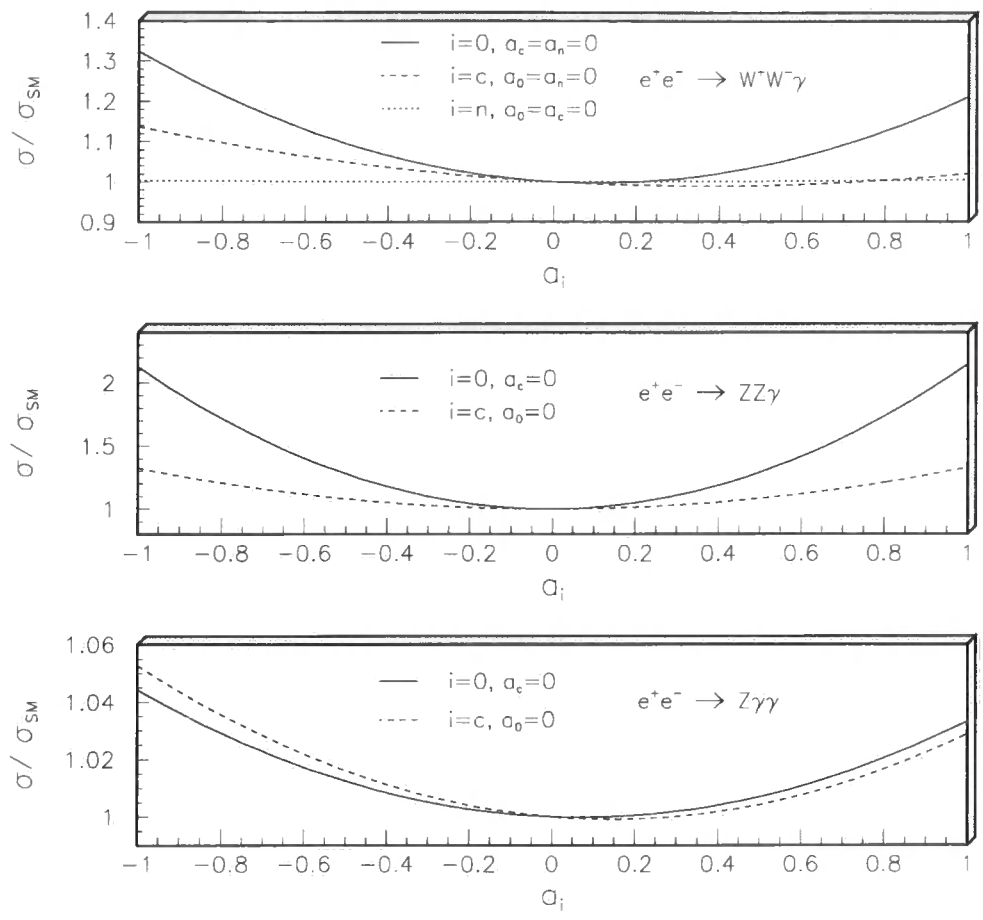

Figure 2.3: Influence of the anomalous parameters on the total cross sections, normalised to their SM values, at $\sqrt{s} = 500$ GeV.

As expected the dependence on the a_i is quadratic, since they appear linearly in the matrix element. The fact that the minimum of the curves is close to the SM point $a_i = 0$ shows that the interference between the anomalous and standard parts of the matrix element is small. The anomalous parameters have a markedly different effect on the three cross sections. Evidently a_0 has the largest influence, particularly on $\sigma(ZZ\gamma)$. The reason for this is easily understood. The anomalous process $e^+e^- \to \gamma^* \to ZZ\gamma$ has a much larger impact on

$\sigma(ZZ\gamma)$ since there are only six other SM diagrams. In contrast, $e^+e^- \to \gamma^* \to W^+W^-\gamma$ has a much larger SM 'background' set of diagrams to contend with. Note also that the anomalous contributions are enhanced by a factor $1/\cos^4\theta_w$ compared to the $WW\gamma\gamma$ vertex. At this collider energy also the possibility of longitudinal polarized W and Z bosons becomes evident: even though the same number of diagrams contributes to $ZZ\gamma$ production as to $Z\gamma\gamma$ production, far tighter bounds on the anomalous couplings can be expected from the former process.

Of course the important question is which of the three processes offers the best chance of detecting an anomalous quartic coupling at a given collider energy. To answer this we need to combine the information from Figs. 2.2 and 2.3 to see whether enhanced sensitivity can overcome a smaller overall event rate. We also need to consider *correlations* between different anomalous contributions to the same cross section. Note here that the magnitude of the SM cross section as well as the luminosity of the collider enter the absolute sensitivity. The standard deviation $\pm 1\,\sigma$ on the cross section is defined as

$$\pm 1\,\sigma \;=\; \pm\sqrt{\frac{\sigma_{\rm SM}}{\mathcal{L}}}\,. \tag{2.13}$$

We consider two experimental scenarios: unpolarised e^+e^- collisions at 200 GeV with $\int \mathcal{L} = 150$ pb^{-1}, and at 500 GeV with $\mathcal{L} = 300$ fb^{-1}/year[4]. Starting with the $W^+W^-\gamma$ process, Figure 2.4 shows the contours in the (a_i, a_j) plane that correspond to $+2, +3\,\sigma$ deviations from the SM cross section at $\sqrt{s} = 200$ GeV. Note that there are three ellipses, one for each combination of the three anomalous couplings. Evidently the sensitivity to a_0 and a_c is comparable, corresponding to $a_i < \mathcal{O}(100)$ for this luminosity.[5] The corresponding limit on a_n is some three to four times larger. Figure 2.5 shows the same contours but now at 500 GeV. The dramatic improvement in sensitivity (now $a_i < \mathcal{O}(1)$) comes partly from the higher collision energy (which allows for more energetic photons) but mainly from the much higher luminosity. A correlation between the effects of a_0 and a_c (solid ellipses) is noticeable at this energy.

[4]In the following we use the expected integrated luminosity for a run of one year [34].

[5]Note that any anomalous parameter a_i too large might result in an instability in the perturbative approach. Note also that for a more realistic value of $\Lambda = 1$ TeV the anomalous parameter are rescaled to even bigger values.

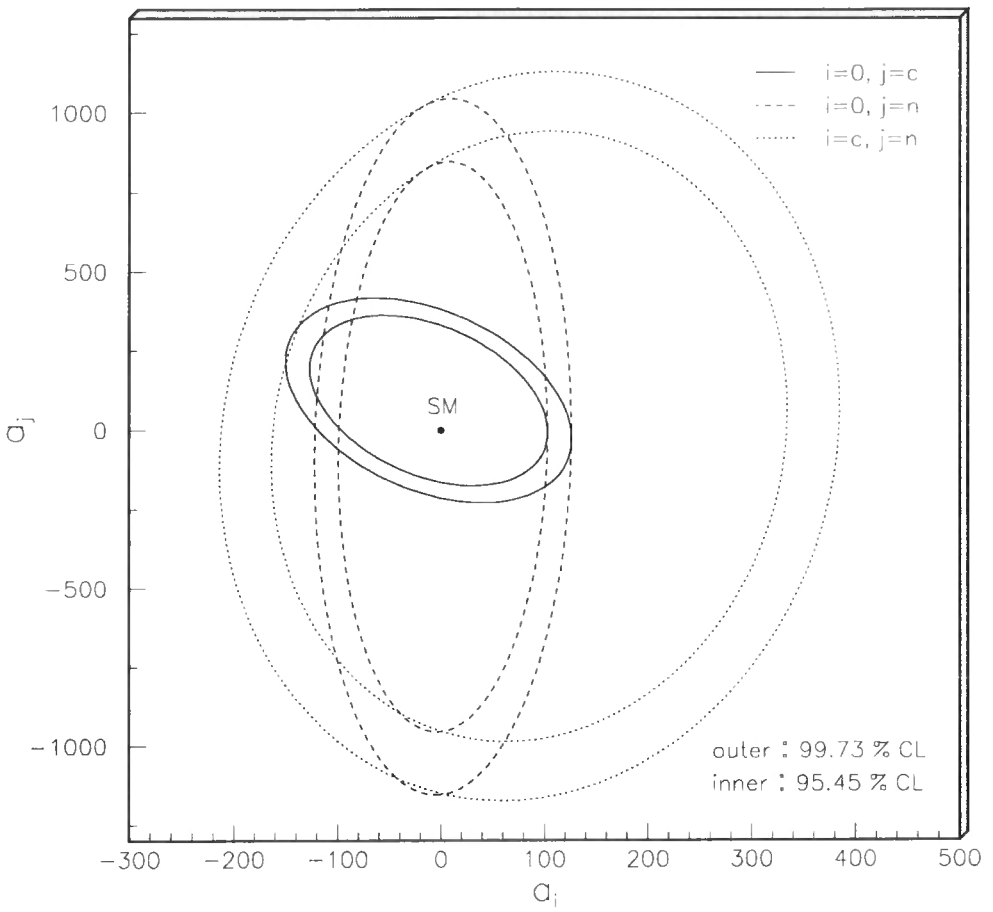

Figure 2.4: Contour plots for $+2, +3\,\sigma$ deviations from the SM $e^+e^- \to W^+W^-\gamma$ total cross section at $\sqrt{s} = 200$ GeV with $\int \mathcal{L} = 150$ pb^{-1}, when two of the three anomalous couplings are non-zero.

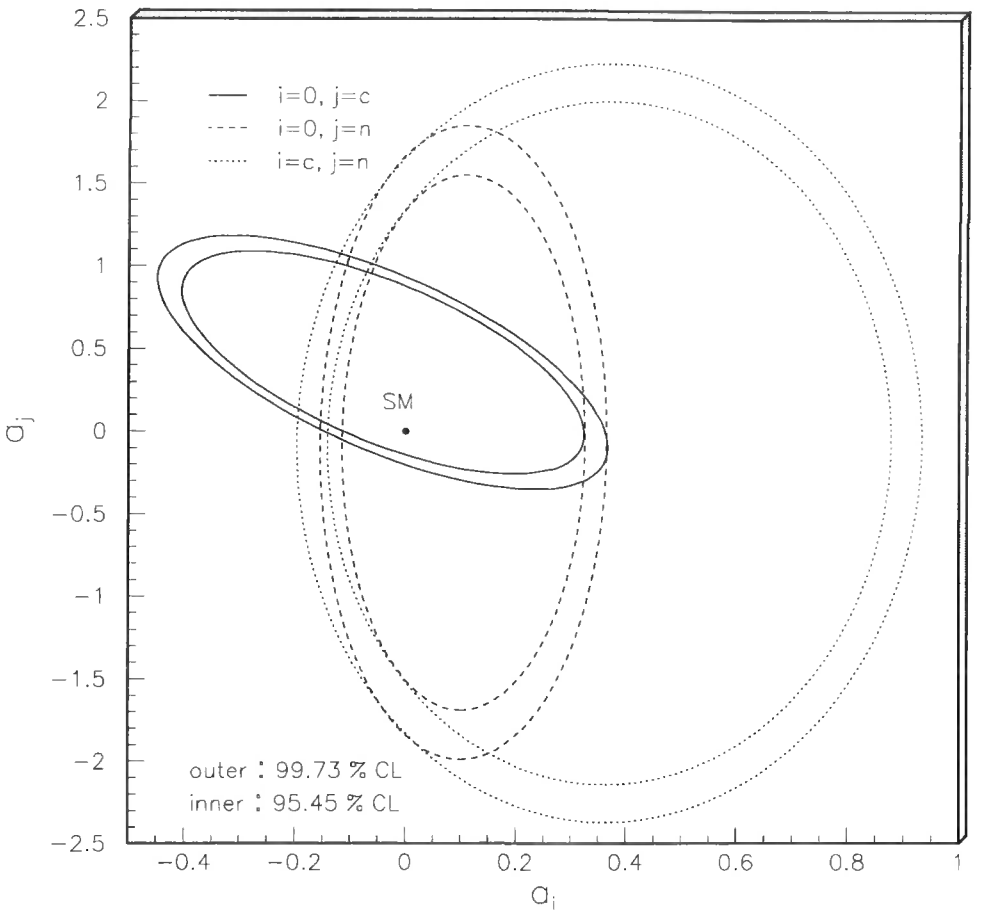

Figure 2.5: As for Figure 2.4, but for $\sqrt{s} = 500$ GeV with $\int \mathcal{L} = 300$ fb^{-1}.

We have already anticipated a significant improvement in sensitivity for this process when the beams are polarised. Specifically, with right-handed electrons (and left-handed positrons) we suppress a large number of SM 'background' diagrams where the $W^{\pm}$ are attached to the fermion line. The effect of 100% beam polarisation of this type is shown in Figure 2.6. Assuming the *same* luminosity we obtain a factor of approximately 3 improvement in the sensitivity to an individual anomalous coupling.

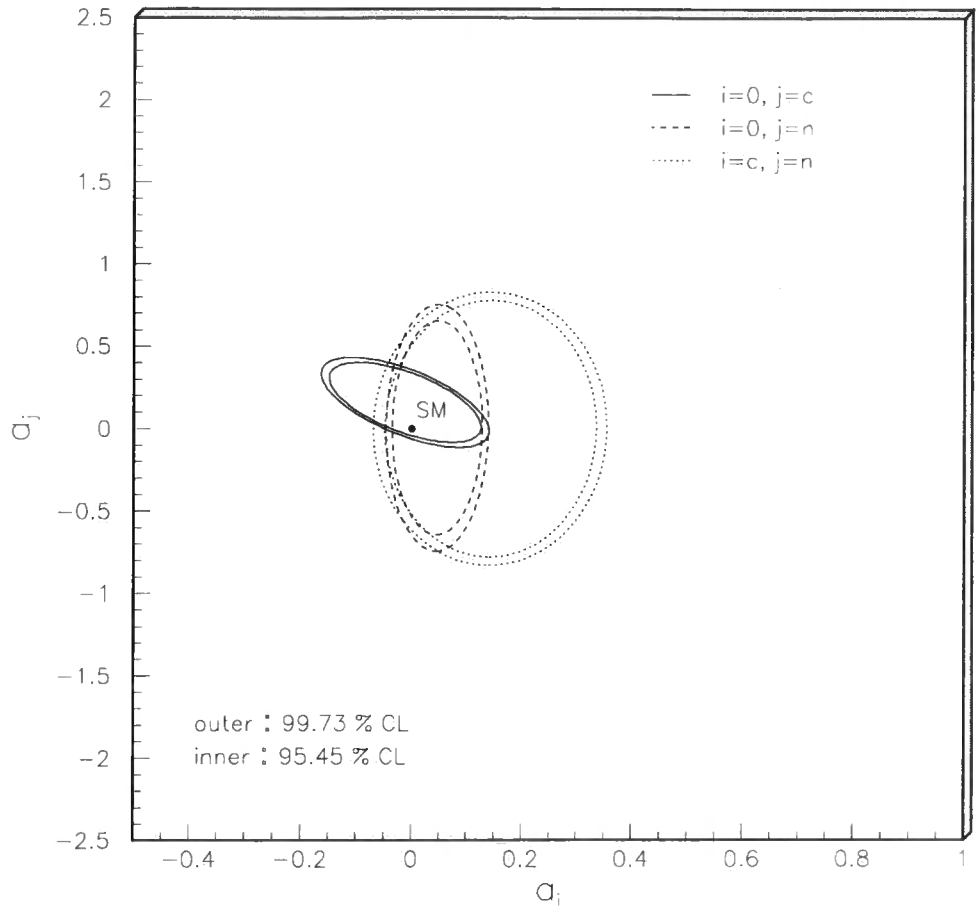

Figure 2.6: As for Figure 2.5, but with 100% beam polarisation.

Turning to the sensitivity of the $ZZ\gamma$ and $Z\gamma\gamma$ processes, Figure 2.7 shows the sensitivity of the latter to a_0 and a_c at $\sqrt{s} = 200$ GeV with $\int \mathcal{L} = 150$ pb^{-1} and unpolarised beams.[6] For comparison, we also show the corresponding $W^+W^-\gamma$ contours from Figure 2.4. The $Z\gamma\gamma$ process gives a significant improvement in sensitivity, particularly for a_c. Since the SM cross sections at this energy are comparable (see Figure 2.2), the improvement comes mainly from

[6]With our choice of photon cuts ($E_\gamma > 20$ GeV) $\sigma(ZZ\gamma)$ is essentially zero at this collision energy.

the enhanced sensitivity of the matrix element to the anomalous couplings in the $Z\gamma\gamma$ case.

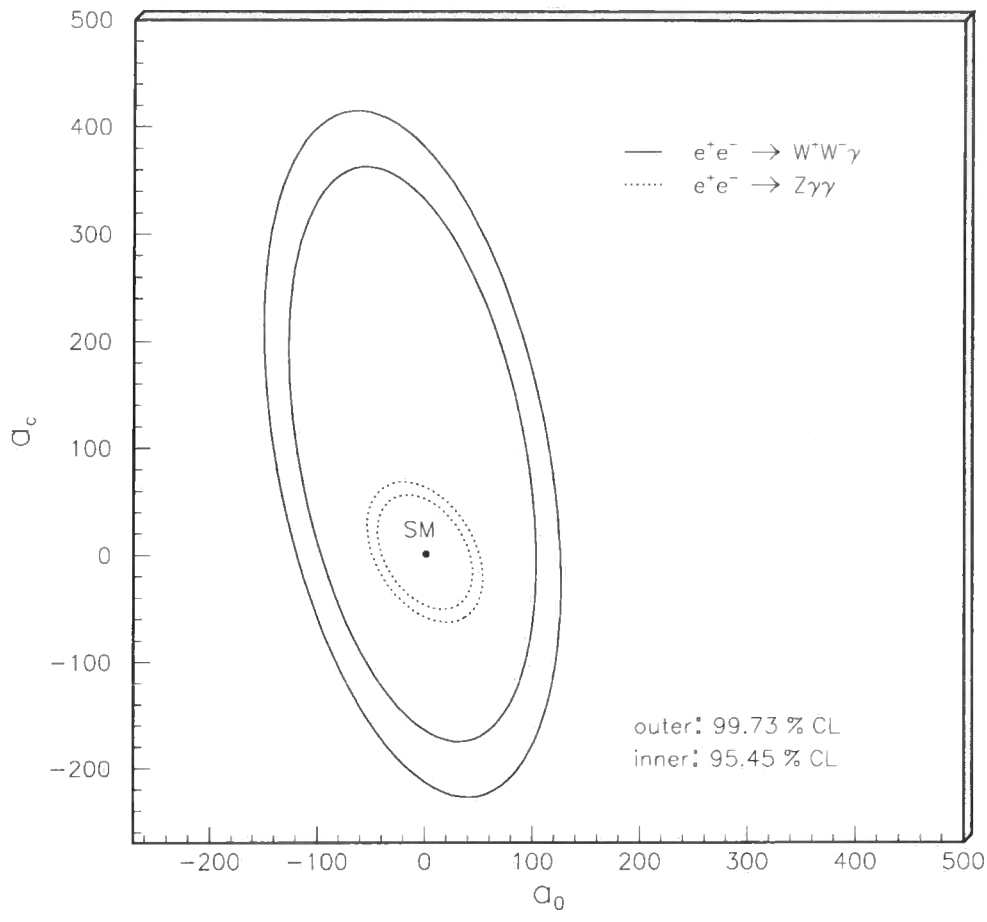

Figure 2.7: Contour plots for $+2, +3\,\sigma$ deviations from the SM $e^+e^- \to Z\gamma\gamma$ total cross section at $\sqrt{s} = 200$ GeV with $\int \mathcal{L} = 150$ pb^{-1}. For comparison, the corresponding contours for the $e^+e^- \to W^+W^-\gamma$ process from Figure 2.4 are also shown.

Finally, Figure 2.8 compares the sensitivity of all three processes to a_0 and a_c at $\sqrt{s} = 500$ GeV with $\int \mathcal{L} = 300$ fb^{-1} and unpolarised beams. The best sensitivity is now provided by the $ZZ\gamma$ process (particularly for a_c), despite the fact that it has the smallest cross section of all the three processes. Note that polarising the beams has little effect on the sensitivity of the $ZZ\gamma$ and $Z\gamma\gamma$ processes to the anomalous couplings, since the left-handed

and right-handed couplings of the Z to the electron are similar.

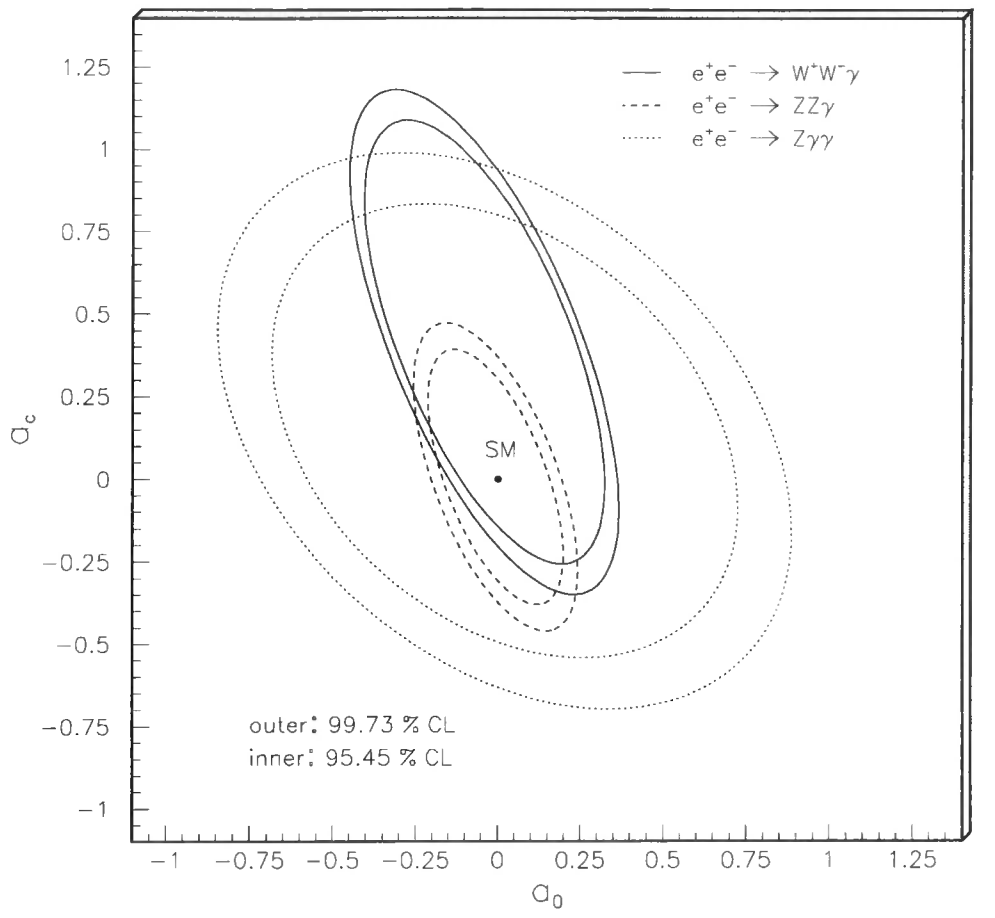

Figure 2.8: As for Figure 2.7, but for $\sqrt{s} = 500$ GeV with $\int \mathcal{L} = 300$ fb^{-1} and including also the $e^+e^- \to ZZ\gamma$ process.

From an experimental point of view it is a challenge to measure the total cross section of triple vector boson production to set direct limits on anomalous quartic couplings. Using the event generator here developed, for $e^+e^- \to W^+W^-\gamma$, the OPAL collaboration (at LEP2) was the first to present direct bounds on all three anomalous couplings [35]. This was followed by bounds from L3 (LEP2) [36] analyzing the process $e^+e^- \to Z\gamma\gamma$, and recently $e^+e^- \to W^+W^-\gamma$ [37] – again based on the comparison with our Monte Carlo program.

Clearly higher centre of mass energies and luminosities are required to exclude the possibility of anomalous quartic couplings. Among today's available colliders, the Tevatron $p\bar{p}$ collider at Fermilab seems – at first sight – to be such a machine. Unfortunately the wide range of partonic center of mass energies $\hat{s}$ makes a universal analysis very difficult, form factors are needed. The small tail of the differential cross section containing hard (high energetic) photons is the dominant source for anomalous contributions to the total cross section $p\bar{p} \to W^+W^-\gamma$.

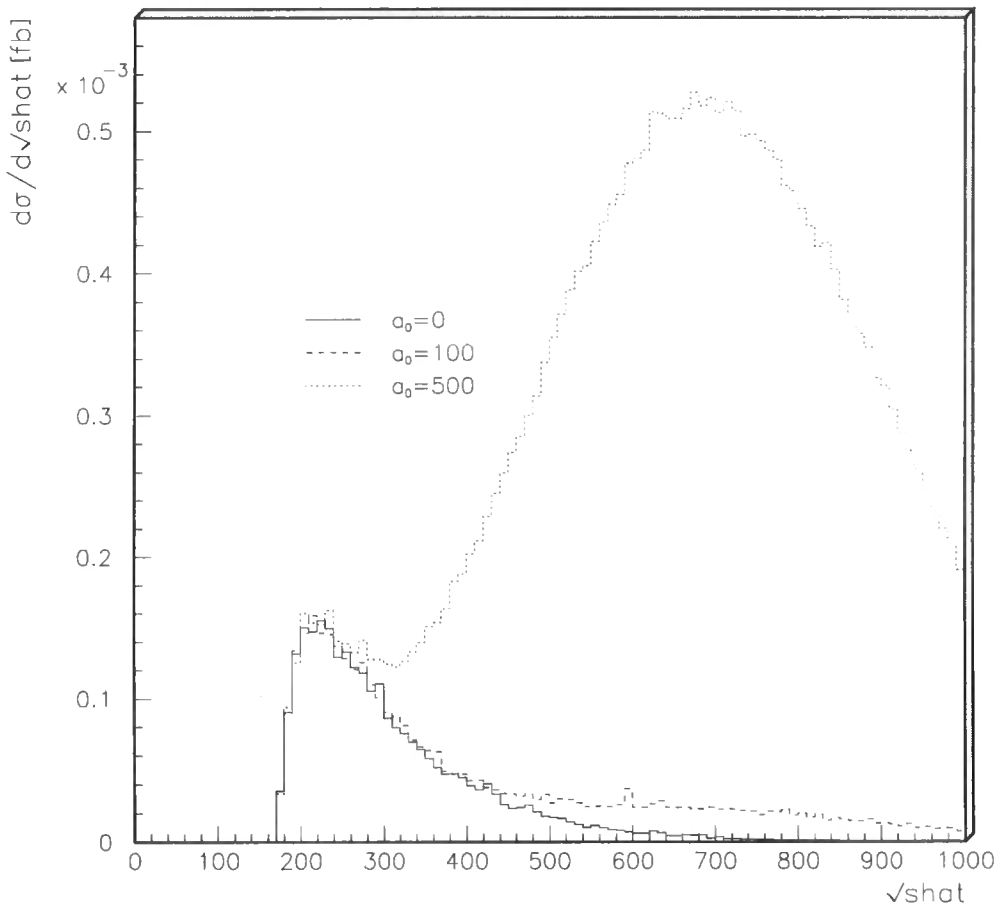

Figure 2.9: Differential cross sections $\mathrm{d}\,\sigma/\mathrm{d}\hat{s}$ for the process $p\bar{p} \to W^+W^-\gamma$ with various values for the anomalous coupling $a_o = 0$, 100, 500.

The anomalous Lagrangian described above can naturally only be understood as an *effective* low energy Lagrangian attempting to simulate new physics far below the scale Λ. As such the analysis of anomalous quartic couplings at a hadron collider becomes rather intriguing.

2.3.2 Vector Boson Mediation

The WW-fusion process $e^+e^- \to \nu_e\bar{\nu}_e\gamma\gamma$ has a very clean experimental signature of two isolated photons and missing energy. Hence we study the dependence of the $e^+e^- \to \nu_e\bar{\nu}_e\gamma\gamma$ WW-fusion cross section on the two anomalous couplings a_0 and a_c. Note that by 'WW-fusion' we mean the contribution of the Feynman diagrams shown in Fig. 2.10 to the cross section.

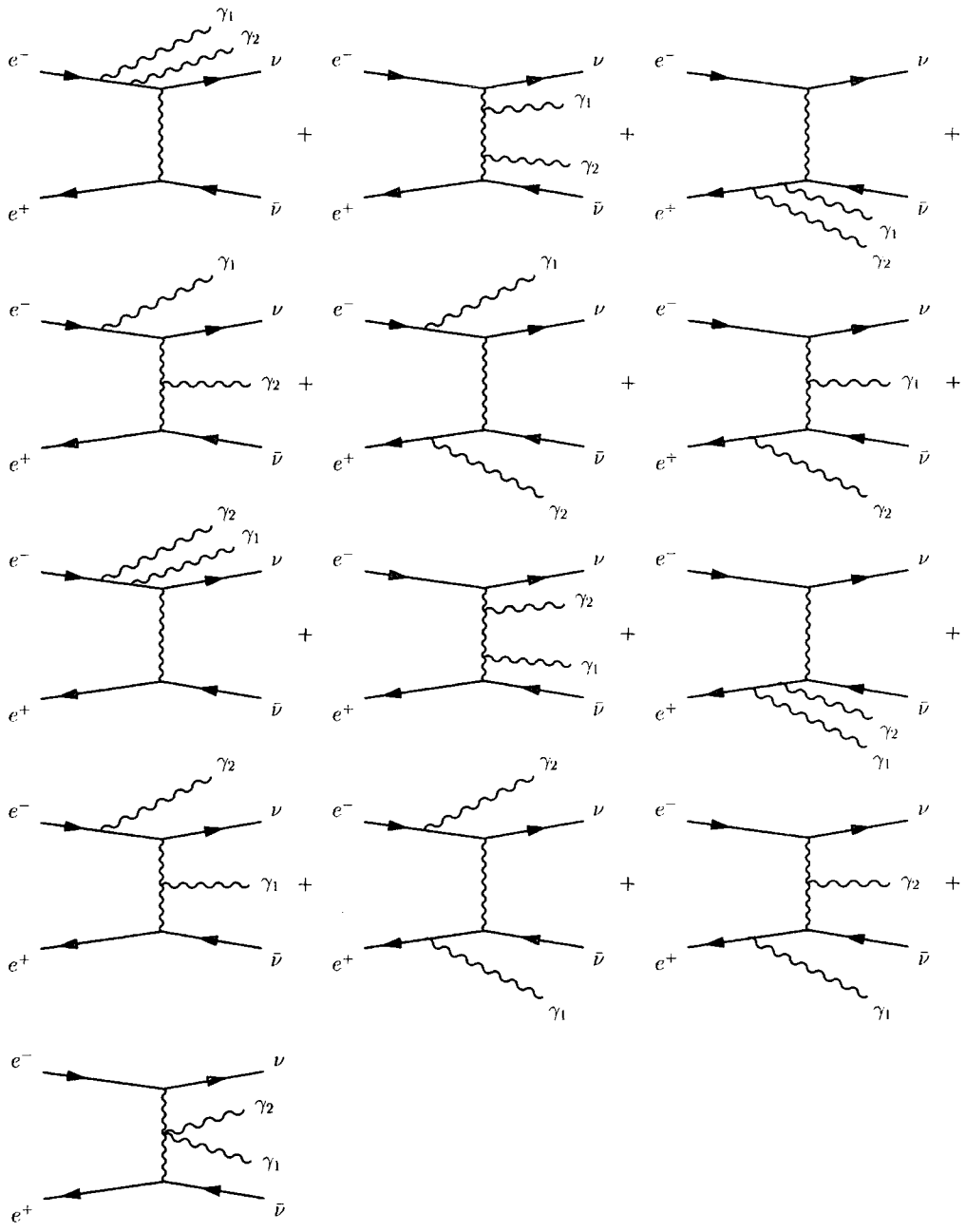

Figure 2.10: Feynman diagrams contributing to the WW-fusion $e^+e^- \to \nu_e\bar{\nu}_e\gamma\gamma$ process.

The SM calculation is based on MADGRAPH [33]. As already stated, we apply a cut on the photon energy $E_\gamma > 20$ GeV to take care of the infrared singularity, and a cut on the

photon rapidity $|\eta_\gamma| < 2$ to avoid collinear singularities.

We do not include contributions from $e^+e^- \to Z\gamma\gamma \to \nu_e\bar{\nu}_e\gamma\gamma$, which obviously do not involve the $WW\gamma\gamma$ vertices. These have been studied in Ref. [18][7]. In practice, they can be straightforwardly removed by imposing cuts on the missing mass $M_{\nu_e\bar{\nu}_e}$ ($M_{\nu_e\bar{\nu}_e} < M_Z$). Nevertheless it has to be said that the $ZZ\gamma\gamma$ vertex has the identical anomalous structure, only the overall coupling is different.

We first consider the SM cross section for the process of interest, i.e. with all anomalous couplings set to zero. Figure 2.11 shows the collider energy dependence of the $e^+e^- \to \nu_e\bar{\nu}_e\gamma\gamma$ WW-fusion cross section. In the LEP2 energy region the total cross section is O(1 fb).

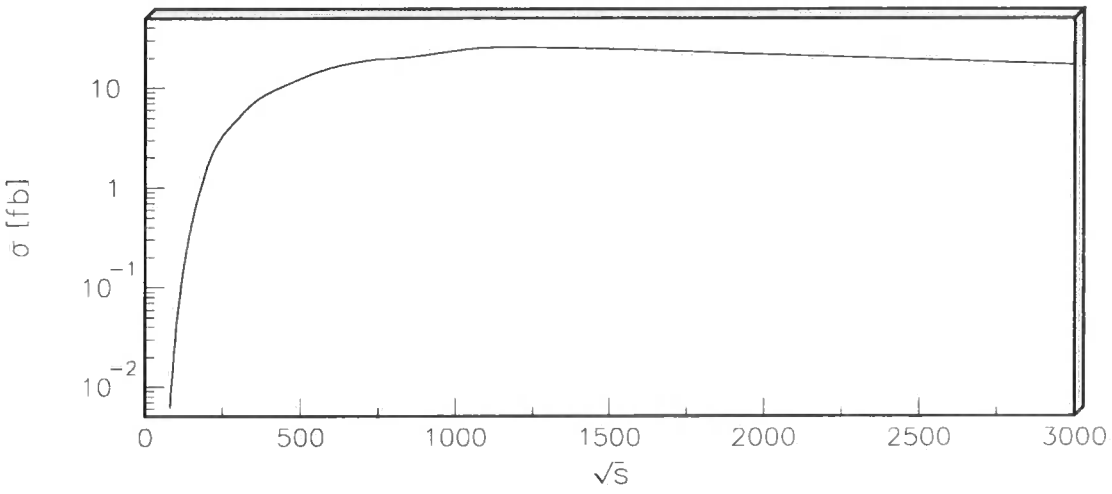

Figure 2.11: Total SM cross section for $e^+e^- \to \nu_e\bar{\nu}_e\gamma\gamma$ via WW-fusion (in fb) as a function of $\sqrt{s}$ (in GeV) with $E_\gamma > 20$ GeV and $|\eta_\gamma| < 2$.

To study any anomalous effects on the total cross section we need to consider the *correlations* between the two different anomalous contributions.

[7]Note that in the previous section [18] strictly $e^+e^- \to Z\gamma\gamma$ has been studied and for comparison with the present WW-fusion analysis the branching ratio $\Gamma(Z \to \nu_e\bar{\nu}_e)$ has to be taken into account as well. This will result in weaker bounds due to the smaller cross section.

To obtain quantitative results, we consider the experimental scenario of unpolarised e^+e^- collisions at 200 GeV with $\int \mathcal{L} = 150$ pb^{-1}.

Figure 2.12 shows the contours in the (a_0, a_c) plane that correspond to $+2, +3\,\sigma$ deviations from the SM cross section at $\sqrt{s} = 200$ GeV.

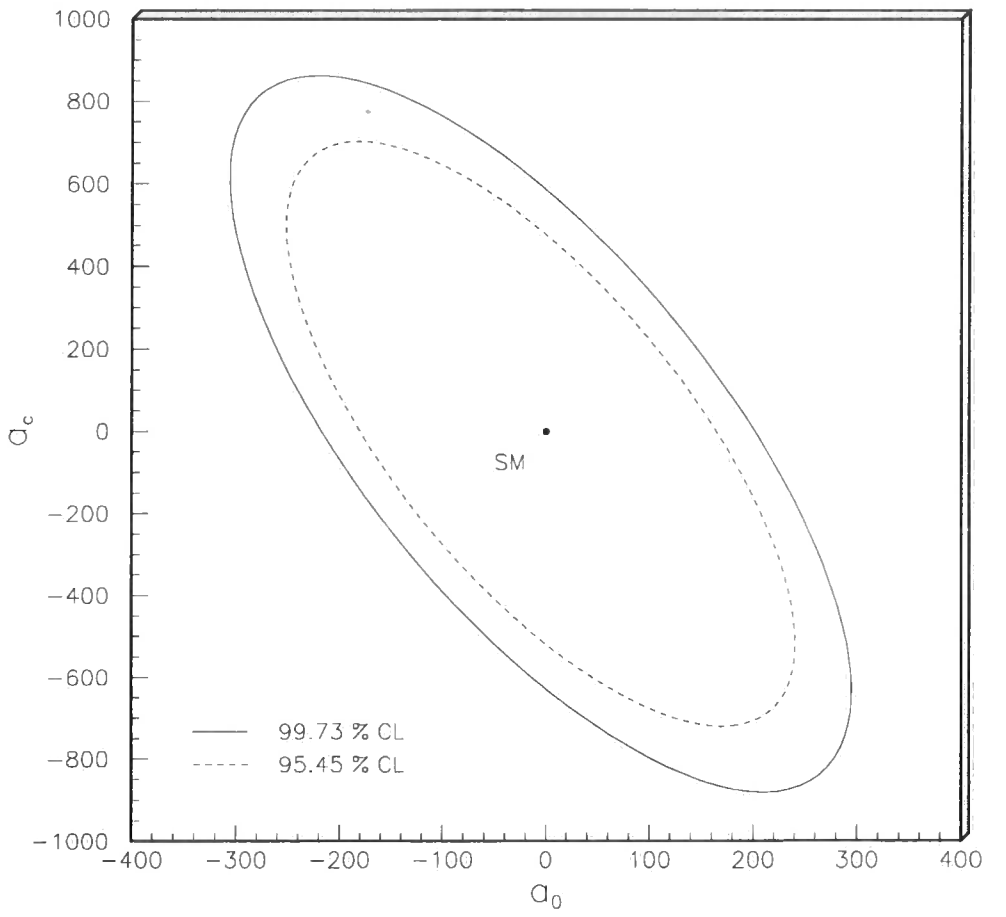

Figure 2.12: Contour plots for $+2, +3\,\sigma$ deviations from the WW-fusion SM $e^+e^- \to \nu_e\bar{\nu}_e\gamma\gamma$ total cross section at $\sqrt{s} = 200$ GeV with $\int \mathcal{L} = 150$ pb^{-1}.

From the purely phenomenological point of view the constraints obtained from the process $e^+e^- \to \nu_e\bar{\nu}_e\gamma\gamma$ via WW-fusion are not competitive with those expected from analysing $WW\gamma$ production and especially from $Z\gamma\gamma$ production. The reason is that although the

sensitivity to anomalous contributions is in general increased (i. e. lower ratio of SM-background to signal and increased phase space due to massless final states) the total cross section itself is 2 orders of magnitude smaller than those for $WW\gamma$ production or $Z\gamma\gamma$ production. Thus with the relatively small luminosity feasible for LEP2 there is little hope that advantages such as the particularly clean experimental environment will make up for the small cross section, and in that case we would expect the tighter bounds on the anomalous parameter to be obtained from analysing $Z\gamma\gamma$ production.

Nevertheless, since only massless particles are produced, experimental data from basically any LEP2 centre of mass energy can be used to increase the overall integrated luminosity, and since the process *is* highly sensitive to anomalous couplings there is a chance that this process could actually in practice be leading to the tightest bounds. Of course in the end this can only be decided by a proper experimental data analysis.

For a future linear collider, with for example $\sqrt{s} = 500$ GeV, the process $e^+e^- \to \nu_e\bar{\nu}_e\gamma\gamma$ becomes even less competitive, since at that energy the enlarged phase space of massless particles becomes even less important. Note also that at this energy the possibility of producing longitudinally polarised W, Z bosons does increase the sensitivity to anomalous couplings considerably [18]. In the WW-fusion process we do not have that opportunity since the W bosons are bound to be 'internal' particles with no preferred polarization state.

2.4 Conclusions

We have investigated the sensitivity of the processes $e^+e^- \to W^+W^-\gamma$, $ZZ\gamma$, $Z\gamma\gamma$ and $e^+e^- \to \nu_e\bar{\nu}_e\gamma\gamma$ to genuine anomalous quartic couplings (a_0, a_c, a_n) at the canonical centre-of-mass energies $\sqrt{s} = 200$ GeV (LEP2) and 500 GeV (LC). Key features in determining the sensitivity for a given process and collision energy, apart from the fundamental process dynamics, are the available photon energy E_γ, the ratio of anomalous diagrams to SM 'background' diagrams, and the polarisation state of the weak bosons [28].

At $\sqrt{s} = 200$ GeV the process $e^+e^- \to Z\gamma\gamma$ leads to the tightest bounds on the contour

of (a_0, a_c), while the process $e^+e^- \to W^+W^-\gamma$ is needed to set bounds also on a_n. Note that the contours of (a_0, a_n) and (a_c, a_n) can then be improved using the knowledge of the tighter bounds on the contour of (a_0, a_c) from $Z\gamma\gamma$ production. At this energy $Z\gamma\gamma$ benefits kinematically from producing only one massive boson, which leaves more energy for the photons as well as having fewer 'background' diagrams. On the other hand $W^+W^-\gamma$ production at this energy suffers from the lack of phase space available for energetic photon emission, although this is partially compensated by the production of longitudinal bosons, which gives rise to higher sensitivity to the anomalous couplings.

At $\sqrt{s} = 500$ GeV, the effects mentioned above conspire in a somewhat different way. All three processes are now well above their threshold, and hence the availability of phase space for energetic photons is less of an issue. The importance of the longitudinal polarisation of the massive bosons increases and even though the same number of diagrams contributes to $ZZ\gamma$ production as to $Z\gamma\gamma$ production, far tighter bounds on the anomalous couplings can be expected from the former process. The production of longitudinally polarised bosons is comparable in the $W^+W^-\gamma$ and $ZZ\gamma$ processes, but the higher signal to background ratio for the latter leads to a better sensitivity to a_0 and a_c.[8]

The ability to polarise the beams leads to a significant improvement in the sensitivity of the $W^+W^-\gamma$ process, since about a third of the contributing diagrams are removed. With polarised beams the tightest bounds now come from this process. The sensitivity of the $e^+e^- \to ZZ\gamma$ process is hardly affected by beam polarisation.

The 500 GeV comparison emphasises the importance of the longitudinal polarisation states of the massive bosons ($ZZ\gamma$ and $Z\gamma\gamma$ are more or less comparable otherwise). This suggests that the $e^+e^- \to W^+W^-Z$ process should be more sensitive to anomalous couplings than $e^+e^- \to W^+W^-\gamma$, since all three final-state particles can be longitudinally polarised. With the expected linear collider luminosity, the somewhat smaller cross section should not be an issue, and the ratio of background to signal diagrams is the same as for $W^+W^-\gamma$ production. Unfortunately this process is only sensitive to a_n.[9] Furthermore, since there is no photon in the final state, 4-dimensional operators can also contribute to anomalous couplings (i.e. an

[8] Here again $W^+W^-\gamma$ is still needed for investigating a_n.

[9] The a_0 and a_c couplings stem from the $VV\gamma\gamma$ vertex.

anomalous W^+W^-ZZ vertex) and the analysis becomes significantly more complicated.

The constraints obtained from the process $e^+e^- \to \nu_e\bar{\nu}_e\gamma\gamma$ via WW-fusion are not competitive with those expected from analysing $WW\gamma$ production and especially from $Z\gamma\gamma$ production.

Finally it is important to emphasise that in our study we have only considered 'genuine' quartic couplings from new six-dimensional operators. We have assumed that all other anomalous couplings are zero, including the trilinear ones. Since the number of possible couplings and correlations is so large, it is in practice very difficult to do a combined analysis of *all* couplings simultaneously. In fact, it is not too difficult to think of new physics scenarios in which effects are only manifest in the quartic interactions. One example would be a very heavy excited W resonance produced and decaying as in $W^+\gamma \to W^* \to W^+\gamma$.
In principle, any non-zero trilinear coupling could affect the limits obtained on the quartic couplings. For example, in equation (2.4) we showed explicitly how a non-zero trilinear coupling (λ) can generate an anomalous $WW\gamma\gamma$ quartic interaction to compete with the 'genuine' ones that we have considered. The (dimensionless) strength of the former is $eg\lambda$, while for the latter it is $e^2 a_i \langle E_{ext.}\rangle\langle E_{int.}\rangle/\Lambda^2$, where $E_{ext.}$ and $E_{int.}$ are the typical energy scales of the photons entering the vertex. (Here we are considering, as a specific example, the $e^+e^- \to W^+W^-\gamma$ process.) Since $\Lambda = M_W$, $\langle E_{ext.}\rangle \sim 25$ GeV and $E_{int.} \sim [5\sqrt{s} + 4(\sqrt{s} - \langle E_{ext.}\rangle)]/9 \sim 190$ GeV , both for $\sqrt{s} = 200$ GeV, we see immediately that the relative contributions of the two types of couplings are in the approximate ratio $3\lambda : a_i$. Now, at LEP2 upper limits on trilinear couplings like λ are already $\mathcal{O}(0.1)$ [25, 26]. In contrast, we have shown that the limits achievable on the a_i are $\mathcal{O}(100)$. Hence we already know that the anomalous trilinear couplings have a minimal impact on our analysis.
The same argument holds at higher collider energies. The limits on the trilinear couplings will always be so much smaller than those on the quartic couplings, that they can safely be ignored in studies of the latter.

Chapter 3

Radiation Zeros

3.1 Introduction

In certain high–energy scattering processes involving charged particles and the emission of one or more photons, the scattering amplitude vanishes for particular configurations of the final–state particles. Such configurations are known as *radiation zeros* or *null zones*. The study of these radiation zeros (RAZ) dates back to the late 1970s [38] , where they were identified in the process $q\bar{q}' \to W\gamma$ as points in phase-space for which the total cross section vanishes.

Today [39, 40] it is understood that the zeros are due to a cancellation which can be regarded as a destructive interference of radiation patterns induced by the charge of the participating particles. The fact that gauge symmetry is a vital ingredient for the cancellation to occur means that radiation zeros can be used to probe physics beyond the standard model. For example, 'anomalous' electroweak gauge boson couplings destroy the delicate cancellations necessary for a zero to occur.

In recent years there have been many studies exploring the phenomenological aspects of radiation zeros, see for example Ref. [39] and references therein. Following the work on physical radiation zeros (e. g. within the physical phase space of the process such as $u\bar{d} \to W^+\gamma$ [38]) unphysical radiation zeros have been found on the edge of phase space in the process $e^+\nu \to W^+\gamma$ [41]. Investigating the process $q\bar{q}' \to W\gamma\gamma$ it has been found [42] that the zero of the process $q\bar{q}' \to W\gamma$ survives for the case that the two final state photons

are collinear. All those zeros have been classified as *exact* zeros, i. e. the cross section vanishes identically, the scattering amplitude is strictly zero.

The question of approximate zeros, i.e. zeros where the cross section exhibits a dramatic drop, but no true zero has also been addressed [43, 40, 44] in processes like $p\bar{p}, pp \to WW, WZ, ZZ$. It has been found that the zero remains exact for all transverse helicity amplitudes whereas for the longitudinal amplitudes (i. e. the ones associated with the mass of the gauge boson) strong gauge cancellations are still taking place but the zero is no longer exact, in fact it becomes energy dependent.

On top of all this, so-called exotic zeros haven been studied, such as zeros originating from the emission of gluons instead of photons [44, 45]. There is little hope of ever experimentally detecting those zeros because they are washed out by the sum and/or average of the colour charge as well as being spoiled by hadronisation effects. Even more living up to their name are zeros caused by the emission of massless supersymmetric particles such as photinos and sphotinos [46] as well as szeros and xeros [47].

Only recently a whole new category of radiation zeros, so-called TypeII radiation zeros or planar zeros, were established by Heyssler and Stirling [48]. Demanding the whole scattering process to take place within the same plane it becomes possible to overcome the theorem of equal charged particles, which requires the particles taking part in the scattering process to have all either positive or negative charge [40].

Experimental evidence for the zeros predicted in [38] has also been found at the Fermilab Tevatron $p\bar{p}$ collider [49]. As already mentioned, the classic process for radiation zeros in high-energy hadron-hadron collisions is $q\bar{q}' \to W\gamma$, where the zero occurs in a 'visible' region of phase space, i.e. away from the phase-space boundaries. It is natural to extend the analysis to more complicated processes involving multiple gauge boson production. At the upgraded Tevatron $p\bar{p}$ and LHC pp colliders, the rates for such events can be quite large.

In this chapter we study in detail the $q\bar{q} \to WW\gamma$ process, and identify the circumstances under which radiation zeros occur. Unlike the $W\gamma$ process, it is not possible to write down a simple analytic expression for the matrix element squared. However, making use of the

soft-photon approximation does allow the zeros to be identified analytically, and a numerical calculation of the full matrix element confirms that although the actual zeros disappear for non-zero photon energies, deep dips do persist for all relevant photon energies. The dips result from delicate cancellations between the various standard model photon emission diagrams, and are 'filled in' by contributions from non-standard gauge boson couplings. We illustrate this explicitly using anomalous quartic couplings.

The chapter is organised as follows. In the following section we review the 'classic' radiation-zero process, $q\bar{q}' \to W\gamma$. In Section 3.3 we extend the analysis to $W^+W^-\gamma$ production, first using analytic methods in the soft-photon limit. We carefully distinguish between photons emitted in the W^+W^- production process and those emitted in the $W \to f\bar{f}$ decay process. We then extend the analysis to non-soft photons using a numerical calculation of the exact matrix element. In Section 3.4 we show how anomalous quartic couplings 'fill in' the dips caused by the radiation zeros. Finally, Section 3.5 presents our summary and conclusions.

3.2 Radiation Zeros in $W\gamma$ Production

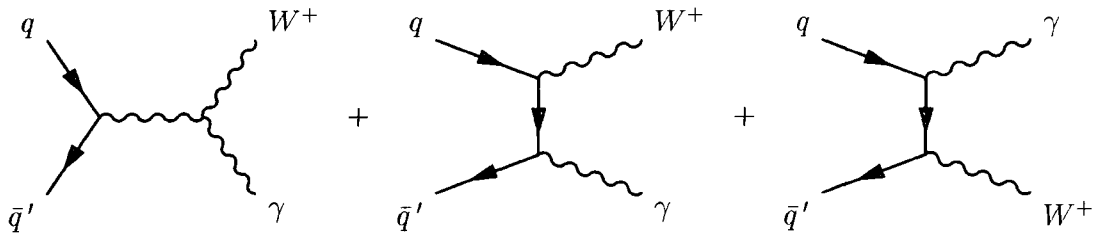

Figure 3.1: Diagrams contributing to the process $q\bar{q}' \to W^+\gamma$.

The classic scattering process which exhibits a radiation zero is $q\bar{q}' \to W^+\gamma$. The amplitude for this can be calculated analytically — there are three Feynman diagrams, shown in Fig. 3.1. With momenta labelled as

$$\begin{aligned} q(p_1) + \bar{q}'(p_2) &\to W^+(k^+) + \gamma(k) \\ W^+(k^+) &\to \nu_l(r_4) + l^+(r_3)\,, \end{aligned} \tag{3.1}$$

the matrix element is

$$\begin{aligned} \mathcal{M} &= \frac{2\,ieg}{\sqrt{2}\,p_2\cdot k}\,\mathcal{C}\,\{t(r_4,p_2)\,s(k,p_1)\,[s(p_1,r_3)\,t(p_1,p_2)\,+\,s(k,r_3)\,t(p_2,k)]\} \\ \mathcal{C} &= \frac{1}{p^2-M_W^2}+\frac{Q_q}{(p_1-k)^2}\,, \end{aligned} \tag{3.2}$$

where $p = p_1 + p_2 = k^+ + k$. Here we have used the spinor technique of Ref. [9], with photon polarisation vector[1] $\epsilon^*_{+\mu}(k) = (1/\sqrt{4\,p_2\cdot k})\;\bar{u}_+(k)\gamma_\mu u_+(p_2)$. The spinor products are defined by

$$s(p_i,p_j) = \bar{u}_+(p_i)u_-(p_j), \qquad t(p_i,p_j) = \bar{u}_-(p_i)u_+(p_j)\,, \tag{3.3}$$

and all fermion masses are set to zero.

The cross section $\sigma \sim |\mathcal{M}|^2$ therefore vanishes when $\mathcal{C} = 0$, i.e.

$$\frac{1}{p^2-M_W^2} = \frac{Q_q}{2\,p_1\cdot k}\,. \tag{3.4}$$

We next introduce the momentum four-vectors

$$\begin{aligned} {p_1}^\mu &= (E,0,0,E) \\ {p_2}^\mu &= (E,0,0,-E) \\ {k_+}^\mu &= \left(\frac{4\,E^2+M_W^2}{4\,E},\,\frac{4\,E^2-M_W^2}{4\,E}\,\sin\Theta\,,\,0\,,\,\frac{4\,E^2-M_W^2}{4\,E}\,\cos\Theta\right) \\ k^\mu &= \left(\frac{4\,E^2-M_W^2}{4\,E},\,-\frac{4\,E^2-M_W^2}{4\,E}\,\sin\Theta\,,\,0\,,\,-\frac{4\,E^2-M_W^2}{4\,E}\,\cos\Theta\right)\,, \end{aligned} \tag{3.5}$$

where Θ is the angle between the incoming quark and the W^+, $\theta_\gamma = \Theta + \pi$, and E is the beam energy of the scattering particles. Substituting into (3.4) gives the condition for a radiation zero [38]:

$$\cos\Theta \;=\; -1 \,+\, 2\,Q_q\,. \tag{3.6}$$

[1]The expression in (3.2) actually corresponds to a positive helicity photon. For a negative helicity photon, a similar expression is obtained. Both amplitudes exhibit the same radiation zero.

In other words, the cross section vanishes when the photon is produced at an angle[2]

$$\cos\theta_\gamma{}^{RAZ} = 1 - 2Q_q = -\frac{1}{3} \qquad \text{for } q = u\,. \tag{3.7}$$

$$\tag{3.8}$$

The angle θ_γ for which the cross section vanishes is independent of the photon energy, in particular it is unchanged in the soft-photon limit, $k^\mu \to 0$, which is realised as the beam energy decreases to its threshold value, $2E \to M_W$. In this limit we can use the *eikonal approximation* to locate the position of the zero. Since for more complicated processes we may only be able to obtain an analytic expression in this approximation, it is worth repeating the above calculation in the soft-photon limit to check that we do indeed obtain the same result.

We start from the matrix element for the process $q\bar{q}' \to W^+$:

$$i\mathcal{M}_0 = \bar{u}_-(p_2)\left(i\frac{g}{\sqrt{2}}\right)\gamma^\nu\, u_-(p_1)\,\epsilon^*_\nu(k_+)\,. \tag{3.9}$$

In the soft-photon limit one can neglect the momentum k in the numerators of the internal fermion propagators, in the $WW\gamma$ vertex, and in the overall energy-momentum conservation constraint (i.e. $p = k_+ = p_1 + p_2$), which leads to

$$\mathcal{M} = (-e)\,\mathcal{M}_0\,\epsilon^*_\mu(k)\,j^\mu \tag{3.10}$$

where the eikonal factor j^μ is given by

$$j^\mu = Q_q\frac{{p_1}^\mu}{p_1\cdot k} + (1-Q_q)\frac{{p_2}^\mu}{p_2\cdot k} - \frac{{k_+}^\mu}{k_+\cdot k}\,. \tag{3.11}$$

The three terms in j^μ come from the $u-$, $t-$ and $s-$channel diagrams respectively or, equivalently, a soft photon radiated off the incoming quark, incoming antiquark, and outgoing W^+. Note that gauge invariance implies $k_\mu \cdot j^\mu = 0$.

Radiation zeros are now obtained for $\epsilon^*(k)\cdot j = 0$. Choosing

$$\begin{aligned} k^\mu &= E_\gamma\,(1, \sin\theta_\gamma, 0, \cos\theta_\gamma) \\ \epsilon_1^\mu &= (0,0,1,0) \\ \epsilon_2^\mu &= (0, -\cos\theta_\gamma, 0, \sin\theta_\gamma) \end{aligned} \tag{3.12}$$

[2]A similar condition holds for the process $q\bar{q}' \to W^-\gamma$: $\cos\theta_\gamma{}^{RAZ} = 1 + 2Q_q = \frac{1}{3}$, for $q = d$.

gives

$$\epsilon^*(k) \cdot j = -Q_q \frac{\sin\theta_\gamma}{1-\cos\theta_\gamma} + (1-Q_q)\frac{\sin\theta_\gamma}{1+\cos\theta_\gamma} = 0\,, \tag{3.13}$$

or equivalently

$$\cos\theta_\gamma{}^{RAZ} = 1 - 2Q_q\,. \tag{3.14}$$

This is exactly the same condition as (3.7), as expected.

3.3 Radiation Zeros in $W^+W^-\gamma$ Production

In this section we extend the analysis to investigate radiation zeros in the process $q\bar{q} \to W^+W^-\gamma \to f_1\bar{f}_2 f_3\bar{f}_4\gamma$. The contributing Feynman diagrams are shown in Fig. 3.2. Note that both γ and Z exchange are included in the $s-$channel diagrams.

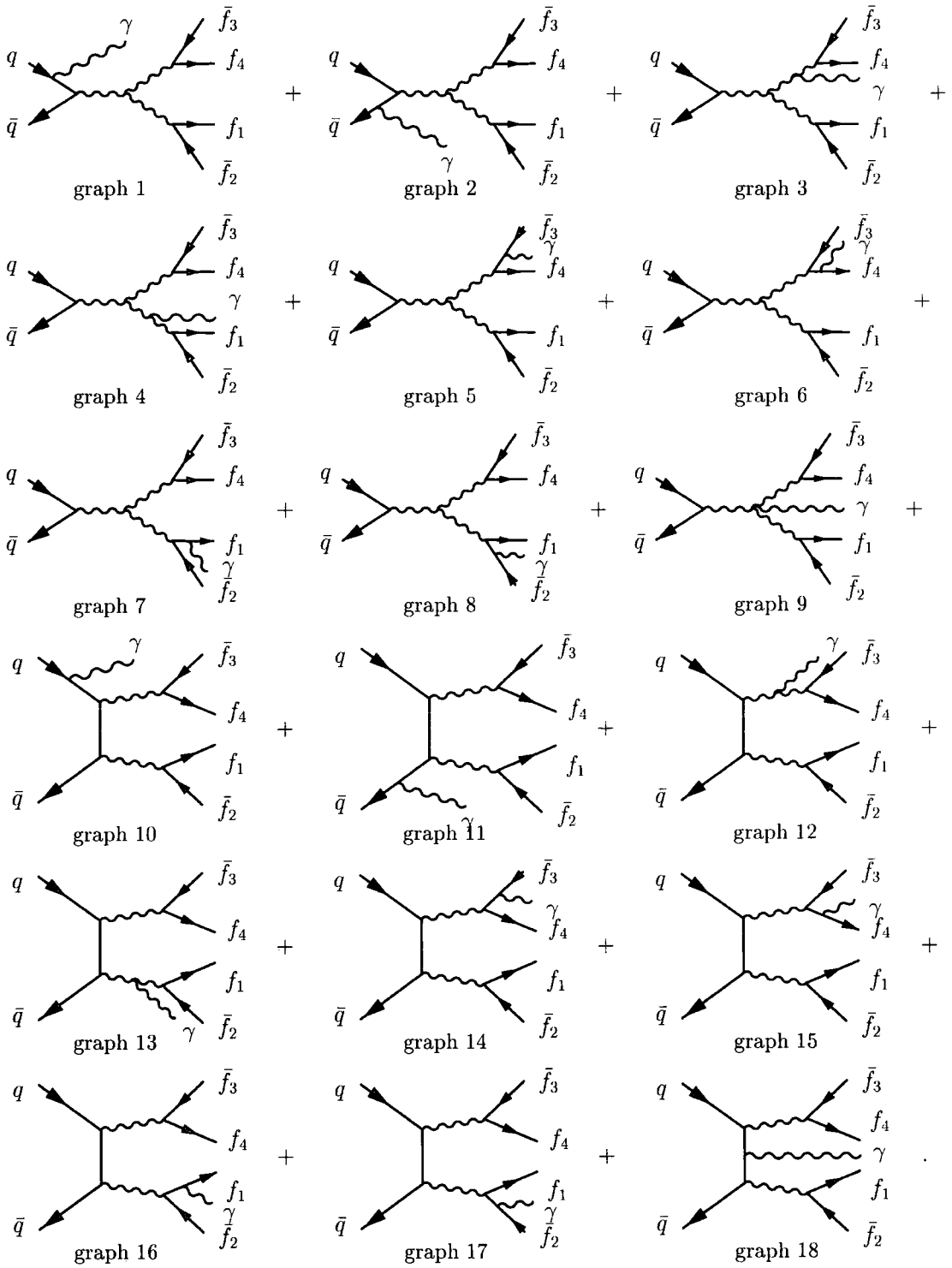

Figure 3.2: Feynman diagrams for the process $q\bar{q} \to W^+W^-\gamma \to f_1\bar{f}_2\bar{f}_3f_4\gamma$.

3.3.1 The soft photon case

We first calculate the matrix element in the soft-photon approximation. Once again the matrix element can be factorized:

$$\mathcal{M} = (-e)\, \mathcal{M}_0\, \epsilon^*_\mu(k)\, j^\mu \tag{3.15}$$

where $\mathcal{M}_0$ is the $(q\bar{q} \to W^+W^-)$ matrix element without photon radiation, and the eikonal current is

$$\begin{aligned} -j^\mu \;=\; & \left(Q_3 \frac{{r_3}^\mu}{r_3 \cdot k} + (1-Q_3) \frac{{r_4}^\mu}{r_4 \cdot k} - \frac{{k_+}^\mu}{k_+ \cdot k} \right) \frac{k_+^2 - \overline{M}^2}{(k_+ + k)^2 - \overline{M}^2} \\ & - \left(Q_1 \frac{{r_1}^\mu}{r_1 \cdot k} + (1-Q_1) \frac{{r_2}^\mu}{r_2 \cdot k} - \frac{{k_-}^\mu}{k_- \cdot k} \right) \frac{k_-^2 - \overline{M}^2}{(k_- + k)^2 - \overline{M}^2} \\ & + \left(-Q_q \frac{{p_1}^\mu}{p_1 \cdot k} - Q_{\bar{q}} \frac{{p_2}^\mu}{p_2 \cdot k} + \frac{{k_+}^\mu}{k_+ \cdot k} - \frac{{k_-}^\mu}{k_- \cdot k} \right) \\ = \; & D^{+\mu} - D^{-\mu} + P^\mu \end{aligned} \tag{3.16}$$

with $Q_i = |Q_i| > 0$, $Q_{\bar{q}} = -Q_q$, r_i the momenta of the final-state f_i fermions, $k_\pm$ the momenta of the $W^\pm$ and $\overline{M} = M_W - i\Gamma_W/2$. This result is appropriate for both right-handed and left-handed quark scattering, although $\mathcal{M}_0$ is of course different in the two cases. In deriving (3.16) we have made use of the partial fraction

$$\frac{1}{k_\pm^2 - \overline{M}^2} \frac{1}{(k_\pm + k)^2 - \overline{M}^2} = \frac{1}{2\, k_\pm \cdot k} \left(\frac{1}{k_\pm^2 - \overline{M}^2} - \frac{1}{(k_\pm + k)^2 - \overline{M}^2} \right) \tag{3.17}$$

to split the contributions involving photon emission from the final-state W bosons into two pieces corresponding to photon emission *before* and *after* the boson goes on mass shell [50, 51]. This is illustrated in Fig. 3.3.

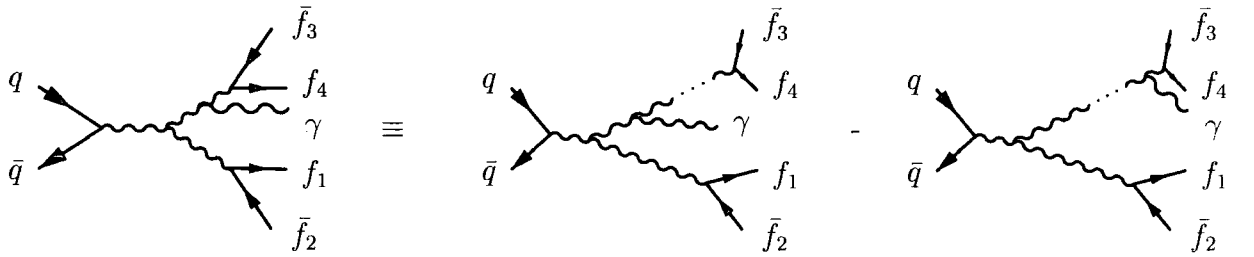

Figure 3.3: Partial fractioning of photon emission off a final-state W boson.

To obtain the cross section one has to integrate over the virtual momenta $k_\pm$:

$$\sigma \sim \int dk_+^2\, dk_-^2 \sum |\mathcal{M}|^2 \simeq \left(\frac{\pi}{M_W \Gamma_W}\right)^2 \sum |\widetilde{\mathcal{M}}_0|^2\, e^2\, \mathcal{I} \tag{3.18}$$

with

$$\begin{aligned} \mathcal{M}_0 &= \widetilde{\mathcal{M}}_0 \frac{1}{k_+^2 - \overline{M}^2} \frac{1}{k_-^2 - \overline{M}^2} \\ \mathcal{I} &\equiv \left(\frac{M_W \Gamma_W}{\pi}\right)^2 \int dk_+^2\, dk_-^2\, (-j \cdot j^*) \frac{1}{|k_+^2 - \overline{M}^2|^2} \frac{1}{|k_-^2 - \overline{M}^2|^2}\,, \end{aligned} \tag{3.19}$$

where we have put the W bosons effectively on their mass shell ($k_\pm^2 = M_W^2$). Performing the $k_\pm^2$ integrals by completing the contours in an appropriate half plane and using Cauchy's theorem eventually leads to

$$\mathcal{I} = |P|^2 + |D^+|^2 + |D^-|^2 - 2\mathrm{Re}\,[D^+ D^{-*}] + 2\mathrm{Re}\,[P(D^{+*} - D^{-*})]\,, \tag{3.20}$$

with

$$
\begin{aligned}
|P|^2 &= Q_q^2\,\widehat{p_1p_1} + Q_{\bar q}^2\,\widehat{p_2p_2} + \widehat{k_+k_+} + \widehat{k_-k_-} + 2\,Q_qQ_{\bar q}\,\widehat{p_1p_2} \\
&\quad -2\,Q_q\,\widehat{p_1k_+} + 2\,Q_{\bar q}\,\widehat{p_2k_-} + 2\,Q_q\,\widehat{p_1k_-} - 2\,Q_{\bar q}\,\widehat{p_2k_+} - 2\,\widehat{k_+k_-} \\
|D^+|^2 &= Q_3^2\,\widehat{r_3r_3} + (1-Q_3)^2\,\widehat{r_4r_4} + \widehat{k_+k_+} + 2\,Q_3(1-Q_3)\,\widehat{r_3r_4} \\
&\quad -2\,Q_3\,\widehat{r_3k_+} - 2\,(1-Q_3)\,\widehat{r_4k_+} \\
|D^-|^2 &= Q_1^2\,\widehat{r_1r_1} + (1-Q_1)^2\,\widehat{r_2r_2} + \widehat{k_-k_-} + 2\,Q_1(1-Q_1)\,\widehat{r_1r_2} \\
&\quad -2\,Q_1\,\widehat{r_1k_-} - 2\,(1-Q_1)\,\widehat{r_2k_-} \\
2\mathrm{Re}\,[D^+\,D^{-*}] &= -2\,\chi_{+-}\Big(Q_1Q_3\,\widehat{r_1r_3} + Q_1(1-Q_3)\,\widehat{r_1r_4} - Q_1\,\widehat{r_1k_+} \\
&\quad +(1-Q_1)Q_3\,\widehat{r_2r_3} + (1-Q_1)(1-Q_3)\,\widehat{r_2r_4} \\
&\quad -(1-Q_1)\,\widehat{r_2k_+} - Q_3\,\widehat{r_3k_-} - (1-Q_3)\,\widehat{r_4k_-} + \widehat{k_+k_-}\Big) \\
2\mathrm{Re}\,[P(D^{+*} - D^{-*})] &= 2\,\chi_+\Big(- Q_qQ_3\,\widehat{r_3p_1} - Q_{\bar q}Q_3\,\widehat{r_3p_2} + \widehat{k_+k_-} + Q_3\,\widehat{r_3k_+} - Q_3\,\widehat{r_3k_-} \\
&\quad -(1-Q_3)Q_q\,\widehat{r_4p_1} - (1-Q_3)Q_{\bar q}\,\widehat{r_4p_2} - \widehat{k_+k_+} \\
&\quad +(1-Q_3)\,\widehat{r_4k_+} - (1-Q_3)\,\widehat{r_4k_-} + Q_q\,\widehat{k_+p_1} + Q_{\bar q}\,\widehat{k_+p_2}\Big) \\
&\quad -2\chi_-\Big(- Q_1Q_q\,\widehat{r_1p_1} - Q_1Q_{\bar q}\,\widehat{r_1p_2} + Q_1\,\widehat{r_1k_+} + \widehat{k_-k_-} - Q_1\,\widehat{r_1k_-} \\
&\quad -(1-Q_1)Q_q\,\widehat{r_2p_1} - (1-Q_1)Q_{\bar q}\,\widehat{r_2p_2} + (1-Q_1)\,\widehat{r_2k_+} \\
&\quad -(1-Q_1)\,\widehat{r_2k_-} + Q_q\,\widehat{k_-p_1} + Q_{\bar q}\,\widehat{k_-p_2} - \widehat{k_-k_+}\Big)\,,
\end{aligned}
\tag{3.21}
$$

with $k_\pm^2 = M_W^2$. The 'antennae' appearing in this expression are defined by

$$
\widehat{p_1p_2} = \frac{p_1\cdot p_2}{p_1\cdot k\;\; p_2\cdot k} \tag{3.22}
$$

and the profile functions [50, 51] by

$$\begin{aligned}\chi_{+-} &= \frac{[(k\cdot k_+)(k\cdot k_-)+(\Gamma_W M_W)^2](\Gamma_W M_W)^2}{[(k\cdot k_+)^2+(\Gamma_W M_W)^2][(k\cdot k_-)^2+(\Gamma_W M_W)^2]} \\ \chi_{+} &= \frac{(\Gamma_W M_W)^2}{(k\cdot k_+)^2+(\Gamma_W M_W)^2} \\ \chi_{-} &= \frac{(\Gamma_W M_W)^2}{(k\cdot k_-)^2+(\Gamma_W M_W)^2} \quad .\end{aligned} \tag{3.23}$$

This result agrees with that given in Ref. [52], where the distribution of soft radiation accompanying W^+W^- production in e^+e^- annihilation was studied. The profile functions have two important limits that have to be distinguished carefully.

(a) $E_\gamma \ll \Gamma_W \ll M_W$

The photon is far softer than the W is off mass shell, which leads to $\chi_{+-} = \chi_- = \chi_+ = 1$. The timescale for photon emission is much longer than the W lifetime, and so the photon 'sees' only the external fermions. The whole current contributes and rather than solving $\mathcal{I} = 0$ to find radiation zeros we can determine the values of k^μ for which

$$\epsilon^*(k)\cdot j = 0\,. \tag{3.24}$$

To simplify the calculation slightly we consider only *leptonic* decays of the W bosons[3]. The eikonal current then reduces to[4]

$$-j^\mu = \frac{r_3^\mu}{r_3\cdot k} - \frac{r_1^\mu}{r_1\cdot k} - Q_q\left(\frac{p_1^\mu}{p_1\cdot k} - \frac{p_2^\mu}{p_2\cdot k}\right)\,. \tag{3.25}$$

Here, r_3 is the four-momentum of the outgoing antilepton with charge $+1$ and r_1 is the four-momentum of the outgoing lepton with charge -1. It turns out that the only solutions of

[3]The hadronic W decay case, $W \to q\bar{q}'$ simply introduces a few extra terms, but the results are qualitatively unchanged.

[4]Note that in the soft limit the ratio of propagators in (3.16) is $\frac{k_\pm^2-\overline{M}^2}{(k_\pm+k)^2-\overline{M}^2} \to 1$.

$\epsilon^*(k)\cdot j = 0$ occur when the scattering is *planar*, i.e. all incoming and outgoing three-momenta lie in the same plane.[5] If, as in (3.12), we take one polarisation vector ϵ_1^* perpendicular to this plane, and the other ϵ_2^* in the plane and orthogonal to the photon three-momentum, then $\epsilon_1^*(k) \cdot j = 0$ is trivially satisfied and $\epsilon_2^*(k) \cdot j = 0$ leads to an implicit equation for the photon production angle θ_γ which corresponds to a radiation zero:

$$\cot\frac{\theta_{1\gamma}}{2} - \cot\frac{\theta_{3\gamma}}{2} - Q_q\left(\cot\frac{\theta_\gamma}{2} + \tan\frac{\theta_\gamma}{2}\right) = 0\ , \tag{3.26}$$

with $\theta_{1\gamma} = \theta_1 - \theta_\gamma$ and $\theta_{3\gamma} = \theta_3 - \theta_\gamma$ and where the lepton four-momentum vectors are

$$\begin{aligned} r_1^\mu &= E_1(1, \sin\theta_1, 0, \cos\theta_1) \\ r_3^\mu &= E_3(1, \sin\theta_3, 0, \cos\theta_3)\ . \end{aligned} \tag{3.27}$$

Depending on the values of θ_1 and θ_3, (3.26) has either two solutions ($\theta_1 > \theta_3 > \pi$ or $\theta_1 < \theta_3 < \pi$) or no solutions[6]. This is illustrated in Figs. 3.4(a) and 3.4(b) respectively. The radiation pattern given by (3.26) is plotted as a function of θ_γ for 'typical' values of the lepton production angles, chosen such that the zeros (in the former case) are clearly visible.

[5]The planarity condition gives rise to the so-called Type II zeros discovered recently [48].

[6]One solution if either $\theta_1 = \pi$ or $\theta_3 = \pi$.

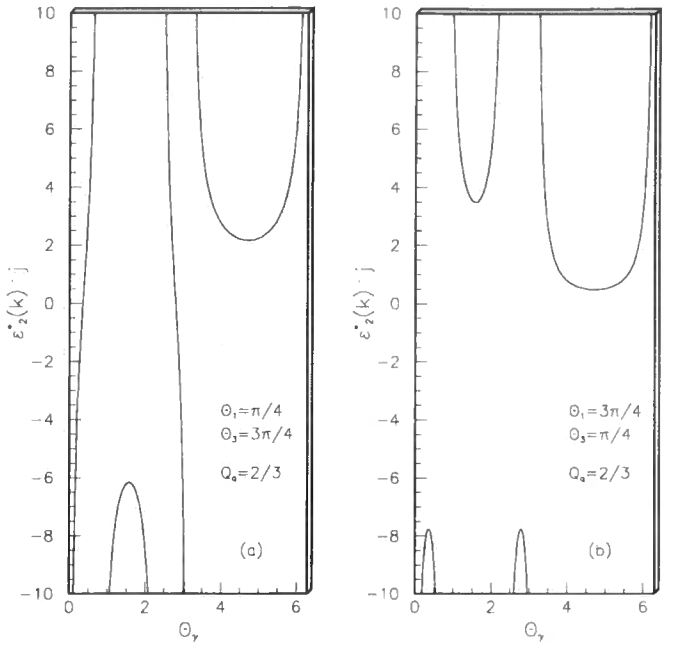

Figure 3.4: The radiation pattern of (3.26). Two (a) or no (b) radiation zeros are visible.

The generalisation to the case of arbitrary W decays is straightforward. Thus for

$$\begin{aligned} W^- &\rightarrow f_1(r_1, -Q_1) + \bar{f}_2(r_2, -Q_2 = -(1-Q_1)) \\ W^+ &\rightarrow \bar{f}_3(r_3, Q_3) + f_4(r_4, Q_4 = 1-Q_3)\ , \end{aligned} \tag{3.28}$$

(3.26) becomes

$$\begin{aligned} -2Q_q \frac{1}{\sin\theta_\gamma} + Q_1 \frac{\sin\theta_{1\gamma}}{1-\cos\theta_{1\gamma}} - (1-Q_1)\frac{\sin\theta_{2\gamma}}{1+\cos\theta_{2\gamma}} \\ -Q_3 \frac{\sin\theta_{3\gamma}}{1-\cos\theta_{3\gamma}} + (1-Q_3)\frac{\sin\theta_{4\gamma}}{1+\cos\theta_{4\gamma}} = 0. \end{aligned} \tag{3.29}$$

There are now either 4, 2 or 0 radiation zeros, depending on the relative orientation in the plane of the initial- and final-state particles.

(b) $\Gamma_W \ll E_\gamma \ll M_W$ When the photon is far harder in energy than the W is off mass shell (but still soft compared to the W masses and energies), the timescale for photon emission is much shorter than the W lifetime. As far as the photon is concerned, the overall process separates into 'W production' and 'W decay' pieces, with no interference between

them. Formally, in this limit the profile functions are $\chi_{+-} = \chi_- = \chi_+ = 0$. Therefore all the interference terms in (3.21) vanish, and to find zeros one has to solve

$$\mathcal{I} = |P|^2 + |D^+|^2 + |D^-|^2 = 0 \,. \tag{3.30}$$

Since each of these quantities is positive definite they have to vanish separately:

$$\begin{aligned} |P|^2 &= 0 \text{ RAZ of } q\bar{q} \to WW\gamma \\ |D^+|^2 &= 0 \text{ RAZ of } W^+ \to \bar{f}_3 f_4 \gamma \\ |D^-|^2 &= 0 \text{ RAZ of } W^- \to f_1 \bar{f}_2 \gamma \quad . \end{aligned} \tag{3.31}$$

Fortunately, the zeros of each are well-separated in phase space in regions that can be isolated experimentally. Thus in practice an energetic photon can be classified as a 'production' or a 'decay' photon depending on whether it reconstructs to an invariant mass M_W when combined with the W fermion decay products. Provided $E_\gamma \gg \Gamma_W$ this classification is in principle unambiguous. The radiation zeros for $W^\pm \to f\bar{f}'\gamma$ decay have been known for some time, and in fact are directly analogous to those for $q\bar{q}' \to W^\pm\gamma$ discussed in the previous section.

We therefore restrict our attention to the zeros of $q\bar{q} \to W^+W^-\gamma$, given by $|P|^2 = 0$, where the W bosons are now considered *on-shell stable particles.* It is straightforward to derive the expression for the current in this case (cf. (3.16)):

$$-j^\mu = -\frac{k_-^\mu}{k_- \cdot k} + \frac{k_+^\mu}{k_+ \cdot k} - Q_q \left(\frac{p_1^\mu}{p_1 \cdot k} - \frac{p_2^\mu}{p_2 \cdot k} \right) . \tag{3.32}$$

Then solving $\epsilon^*(k) \cdot j = 0$ leads to

$$\tan\theta_\gamma = \frac{-\beta \sin\Theta - 2\,Q_q\beta^2 \cos\Theta \sin\Theta \pm \sqrt{\beta^2 \sin^2\Theta + 4\,Q_q(\beta^2-1)\,(Q_q + \beta\cos\Theta)}}{2\,(-\beta\cos\Theta - Q_q + Q_q\,\beta^2 \sin^2\Theta)} \tag{3.33}$$

where $\beta = (1 - M_W^2/E^2)^{\frac{1}{2}} < 1$ is the velocity of the W, Θ is the angle between the W^- and the incoming quark, and E is the beam energy. Note that again these results correspond to all incoming and outgoing particles lying in the same plane. One interesting feature of this result is that there is now a certain minimum beam energy, for a given Θ and Q_q, which

is required to set up the environment for radiation zeros (the square root in (3.33) has to be positive). For example, for $\Theta = \pi/2$ the critical energy is $E_{crit.} = M_W(1 + 4Q_q^2)^{\frac{1}{2}}$. For energies $E > E_{crit.}$ four radiation zeros are present (due to the $\pm$ and the periodicity of tan). For $E = E_{crit.}$ there are only two radiation zeros (the square root vanishes) and there are none for $E < E_{crit.}$.

3.3.2 The general case

In the previous section we have found radiation zeros in the soft-photon approximation. In order to extend these results to arbitrary photon energies we have to consider the full matrix element, i.e. the sum of all the diagrams in Fig. 3.2. Since we are interested now in the case when $\Gamma_W \ll E_\gamma$, we can again make use of the partial fraction technique to factorise the full matrix element into production and decay parts, exactly as in Eqs. (3.30) and (3.31). As in the previous section we focus on the $WW\gamma$ production process:

$$\begin{aligned} d\sigma &= \frac{1}{2s} d\Phi_3 \, d\Phi_2^+ \, d\Phi_2^- \, \Big| \mathcal{M}_1 + \mathcal{M}_2 + \mathcal{M}_3 + \mathcal{M}_4 + \mathcal{M}_9 \\ &\qquad + \mathcal{M}_{10} + \mathcal{M}_{11} + \mathcal{M}_{12} + \mathcal{M}_{13} + \mathcal{M}_{18} \Big|^2 \end{aligned} \tag{3.34}$$

where the subscript refers to the diagrams of Fig. 3.2.[7] The final-state fermion parts of these diagrams are integrated over the two-body phase spaces to give two branching ratio ($W \to f\bar{f}$) factors. The photon can be emitted off either the two initial-state quarks, the two final-state W's, the internal lines (W's as well as the $t-$channel quark) or from the four boson vertex. We next have to specify the three-body phase space configuration. To simplify the kinematics we choose to fix the direction of the W^- by Θ, and the energy and the angle of the photon by E_γ and θ_γ respectively. An overall azimuthal angle is disregarded and, more importantly, the incoming and outgoing particles are required to lie in a *plane*, defined by $\Phi = \phi_\gamma = 0°$.[8] Given the initial quark momenta p_1, p_2, the W^+ four-momentum

[7] Note that only the first part of the partial fraction (3.17) is to be taken for $\mathcal{M}_3, \mathcal{M}_4, \mathcal{M}_{12}$ and $\mathcal{M}_{13}$.

[8] We show later that there are no radiation zeros for *non-planar* configurations.

is then constrained by energy-momentum conservation:

$$\begin{aligned} p_1^\mu &= E(1,0,0,1) \\ p_2^\mu &= E(1,0,0,-1) \\ k^\mu &= E_\gamma(1,\sin\theta_\gamma,0,\cos\theta_\gamma) \\ k_-^\mu &= (E_W,\sqrt{E_W^2-M_W^2}\,\sin\Theta,0,\sqrt{E_W^2-M_W^2}\,\cos\Theta) \\ k_+^\mu &= (2E-E_\gamma-E_W,-(E_\gamma\sin\theta_\gamma+\sqrt{E_W^2-M_W^2}\,\sin\Theta),0, \\ &\qquad -(E_\gamma\cos\theta_\gamma+\sqrt{E_W^2-M_W^2}\,\cos\Theta)) \end{aligned} \tag{3.35}$$

where E_W is determined by the constraint $k_+^2 = M_W^2$ and is given by

$$\begin{aligned} E_W &= \{-2EE_\gamma^2-4E^3+6E^2E_\gamma+[E_\gamma^2\cos^2(\theta_\gamma-\Theta)\,(-8E^3E_\gamma+4E^2E_\gamma^2 \\ &\quad +M_W^2E_\gamma^2\cos^2(\theta_\gamma-\Theta)+4E^4-4E^2M_W^2+4EE_\gamma M_W^2-E_\gamma^2M_W^2)]^{\frac{1}{2}}\} \\ &\quad /\,[E_\gamma^2\cos^2(\theta_\gamma-\Theta)-4E^2+4EE_\gamma-E_\gamma^2] \quad . \end{aligned} \tag{3.36}$$

In terms of these variables the three-body phase space integration is

$$d\,\Phi_3(k_+,k_-,k) = \frac{E_W E_\gamma}{4(2\pi)^5}\,\frac{d\cos\Theta\,d\Phi\;dE_\gamma\,d\cos\theta_\gamma\,d\phi_\gamma}{\left|-4E+2E_\gamma-2E_W E_\gamma\cos(\theta_\gamma-\Theta)/\sqrt{E_W^2-M_W^2}\right|^2}\,. \tag{3.37}$$

We first consider the differential cross section as a function of θ_γ, with all other variables kept fixed. For input parameters we take [53]

$$\begin{aligned} &M_W = 80.41\ \text{GeV}, \quad M_Z = 91.187\ \text{GeV}\ , \quad e^2 = 4\pi/137.035, \\ &g = e/\sin\theta_w\ , \qquad \sin^2\theta_w = 0.23\ , \end{aligned} \tag{3.38}$$

and in the following plots we also fix, for sake of illustration,

$$Q_q = \frac{2}{3}\,, \qquad E = 500\ \text{GeV}\,, \qquad \Theta = \frac{2\pi}{3}\,. \tag{3.39}$$

Fig. 3.5 shows the θ_γ dependence of the differential $u\bar{u} \to W^+W^-\gamma$ cross section, for a selection of photon energies E_γ[9]. It is immediately apparent that an actual zero of the

[9]Strictly, in order to separate out the $WW\gamma$ process in the first place we have to assume $E_\gamma \gg \Gamma_W$. However, to investigate and illustrate the disappearance of the zero it is convenient to formally consider all E_γ values down to zero. Of course the lower energy limit on physically observable photons is much higher.

cross section is only achieved in the limit $E_\gamma \to 0$. Increasing the photon energy gradually 'fills in' the dip. The reason is that for non-soft photons additional diagrams (9 and 18 in Fig. 3.2) contribute and these give rise to a non-zero cross section at the positions of the zeros.[10] The points at the bottom of the dips in Fig. 3.5 are actually the minimum values of the corresponding cross sections[11]. In fact it can be shown that for E_γ not too large, $\sigma_{\min} \propto {E_\gamma}^2$. At high photon energies the dips disappear altogether and the cross section assumes a different shape.

[10]This is in contrast to the process $eq \to eq\gamma$ studied in Ref. [48] where *all* diagrams contribute in the soft-photon limit, and where the radiation zeros persist for $E_\gamma \neq 0$.

[11]The angles at which the minima occur are very close to the RAZ angle in the soft-photon limit, as can be seen in Fig. 3.5.

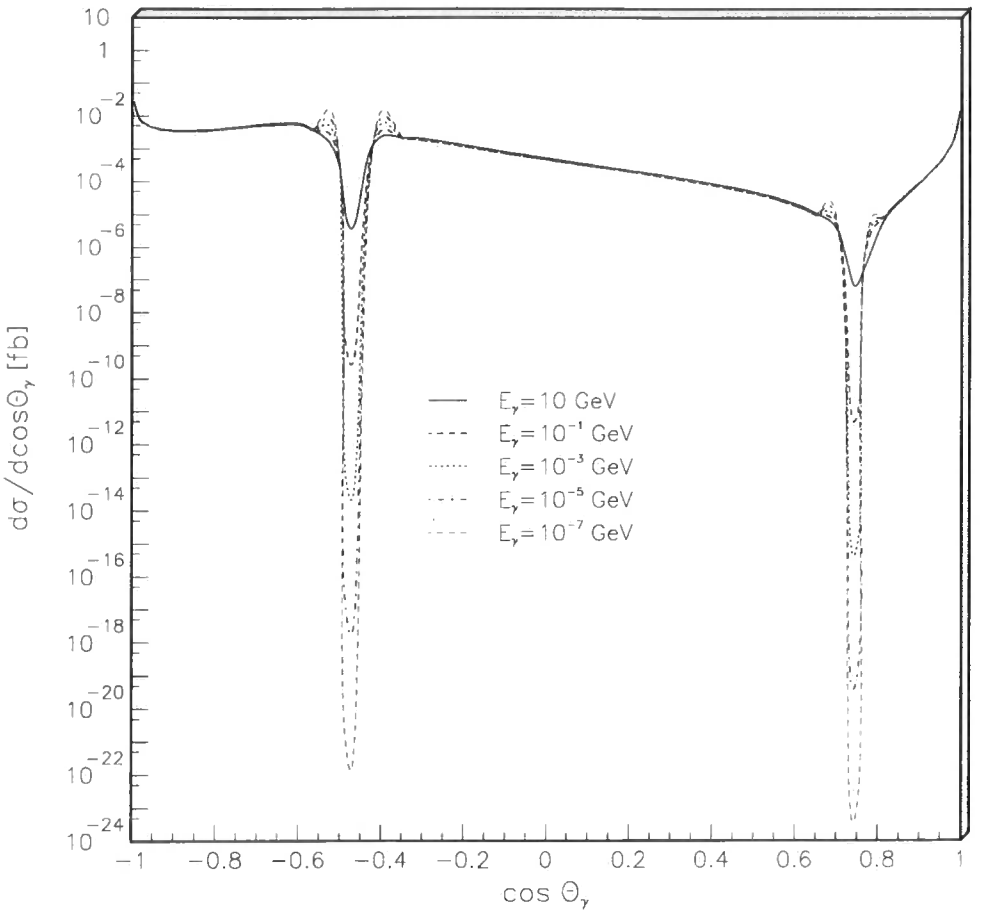

Figure 3.5: Differential cross section for the process $u\bar{u} \to W^+W^-\gamma$.

Note that the 'zeros'/ dips both lie in the angular region between the outgoing W^- and the incoming u, and by symmetry between the outgoing W^+ and the incoming $\bar{u}$. Further note that for a given E_γ, σ_{min} differs by a factor ~ 100 due to the asymmetric (with respect to the photon emission angle) contribution from diagram 18.

To confirm that we do indeed have a Type II (planar configuration) radiation zero, we next recalculate the $\cos\theta_\gamma$ distribution for $\phi_\gamma \neq 0°$. We choose a small non-zero photon energy $E_\gamma = 10^{-5}$ GeV such that the dip is clearly visible for $\phi_\gamma = 0°$. The results are shown in Fig. 3.6[12]. For ϕ_γ well away from zero, there is no hint of a dip in the cross section.

[12]Note the different scale compared to Fig. 3.5.

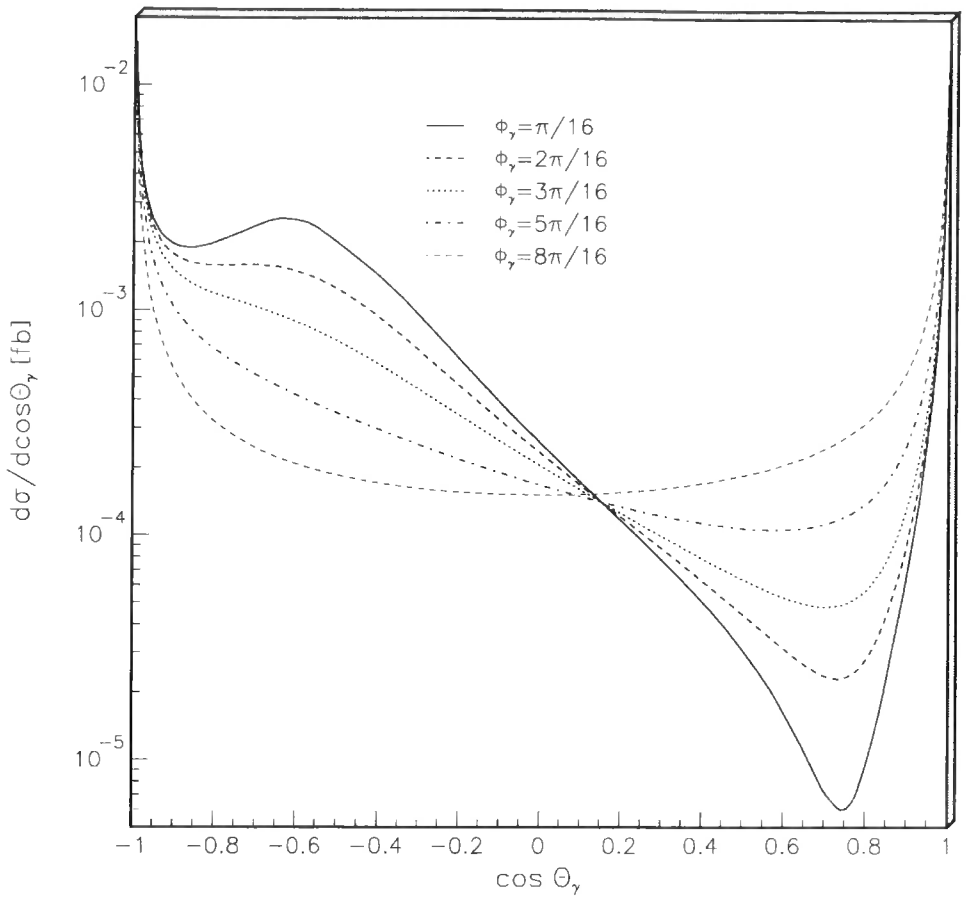

Figure 3.6: Same as Fig. 3.5 for $E_\gamma = 10^{-5}$ GeV and various ϕ_γ.

The results displayed in the above figures correspond to $u\,\bar{u}$ scattering. Similar results are obtained for $d\,\bar{d}$ and e^+e^- scattering, i.e. exact Type II zeros are only found in the soft-photon limit where they are given by (3.33). The position of the zeros depends on the incoming fermions' electric charge, and on the scattering angles and velocities of the W bosons. For non-soft photons the dips are filled in, but still remain clearly visible for photon energies up to $\mathcal{O}(10\text{ GeV})$.

3.4 Anomalous gauge boson couplings

As discussed in the Introduction, the existence of radiation zeros is in general destroyed by the presence of anomalous gauge boson couplings.
The impact of anomalous trilinear couplings on the radiation zeros in the $q\bar{q}' \to W\gamma$ process was considered in Ref. [54]. As expected, the zeros are removed for non-zero values of the anomalous parameters. Such couplings would also affect the zeros in the $WW\gamma$ case. However there are already quite stringent limits on these trilinear couplings from the Tevatron $p\bar{p} \to W\gamma X$ [55] and LEP2 $e^+e^- \to W^+W^-$ processes [25, 26]. We therefore neglect them here and concentrate on genuine anomalous quartic couplings . The $WW\gamma$ process is in fact the simplest one which is sensitive to *quartic* couplings. It is natural therefore to consider the implications of anomalous quartic couplings on the radiation zeros discussed in the previous section.

Let us consider first the differential cross section in the planar configuration as a function of θ_γ, just as we did in the previous section, but now in the presence of non-zero values of the three anomalous parameters a_0, a_c and a_n introduced in (2.8), (2.9) and (2.10). From the Lagrangian it can be seen that any anomalous contribution is *linear* in E_γ. Soft photons are 'blind' to the anomalous couplings and therefore the zeros in the $k^\mu \to 0$ limit survive. For moderate photon energies, the dips in the SM cross section will be filled in by contributions proportional to a_i and ${a_i}^2$. The higher the photon energy, the more dramatic the effect, although of course the dips become less well defined too. In principle, therefore, one should optimize the photon energy, to make it small enough to maintain the zeros but at the same time large enough to gain measurable deviations from the SM prediction. Since the anomalous contributions originate in the four boson vertex in the s-channel, one can also increase the sensitivity to them by considering only right-handed initial quarks, for which the t-channel contributions are absent.[13]

[13]Unfortunately in doing so one also decreases the total cross section by roughly 2 orders of magnitude, so again it has to be seen whether the sensitivity to new physics is in fact increased in practice.

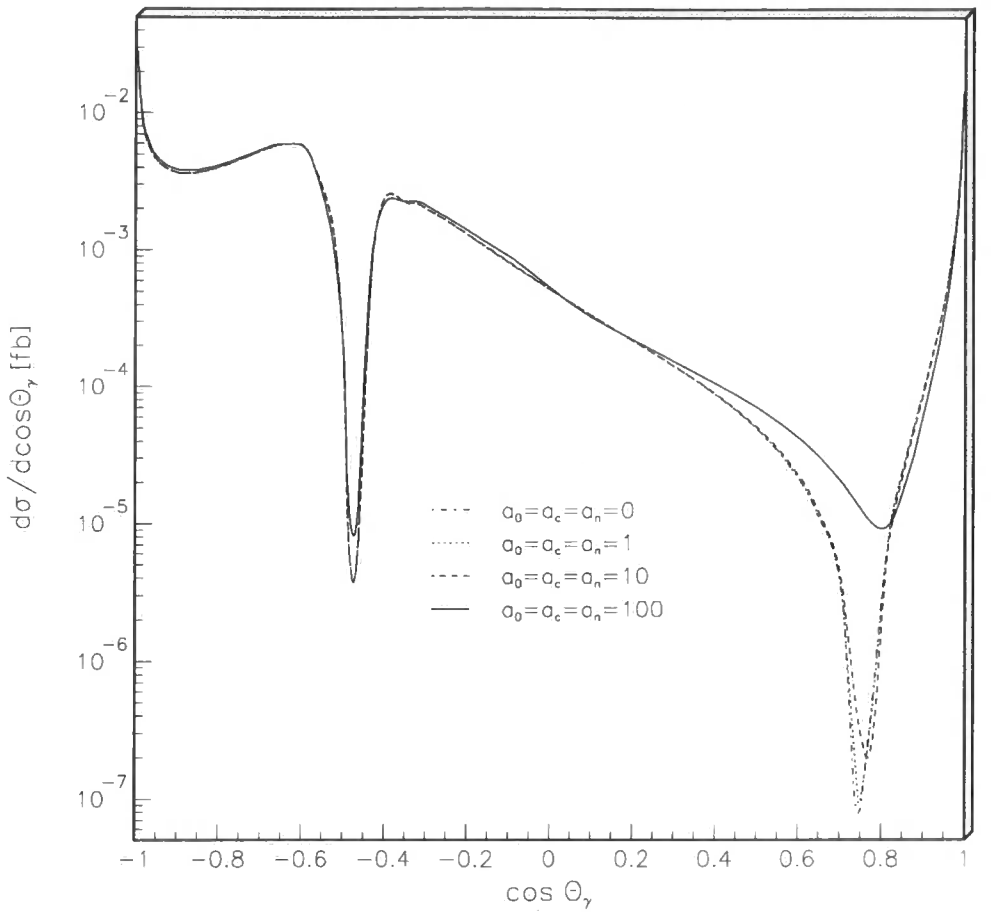

Figure 3.7: Differential cross section for the process $u\bar{u} \to W^+W^-\gamma$ with $E_\gamma = 1$ GeV. The curves correspond to different values of the anomalous parameters introduced in the text.

Fig. 3.7 shows the θ_γ dependence of the $u\bar{u} \to WW\gamma$ cross section for $E_\gamma = 1$ GeV, for the same configuration and parameters as in Fig. 3.5 (see Eqs. (3.38,3.39)). The curves correspond to different (positive) values of the anomalous parameters [14]. The anomalous contribution is approximately isotropic in θ_γ. Therefore because the dips have different depths one gets filled in more rapidly than the other. This is evident in the figure, where the dip at $\cos\theta_\gamma \sim 0.75$ is already filled in for $a_i \sim \mathcal{O}(100)$, whereas the steep dip at $\cos\theta_\gamma \sim -0.48$ is still very apparent. This shows it is advantageous to focus on certain regions

[14] To make quantitative predictions the anomalous parameter Λ appearing in Eqs. (2.8,2.9,2.10) has to be fixed. We choose $\Lambda = M_W$; any other choice results in a trivial rescaling of the anomalous parameters a_0, a_c and a_n. See the discussion in [18]. The anomalous parameters can also be negative, which leads to results similar to those in Fig. 3.7.

of photon phase space in order to increase the sensitivity to the anomalous couplings. Of course, this requires very high luminosity to ensure a large enough event rate in these regions.

3.5 Conclusions

We have investigated the (Type II) radiation zeros of the process $q\bar{q} \to W^+W^-\gamma \to f_1\bar{f}_2\bar{f}_3f_4\gamma$. In the soft-photon limit ($\Gamma_W \ll E_\gamma \ll M_W$) the cross section vanishes for certain values of the photon and $W^\pm$ production angles, for which analytic expressions have been derived (3.33). For non-zero photon energies the zeros disappear, but for energies not too large the photon angular distribution still exhibits deep dips centred on the positions of the soft-photon zeros. The subtle cancellations leading to the zeros in the soft-photon limit still takes place, but for non-soft photons two additional diagrams (9 and 18) have to be considered and σ_{min} is exactly that contribution. In the 'classic' process $q\bar{q}' \to W^+\gamma$ there are no further diagrams for non-soft photons and the zeros survive for all photon energies. Although we have concentrated on the quark scattering process $q\bar{q} \to W^+W^-\gamma$ our results apply equally well to $e^+e^- \to W^+W^-\gamma$ by setting $Q_q = -1$. Note that, as for quark antiquark scattering, the zeros in the e^+e^- (soft-photon) case are in the 'visible' regions of phase space, in contrast to those in the analogous 'classical' process $e^+\nu_e \to W^+\gamma$. Furthermore for e^+e^- scattering diagram 9 (scattering via t-channel exchange) is not present and direct access to the four boson vertex is given for non-soft photons, i.e. the four boson vertex is the only contribution to the cross section at the position of the zeros.

We have also studied the effect of including non-zero anomalous quartic couplings. These contributions increase with increasing photon energy and fill in the dips present in the standard model. In principle, therefore, the vicinity of the radiation zeros is the most sensitive part of phase space to these anomalous four boson couplings.

In practice however, we learned from the previous chapter that by analyzing the full phase-space of $WW\gamma$ production (*i.e. not* being constrained to planar configurations) increases the sensitivity to anomalous quartic couplings. Our analysis has been entirely theoretical. Having established that there *are* regions of phase space where the cross section is heavily

suppressed, the next step is to see to what extent the phenomenon persists when hadronisation, radiative corrections, smearing, boost, detector etc. effects are taken into account, in the context, for example, of a possible measurement at the Tevatron or LHC hadron colliders. In this respect, a high energy, high luminosity e^+e^- linear collider could provide a cleaner environment for studying $WW\gamma$ production in this way.

Notice that we do not anticipate a large effect from perturbative QCD corrections. This conclusion is based on the study of Ref. [56] where the full $\mathcal{O}(\alpha_s)$ corrections to the $W\gamma$ process were calculated. It was shown (Fig. 6 of Ref. [56]) that the radiation zero present at Born level was essentially unchanged by the NLO corrections.

Chapter 4

Electroweak Radiative Corrections

To match the expected experimental precision at future linear colliders, improved theoretical predictions beyond next-to-leading order are required. At the anticipated energy scale of $\sqrt{s} = 1$ TeV the electroweak virtual corrections are strongly enhanced by collinear-soft Sudakov logarithms of the form $\log^2(s/M^2)$, with M being the generic mass scale of the W and Z bosons. By choosing an appropriate gauge, we have developed a formalism to calculate such corrections for arbitrary electroweak processes. As an example we consider here the processes $e^+e^- \to f\bar{f}$ and $e^+e^- \to W_T^+W_T^-$, $W_L^+W_L^-$ and study the perturbative structure of the electroweak Sudakov logarithms by means of an explicit two-loop calculation. In this way we investigate how the Standard Model, with its mass gap between the photon and Z boson in the neutral sector, compares to unbroken theories like QED and QCD. In contrast to what is known for unbroken theories we find that the Sudakov logarithms are not exclusively given by the so-called rainbow diagrams, owing to the mass gap and the charged-current interactions. In spite of this, we nevertheless observe that the two-loop corrections are consistent with an exponentiation of the one-loop corrections. In this sense the Standard Model behaves like an unbroken theory at high energies.

We give a description of our formalism, which is based on the Coulomb gauge, and extend it to reactions with transverse and longitudinal (massive) gauge bosons in the final state. Especially the treatment of the longitudinal gauge bosons requires some special attention. In order to cover all the relevant features and subtleties of our method, it is sufficient to restrict the discussion to the virtual corrections. In fact, since the Sudakov logarithms originate from

the exchange of soft, effectively on-shell gauge bosons, many of the features derived for these virtual corrections are intimately related to properties of the corresponding real-gauge-boson emission processes.

4.1 Introduction

At the next generation of colliders center-of-mass energies will be reached that largely exceed the electroweak scale. For instance, the energy at a future linear e^+e^- collider is expected to be in the TeV range [34]. At these energies one enters the realm of large perturbative corrections. Even the effects arising from weak corrections are expected to be of the order of 10% or more [57, 58], i.e. just as large as the well-known electromagnetic corrections. In order not to jeopardize any of the high-precision studies at these high-energy colliders, it is therefore indispensable to improve the theoretical understanding of the radiative corrections in the weak sector of the Standard Model (SM). In particular this will involve a careful analysis of effects beyond first order in the perturbative expansion in the (electromagnetic) coupling $\alpha = e^2/(4\pi)$.

The dominant source of radiative corrections at TeV-scale energies is given by logarithmically enhanced effects of the form $\alpha^n \log^m(M^2/s)$ for $m \leq 2n$, involving particle masses M well below the collider energy $\sqrt{s}$. A natural way of controlling the theoretical uncertainties would therefore consist in a comprehensive study of these large logarithms, taking into account all possible sources (i.e. ultraviolet, soft, and collinear). In first approximation the so-called Sudakov logarithms $\propto \alpha^n \log^{2n}(M^2/s)$, arising from collinear-soft singularities [59], constitute the leading contribution to the large electroweak correction factors. Recent studies have focused on these Sudakov effects in fermionic processes like $e^+e^- \to f\bar{f}$ [60, 61, 62][1]. Unfortunately the three independent studies are in mutual disagreement, exhibiting strikingly different higher-order results already for the virtual corrections. The main cause for the differences can be traced back to the use of different assumptions concerning the exponentiation properties of the Sudakov logarithms in the SM. Many of these assumptions

[1]The recent paper [63] is in agreement with our findings [21]

are based on the analogy with unbroken theories like QED and QCD, where the resummation of the higher-order effects amounts to an exponentiation of the one-loop corrections (see for instance Refs. [59] and [64, 65, 66]). However, the SM is a broken gauge theory with a large mass gap in the neutral sector between the massless photon and the massive Z boson, making it a theory with more than one mass scale. As such it remains to be seen how much of the analogy with unbroken theories actually pertains to the SM.

We therefore focus on the virtual Sudakov logarithms in the reactions $e^+e^- \to f\bar{f}$, and $e^+e^- \to W_T^+W_T^-$, $W_L^+W_L^-$, in an attempt to clarify how the $\mathcal{O}(\alpha^2)$ effects relate to the $\mathcal{O}(\alpha)$ ones. In this way we identify to what extent the SM behaves like an unbroken theory at high energies. Moreover, since the Sudakov logarithms originate from the exchange of soft, effectively on-shell gauge bosons, many of the features derived for the virtual corrections are intimately related to properties of the corresponding real-gauge-boson emission processes.

4.2 Electroweak Sudakov Logarithms in the Coulomb gauge

In order to facilitate the calculation of the one- and two-loop Sudakov logarithms, we work in the Coulomb gauge for both massless and massive gauge bosons. In the Coulomb gauge the gauge fixing Lagrangian for massive W bosons[2] is given by

$$\mathcal{L}_{GF} = -\lambda \left[\left(\partial_\mu - \frac{n\cdot\partial}{n^2} n_\mu \right) W^{+\mu} \right] \left[\left(\partial_\nu - \frac{n\cdot\partial}{n^2} n_\nu \right) W^{-\nu} \right] \tag{4.1}$$

with the temporal gauge vector $n^\mu = (1,0,0,0)$. Let us select the bilinear interactions in the $W\phi$ - sector from the SM Lagrangian (1.1). From the kinetic term of the W bosons we obtain

$$-\frac{1}{4}\mathbf{W}_{\mu\nu}\mathbf{W}^{\mu\nu} \xrightarrow{\text{bilinear}} -\frac{1}{4}\left(\partial_\mu \mathbf{W}_\nu - \partial_\nu \mathbf{W}_\mu\right)\left(\partial^\mu \mathbf{W}^\nu - \partial^\nu \mathbf{W}^\mu\right)$$

[2]The $Z\chi$ and the photon sector can be treated similarly. We will give those results without explicit derivation later.

$$\xrightarrow[\text{content}]{\text{charged}} -\frac{1}{4}\left(2\,\frac{1}{2}\left[\partial_\mu\left(W_\nu^+ + W_\nu^-\right)\partial^\mu\left(W^{+\nu} + W^{-\nu}\right) - \partial_\mu\left(W_\nu^+ - W_\nu^-\right)\partial^\mu\left(W^{+\nu} - W^{-\nu}\right)\right]\right.$$

$$\left.-2\,\frac{1}{2}\left[\partial_\mu\left(W_\nu^+ + W_\nu^-\right)\partial^\nu\left(W^{+\mu} + W^{-\mu}\right) - \partial_\mu\left(W_\nu^+ - W_\nu^-\right)\partial^\nu\left(W^{+\mu} - W^{-\mu}\right)\right]\right) \tag{4.2}$$

$$= -\left(\partial_\mu W_\nu^+\right)\left(\partial^\mu W^{-\nu}\right) + \left(\partial_\mu W^{+\mu}\right)\left(\partial^\nu W_\nu^-\right). \tag{4.3}$$

In the ϕ sector we need the covariant derivative (1.4)

$$D_\mu = \partial_\mu - ig\,\mathbf{I}\cdot\mathbf{W}_\mu + ig'\,\frac{Y}{2}\,B_\mu$$

$$\xrightarrow[\text{content}]{\text{charged}} \begin{pmatrix} \partial_\mu & 0 \\ 0 & \partial_\mu \end{pmatrix} - \frac{i\,g}{\sqrt{2}}\begin{pmatrix} 0 & W_\mu^+ \\ W_\mu^- & 0 \end{pmatrix} \tag{4.4}$$

and with

$$\phi(x) = \begin{pmatrix} \phi^+(x) \\ \dfrac{1}{\sqrt{2}}\left(v + H(x) + i\,\chi(x)\right) \end{pmatrix} \to \begin{pmatrix} \phi^+ \\ v/\sqrt{2} \end{pmatrix} \tag{4.5}$$

$$\left(D_\mu\,\phi\right) \xrightarrow[\text{charged}]{\text{linear}} \begin{pmatrix} \partial_\mu & -\dfrac{ig}{\sqrt{2}}\,W_\mu^+ \\ -\dfrac{ig}{\sqrt{2}}\,W_\mu^- & \partial_\mu \end{pmatrix}\begin{pmatrix} \phi^+ \\ v/\sqrt{2} \end{pmatrix} = \begin{pmatrix} \partial_\mu\phi^+ - \dfrac{igv}{2}W_\mu^+ \\ 0 \end{pmatrix}. \tag{4.6}$$

Hence

$$\left(D^\mu\,\phi\right)^\dagger\left(D_\mu\,\phi\right) \xrightarrow[\text{charged}]{\text{bilinear}} \left(\partial^\mu\,\phi^- + \frac{igv}{2}\,W^{-\mu}\;,\;0\right)\begin{pmatrix} \partial_\mu\,\phi^+ - \dfrac{igv}{2}\,W_\mu^+ \\ 0 \end{pmatrix}$$

$$= \left(\partial^\mu\,\phi^-\right)\left(\partial_\mu\,\phi^+\right) - \frac{igv}{2}\left[W_\mu^+\left(\partial^\mu\,\phi^-\right) - W^{-\mu}\left(\partial_\mu\,\phi^+\right)\right] + \left(\frac{gv}{2}\right)^2 W_\mu^+\,W^{-\mu}. \tag{4.7}$$

Making use of $M_W = vg/2$ (1.9) and bringing the derivative in front of the W fields yields the bilinear Lagrangian in the $W\phi$ - sector in the Coulomb gauge

$$\begin{aligned}\mathcal{L}_{W-\phi\,int.} \;=\; & (\partial^\mu W_\mu^+)(\partial^\nu W_\nu^-) - (\partial_\mu W_\nu^+)(\partial^\mu W^{-\nu}) + (\partial_\mu\phi^+)(\partial^\mu\phi^-) \\ & + iM_W[(\partial^\mu W_\mu^+)\phi^- - (\partial^\nu W_\nu^-)\phi^+] + M_W^2\,W_\mu^+ W^{-\mu} \\ & - \lambda\left[\left(\partial_\mu - \frac{n\cdot\partial}{n^2}n_\mu\right)W^{+\mu}\right]\left[\left(\partial_\nu - \frac{n\cdot\partial}{n^2}n_\nu\right)W^{-\nu}\right]\end{aligned} \tag{4.8}$$

and hence the interaction matrix can be written as

$$\begin{pmatrix} -i\left[(k^2 - M_w^2)\,g^{\mu\nu} - k^\mu k^\nu + \lambda\left(k^\mu - \frac{n\cdot k}{n^2}n^\mu\right)\left(k^\nu - \frac{n\cdot k}{n^2}n^\nu\right)\right] & \pm i\,M_w k^\mu \\ \pm i\,M_w k^\nu & i\,k^2 \end{pmatrix} \tag{4.9}$$

$$= \begin{pmatrix} W_\mu^\pm, k \sim\!\!\blacktriangleright\!\!\bullet\!\!\blacktriangleright\!\!\sim W_\nu^\pm, k & W_\mu^\pm, k \sim\!\!\blacktriangleright\!\!\bullet\!\!\rightarrow \phi^\pm, k \\ \phi^\pm, k \text{ - }\blacktriangleright\!\!\bullet\!\!\blacktriangleright\!\!\sim W_\nu^\pm, k & \phi^\pm, k \text{ - }\blacktriangleright\!\!\bullet\!\!\rightarrow \phi^\pm, k \end{pmatrix}. \tag{4.10}$$

with $\pm$ in (4.9) corresponding to $W^\pm$.

The propagators in the coloumb gauge are obtained by inverting the interaction matrix and taking the limit $\lambda \to \infty$.

$$\begin{pmatrix} \sim\!\!\blacktriangleright\!\!\bullet\!\!\blacktriangleright\!\!\sim & \sim\!\!\blacktriangleright\!\!\bullet\!\!\rightarrow \\ \text{-}\blacktriangleright\!\!\bullet\!\!\blacktriangleright\!\!\sim & \text{-}\blacktriangleright\!\!\bullet\!\!\rightarrow \end{pmatrix} \begin{pmatrix} P_{\nu\rho} & M_\nu^\pm \\ M_\rho^\pm & P \end{pmatrix} = \begin{pmatrix} -\delta^\mu{}_\rho & 0 \\ 0 & -1 \end{pmatrix}. \tag{4.11}$$

This leads to the explicit form of the propagators

$W^\pm$ $W^\pm$, μ, ν, k : $$P_{\mu\nu} = \frac{-i}{k^2 - M_w^2 + i\epsilon}\left(g_{\mu\nu} + \frac{k_\mu k_\nu}{\vec{k}^2} - k_0\frac{k_\mu n_\nu + k_\nu n_\mu}{\vec{k}^2}\right) \tag{4.12}$$

$W^\pm$ $\phi^\pm$, μ, k : $$M_\mu^\pm = \frac{\mp i\,M_w}{k^2 - M_w^2 + i\epsilon}\frac{k_0}{\vec{k}^2}n_\mu \tag{4.13}$$

$\phi^\pm$ $W^\pm$, ν, k : $$M_\nu^\pm = \frac{\mp i\,M_w}{k^2 - M_w^2 + i\epsilon}\frac{k_0}{\vec{k}^2}n_\nu \tag{4.14}$$

$\phi^\pm$ $\phi^\pm$, k : $$P = \frac{i}{k^2 - M_w^2 + i\epsilon}\left(1 + \frac{M_w^2}{\vec{k}^2}\right), \tag{4.15}$$

In the neutral sector the propagators for the Z boson are given by

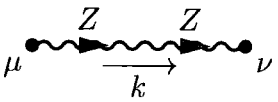

$$: \quad P_{\mu\nu} = \frac{-i}{k^2 - M_z^2 + i\,\epsilon} \left(g_{\mu\nu} + \frac{k_\mu k_\nu}{\vec{k}^2} - k_0 \frac{k_\mu n_\nu + k_\nu n_\mu}{\vec{k}^2} \right) \tag{4.16}$$

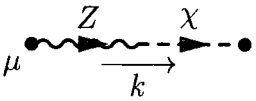

$$: \quad M_\mu = \frac{M_z}{k^2 - M_z^2 + i\,\epsilon} \frac{k_0}{\vec{k}^2} n_\mu \tag{4.17}$$

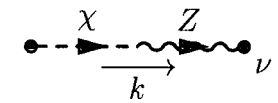

$$: \quad M_\nu = \frac{M_z}{k^2 - M_z^2 + i\,\epsilon} \frac{k_0}{\vec{k}^2} n_\nu \tag{4.18}$$

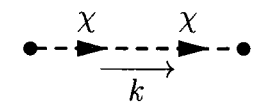

$$: \quad P = \frac{i}{k^2 - M_z^2 + i\,\epsilon} \left(1 + \frac{M_z^2}{\vec{k}^2} \right), \tag{4.19}$$

and for the photon

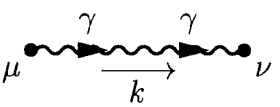

$$: \quad P_{\mu\nu} = \frac{-i}{k^2 + i\,\epsilon} \left(g_{\mu\nu} + \frac{k_\mu k_\nu}{\vec{k}^2} - k_0 \frac{k_\mu n_\nu + k_\nu n_\mu}{\vec{k}^2} \right). \tag{4.20}$$

The power of this gauge choice lies in the fact that in the kinematical region of interest the gauge-boson propagators become effectively transverse:

$$\begin{aligned} P^{\mu\nu}(k) &= -\,i\,\frac{\vec{k}^2\, g^{\mu\nu} + k^\mu k^\nu - k^0\,(k^\mu n^\nu + n^\mu k^\nu)}{\vec{k}^2\,(k^2 - M^2 + i\epsilon)} \\ &= \frac{-\,i}{k^2 - M^2 + i\epsilon} \left[Q^{\mu\nu}(k) - \frac{k^2}{\vec{k}^2}\, n^\mu n^\nu \right]. \end{aligned} \tag{4.21}$$

The tensor

$$Q_{\mu\nu}(k) = -\sum_{\lambda=\pm} \epsilon_\mu(k,\lambda)\, \epsilon_\nu^\star(k,\lambda) \tag{4.22}$$

is the polarization sum for the transverse helicity states. Therefore the gauge bosons are effectively transverse if $k^2 \ll \vec{k}^2$, which is the case for collinear gauge-boson emission at high energies ($k^2 \propto M^2$ and $\vec{k}^2 \approx k_0^2 \gg M^2$). As a result of the effective transversality, the virtual Sudakov logarithms originating from vertex, box etc. corrections are suppressed[3] (provided all kinematical invariants are of the same order as the CM energy squared).

[3]We will come back to that later, once we have established all the necessary ingredients.

Hence, all virtual Sudakov logarithms are contained exclusively in the self-energies of the external on-shell particles [65, 23] or the self-energies of any intermediate particle that happens to be effectively on-shell.[4] The latter is, for instance, needed for the production of near-resonance unstable particles. The elegance of this method lies in its universal nature. Once all self-energies to all on-shell/on-resonance SM particles have been calculated, the prediction of the Sudakov form factor for an *arbitrary* electroweak process becomes trivial. The relevant self-energies for the calculation of the Sudakov logarithms involve the exchange of collinear-soft gauge bosons, including their potential mixing with the corresponding would-be Goldstone bosons. The collinear-soft exchange of fermions and ghosts leads to suppressed contributions, since the propagators of these particles do not have the required pole structure[5].

4.2.1 The external wave-function factors

The calculation of the external wave-function factors for fermions is non-trivial [67] but no further complications arise in the Coulomb gauge. For massive gauge bosons, however, the mixing with the corresponding component of the Higgs doublet introduces an additional complication. For instance, consider the W boson and the would-be Goldstone boson ϕ. For a proper description of the on-shell W bosons we have to define the asymptotic $W^{\rm as}$ field in terms of the interacting W and ϕ fields[6]:

$$W_\mu^{\pm,\rm as}(x) \;=\; Z_W^{-\frac{1}{2}}\, W_\mu^{\pm}(x) \;\pm\; i\,\delta Z_1\,\frac{\partial_\mu \phi^{\pm}(x)}{M_W} + \delta Z_n\, n_\mu n\cdot W^{\pm}(x) + \delta Z_2\,\frac{\partial_\mu\, \partial\cdot W^{\pm}(x)}{M_W^2}, \quad (4.23)$$

in such a way that the free-field propagators are retrieved for $W^{\rm as}$ in the on-shell limit. This fixes the renormalization factors Z and δZ in terms of the self-energies of the interacting fields.

However, the full expression in (4.23) is in fact only needed to guarantee that the asymptotic

[4] Note that similar simplifications can probably be obtained equally well by working in an axial gauge, see for instance Ref. [66] for massless particles.

[5] We come back to that later.

[6] Neutral external gauge bosons and hence an asymptotic state containing the Z boson and the would-be Goldstone boson χ will be investigated elsewhere [23].

vector field satisfies the physical polarization condition

$$\partial^\mu W_\mu^{\pm,\mathrm{as}}(x) = 0\,, \tag{4.24}$$

in the weak limit.

For all practical purposes, *i. e.* calculating S-matrix elements, the asymptotic state will be connected to a source term $\epsilon^\mu(k)$ and it is sufficient to consider

$$W_\mu^{\pm,\mathrm{as}}(x) \to Z_W^{-\frac{1}{2}}\, W_\mu^{\pm}(x) + \delta Z_n\, n_\mu\, n\cdot W^{\pm}(x)\,, \tag{4.25}$$

the two terms containing ∂_μ yielding $\epsilon(k)\cdot k = 0$. In the remainder of this section we will denote those irrelevant terms proportional to k_μ by '...' .

Jumping ahead of ourselves we note already here that for transverse W_T, the second term in (4.25) will also vanish ($\epsilon_T(k)\cdot n = 0$, n being time-like) , whereas for longitudinal W_L the full expression (4.25) will be of relevance.

In order to actually determine the renormalization factor $Z_W^{-\frac{1}{2}}$ and δZ_n we study the field-theoretical prescription of the propagator as the Fourier Transform (FT) of the time-ordered product of the $W_\mu^{\pm\mathrm{as}}$ fields acting on both sides on the vacuum

$$\begin{aligned}
&\mathrm{FT}\,\langle\,0\,|\mathrm{T}\,(\,W_\mu^{+,\mathrm{as}}(x)\,W_\nu^{-,\mathrm{as}}(y)\,)\,|\,0\,\rangle = \\
&= \mathrm{FT}\,\langle\,0\,|\mathrm{T}\,\Big(\big[Z_W^{-\frac{1}{2}}\;W_\mu^{+}(x) + \delta Z_n\;n_\mu\, n\cdot W^{+}(x)\big]\,\big[\,Z_W^{-\frac{1}{2}}\,W_\nu^{-}(y) + \delta Z_n\;n_\nu\, n\cdot W^{-}(y)\,\big]\Big)\,|\,0\,\rangle + \ldots \\
&= \mathrm{FT}\,\langle\,0\,|\mathrm{T}\,\Big(Z_W^{-1}\,W_\mu^{+}(x)\,W_\nu^{-}(y) + \delta Z_n\;Z_W^{-\frac{1}{2}}\,n_\mu\, n\cdot W^{+}(x)\,W_\nu^{-}(y) \\
&\qquad + Z_W^{-\frac{1}{2}}\;\delta Z_n\;W_\mu^{+}(x)\,n_\nu\, n\cdot W^{-}(y) + \delta {Z_n}^2\,n_\mu\, n\cdot W^{+}(x)\;n_\nu\, n\cdot W^{-}(y)\Big)\,|\,0\,\rangle + \ldots\,.
\end{aligned} \tag{4.26}$$

To further specify the above we need to gain knowledge about the propagator of the interacting W fields, *i. e.* we first have to derive the dressed propagators.

The $W^\pm$ boson self energy $i\,\Sigma_{W^\pm}^{\mu\nu}$ can be decomposed into

$$i\,\Sigma_{W^\pm}^{\mu\nu} = i\,\left[\mathrm{g}^{\mu\nu}\,\Sigma_{\mathrm{w,g}} + \mathrm{k}^\mu\mathrm{k}^\nu\,\Sigma_{\mathrm{w,k}} + (\mathrm{k}^\mu\mathrm{n}^\nu + \mathrm{k}^\nu\mathrm{n}^\mu)\,\Sigma_{\mathrm{w,m}} + \mathrm{n}^\mu\mathrm{n}^\nu\,\Sigma_{\mathrm{w,n}}\right] \tag{4.27}$$

Similarly the mixed boson/would-be Goldstone boson self energy can be written as

$$i\,\Sigma_{W^\pm\phi^\pm}^{\mu} = \pm\, i\,\left[k^\mu\,\Sigma_{W^+\phi^+,k} + n^\mu\,\Sigma_{W^+\phi^+,n}\right]\,. \tag{4.28}$$

To all orders in perturbation theory the interaction matrix (4.9) is thus

$$\begin{pmatrix} -i\left[g^{\mu\nu}(k^2 - M_W^2 - \Sigma_{W,g}) + \lambda(k^\mu - k^0 n^\mu)(k^\nu - k^0 n^\nu)\right. \\ \left. - k^\mu k^\nu(1 + \Sigma_{W,k}) - (k^\mu n^\nu + k^\nu n^\mu)\Sigma_{W,m} - n^\mu n^\nu \Sigma_{W,n}\right] & \pm i\left[k^\mu(M_W + \Sigma_{W^+\phi^+,k}) + n^\mu \Sigma_{W^+\phi^+,n}\right] \\ \pm i\left[k^\nu(M_W + \Sigma_{W^+\phi^+,k}) + n^\nu \Sigma_{W^+\phi^+,n}\right] & i\left[k^2 + \Sigma_\phi\right] \end{pmatrix} \tag{4.29}$$

with $\Sigma_\phi = \Sigma_{\phi^\pm}$ the would-be Goldstone boson self energy.

The Dyson-resummed propagator matrix is obtained by inverting this interaction matrix and taking the limit $\lambda \to \infty$. To simplify the calculation we define the following quantities[7]

$$q^\mu \equiv k^\mu - k^0 n^\mu \tag{4.30}$$

$$Q^{\mu\nu} \equiv g^{\mu\nu} - n^\mu n^\nu - \frac{q^\mu q^\nu}{q^2} \tag{4.31}$$

with the useful properties

$$n_\mu Q^{\mu\nu} = q_\mu Q^{\mu\nu} = Q^{\mu\nu} n_\nu = Q^{\mu\nu} q_\nu = 0 \tag{4.32}$$

$$n \cdot q = 0\,, \quad Q^{\mu\nu} Q_{\nu\rho} = Q^\mu{}_\rho\,, \quad q^2 = -\vec{k}^2 \tag{4.33}$$

The dressed-propagator matrix can be written in the generic form

$$\begin{pmatrix} -i\left[A\,Q_{\nu\rho} + B\,q_\nu\,q_\rho + C(q_\nu\,n_\rho + n_\nu\,q_\rho) + D\,n_\nu\,n_\rho\right] & \pm i\left[E\,q_\nu + F\,n_\nu\right] \\ \pm i\left[E\,q_\rho + F\,n_\rho\right] & i\,G \end{pmatrix}. \tag{4.34}$$

Making use of the Ward identities we immediately find $B = C = E = 0$. For the other

[7]Note that $Q^{\mu\nu}$ is identical to (4.22).

coefficients we find explicitly

$$A = \frac{1}{k^2 - M_W^2 - \Sigma_{W,\mathrm{g}}} \tag{4.35}$$

$$D = \Bigg[k^2 - M_W^2 - \Sigma_{W,\mathrm{g}} - 2\,k_0\,\Sigma_{W,m} - \Sigma_{W,n} - k_0^2\,(1 + \Sigma_{W,k}) + \frac{[k_0(M_W + \Sigma_{W+\phi^+,k}) + \Sigma_{W+\phi^+,n}]^2}{k^2 + \Sigma_\phi}\Bigg]^{-1} \tag{4.36}$$

$$F = D\,\frac{k_0\,(M_W + \Sigma_{W+\phi^+,k}) + \Sigma_{W+\phi^+,n}}{k^2 + \Sigma_\phi} \tag{4.37}$$

$$G = \frac{1}{k^2 + \Sigma_\phi} - \frac{F^2}{D}\,. \tag{4.38}$$

Hence (4.26) becomes

$$\begin{aligned}
\mathrm{FT}\,\langle\,0\,|\mathrm{T}\,(\,W_\mu^{+,\mathrm{as}}(x)\,W_\nu^{-,\mathrm{as}}(y)\,)\,|\,0\,\rangle &= (-i)\,Z_W^{-1}\,[A\,Q_{\mu\nu} + D\,n_\mu\,n_\nu] \\
&+ (-i)\,Z_W^{-\frac{1}{2}}\,\delta Z_n\,n_\mu\,[A\,n^\rho\,Q_{\rho\nu} + D\,n^\rho\,n_\rho\,n_\nu] \\
&+ (-i)\,Z_W^{-\frac{1}{2}}\,\delta Z_n\,n_\nu\,[A\,n^\sigma\,Q_{\mu\sigma} + D\,n_\mu\,n^\sigma\,n_\sigma] \\
&+ (-i)\,\delta Z_n{}^2\,n_\mu\,n_\nu\,[A\,n^\rho\,n^\sigma\,Q_{\sigma\rho} + D\,n^\rho\,n_\rho\,n^\sigma\,n_\sigma] + \ldots \\
&= (-i)\,Z_W^{-1}\,A\,Q_{\mu\nu} + (-i)\,\left[Z_W^{-\frac{1}{2}} + \delta Z_n\right]^2 D\,n_\mu\,n_\nu + \ldots\,,
\end{aligned} \tag{4.39}$$

where we have made use of (4.32). The wave-function factors are obtained from the free-field on-shell residue constraint

$$\begin{aligned}
i\,(k^2 - M_{W,\mathrm{phys.}}^2)\,\mathrm{FT}\,\langle\,0\,|\mathrm{T}\,(\,W_\mu^{+,\mathrm{as}}(x)\,W_\nu^{-,\mathrm{as}}(y)\,)\,|\,0\,\rangle\,\Big|_{k^2=M_{W,\mathrm{phys.}}^2} &\equiv -\sum_{\lambda=\pm,0}\epsilon_\mu(k,\lambda)\,\epsilon_\nu^*(k,\lambda) \\
&= \left[Q_{\mu\nu}(k) - \frac{k^2}{\vec{k}^{\,2}}\,n_\mu n_\nu + \ldots\right]\Big|_{k^2=M_{W,\mathrm{phys.}}^2}\,,
\end{aligned} \tag{4.40}$$

where $M_{W,\mathrm{phys.}}$ is the physical mass of the W boson. Using (4.35) and (4.39) we find for the wave-function factor Z_W^{-1}

$$Z_W^{-1} = \frac{k^2 - M_{W,\mathrm{phys.}}^2 - \Sigma_{W,\mathrm{g}}}{k^2 - M_{W,\mathrm{phys.}}^2}\Big|_{k^2=M_{W,\mathrm{phys.}}^2}\,. \tag{4.41}$$

Now, again jumping ahead we can simplify these expressions in the Sudakov limit. In this particular limit $M_W \equiv M_{W,\text{phys.}}$ and hence no mass renormalization has to be performed, since this would imply an explicit energy dependence of the mass counterterm. This means that $\Sigma_{W,g} \sim (k^2 - M_W^2)$ (see section 4.3.2). By making use of similar arguments and taking the W bosons on-shell, D can be simplified in the Sudakov limit ($M_W^2 \ll k_0^2$) to

$$D \to -\frac{M_W^2}{\vec{k}^2} \frac{1}{k^2 - M_W^2 + \Sigma_\phi}. \tag{4.42}$$

Defining $Z_L^{-\frac{1}{2}} \equiv Z_W^{-\frac{1}{2}} + \delta Z_n$ we find

$$Z_L^{-1} = \frac{k^2 - M_W^2 + \Sigma_\phi}{k^2 - M_W^2}\Big|_{k^2=M_W^2}, \tag{4.43}$$

which we will see later is the wave-function factor for longitudinal W bosons.

A few comments are at order here. First, we like to stress the fact that for longitudinal W bosons the $Q_{\mu\nu}$ part of the propagator does not contribute and the remaining term proportional to $n_\mu n_\nu$ is mass suppressed (4.42), even after multiplication with the longitudinal polarization vector yielding a factor k_0/M_W. To be more precise, we first give the remaining coefficients of the Dyson-resummed propagator matrix in the on-shell Sudakov limit

$$F \to \frac{k_0}{M_W} D = -\frac{M_W}{k_0} \frac{1}{k^2 - M_W^2 + \Sigma_\phi} \tag{4.44}$$

$$G \to \frac{1}{k^2 - M_W^2 + \Sigma_\phi}, \tag{4.45}$$

which indeed illustrates that, in the longitudinal sector, the only non mass-suppressed propagator is the one containing exclusively the would-be Goldstone bosons. This is indeed the essence of the so-called Equivalence Theorem. That is, a non-vanishing matrix element for longitudinal W bosons at high energies is equivalent to the corresponding matrix element with the W bosons replaced by the would-be Goldstone bosons ϕ. Hence, at high energies the would-be Goldstone bosons effectively become physical Goldstone bosons, at the expense of the longitudinal degrees of freedom of the massive gauge bosons. This is exactly what one would expect if the SM were to behave like an unbroken theory at high energies.

Before we continue to establish the connection between the wave-function factors and the

calculation of the Sudakov logarithms we summarize the above. The dressed propagators are in the relevant Sudakov limit given by

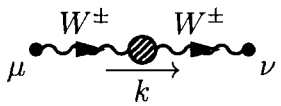

$$: \quad \frac{-i\,Q_{\mu\nu}}{k^2 - M_W^2 - \Sigma_{W,\mathrm{g}} + i\,\epsilon} + \frac{-i\,n_\mu n_\nu}{k^2 - M_W^2 + \Sigma_\phi + i\,\epsilon}\left(-\frac{k^2}{k_0^2}\right) \tag{4.46}$$

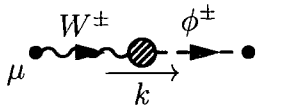

$$: \quad \frac{\mp i\,M_W}{k^2 - M_W^2 + \Sigma_\phi + i\,\epsilon}\,\frac{1}{k_0}\,n_\mu \tag{4.47}$$

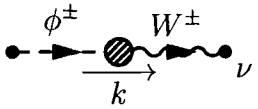

$$: \quad \frac{\mp i\,M_W}{k^2 - M_W^2 + \Sigma_\phi + i\,\epsilon}\,\frac{1}{k_0}\,n_\nu \tag{4.48}$$

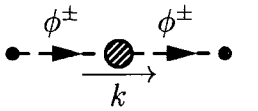

$$: \quad \frac{i}{k^2 - M_W^2 + \Sigma_\phi + i\,\epsilon}\,. \tag{4.49}$$

Now, to finish this section we consider the S-matrix element (the open circle denotes the amputated Green's function and the double line refers to the asymptotic state)

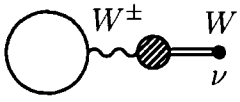

$$i\,(k^2 - M_W^2)\;\epsilon^\nu(k)\Big|_{k^2=M_W^2} =$$

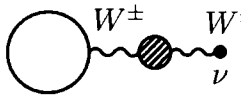

$$i\,(k^2 - M_W^2)\left[Z_W^{-\frac{1}{2}}\;\epsilon^\nu(k) + \delta Z_n\;n^\nu\,\epsilon_0(k)\right]\Big|_{k^2=M_W^2}\,,$$

where we have left the polarization state unspecified, bearing in mind that $\epsilon_T(k)\cdot n = 0$ and $\epsilon_L(k)\cdot n \approx k_0/M_W$ in the high energy limit. Upon amputation of the external legs we find in the relevant Sudakov limit

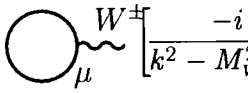

$$\left[\frac{-i\,Q^\mu{}_\nu}{k^2 - M_W^2 - \Sigma_{W,\mathrm{g}}} + \frac{-i\,n^\mu n_\nu}{k^2 - M_W^2 + \Sigma_\phi}\left(-\frac{k^2}{k_0^2}\right)\right] i(k^2 - M_W^2)\left[Z_W^{-\frac{1}{2}}\;\epsilon^\nu(k) + \delta Z_n\,n^\nu\,\epsilon_0(k)\right]\Big|_{k^2=M_W^2}$$

$$=$$

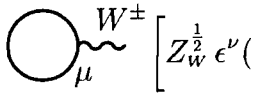

$$\left[Z_W^{\frac{1}{2}}\,\epsilon^\nu(k)\,Q^\mu{}_\nu + Z_L^{\frac{1}{2}}\,n^\mu\left(-\frac{M_W^2}{k_0^2}\right)\epsilon_0(k)\right]\Big|_{k^2=M_W^2}\,.$$

This is the most general result, from which we deduce that for transverse W bosons, with $\epsilon_T^\nu(k)\,Q^\mu{}_\nu = \epsilon_T^\mu(k)$ and $\epsilon_T(k)\cdot n = 0$, the contribution of Sudakov logarithms simply amounts

to multiplying each external transverse W boson line of the matrix element by the factor $Z_W^{\frac{1}{2}}$. For longitudinal W bosons $\epsilon_L^\nu(k)\, Q^\mu{}_\nu = 0$ and $\epsilon_L(k) \cdot n \approx k_0/M_W$ and we find a mass suppressed contribution $\sim M_W/k_0$.

Similarly we obtain for the mixed self-energy

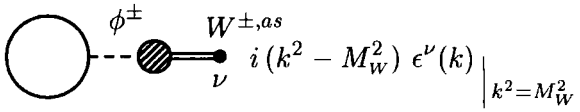

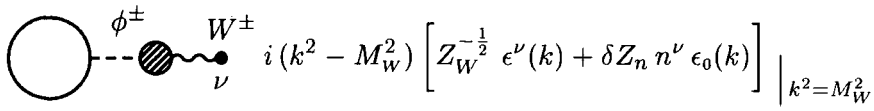

and amputating the legs yields in the relevant Sudakov limit

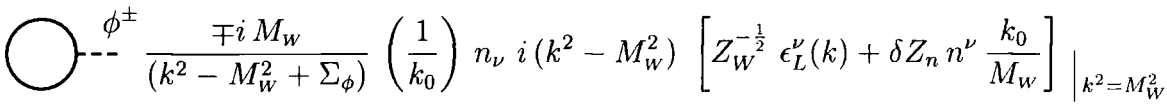

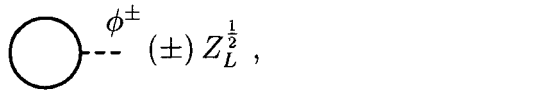

in the case of longitudinal polarization and no contribution in the case of transversely polarized W bosons. That is we find for longitudinal W bosons that the dominant contribution to any physical process originates from the amputated Green's-function where the amputated leg is a would-be Goldstone boson ϕ, provided that the matrix element is not mass suppressed to start with. The contribution where the amputated leg is a W boson contracted with the temporal gauge vector is mass suppressed.

In the Sudakov limit the Equivalence Theorem comes quite naturally out of the above consideration in the Coulomb gauge. This is based on the presence of mixed gauge-boson/would-be Goldstone boson propagators. A minor complication, in the full assessment of the Equivalence Theorem, arises due to these mixed propagators. Namely we have to show that the S-matrix element with the asymptotic state $\phi^{\pm\,\mathrm{as}}$ will not exhibit a leading contribution for the amputated Green's-function where the amputated leg is a W boson. And finally we will have to show that the dominant contribution is again the one where the amputated leg is a would-be Goldstone boson.

In order to study those S-matrix elements we first have to define the asymptotic state for the would-be Goldstone boson: $\phi^{\pm,\mathrm{as}}(x) = Z_\phi^{-\frac{1}{2}}\,\phi^{\pm}(x)$. For the propagator we find

$$\begin{aligned}\mathrm{FT}\,\langle\,0\,|\mathrm{T}\,(\,\phi^{+,\mathrm{as}}(x)\,\phi^{-,\,\mathrm{as}}(y)\,)\,|\,0\,\rangle &= \mathrm{FT}\,\langle\,0\,|\mathrm{T}\,(Z_\phi^{-\frac{1}{2}}\,\phi^{+}(x)\,Z_\phi^{-\frac{1}{2}}\phi^{-}(y)\,)\,|\,0\,\rangle \\ &\to Z_\phi^{-1}\,\frac{i}{k^2 - M_W^2 + \Sigma_\phi + i\,\epsilon}\,,\end{aligned} \tag{4.50}$$

and

$$(-i)\,(k^2 - M_W^2)\,\mathrm{FT}\,\langle\,0\,|\mathrm{T}\,(\,\phi^{+,\mathrm{as}}(x)\,\phi^{-,\,\mathrm{as}}(y)\,)\,|\,0\,\rangle\Big|_{k^2=M_W^2} \equiv 1 \tag{4.51}$$

where we have made use of the dyson-resummed propagator (4.49) and the requirement to retrieve the free-field propagator for the asymptotic states in the on-shell limit. Hence the wave-function factor Z_ϕ^{-1} is given by (compare to (4.43))

$$Z_\phi^{-1} = \frac{k^2 - M_W^2 + \Sigma_\phi}{k^2 - M_W^2}\Big|_{k^2=M_W^2} = Z_L^{-1}\,. \tag{4.52}$$

For the mixed S-matrix element we find

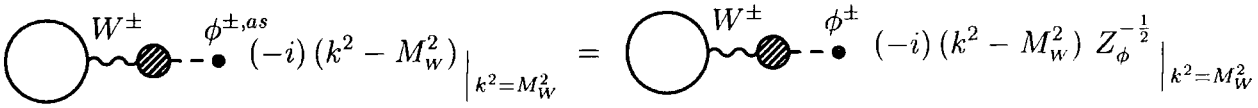

and amputating the legs leads in the relevant Sudakov limit to

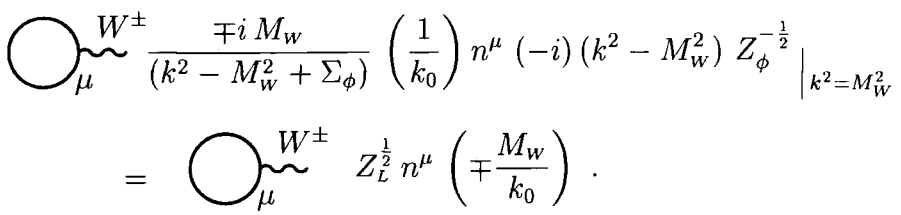

This again leads to mass suppression, which is what we had to show.

Similarly we obtain for the scalar self-energy

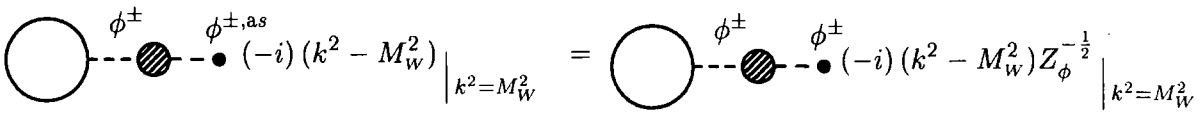

and amputation yields in the usual limit

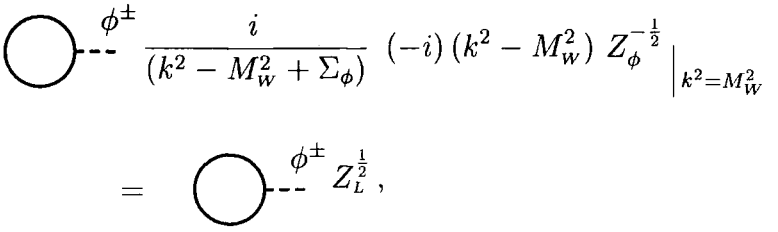

which is not only the leading contribution, but strikingly enough *identical* to the leading contribution we obtained from the asymptotic $W_\mu^{\pm\,\mathrm{as}}$ field. In the high energy Sudakov limit we do not only find the Equivalence Theorem $W_\mu^{\pm\,\mathrm{as}} \to \pm C\,\phi^{\pm\,\mathrm{as}}$ to hold in the Coulomb gauge for massive particles, but we find a very special case of the Equivalence Theorem, *i. e.* $C = 1$ to all orders in perturbation theory, meaning the *identity* of the two particles rather than mere *proportionality.*

We close this section with the following observations and conclusions. For transversely polarized *external* W bosons the mixing with the ϕ field vanishes and the Sudakov correction factor amounts to multiplying each external transverse W boson line of the matrix element by the factor $Z_W^{\frac{1}{2}}$. For longitudinally polarized *external* W bosons the correction factor $Z_W^{\frac{1}{2}}$ is mass suppressed and the dominant Sudakov correction factor amounts to multiplying each external longitudinal gauge boson line of the matrix element by the factor $Z_\phi^{\frac{1}{2}}$. (Provided that the matrix element is not mass suppressed to start with). This statement is a special case of the Equivalence Theorem where effectively the W bosons can be substituted by their would-be Goldstone bosons ϕ in the high energy limit.

4.3 Electroweak one-loop Sudakov logarithms

To establish the formalism that will be used in the following sections we are presenting here the one-loop calculation of the Sudakov logarithms in the Coulomb gauge [21]. For arbitrary final and initial state particles our calculations are in agreement with the well known one-loop contribution to the external wave-function factors $Z = 1 + \delta Z$.

4.3.1 The fermionic self-energy at one-loop level

As mentioned above, in order to determine the Sudakov logarithms in processes like $e^+e^- \to f\bar{f}$ one has to calculate the external self-energies (i.e. the wave-function factors) of all fermions involved in the process.

Consider to this end the fermionic one-loop self-energy $\Sigma_f^{(1)}(p, n, M_1)$, originating from the emission of a gauge boson V_1 with loop-momentum k_1 and mass M_1 from an effectively massless fermion[8] f with momentum p:

$$-i\,\Sigma_f^{(1)}(p,n,M_1) \quad =$$

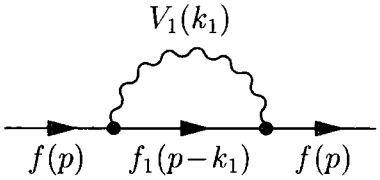

Again n is the unit vector in the time direction, which enters by virtue of using the Coulomb gauge. In the high-energy limit the fermion mass in the numerator of the fermion propagator can be neglected and similarly the contribution involving a mixed gauge-boson – Goldstone-boson propagator can be discarded. The self-energy $\Sigma_f^{(1)}$ then contains an odd number of γ-matrices, leading to the following natural decomposition in terms of the two possible structures $\not{p}$ and $\not{n}$:

$$\Sigma_f^{(1)}(p,n,M_1) \;\approx\; \left[\not{p}\,\Sigma_p^{(1)}(n\cdot p, p^2, M_1) + \not{n}\,\frac{p^2}{n\cdot p}\,\Sigma_n^{(1)}(n\cdot p, p^2, M_1)\right] e^2\,\Gamma_{ff_1V_1}^2 \;. \quad (4.53)$$

The coupling factor $\Gamma_{ff_1V_1}$ is defined according to

$$\Gamma_{ff_1V_1} \;=\; V_{ff_1V_1} - \gamma_5\,A_{ff_1V_1}\;, \quad (4.54)$$

where $V_{ff_1V_1}$ and $A_{ff_1V_1}$ are the vector and axial-vector couplings of the fermion f to the exchanged gauge boson V_1. In our convention these coupling factors read

$$\Gamma_{ff\gamma} \;=\; -Q_f, \qquad \Gamma_{ffZ} = \frac{(1-\gamma_5)\,I_f^3 - 2\,Q_f\,\sin^2\theta_w}{2\cos\theta_w\,\sin\theta_w}, \qquad \Gamma_{ff'W} = \frac{(1-\gamma_5)}{2\sqrt{2}\,\sin\theta_w}\;. \quad (4.55)$$

Here I_f^3 is the quantum number corresponding to the third component of the weak isospin, $e\,Q_f$ is the electromagnetic charge, and θ_w is the weak mixing angle. We have denoted the

[8]The massive case can be treated in a similar way since no mass renormalization is required. See previous section.

isospin partner of f with f'.

The contribution to the external wave-function factor now amounts to multiplying the self-energy by $i/\not{p}$ on the side where it is attached to the rest of the scattering diagram and by the appropriate fermion source on the other side. Finally the square root should be taken of the external wave-function factor, i.e. the one-loop contribution should be multiplied by the usual factor $1/2$. For an initial-state fermion, for example, one obtains[9]

$$\begin{aligned}\frac{1}{2}\,\frac{i}{\not{p}}\left[-i\,\Sigma_f^{(1)}(p,n,M_1)\right]u_f(p) &\approx \frac{e^2}{2}\,\Gamma^2_{ff_1V_1}\left[\Sigma_p^{(1)}(n\cdot p,m_f^2,M_1)+2\,\Sigma_n^{(1)}(n\cdot p,m_f^2,M_1)\right]u_f(p)\\ &\equiv \frac{1}{2}\,\delta Z_f\,u_f(p)\;, \end{aligned} \tag{4.56}$$

where m_f is the mass of the external fermion and $\sqrt{s}=2\,p_0$ is the center-of-mass energy of the process $e^+e^-\to f\bar{f}$. This contribution to the external wave-function factor $Z_f=1+\delta Z_f$ can be extracted from the full fermionic self-energy by means of the projection

$$\begin{aligned}\delta Z_f^{(1)}(V_1) &= \frac{i}{2\,p_0}\,\bar{u}_f(p)\left\{\frac{\partial}{\partial p_0}\left[-i\,\Sigma_f^{(1)}(p,n,M_1)\right]\right\}u_f(p)\\ &= \frac{i}{2\,p_0}\,\bar{u}_f(p)\left\{\frac{\partial}{\partial\,p_0}\int\frac{\mathrm{d}^4k_1}{(2\,\pi)^4}\,(ie\,\gamma_\nu\,\Gamma_{ff_1V_1})\,\frac{i}{(\not{p}-\not{k}_1)-m_f+i\epsilon}\,(ie\,\gamma_\mu\,\Gamma_{ff_1V_1})\,P^{\mu\nu}(k_1)\right\}u_f(p)\\ &\approx \frac{-e^2}{2\,p_0}\,\bar{u}_f(p)\int\frac{\mathrm{d}^4k_1}{(2\,\pi)^4}\,\frac{(\gamma_\nu\not{p})\,\gamma^0\,(\not{p}\,\gamma_\mu)}{[(p-k_1)^2-m_f^2+i\epsilon]^2}\,P^{\mu\nu}(k_1)\,\Gamma^2_{ff_1V_1}\,u_f(p)\\ &\approx -\,e^2\,\Gamma^2_{ff_1V_1}\int\frac{\mathrm{d}^4k_1}{(2\,\pi)^4}\,\frac{4\,p_\mu\,p_\nu}{[(p-k_1)^2-m_f^2+i\epsilon]^2}\,P^{\mu\nu}(k_1)\;, \end{aligned} \tag{4.57}$$

where we have made use of (A.176) and $\bar{u}_f(p)\,\gamma^0 u_f(p)=2\,p_0$ as well as

$$\frac{\partial}{\partial\,p_\mu}\,\frac{1}{\not{p}}=-\frac{1}{\not{p}}\,\gamma^\mu\,\frac{1}{\not{p}}\,. \tag{4.58}$$

Note also that the loop-momentum k_1 has been neglected in the numerator of the fermion propagator, since only collinear-soft gauge-boson momenta will give rise to the Sudakov logarithms. The mass of the fermion inside the loop, m_{f_1}, is at best of the order of the

[9] For an outgoing fermion one obtains $\frac{1}{2}\,\bar{u}_f(p)\,\delta\,\tilde{Z}_f^{(1)}$, where $\delta\,\tilde{Z}_f^{(1)}$ can be derived from $\delta\,Z_f^{(1)}$ by reversing the sign in front of γ_5.

Z-boson mass (for the top-quark). At the leading-logarithmic level it therefore only enters as an independent mass scale if the exchanged gauge boson is a photon (i.e. $m_{f_1} = m_f$), where the fermion mass is needed for the regularization of collinear singularities.
In the last step of (4.57) we have exploited the fact that $\delta Z_f^{(1)}$ will be multiplied on the right by $u_f(p)$, so writing $\Gamma^2_{ff_1V_1}$ or its projections on left/right-handed chiral couplings $(V_{ff_1V_1} \pm A_{ff_1V_1})^2$ is effectively equivalent.
Making use of the explicit form of the propagator in the coulomb gauge (4.21) the numerator can be simplified

$$\begin{aligned}(i)\left[k_1^2 - M_1^2 + i\epsilon\right] 4\, p_\mu\, p_\nu\, P^{\mu\nu}(k_1) &\approx \frac{4}{\vec{k_1}^2}\left[(p\cdot k_1)^2 - k_{1\,0}\, p_0\, 2\,(p\cdot k_1)\right] \\ &= \frac{1}{\vec{k_1}^2}\left[(p-k_1)^2 - p^2 - k_1^2\right]^2 + \frac{4\,k_{1\,0}\,p_0}{\vec{k_1}^2}\left[(p-k_1)^2 - p^2 - k_1^2\right].\end{aligned} \tag{4.59}$$

As we will see below, in order to obtain double logarithms the fermion as well as the gauge boson propagator are needed. Now $p^2 = m_f^2$ and the terms k_1^2 and $(p-k_1)^4$ will kill one of the types of denominators. Thus we are left with

$$(i)\left[k_1^2 - M_1^2 + i\epsilon\right] 4\, p_\mu\, p_\nu\, P^{\mu\nu}(k_1) \;\approx\; \frac{4\,k_{1\,0}\,p_0}{\vec{k_1}^2}\left[(p-k_1)^2 - m_f^2\right]. \tag{4.60}$$

Therefore

$$\delta\, Z_f^{(1)}(V_1) \;\approx\; -e^2\,\Gamma^2_{ff_1V_1}\int \frac{\mathrm{d}^4k_1}{(2\,\pi)^4}\,\frac{4\,k_{1\,0}\,p_0}{\vec{k_1}^2}\,\frac{-i}{[(p-k_1)^2 - m_f^2 + i\epsilon]\,[k_1^2 - M_1^2 + i\epsilon]}, \tag{4.61}$$

Having two canonical momenta at our disposal, i.e. p and n, we define the following Sudakov parametrisation of the gauge-boson loop-momentum k_1:

$$k_1 = v_1\, q + u_1\, \bar{q} + k_{1_\perp}\,, \tag{4.62}$$

with

$$\begin{aligned} p^\mu &\equiv (E, \beta_f E, 0, 0)\,, & \beta_f &= \sqrt{1 - m_f^2/E^2}\,, & s &= 4\,E^2, \\ q^\mu &= (E, E, 0, 0)\,, & \bar{q}^\mu &= (E, -E, 0, 0)\,, & k_{1_\perp}^\mu &= (0, 0, \vec{k}_{1_\perp})\,. \end{aligned} \tag{4.63}$$

In terms of this parametrisation, the integration measure d^4k_1, the invariants $(p\cdot k_1)$ and k_1^2, and the gauge-boson energy k_1^0 read

$$\begin{aligned}
\mathrm{d}^4k_1 &= \pi\frac{s}{2}\,\mathrm{d}v_1\,\mathrm{d}u_1\,\mathrm{d}\vec{k}_{1_\perp}^{\,2}\;,\\
(p\cdot k_1) &= \frac{s}{4}\left[v_1\,(1-\beta_f)+u_1\,(1+\beta_f)\right]\approx\frac{s}{2}\left(u_1+\frac{m_f^2}{s}\,v_1\right)\;,\\
k_1^2 &= s\,v_1\,u_1-\vec{k}_{1_\perp}^{\,2}\qquad\text{and}\qquad k_1^0=\frac{\sqrt{s}}{2}\,(v_1+u_1)\;.
\end{aligned}\tag{4.64}$$

The term containing the fermion mass m_f is needed for the exchange of photons only, regulating the collinear singularity at $u_1 = 0$. For the exchange of a massive gauge boson the mass M_1 will be the dominant collinear as well as infrared regulator.

The v_1-integration is restricted to the interval $0 \le v_1 \le 1$, as a result of the requirement of having poles in both hemispheres of the complex u_1-plane. The residue is then taken in the lower hemisphere in the pole of the gauge-boson propagator: $s\,v_1\,u_1^{\mathrm{res}} = \vec{k}_{1_\perp}^{\,2} + M_1^2 \equiv s\,v_1\,y_1$. Finally, $\vec{k}_{1_\perp}^{\,2}$ is substituted by y_1, with the condition $\vec{k}_{1_\perp}^{\,2} \ge 0$ translating into $v_1\,y_1 \ge M_1^2/s$. The one-loop Sudakov contribution to δZ_f now reads

$$\begin{aligned}
\delta\,Z_f^{(1)}(V_1) &\approx -\frac{\alpha}{\pi}\,\Gamma^2_{ff_1V_1}\int_0^\infty \mathrm{d}y_1\int_0^1 \mathrm{d}v_1\,\frac{\Theta(v_1y_1-\frac{M_1^2}{s})}{(y_1+\frac{m_f^2}{s}v_1)\,(v_1+y_1)}\\
&\approx -\frac{\alpha}{\pi}\,\Gamma^2_{ff_1V_1}\int_0^1\frac{\mathrm{d}y_1}{y_1}\int_{y_1}^1\frac{\mathrm{d}z_1}{z_1}\,\mathcal{K}^{(1)}(s,m_f^2,M_1,y_1,z_1)\;,
\end{aligned}\tag{4.65}$$

with the integration kernel $\mathcal{K}^{(1)}$ given by

$$\mathcal{K}^{(1)}(s,m_f^2,M_1,y_1,z_1) = \Theta\Big(y_1z_1-\frac{M_1^2}{s}\Big)\,\Theta\Big(y_1-\frac{m_f^2}{s}\,z_1\Big)\;.\tag{4.66}$$

Here we introduced the energy variable $z_1 = v_1 + y_1$ and made use of the fact that only collinear-soft gauge-boson momenta are responsible for the quadratic large-logarithmic effects: $y_1,\, z_1 \ll 1$. As a result, the gauge boson inside the loop is effectively on-shell and transversely polarized (see (4.21) with $k^2 \ll \vec{k}^2$ in the collinear regime). The same result can be obtained by means of the dispersion method. The dispersion method proceeds via the computation of the absorptive part by applying the Cutkosky cutting rule, which

effectively puts both the internal gauge boson and fermion on-shell, whereas the external fermion becomes off-shell. Subsequently the real part is obtained by using dispersion-integral (Cauchy-integral) techniques, turning the internal fermion off-shell and allowing the external fermion to be on-shell.

The exchanged gauge boson can either be a massless photon (γ) or one of the massive weak bosons (W or Z). The associated mass gap gives rise to distinctive differences in the two types of contributions. Bearing in mind that the SM is not parity conserving and making use of (D.217) and (D.218) we present the one-loop Sudakov correction factors for right- and left-handed fermions/antifermions separately:

$$\delta Z_{f_R}^{(1)}(\gamma) = \left[\left(\frac{Y_f^R}{2}\right)^2\right] \mathrm{L}_\gamma(\lambda, m_f) = Q_f^2\, \mathrm{L}_\gamma(\lambda, m_f)\ , \tag{4.67a}$$

$$\delta Z_{f_L}^{(1)}(\gamma) = \left[\left(I_f^3\right)^2 + I_f^3 Y_f^L + \left(\frac{Y_f^L}{2}\right)^2\right] \mathrm{L}_\gamma(\lambda, m_f) = Q_f^2\, \mathrm{L}_\gamma(\lambda, m_f)\ , \tag{4.67b}$$

$$\delta Z_{f_R}^{(1)}(W) = 0\ , \tag{4.67c}$$

$$\delta Z_{f_L}^{(1)}(W) = \frac{1}{2\sin^2\theta_\mathrm{w}}\, \mathrm{L}(M, M)\ , \tag{4.67d}$$

$$\delta Z_{f_R}^{(1)}(Z) = \frac{\sin^2\theta_\mathrm{w}}{\cos^2\theta_\mathrm{w}} \left(\frac{Y_f^R}{2}\right)^2 \mathrm{L}(M, M) = \left[\left(\frac{Y_f^R}{2\cos\theta_\mathrm{w}}\right)^2 - Q_f^2\right] \mathrm{L}(M, M)\ , \tag{4.67e}$$

$$\begin{aligned} \delta Z_{f_L}^{(1)}(Z) &= \left[\frac{\cos^2\theta_\mathrm{w}}{\sin^2\theta_\mathrm{w}} \left(I_f^3\right)^2 - I_f^3 Y_f^L + \frac{\sin^2\theta_\mathrm{w}}{\cos^2\theta_\mathrm{w}} \left(\frac{Y_f^L}{2}\right)^2\right] \mathrm{L}(M, M) \\ &= \left[\frac{1}{4\sin^2\theta_\mathrm{w}} + \left(\frac{Y_f^L}{2\cos\theta_\mathrm{w}}\right)^2 - Q_f^2\right] \mathrm{L}(M, M)\ , \end{aligned} \tag{4.67f}$$

with

$$\mathrm{L}(M_1, M_2) = -\frac{\alpha}{4\pi} \log\left(\frac{M_1^2}{s}\right) \log\left(\frac{M_2^2}{s}\right)\ , \tag{4.68}$$

$$\mathrm{L}_\gamma(\lambda, M_1) = -\frac{\alpha}{4\pi} \left[\log^2\left(\frac{\lambda^2}{s}\right) - \log^2\left(\frac{\lambda^2}{M_1^2}\right)\right]\ , \tag{4.69}$$

and $\delta Z_{f_R}^{(1)} = \delta Z_{f_L}^{(1)}$ for all three gauge bosons.

Note that these correction factors are the same for incoming as well as outgoing particles. In Eq. (4.67) $Y_f^{R,L}$ denotes the right- and left-handed hypercharge of the external fermion,

which is connected to the third component of the weak isospin I_f^3 and the electromagnetic charge $e\,Q_f$ through the Gell-Mann – Nishijima relation $Q_f = I_f^3 + Y_f^{R,L}/2$. The parameter λ is the fictitious (infinitesimally small) mass of the photon needed for regularizing the infrared singularity at $z_1 = 0$. For the sake of calculating the leading Sudakov logarithms, the masses of the W and Z bosons can be represented by one generic mass scale M.
In the process $e^+e^- \to f\bar{f}$ the one-loop correction factors presented in Eq. (4.67) contribute in the following way to the polarized matrix element, bearing in mind that at high energies the helicity eigenstates are equivalent to the chiral eigenstates:

$$\mathcal{M}^{1-\text{loop, sudakov}}_{e_R^+ e_L^- \to f_L \bar{f}_R} = \frac{1}{2}\left[\delta Z^{(1)}_{e_R^+} + \delta Z^{(1)}_{e_L^-} + \delta Z^{(1)}_{f_L} + \delta Z^{(1)}_{\bar{f}_R}\right] \mathcal{M}^{\text{born}}_{e_R^+ e_L^- \to f_L \bar{f}_R}\,, \tag{4.70}$$

and similar expressions for the other possible helicity combinations.

As promised, we come back to the issue of possible contributions to the Sudakov correction factor from self energies with fermions or ghosts in the upper loop. We saw in this section that the $1/\vec{k}^2$ part of the gauge boson propagator in the Coulomb gauge is crucial for obtaining double logarithmic contributions. Obviously the fermion propagator does not exhibit this feature. The ghost propagator contains the required $1/\vec{k}^2$, but lacks the pole structure $1/(k^2 - M^2)$ and hence no contribution to the Sudakov correction factor can be obtained.

To end the one-loop section on fermionic corrections we finally show the suppression of vertex corrections. The line of argument holds for box corrections as well.
We consider the following vertex correction where we assume for simplicity the exchanged particle as well as the incoming particle to be a photon

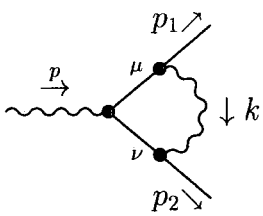

$$\sim \int \frac{\mathrm{d}^4k}{(2\,\pi)^4}\,\bar{u}(p_2)\,\gamma_\nu\,\frac{1}{[(\not{p}_2 - \not{k}) - m]}\,\not{\epsilon}(p)\,\frac{-1}{[(\not{p}_1 + \not{k}) + m]}\,\gamma_\mu\,P^{\mu\nu}(k)\,u(p_1)$$

$$\approx -\bar{u}(p_2)\,\not{\epsilon}(p)u(p_1)\int \frac{\mathrm{d}^4k}{(2\,\pi)^4}\,\frac{4\,p_{1\,\mu}\,p_{2\,\nu}\,P^{\mu\nu}(k)}{[(p_1+k)^2 - m^2]\,[(p_2-k)^2 - m^2]}\,. \tag{4.71}$$

With the Sudakov parametrisation $k = x\,p_1 + y\,p_2 + k_\perp$ and say $p_1^\mu \approx E(1,1,0,0)$ and

$p_2^\nu \approx E(1,-1,0,0)$ we obtain

$$i[k^2+i\epsilon]\, p_{1\,\mu}\, p_{2\,\nu}\, P^{\mu\nu}(k) = \left[p_1\cdot p_2 + \frac{p_1\cdot k\; p_2\cdot k}{\vec{k}^2} - \frac{k_0}{\vec{k}^2}\,(\,p_{1\,0}\,p_2\cdot k\; + p_{2\,0}\,p_1\cdot k\,)\right] \tag{4.72}$$

$$\approx \left[2\,E^2 + \frac{2\,E^2\,y\;\;2\,E^2\,x}{E^2\,(x+y)^2} - \frac{E^2\,(x+y)\;2\,E^2\,(y+x)}{E^2\,(x+y)^2}\right] \tag{4.73}$$

$$= \left[4\,E^2\,\frac{x\,y}{(x+y)^2}\right] \tag{4.74}$$

where we have made use of the on-shell condition $\vec{k}_\perp^2 \approx 4\,E^2\,x\,y$ and neglected mass terms. The remaining term will *not* lead to Sudakov logarithms since the numerator will kill both poles originating from the fermion propagators. Hence we conclude that the only term leading to Sudakov logarithms, *i. e.* $k_0\,(k^\mu n^\nu + n^\mu k^\nu)/\vec{k}^2$, is effectively rendered inactive for vertex corrections.[10]

The same argument holds for box corrections where again the $g_{\mu\nu}$ part of the propagator cancels the for Sudakov logarithms relevant part of the propagator.

4.3.2 The bosonic self-energy at one-loop level

In this section we are calculating the W boson self energy. As we have seen in section (4.2.1) transverse and longitudinal gauge bosons have to be treated separately. To all orders in perturbation theory the Sudakov correction factor for transverse W bosons is given by $Z_W^{\frac{1}{2}}$, for longitudinal W bosons by $Z_L^{\frac{1}{2}}$, which is obtained from the scalar ϕ self energy, which we will calculate in the next section. In this section we are calculating the one-loop Sudakov correction factor for transverse W bosons, *i. e.* $\delta Z_{W_T}^{(1)} = Z_{W_T} - 1$.

In the bosonic sector a substantial complication arises in the calculation of Sudakov logarithms which can be traced back to the presence of the mixed gauge-boson/would-be Goldstone boson propagator. The method of extracting the external wave-function factor Z from the full self energy by means of the derivative projection 'trick' has to be carefully reconsidered. In fact, as we will see later, the derivative-projection method is applicable for diagonal self energies, *i. e.* the amputated legs on both sides being the same particle. So

[10] Recall that in the case of the self energy $p\cdot p = m_f^2 \approx 0$ and the for Sudakov logarithms relevant term survives.

it applies to the charged W bosons. In the neutral sector where we have to deal with the mixing of the photon and the Z bosons more care is needed in defining the proper asymptotic states and the full analysis is postponed [23]. However, in the calculation of two-loop Sudakov correction factors the one-loop self energies of the neutral sector are indispensable. Therefore we come back to the neutral sector at the end of this section and derive some important features.

As we saw in section 4.2.1 the Sudakov correction factor for transverse gauge bosons amounts to multiplying the external line of the matrix element by $Z_W^{\frac{1}{2}}$. Recalling, that

$$Z_W^{-1} = \frac{k^2 - M_W^2 - \Sigma_{W,\mathrm{g}}}{k^2 - M_W^2}\Big|_{k^2=M_W^2},$$

and hence we have to calculate the $\mathrm{g}_{\mu\nu}$ part of the W self energy. We first have to select the contributing diagrams. The legs are amputated and hence fixed to be W bosons. That leaves 4×4 possible combinations of scalar, mixed and gauge-boson particle states in the upper and lower part of the loop, which are displayed in Fig. (4.1).

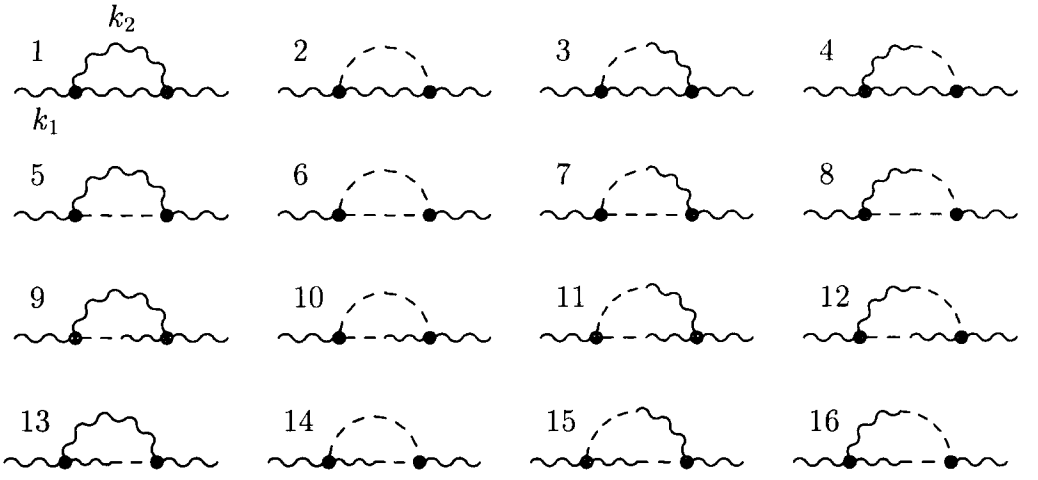

Figure 4.1: Possible contributions to the one-loop W self energy.

The only way to obtain $\mathrm{g}_{\mu\nu}$ contributions of the W self energy is if the lower particle in the loop, which by convention is the energetic one, is a gauge boson. The mixed- and scalar-propagator do not contain a $\mathrm{g}_{\alpha\beta}$ term and hence there is no way to contract the Lorenz index ν through to the other side of the diagram. In principle another way to achieve this

is by having a gauge boson as upper (soft) particle in the loop. However, as we have seen in the previous section, the presence of $1/|\vec{k}_2|$ is crucial for obtaining double logarithms. This eliminates the $g_{\alpha\beta}$ term in the propagator of the soft gauge boson as well as the $g_{\mu\nu}$ term from the tensor reduction of $k_{2\,\mu}k_{2\,\nu}/\vec{k}_2^{\,2} \xrightarrow{g_{\mu\nu}} k_{2\,\perp\mu}k_{2\,\perp\nu}/\vec{k}_2^{\,2} \leq 1$. Hence we are left with the first four diagrams, out of which diagram (2) does not contribute since the scalar propagator exhibits the required pole structure only at next to leading order $\sim M_W^2$ and an additional factor of M_W^2 originating from the two vertices leads to an overall mass suppressed contribution.

We start by calculating the $g_{\mu\nu}$ part of the W self energy of diagram (1) ($M_1 = M_2 = M_W$):

$$i\,\Sigma^{(1),V_4}_{W^\pm,\mu\nu}(V_3) \quad = \quad$$

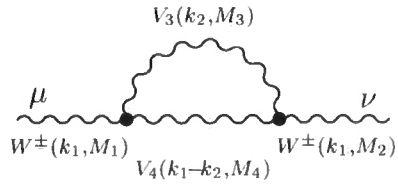

yielding

$$i\,\Sigma^{(1),V_4}_{W^\pm,\mu\nu}(V_3) = \int \frac{\mathrm{d}^4k_2}{(2\,\pi)^4}\,P^{\sigma\sigma'}(k_2)\,P^{\rho\rho'}(k_1-k_2)\,(ie\,G_{134})\,V_{\mu\sigma\rho}\,(ie\,G_{243})\,V_{\rho'\sigma'\nu}\,. \tag{4.75}$$

The totally antisymmetric coupling $e\,G_{ijl}$ is the triple gauge-boson coupling with all three gauge-boson lines (i,j,l) defined to be incoming at the interaction vertex, *i. e.* $G_{134}\,G_{243} = G_{W^\pm V_3 V_4}\,G_{W^\mp V_4^\dagger V_3^\dagger} = G^2_{W^\pm V_3 V_4}$ in the above expression. In our convention this coupling is fixed according to $G_{\gamma W^+W^-} = 1$ and $G_{ZW^+W^-} = -\cos\theta_\mathrm{w}/\sin\theta_\mathrm{w}$. The tensor structures of the two triple gauge boson interactions read

$$\begin{aligned} V_{\mu\sigma\rho} &= (k_1+k_2)_\rho\,\mathrm{g}_{\mu\sigma} + (-\mathrm{k}_2+\mathrm{k}_1-\mathrm{k}_2)_\mu\,\mathrm{g}_{\sigma\rho} + (-\mathrm{k}_1+\mathrm{k}_2-\mathrm{k}_1)_\sigma\,\mathrm{g}_{\mu\rho} \\ &\to -(2\,k_1-k_2)_\sigma\,\mathrm{g}_{\mu\rho} \qquad (4.76) \\ V_{\rho'\sigma'\nu} &= -\Big[(k_2-k_1+k_2)_\nu\,\mathrm{g}_{\sigma'\rho'} + (\mathrm{k}_1-\mathrm{k}_2+\mathrm{k}_1)_{\sigma'}\,\mathrm{g}_{\rho'\nu} + (-\mathrm{k}_1-\mathrm{k}_2)_{\rho'}\,\mathrm{g}_{\sigma'\nu}\Big] \\ &\to -(2\,k_1-k_2)_{\sigma'}\,\mathrm{g}_{\rho'\nu} \qquad (4.77) \end{aligned}$$

where we have selected the part eventually leading to $g_{\mu\nu}$ once we consider $P^{\rho\rho'}(k_1-k_2) \to (-i)\,\mathrm{g}^{\rho\rho'}/[(\mathrm{k}_1-\mathrm{k}_2)^2 - \mathrm{M}_4^2 + \mathrm{i}\epsilon\,]$ (see discussion above).

Let us leave the soft particle V_3 unspecified for the time being, *i. e.* $V_3 = \gamma, Z, W$ are all possible. With

$$\begin{aligned}
&(i)\left[k_2^2 - M_3^2 + i\epsilon\right](2\,k_1 - k_2)_\sigma\,(2\,k_1 - k_2)_{\sigma'}\;P^{\sigma\sigma'}(k_2) \\
&\qquad\approx\;(2\,k_1 - k_2)_\sigma\,(2\,k_1 - k_2)_{\sigma'}\left[\frac{-k_{2\,0}}{\vec{k}_2^{\,2}}\left(k_{2\,\sigma}\,n_{\sigma'} + n_\sigma\,k_{2\,\sigma'}\right)\right] \\
&\qquad\approx\;-\frac{2\,k_{2\,0}}{\vec{k}_2^{\,2}}\left[(2\,k_1\cdot k_2 - k_2^2)\,(2\,k_{1\,0} - k_{2\,0})\right] \\
&\qquad\approx\;\frac{4\,k_{1\,0}\,k_{2\,0}}{\vec{k}_2^{\,2}}\left((k_1 - k_2)^2 - k_1^2 - k_2^2 + k_2^2\right). \qquad (4.78)
\end{aligned}$$

we then obtain for the $g_{\mu\nu}$ part of the W boson self energy

$$\begin{aligned}
i\,\Sigma_{W,\mathrm{g}}^{(1),V_4}(V_3) &\approx\; e^2\,G_{134}\,G_{243}\int\frac{\mathrm{d}^4k_2}{(2\,\pi)^4}\,\frac{(2\,k_1 - k_2)_\sigma\,(2\,k_1 - k_2)_{\sigma'}\,i\,P^{\sigma\sigma'}(k_2)}{[(k_1 - k_2)^2 - M_4^2 + i\epsilon\,]} \\
&\approx\; e^2\,G_{134}\,G_{243}\int\frac{\mathrm{d}^4k_2}{(2\,\pi)^4}\,\frac{4\,k_{1\,0}\,k_{2\,0}}{\vec{k}_2^{\,2}}\,\frac{\left((k_1 - k_2)^2 - M_4^2\;+ M_4^2 - k_1^2\right)}{[(k_1 - k_2)^2 - M_4^2 + i\epsilon\,]\,[k_2^2 - M_3^2 + i\epsilon\,]} \\
&\approx\; -\,e^2\,G_{134}\,G_{243}\int\frac{\mathrm{d}^4k_2}{(2\,\pi)^4}\,\frac{4\,k_{1\,0}\,k_{2\,0}}{\vec{k}_2^{\,2}}\,\frac{\left(k_1^2 - M_4^2\right)}{[(k_1 - k_2)^2 - M_4^2 + i\epsilon\,]\,[k_2^2 - M_3^2 + i\epsilon\,]}\,, \qquad (4.79)
\end{aligned}$$

in the Sudakov limit.

In the case of V_3 being a neutral gauge boson (N) and hence V_4 being the W boson ($M_4 = M_W$) we are left with

$$i\,\Sigma_{W,\mathrm{g}}^{(1)}(\gamma) = [k_1^2 - M_W^2]\;\mathcal{F}(\lambda, M_W) \qquad (4.80)$$

$$i\,\Sigma_{W,\mathrm{g}}^{(1)}(Z) = \frac{\cos^2\theta_\mathrm{w}}{\sin^2\theta_\mathrm{w}}\,[k_1^2 - M_W^2]\;\mathcal{F}(M_Z, M_W)\,, \qquad (4.81)$$

with

$$\mathcal{F}(M_3, M_4) = -(e)^2\int\frac{\mathrm{d}^4k_2}{(2\,\pi)^4}\,\frac{4\,k_{1\,0}\,k_{2\,0}}{\vec{k}_2^{\,2}}\,\frac{1}{[(k_1 - k_2)^2 - M_4^2 + i\epsilon\,]\,[k_2^2 - M_3^2 + i\epsilon\,]}\,. \qquad (4.82)$$

Now from (4.41) we recall that

$$\delta Z_{W_T}^{(1)} = \frac{\Sigma_{W,\mathrm{g}}^{(1)}}{(k_1^2 - M_W^2)}\,\Big|_{k_1^2 = M_W^2}\,. \qquad (4.83)$$

and hence the Sudakov correction factor reads

$$\delta Z^{(1)}_{W_T}(N) = (-i)\, G_{134}\, G_{243}\, \mathcal{F}(M_N, M_W)\,. \tag{4.84}$$

Note here that diagrams (3) and (4) do *not* contribute in the above case of V_3 being a neutral particle. Firstly the photon does not have a would-be Goldstone boson partner. Secondly the $Z\chi$ and χZ mixing propagator is at both ends attached to two W bosons and a quick check of the Feynman rules in Appendix B reveals that the χ does not couple to two W bosons. Hence the diagrams (3) and (4) don't contribute.
Apart from the couplings (4.84) is identical to (4.61). Hence the required steps to eventually obtain the double logarithms are identical to the ones given explicitly in the fermion sector. The one-loop Sudakov correction factor for transverse W bosons is for the photon and the Z boson respectively

$$\delta Z^{(1)}_{W_T}(\gamma) = Q_W^2\, \mathrm{L}_\gamma(\lambda, M)\,, \tag{4.85a}$$

$$\delta Z^{(1)}_{W_T}(Z) = \frac{\cos^2\theta_\mathrm{w}}{\sin^2\theta_\mathrm{w}}\, \mathrm{L}(M,M) = \left[\frac{1}{\sin^2\theta_\mathrm{w}} - Q_W^2\right] \mathrm{L}(M,M) \tag{4.85b}$$

with $\mathrm{L}_\gamma(\lambda, M)$ and $\mathrm{L}(M,M)$ being defined in (4.69) and (4.68).

Now, for V_3 being the W boson and hence V_4 being either a photon or a Z boson we have to calculate diagrams (3) and (4). Leaving the charge of the mixed propagator general, we obtain

$i\,\Sigma^{(1),N}_{W^\pm,\mu\nu}(\phi W)$ =

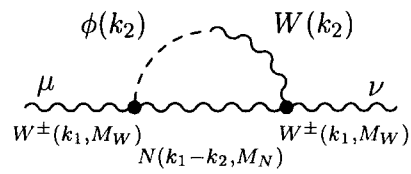

$$= \int \frac{\mathrm{d}^4 k_2}{(2\,\pi)^4}\, (-ie\,\widetilde{G}_N\, M_W)\, \mathrm{g}_{\mu\rho}\, \mathrm{P}^{\rho\rho'}(\mathrm{k}_1 - \mathrm{k}_2)\, \frac{\mp \mathrm{i}\mathrm{M}_\mathrm{W}}{[\mathrm{k}_2^2 - \mathrm{M}_\mathrm{W}^2 + \mathrm{i}\epsilon\,]}\, \frac{\mathrm{k}_{20}}{\vec{\mathrm{k}}_2^{\,2}}\, \mathrm{n}^{\sigma'}\, (\mathrm{ie}\,\mathrm{G}_{\mathrm{W}\mp\mathrm{NW}\pm})\, \mathrm{V}_{\rho'\sigma'\nu} \tag{4.86}$$

where we have introduced the abbreviation $\widetilde{G}_\gamma = 1$ and $\widetilde{G}_Z = \sin\theta_\mathrm{w}/\cos\theta_\mathrm{w}$. Again the triple

gauge boson vertex can be simplified according to (4.77): $V_{\rho'\sigma'\nu} \to [-(2\,k_1 - k_2)_{\sigma'}\,g_{\rho'\nu}]$. Considering that the $k_{2\sigma'}$ term contracted with $n^{\sigma'}$ together with the already present k_{20} will kill the crucial $1/\vec{k_2}^{\,2}$ we can safely ignore it. Selecting the $g_{\mu\nu}$ part this can be written as

$$i\,\Sigma^{(1),N}_{W,\mathrm{g}}\,(\phi W) = -(e)^2\,\widetilde{G}_N\,G_{W^\mp N W^\pm}\int\frac{\mathrm{d}^4k_2}{(2\,\pi)^4}\,\frac{2\,k_{20}\,k_{10}}{\vec{k_2}^{\,2}}\,\frac{\mp M_W^2}{[(k_1-k_2)^2-M_N^2+i\epsilon\,]\,[k_2^2-M_W^2+i\epsilon\,]}\,, \tag{4.87}$$

and for the contribution from diagram (4) we can immediately write

$$i\,\Sigma^{(1),N}_{W,\mathrm{g}}\,(W\phi) = -(e)^2\,\widetilde{G}_N\,G_{W^\pm W^\mp N}\int\frac{\mathrm{d}^4k_2}{(2\,\pi)^4}\,\frac{2\,k_{20}\,k_{10}}{\vec{k_2}^{\,2}}\,\frac{\mp M_W^2}{[(k_1-k_2)^2-M_N^2+i\epsilon\,]\,[k_2^2-M_W^2+i\epsilon\,]}\,. \tag{4.88}$$

Note that due to $G_{W^\pm W^\mp N} = G_{W^\mp N W^\pm}$ (4.87) and (4.88) are identical.

Hence upon adding up all three contributions (*i. e.* the gauge-boson propagator and the two mixed propagators) we find for the neutral particle being a photon, $[G_{W^\pm W^\mp\gamma} = G_{W^\mp\gamma W^\pm} = \pm 1\,,\ \widetilde{G}_\gamma = 1]$

$$i\,\Sigma^{(1),\gamma}_{W,\mathrm{g}}(W{+}\phi W{+}W\phi) = \left([k_1^2-\lambda^2]-M_W^2\right)\,\mathcal{F}(M_W,\lambda)\,, \tag{4.89}$$

where we can neglect the photon mass λ in the prefactor.

For the neutral particle being the Z boson, $[G_{W^\pm W^\mp Z} = G_{W^\mp Z W^\pm} = \mp\cos\theta_\mathrm{w}/\sin\theta_\mathrm{w}$, $\widetilde{G}_Z = \sin\theta_\mathrm{w}/\cos\theta_\mathrm{w}]$ and making use of $M_Z^2\,\cos^2\theta_\mathrm{w} = M_W^2$ we find

$$\begin{aligned} i\,\Sigma^{(1),Z}_{W,\mathrm{g}}(W{+}\phi W{+}W\phi) &= \left(\frac{\cos^2\theta_\mathrm{w}}{\sin^2\theta_\mathrm{w}}\,[k_1^2-M_Z^2]+M_W^2\right)\,\mathcal{F}(M_W,M_Z) \\ &= \left(k_1^2\,\frac{\cos^2\theta_\mathrm{w}}{\sin^2\theta_\mathrm{w}}-\frac{M_W^2}{\sin^2\theta_\mathrm{w}}+M_W^2\right)\,\mathcal{F}(M_W,M_Z) \\ &= \left(\frac{\cos^2\theta_\mathrm{w}}{\sin^2\theta_\mathrm{w}}[k_1^2-M_W^2]\right)\,\mathcal{F}(M_W,M_Z)\,, \end{aligned} \tag{4.90}$$

with $\mathcal{F}$ defined in (4.82). For the Sudakov correction factor we find a contribution to $\delta Z^{(1)}_{W_T}$ of the generic form[11]

$$-\,e^2\,G_{134}\,G_{243}\int\frac{\mathrm{d}^4k_2}{(2\,\pi)^4}\,\frac{4\,k_{10}\,k_{20}}{\vec{k_2}^{\,2}}\,\frac{-i}{[(k_1-k_2)^2-M_4^2+i\epsilon\,]\,[k_2^2-M_3^2+i\epsilon\,]} \tag{4.91}$$

[11] Note that the product of the two triple gauge boson vertices is even under the replacement $W^+ \leftrightarrow W^-$.

using the labelling $1 \ldots 4$ defined in the 'pure' gauge boson self energy. This expression is in perfect agreement with (4.84). Upon summation over the internal neutral particles we obtain

$$\begin{aligned}\delta Z^{(1)}_{W_T}\,(W+\phi W+W\phi) &= \frac{1}{\sin^2\theta_{\rm w}}\,{\rm L}(M,M)+Q_W^2\left[{\rm L}(M,M)-{\rm L}(M,M)\right]\\ &= \frac{1}{\sin^2\theta_{\rm w}}\,{\rm L}(M,M)\end{aligned} \tag{4.92}$$

again with $\mathrm{L}(M,M)$ being defined in (4.68).

Once having established this we might wonder whether in this particular case of a diagonal W self energy the derivative 'trick' would have led to the same result. Assume we could have used

$$\begin{aligned}\delta Z_{W_T} &= \frac{i}{2\,k_{1\,0}}\,\epsilon_T^{\mu}(k_1)\left\{\frac{\partial}{\partial\,k_{1\,0}}\left[i\Sigma^{(1)}_{W^{\pm},\mu\nu}(V_3)\right]\right\}\epsilon_T^{*\,\nu}(k_1)\\ &\approx \frac{i}{2\,k_{1\,0}}\,\epsilon_T^{\mu}(k_1)\left\{\frac{\partial}{\partial\,k_{1\,0}}\left[\int\frac{{\rm d}^4k_2}{(2\,\pi)^4}\,P^{\sigma\sigma'}(k_2)\,P^{\rho\rho'}(k_1-k_2)\,(ie\,G_{134})\,V_{\mu\sigma\rho}\,(ie\,G_{243})\,V_{\rho'\sigma'\nu}\right]\right\}\epsilon_T^{*\,\nu}(k_1)\,.\end{aligned} \tag{4.93}$$

Here the contraction with the transverse polarization vectors $\epsilon_T^{\mu}(k_1)$ and $\epsilon_T^{*\,\nu}(k_1)$ projects on $-\mathrm{g}_{\mu\nu}$ and the derivative $\frac{1}{2\,k_{1\,0}}\,\frac{\partial}{\partial k_{1\,0}}$ projects on the on-shell wave-function factor. The latter hinges on the fact that $\Sigma^{(1)}_{W,\mathrm{g}}\sim(k_1^2-M_W^2)$. The vertex structures simplify to $V_{\mu\sigma\rho}\approx -2\,k_{1\,\sigma}\,\mathrm{g}_{\mu\rho}$ and $V_{\rho'\sigma'\nu}\approx -2\,k_{1\,\sigma'}\,\mathrm{g}_{\rho'\nu}$ since here we can neglect the momentum k_2 with respect to k_1. [This will at the most lead to a term $\sim k_2^2$. Since the factor $\frac{1}{k_1^2-M_W^2}$ has been replaced by the derivative in this approach, such a term is suppressed.] Making use of $\epsilon_T(k_1)\cdot k_1=0$, $\epsilon_T(k_1)\cdot\epsilon_T^{*}(k_1)=-1$ and $\epsilon_T(k_1)\cdot n=0$ we find

$$\begin{aligned}\delta Z_{W_T} &\approx \frac{-i\,e^2}{2\,k_{1\,0}}\,\epsilon_T^{\mu}(k_1)\left\{\frac{\partial}{\partial\,k_{1\,0}}\left[\int\frac{{\rm d}^4k_2}{(2\,\pi)^4}\,4\,k_{1\,\sigma}\,k_{1\,\sigma'}\,P^{\sigma\sigma'}(k_2)\,P^{\mu\nu}(k_1-k_2)\,G_{134}\,G_{243}\right]\right\}\epsilon_T^{*\,\nu}(k_1)\\ &\approx \frac{-i\,e^2}{2\,k_{1\,0}}\,\epsilon_T^{\mu}(k_1)\left\{\frac{\partial}{\partial\,k_{1\,0}}\left[\int\frac{{\rm d}^4k_2}{(2\,\pi)^4}\,4\,k_{1\,\sigma}\,k_{1\,\sigma'}\,P^{\sigma\sigma'}(k_2)\,\frac{\mathrm{g}^{\mu\nu}\,(-\mathrm{i})}{[(k_1-k_2)^2-M_4^2+i\epsilon\,]}\,G_{134}\,G_{243}\right]\right\}\epsilon_T^{*\,\nu}(k_1)\\ &= -e^2\,G_{134}\,G_{243}\int\frac{{\rm d}^4k_2}{(2\,\pi)^4}\,\frac{4\,k_{1\,\sigma}\,k_{1\,\sigma'}\,P^{\sigma\sigma'}(k_2)}{[(k_1-k_2)^2-M_4^2+i\epsilon\,]^2}\,.\end{aligned} \tag{4.94}$$

And, indeed, for the diagonal self energy (*i. e.* the same particle in both amputated legs) we find agreement between the two methods.

Now, we jump slightly ahead and also present the full self energy for neutral particles, which is needed later at two loop level for the so-called 'frog' diagrams. In those diagrams the neutral particles are effectively transverse, but not necessarily on-shell (being virtual particles). Hence the precise definition of the asymptotic states in the neutral sector is not an issue. It is important to notice that we will need the full one-loop self energy (rather than the derivative) to calculate the contribution from the 'frog' diagrams, the reason being that the external legs are not necessarily on-shell. In the case of the one-loop γZ-mixing self energy it is even impossible that both external legs are on-shell.

From (4.79), (4.87) and (4.88), inserting the appropriate couplings, we obtain[12]

$$i\,\Sigma^{(1)}_{\gamma\gamma,\mathrm{g}}(W{+}\phi W{+}W\phi) = \left([k_1^2 - M_W^2] + M_W^2\right)\,\mathcal{F}(M_W, M_W) \tag{4.95}$$

$$i\,\Sigma^{(1)}_{ZZ,\mathrm{g}}(W{+}\phi W{+}W\phi) = \left(\frac{\cos^2\theta_\mathrm{w}}{\sin^2\theta_\mathrm{w}}\,[k_1^2 - M_W^2] - M_W^2\right)\,\mathcal{F}(M_W, M_W) \tag{4.96}$$

$$i\,\Sigma^{(1)}_{\gamma Z,\mathrm{g}}(W{+}\phi W{+}W\phi) = \left(-\frac{\cos\theta_\mathrm{w}}{\sin\theta_\mathrm{w}}\,[k_1^2 - M_W^2] - \frac{1}{2}\left(\frac{\cos\theta_\mathrm{w}}{\sin\theta_\mathrm{w}} - \frac{\sin\theta_\mathrm{w}}{\cos\theta_\mathrm{w}}\right) M_W^2\right)\,\mathcal{F}(M_W, M_W) \tag{4.97}$$

$$i\,\Sigma^{(1)}_{Z\gamma,\mathrm{g}}(W{+}\phi W{+}W\phi) = \left(-\frac{\cos\theta_\mathrm{w}}{\sin\theta_\mathrm{w}}\,[k_1^2 - M_W^2] + \frac{1}{2}\left(\frac{\sin\theta_\mathrm{w}}{\cos\theta_\mathrm{w}} - \frac{\cos\theta_\mathrm{w}}{\sin\theta_\mathrm{w}}\right) M_W^2\right)\,\mathcal{F}(M_W, M_W) \tag{4.98}$$

with $\mathcal{F}$ being defined in (4.82). Hence

$$i\,\Sigma^{(1)}_{\gamma\gamma,\mathrm{g}}(W{+}\phi W{+}W\phi) = \left[\,k_1^2\,\right]\,\mathcal{F}(M_W, M_W) \tag{4.99}$$

$$i\,\Sigma^{(1)}_{ZZ,\mathrm{g}}(W{+}\phi W{+}W\phi) = \frac{\cos^2\theta_\mathrm{w}}{\sin^2\theta_\mathrm{w}}\left[\,k_1^2 - M_Z^2\,\right]\,\mathcal{F}(M_W, M_W) \tag{4.100}$$

$$i\,\Sigma^{(1)}_{\gamma Z,\mathrm{g}}(W{+}\phi W{+}W\phi) = i\,\Sigma^{(1)}_{Z\gamma,\mathrm{g}}(W{+}\phi W{+}W\phi) = -\frac{\cos\theta_\mathrm{w}}{\sin\theta_\mathrm{w}}\left(\frac{1}{2}k_1^2 + \frac{1}{2}[\,k_1^2 - M_Z^2\,]\right)\,\mathcal{F}(M_W, M_W)\,, \tag{4.101}$$

or generically

$$i\,\Sigma^{(1)}_{N_1N_2,\mathrm{g}}(W{+}\phi W{+}W\phi) = G_{134}G_{243}\left(\frac{1}{2}\,[\,k_1^2 - M_{N_1}^2\,] + \frac{1}{2}\,[\,k_1^2 - M_{N_2}^2\,]\right)\mathcal{F}(M_W, M_W)\,, \tag{4.102}$$

[12]Note the slight change of notation. The outside legs being neutral implies that both gauge bosons in the loop are W bosons and we don't indicate V_4 any further, but we do indicate the two possibly different particles in the external legs. Note also that the same results are obtained in the case of V_4 being the *soft* gauge boson.

with $G_{134}G_{243} = G_{N_1W^\pm W^\mp}\, G_{N_2W^\pm W^\mp}$. From this generic expression we see that the diagonal self energies (with $N_1 = N_2 = N$) are proportional to the inverse pole $(k_1^2 - M_N^2)$. The corresponding proportionality factor could just as well have been derived with the derivative approach, as we have seen for the W boson self energy. This is not true for the mixed (γZ) self energy in view of the occurrence of two inverse poles in the full expression.

4.3.3 The scalar self-energy at one-loop level

As mentioned before, in the high energy limit the Equivalence Theorem applies and longitudinal gauge bosons solely appear with the quantum numbers of scalars. Hence discussing longitudinal $W^\pm$ bosons in the final state is intimately related to the study of scalar particles (would-be Goldstone bosons $\phi^\pm$) in the final state. Again the machinery is the same but let us give the key formulae for completeness.

Consider the scalar one-loop self-energy $\Sigma_\phi^{(1)}(p, n, M_1)$, originating from the emission of a gauge boson V_1 with loop-momentum k_1 and mass M_1 from a would-be Goldstone boson $\phi^\pm$ with the momentum p:

$$i\,\Sigma_{\phi^\pm}^{(1)}(p, n, M_1) \quad = \quad$$

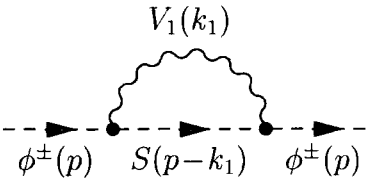

where S is either a $\phi^\pm$ if the exchanged gauge boson is a photon or a Z, or if the exchanged gauge boson is a $W^\pm$, S stands for either the Higgs particle H or χ. The corresponding one-loop contribution to the external wave-function factor $Z_\phi = 1 + \delta Z_\phi$ can be obtained by means of the projection

$$\begin{aligned}
\delta Z_\phi &= \frac{i}{2\,p_0}\left\{\frac{\partial}{\partial p_0}\left[i\,\Sigma_{\phi^\pm}^{(1)}(p, n, M_1)\right]\right\} \\
&\approx \frac{i}{2\,p_0}\left\{\frac{\partial}{\partial p_0}\left[\int \frac{\mathrm{d}^4k_1}{(2\,\pi)^4}\,(ie\,G_{V_1\phi^\pm S})\,(p + p - k_1)_\mu\,P^{\mu\nu}(k_1)\,\frac{i}{[(p-k_1)^2 - M_1^2 + i\epsilon\,]}\right.\right. \\
&\qquad \left.\left. \times\,(ie\,G^*_{V_1\phi^\pm S})\,(p + p - k_1)_\nu\right]\right\}, \\
&\approx -e^2\,|G_{V_1\phi^\pm S}|^2 \int \frac{\mathrm{d}^4k_1}{(2\,\pi)^4}\,\frac{4\,p_\mu\,p_\nu\,P^{\mu\nu}(k_1)}{[(p-k_1)^2 - M_1^2 + i\epsilon\,]^2}\,,
\end{aligned} \tag{4.103}$$

with $G_{V_1\phi^\pm S}$ given in Appendix B.

Hence we obtain the following expression for the one-loop Sudakov correction to the external wave-function factor for scalar particles:

$$\delta Z_\phi^{(1)}(\gamma) = Q_\phi^2 \, \mathrm{L}_\gamma(\lambda, M) \,, \tag{4.104a}$$

$$\begin{aligned} \delta Z_\phi^{(1)}(Z) &= \frac{(1-2\cos^2\theta_\mathrm{w})^2}{4\cos^2\theta_\mathrm{w}\sin^2\theta_\mathrm{w}} \mathrm{L}(M,M) \\ &= \left[\frac{1}{4\sin^2\theta_\mathrm{w}} + \frac{1}{4\cos^2\theta_\mathrm{w}} - Q_\phi^2\right] \mathrm{L}(M,M) \,, \end{aligned} \tag{4.104b}$$

$$\delta Z_\phi^{(1)}(W) = \frac{1}{2\sin^2\theta_\mathrm{w}} \mathrm{L}(M,M) \,, \tag{4.104c}$$

with $\mathrm{L}_\gamma(\lambda, M)$ and $\mathrm{L}(M,M)$ being defined in (4.69) and (4.68).

4.3.4 General one-loop Sudakov logarithms

Gathering the knowledge from the previous three sections we are now prepared to make general statements. Upon summation over the allowed gauge-boson exchanges, one obtains the following expression for the full one-loop Sudakov correction to the external wave-function factor for an arbitrary particle with mass m, charge Q and hypercharge Y:

$$\boxed{\delta Z^{(1)} = \left[\frac{C_2(R)}{\sin^2\theta_\mathrm{w}} + \left(\frac{Y}{2\cos\theta_\mathrm{w}}\right)^2\right] \mathrm{L}(M,M) + Q^2\left[\mathrm{L}_\gamma(\lambda,m) - \mathrm{L}(M,M)\right]} \,. \tag{4.105}$$

Here $C_2(R)$ is the $SU(2)$ Casimir operator of the external particle. So, $C_2(R) = C_F = 3/4$ for the fermions and longitudinal gauge bosons (read: Goldstone bosons), which are in the fundamental representation, and $C_2(R) = C_A = 2$ for transverse gauge bosons, which are in the adjoint representation. Note that the terms proportional to Q^2 in (4.105) are the result of the mass gap between the photon and the weak bosons.

We have applied these one-loop Sudakov correction factors to the reactions $e^+e^- \to W_T^+W_T^-$, $W_L^+W_L^-$ and found perfect agreement with the high-energy approximation in Ref. [58], which confirms the afore-mentioned differences between transverse and longitudinal degrees

of freedom. To illustrate the above we give two examples of transversely and longitudinally polarized W bosons. For $e_L^- e_R^+ \to W_T^+ W_T^-$ the Sudakov double logarithms are obtained from

$$\begin{aligned}\sigma^{1-\text{loop, sudakov}}_{e_R^+ e_L^- \to W_T^+ W_T^-} &= 2\left[\delta Z^{(1)}_{e_L^-} + \delta Z^{(1)}_{W_T}\right] \sigma^{\text{born}}_{e_R^+ e_L^- \to W_T^+ W_T^-} \\ &= \left[\frac{1 + 2\cos^2\theta_\text{w} + 8\cos^4\theta_\text{w}}{2\,\cos^2\theta_\text{w}\,\sin^2\theta_\text{w}}\,\text{L}(M,M) + 2\big(\text{L}_\gamma(\lambda, m_e) + \text{L}_\gamma(\lambda, M)\big)\right] \sigma^{\text{born}}_{e_R^+ e_L^- \to W_T^+ W_T^-}\,,\end{aligned} \tag{4.106}$$

and for $e_L^+ e_R^- \to W_L^+ W_L^-$ from

$$\begin{aligned}\sigma^{1-\text{loop, sudakov}}_{e_R^- e_L^+ \to W_L^+ W_L^-} &= 2\left[\delta Z^{(1)}_{e_R^-} + \delta Z^{(1)}_{\phi}\right] \sigma^{\text{born}}_{e_R^- e_L^+ \to W_L^+ W_L^-} \\ &= \left[\frac{5 - 10\cos^2\theta_\text{w} + 8\cos^4\theta_\text{w}}{2\,\cos^2\theta_\text{w}\,\sin^2\theta_\text{w}}\,\text{L}(M,M) + 2\big(\text{L}_\gamma(\lambda, m_e) + \text{L}_\gamma(\lambda, M)\big)\right] \sigma^{\text{born}}_{e_R^- e_L^+ \to W_L^+ W_L^-}\,,\end{aligned} \tag{4.107}$$

in agreement with the leading contributions $\sim \text{L}(M,M)$ in Eq. (12) of Ref. [58]. The overall factor of two originates from the two final and two initial state particles.

4.4 Electroweak two-loop Sudakov logarithms

For high precision measurements it will become crucial to probe beyond leading order in α and hence theoretical predictions of this accuracy are needed. Eventually it might become inevitable to re-sum those large logarithms to all orders in perturbation theory. To this end let us start with the calculation of two-loop Sudakov correction factors. Again the calculation is very similar for the various types of external ('baseline') particles. We use the fermion case as the major example to illustrate all the subtleties and then briefly give the results for transverse and longitudinal W bosons (that is would-be Goldstone bosons) in the following sections.

4.4.1 The fermionic self-energy at two-loop level

At two-loop accuracy one has to take the following five generic sets of diagrams into account:

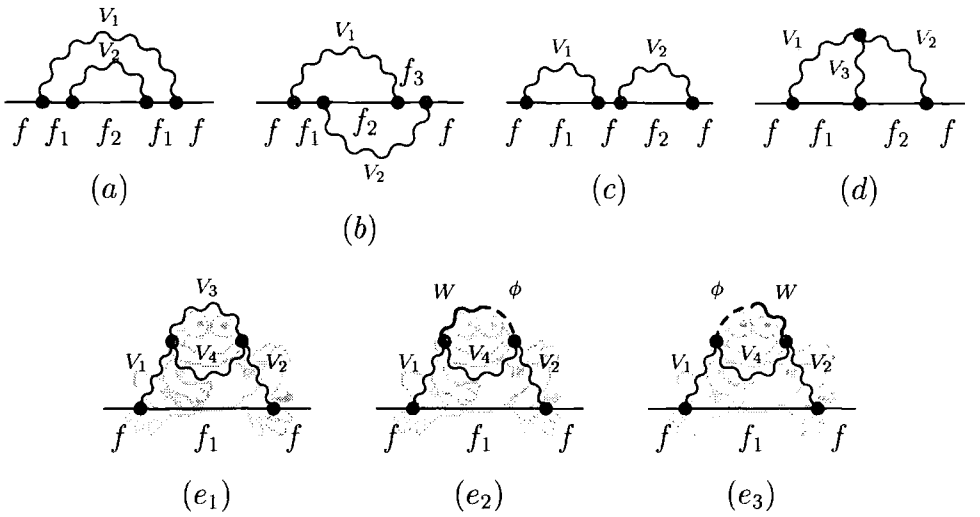

The fermions f_i are fixed by the exchanged gauge bosons V_i. Various cancellations are going to take place between all these diagrams. In unbroken theories like QED and QCD merely the so-called 'rainbow' diagrams of set (a) survive. The same holds if all gauge bosons of the theory would have a similar mass. The unique feature of the SM is that it is only partially broken, with the electromagnetic gauge group $U(1)_{\rm em} \neq U(1)_Y$ remaining unbroken. As such three of the four gauge bosons will acquire a mass, whereas the photon remains massless and will interact with the charged massive gauge bosons ($W^{\pm}$). As a consequence, merely calculating the 'rainbow' diagrams will *not* lead to the correct result.

To illuminate the above let us study each of the generic five topologies separately.

Let the outer loop-momentum of the 'rainbow' diagram of set (a) be denoted k_1 and the inner loop-momentum k_2. For simplicity we use the generic mass m_f for every fermion and do not distinguish between different fermion species. At one-loop level we learned that the fermion mass is only needed as a cut-off parameter to regularize the collinear singularity if the soft exchanged gauge boson is a photon. The two-loop fermion self-energy can then be

written as

$$\begin{aligned}\delta Z_f^{(2)}(a) &= \frac{i}{2\,p_0}\,\bar{u}_f(p)\Big\{\frac{\partial}{\partial\,p_0}\int\frac{\mathrm{d}^4k_1}{(2\,\pi)^4}\int\frac{\mathrm{d}^4k_2}{(2\,\pi)^4}\,(ie\,\gamma_\nu\,\Gamma_{ff_1V_1})\,\frac{i}{(\not{p}-\not{k}_1)-m_f+i\epsilon}\,(ie\,\gamma_{\nu'}\,\Gamma_{f_1f_2V_2}) \\ &\quad\times\frac{i}{(\not{p}-\not{k}_1-\not{k}_2)-m_f+i\epsilon}\,(ie\,\gamma_{\mu'}\,\Gamma_{f_1f_2V_2})\,\frac{i}{(\not{p}-\not{k}_1)-m_f+i\epsilon}\,(ie\,\gamma_\mu\,\Gamma_{ff_1V_1}) \\ &\quad\times P^{\mu\nu}(k_1)\,P^{\mu'\nu'}(k_2)\Big\}\,u_f(p) \\ &\approx -(ie)^4\int\frac{\mathrm{d}^4k_1}{(2\,\pi)^4}\int\frac{\mathrm{d}^4k_2}{(2\,\pi)^4}\,\frac{\Gamma^2_{ff_1V_1}\,\Gamma^2_{f_1f_2V_2}\,4\,p_\mu\,p_\nu\;P^{\mu\nu}(k_1)\;\;4\,p_{\mu'}\,p_{\nu'}\;P^{\mu'\nu'}(k_2)}{[(p-k_1)^2-m_f^2+i\epsilon\,]^2\,[(p-k_1-k_2)^2-m_f^2+i\epsilon\,]} \\ &\quad\times\left(\frac{2}{[(p-k_1)^2-m_f^2+i\epsilon\,]}+\frac{1}{[(p-(k_1+k_2))^2-m_f^2+i\epsilon\,]}\right). \qquad (4.108)\end{aligned}$$

Making use of (4.60) and

$$\begin{aligned}(i)\left[k_2^2-M_2^2+i\epsilon\right]4\,p_{\mu\prime}\,p_{\nu'}\;P^{\mu'\nu'}(k_2) &\approx \frac{4\,k_{20}\,p_0}{\vec{k}_2^{\,2}}\left((p-k_2)^2-m_f^2\right) \\ &\approx \frac{4\,k_{20}\,p_0}{\vec{k}_2^{\,2}}\left(\left[(p-(k_1+k_2))^2-m_f^2\right]-\left[(p-k_1)^2-m_f^2\right]\right), \qquad (4.109)\end{aligned}$$

in leading logarithmic approximation the self-energy can be written

$$\begin{aligned}\delta Z_f^{(2)}(a) &\approx (i\,e^2)^2\,\Gamma^2_{ff_1V_1}\,\Gamma^2_{f_1f_2V_2}\int\frac{\mathrm{d}^4k_1}{(2\,\pi)^4}\int\frac{\mathrm{d}^4k_2}{(2\,\pi)^4}\,\frac{4\,k_{10}\,p_0}{\vec{k}_1^{\,2}}\,\frac{4\,k_{20}\,p_0}{\vec{k}_2^{\,2}} \\ &\quad\times\frac{1}{[(p-k_1)^2-m_f^2+i\epsilon\,]\,[(p-(k_1+k_2))^2-m_f^2+i\epsilon\,]\,[k_1^2-M_1^2+i\epsilon\,]\,[k_2^2-M_2^2+i\epsilon\,]} \qquad (4.110)\end{aligned}$$

For the gauge boson momentum k_2 we choose a Sudakov parametrisation equivalent to the one used for k_1, *i. e.*

$$k_2 = v_2\,q + u_2\,\bar{q} + k_{2_\perp}\,, \qquad (4.111)$$

with q and $\bar{q}$ defined in (4.63). The calculation simplifies if we perform the u_2 integration first, taking the residue in the lower hemisphere in the pole of the corresponding gauge boson

propagator. Following the steps of the one-loop calculation we find

$$\begin{aligned}\delta Z_f^{(2)}(a) \approx & \left(-\frac{\alpha}{\pi}\right) \Gamma^2_{ff_1V_1} \int_0^1 \frac{\mathrm{d}y_1}{y_1} \int_{y_1}^1 \frac{\mathrm{d}z_1}{z_1}\, \Theta\Big(y_1 z_1 - \frac{M_1^2}{s}\Big)\, \Theta\Big(y_1 - \frac{m_f^2}{s}\, z_1\Big) \\ & \times \left(-\frac{\alpha}{\pi}\right) \Gamma^2_{f_1 f_2 V_2} \int_0^1 \frac{\mathrm{d}y_2}{(y_2+y_1)} \int_{y_2}^1 \frac{\mathrm{d}z_2}{z_2}\, \Theta\Big(y_2 z_2 - \frac{M_2^2}{s}\Big)\, \Theta\Big(y_2 - \frac{m_f^2}{s}\, z_2\Big) \\ = & \left(-\frac{\alpha}{\pi}\right)^2 \int_0^1 \frac{\mathrm{d}y_1}{y_1} \int_{y_1}^1 \frac{\mathrm{d}z_1}{z_1} \int_0^1 \frac{\mathrm{d}y_2}{y_2} \int_{y_2}^1 \frac{\mathrm{d}z_2}{z_2}\, \Gamma^2_{ff_1V_1}\, \mathcal{K}^{(1)}(s, m_f^2, M_1, y_1, z_1) \\ & \times \Gamma^2_{f_1 f_2 V_2}\, \mathcal{K}^{(1)}(s, m_f^2, M_2, y_2, z_2)\, \Theta(y_2 - y_1) \end{aligned} \tag{4.112}$$

with $\mathcal{K}^{(1)}$ being defined in (4.66).

Being already familiar with the type of simplifications which have to be applied to the self-energies we can omit the very first steps and give the self-energy of set (b) ('crossed rainbow') in the following way

$$\begin{aligned}\delta Z_f^{(2)}(b) = & -(ie)^4 \int \frac{\mathrm{d}^4 k_1}{(2\pi)^4} \int \frac{\mathrm{d}^4 k_2}{(2\pi)^4}\, \Gamma_{ff_1V_1}\, \Gamma_{f_1 f_2 V_2}\, \Gamma_{f_2 f_3 V_1}\, \Gamma_{f f_3 V_2}\, 4\, p_\mu\, p_\nu\, P^{\mu\nu}(k_1)\, 4\, p_{\mu'}\, p_{\nu'}\, P^{\mu'\nu'}(k_2) \\ & \times \frac{1}{[(p-k_1)^2 - m_f^2 + i\epsilon]\,[(p-k_1-k_2)^2 - m_f^2 + i\epsilon]\,[(p-k_2)^2 - m_f^2 + i\epsilon]} \\ & \times \left(\frac{1}{[(p-k_1)^2 - m_f^2 + i\epsilon]} + \frac{1}{[(p-k_1-k_2)^2 - m_f^2 + i\epsilon]} + \frac{1}{[(p-k_2)^2 - m_f^2 + i\epsilon]} \right) \\ \approx & -(i\,e^2)^2 \int \frac{\mathrm{d}^4 k_1}{(2\pi)^4} \int \frac{\mathrm{d}^4 k_2}{(2\pi)^4}\, \Gamma_{ff_1V_1}\, \Gamma_{f_1 f_2 V_2}\, \Gamma_{f_2 f_3 V_1}\, \Gamma_{f f_3 V_2}\, \frac{4\, k_{1\,0}\, p_0}{\vec{k}_1^{\,2}}\, \frac{4\, k_{2\,0}\, p_0}{\vec{k}_2^{\,2}} \\ & \times \frac{1}{[(p-k_1)^2 - m_f^2 + i\epsilon]\,[(p-k_2)^2 - m_f^2 + i\epsilon]\,[k_1^2 - M_1^2 + i\epsilon]\,[k_2^2 - M_2^2 + i\epsilon]}\,. \end{aligned} \tag{4.113}$$

Note here the complete factorization of the two integrals. Thus this contribution can be written

$$\begin{aligned}\delta Z_f^{(2)}(b) = & -\Gamma_{ff_1V_1}\, \Gamma_{f_1 f_2 V_2}\, \Gamma_{f_2 f_3 V_1}\, \Gamma_{f f_3 V_2} \left(-\frac{\alpha}{\pi}\right) \int_0^1 \frac{\mathrm{d}y_1}{y_1} \int_{y_1}^1 \frac{\mathrm{d}z_1}{z_1} \mathcal{K}^{(1)}(s, m_f^2, M_1, y_1, z_1) \\ & \times \left(-\frac{\alpha}{\pi}\right) \int_0^1 \frac{\mathrm{d}y_2}{y_2} \int_{y_2}^1 \frac{\mathrm{d}z_2}{z_2}\, \mathcal{K}^{(1)}(s, m_f^2, M_2, y_2, z_2)\,, \end{aligned} \tag{4.114}$$

Obviously the reducible contribution from set (c) can only be the product of the two

corresponding one-loop contributions

$$\delta Z_f^{(2)}(c) = \left(-\frac{\alpha}{\pi}\right) \Gamma^2_{ff_1V_1} \int_0^1 \frac{\mathrm{d}y_1}{y_1} \int_{y_1}^1 \frac{\mathrm{d}z_1}{z_1} \mathcal{K}^{(1)}(s, m_f^2, M_1, y_1, z_1) \times \left(-\frac{\alpha}{\pi}\right) \Gamma^2_{ff_2V_2} \int_0^1 \frac{\mathrm{d}y_2}{y_2} \int_{y_2}^1 \frac{\mathrm{d}z_2}{z_2} \mathcal{K}^{(1)}(s, m_f^2, M_2, y_2, z_2). \tag{4.115}$$

Unfortunately life is getting harder for the two remaining sets of diagrams. The main complication being that more than two gauge-boson propagators are involved and hence a variety of possible on-shell combinations enlarges the actual number of integrals to be performed. The triple-gauge-boson ('TGB') diagram of set (d) can be written in the following way

$$\begin{aligned}\delta Z_f^{(2)}(d) &= i\,(ie)^4 \int \frac{\mathrm{d}^4k_1}{(2\,\pi)^4} \int \frac{\mathrm{d}^4k_2}{(2\,\pi)^4} \frac{2\,p_\mu\,2\,p_\nu\,2\,p_\rho\; P^{\mu\mu'}(k_1)\,P^{\rho\rho'}(k_1-k_2)\,P^{\nu\nu'}(k_2)\,V_{\mu'\,\rho'\,\nu'}}{[(p-k_1)^2-m_f^2+i\epsilon\,][(p-k_2)^2-m_f^2+i\epsilon\,]} \\ &\quad \times \Gamma_{ff_1V_1}\,\Gamma_{f_1f_2V_3}\,\Gamma_{ff_2V_2}\,G_{132} \left(\frac{1}{[(p-k_1)^2-m_f^2+i\epsilon\,]} + \frac{1}{[(p-k_2)^2-m_f^2+i\epsilon\,]}\right) \\ &\equiv (i\,e^2)^2 \int \frac{\mathrm{d}^4k_1}{(2\,\pi)^4} \int \frac{\mathrm{d}^4k_2}{(2\,\pi)^4} \Gamma_{ff_1V_1}\,\Gamma_{f_1f_2V_3}\,\Gamma_{ff_2V_2}\,G_{132}\,\mathrm{IK}(d)\,,\end{aligned} \tag{4.116}$$

with

$$\begin{aligned}\mathrm{IK}(d) &= -i\,\frac{2\,p_\mu\,2\,p_\nu\,2\,p_\rho\; P^{\mu\mu'}(k_1)\,P^{\rho\rho'}(k_1-k_2)\,P^{\nu\nu'}(k_2)\,V_{\mu'\,\rho'\,\nu'}}{[(p-k_1)^2-m_f^2+i\epsilon\,][(p-k_2)^2-m_f^2+i\epsilon\,]} \\ &\quad \times \left(\frac{1}{[(p-k_1)^2-m_f^2+i\epsilon\,]} + \frac{1}{[(p-k_2)^2-m_f^2+i\epsilon\,]}\right)\end{aligned} \tag{4.117}$$

and

$$V_{\mu'\,\rho'\,\nu'} = (2k_2-k_1)_{\mu'}\,g_{\nu'\rho'} + (-\mathrm{k}_2-\mathrm{k}_1)_{\rho'}\,g_{\mu'\nu'} + (2\,\mathrm{k}_1-\mathrm{k}_2)_{\nu'}\,g_{\mu'\rho'}\,. \tag{4.118}$$

Defining $k_3 \equiv k_1 - k_2$ the integration kernel $\mathrm{IK}(d)$ of (4.116) can be written in the following

way

$$
\begin{aligned}
\mathrm{IK}(d) \approx (-i)\Bigg(& \Big[2\,p_\mu\,(2\,k_2 - k_1)_{\mu'}\,P^{\mu\mu'}(k_1)\Big]\Big[4\,p_\rho\,p_\nu\,P^{\rho\rho'}(k_3)\,P_{\rho'}{}^{\nu}(k_2)\Big] \\
& + \Big[-2\,p_\rho\,(k_1+k_2)_{\rho'}\,P^{\rho\rho'}(k_3)\Big]\Big[4\,p_\mu\,p_\nu\,P^{\mu\mu'}(k_1)\,P_{\mu'}{}^{\nu}(k_2)\Big] \\
& + \Big[2\,p_\nu\,(2\,k_1 - k_2)_{\nu'}\,P^{\nu\nu'}(k_2)\Big]\Big[4\,p_\rho\,p_\mu\,P^{\mu\mu'}(k_1)\,P_{\mu'}{}^{\rho}(k_3)\Big]\Bigg) \\
& \times \left(\frac{[(p-k_1)^2] + [(p-k_2)^2]}{[(p-k_1)^2 - m_f^2 + i\epsilon\,]^2\,[(p-k_2)^2 - m_f^2 + i\epsilon\,]^2}\right) \qquad (4.119)
\end{aligned}
$$

$$
\begin{aligned}
\approx \Bigg(& \left[-2\,[\,(p-k_2)^2 - k_2^2\,] + \frac{2\,k_{1\,0}\,p_0}{\vec{k}_1^{\,2}}\,[\,k_3^2 - k_1^2 - k_2^2\,] + \frac{2\,k_{1\,0}\,k_{2\,0}}{\vec{k}_1^{\,2}}\,[(p-k_1)^2 - k_1^2] + \frac{2\,k_{1\,0}\,p_0}{\vec{k}_1^{\,2}}\,k_1^2\right] \times \\
& \times \left[\frac{4\,k_{3\,0}\,p_0}{\vec{k}_3^{\,2}}\,[\,(p-k_1)^2 - (p-k_2)^2 - k_1^2 + k_2^2\,] + \frac{4\,k_{2\,0}\,p_0}{\vec{k}_2^{\,2}}\,[\,(p-k_2)^2 - k_2^2\,] - \frac{2\,k_{3\,0}\,k_{2\,0}}{\vec{k}_3^{\,2}\,\vec{k}_2^{\,2}} \times\right. \\
& \left. \times \Big[k_{2\,0}\,p_0\,[\,(p-k_1)^2 - k_1^2 - (p-k_2)^2 + k_2^2\,] + k_{3\,0}\,p_0\,[\,(p-k_2)^2 - k_2^2\,] - p_0^2\,[\,k_1^2 - k_2^2 - k_3^2\,]\Big]\right] \\
& + \left[\Big([\,(p-k_2)^2 - k_2^2\,] - \frac{k_{3\,0}\,p_0}{\vec{k}_3^{\,2}}\,[\,k_3^2 - k_1^2 + k_2^2\,] - \frac{k_{3\,0}\,k_{2\,0}}{\vec{k}_3^{\,2}}\,[\,(p-k_1)^2 - k_1^2 - (p-k_2)^2 + k_2^2\,]\Big)\right. \\
& \left. + \Big([\,(p-k_1)^2 - k_1^2\,] - \frac{k_{3\,0}\,p_0}{\vec{k}_3^{\,2}}\,[-k_3^2 - k_1^2 + k_2^2\,] - \frac{k_{3\,0}\,k_{1\,0}}{\vec{k}_3^{\,2}}\,[\,(p-k_1)^2 - k_1^2 - (p-k_2)^2 + k_2^2\,]\Big)\right] \times \\
& \times \left[\frac{4\,k_{1\,0}\,p_0}{\vec{k}_1^{\,2}}\,[\,(p-k_1)^2 - k_1^2\,] + \frac{4\,k_{2\,0}\,p_0}{\vec{k}_2^{\,2}}\,[\,(p-k_2)^2 - k_2^2\,]\right. \\
& \left. - \frac{2\,k_{1\,0}\,k_{2\,0}}{\vec{k}_1^{\,2}\,\vec{k}_2^{\,2}}\Big[p_0\,k_{2\,0}\,[\,(p-k_1)^2 - k_1^2\,] + p_0\,k_{1\,0}\,[\,(p-k_2)^2 - k_2^2] + p_0^2\,[\,k_3^2 - k_1^2 - k_2^2]\Big]\right] \\
& + \left[-2\,[\,(p-k_1)^2 - k_1^2\,] + \frac{2\,k_{2\,0}\,p_0}{\vec{k}_2^{\,2}}\,[\,k_3^2 - k_1^2 - k_2^2\,] + \frac{2\,k_{1\,0}\,k_{2\,0}}{\vec{k}_2^{\,2}}\,[(p-k_2)^2 - k_2^2] + \frac{2\,k_{2\,0}\,p_0}{\vec{k}_2^{\,2}}\,k_2^2\right] \times \\
& \times \left[\frac{4\,k_{3\,0}\,p_0}{\vec{k}_3^{\,2}}\,[\,(p-k_1)^2 - (p-k_2)^2 - k_1^2 + k_2^2\,] + \frac{4\,k_{1\,0}\,p_0}{\vec{k}_1^{\,2}}\,[\,(p-k_1)^2 - k_1^2\,] - \frac{2\,k_{3\,0}\,k_{1\,0}}{\vec{k}_3^{\,2}\,\vec{k}_1^{\,2}} \times\right. \\
& \left. \times \Big[k_{1\,0}\,p_0\,[\,(p-k_1)^2 - k_1^2 - (p-k_2)^2 + k_2^2\,] + k_{3\,0}\,p_0\,[\,(p-k_1)^2 - k_1^2\,] + p_0^2\,[\,k_2^2 - k_1^2 - k_3^2\,]\Big]\right]\Bigg) \\
& \times \left(\frac{[(p-k_1)^2] + [(p-k_2)^2]}{[(p-k_1)^2 - m_f^2 + i\epsilon\,]^2\,[(p-k_2)^2 - m_f^2 + i\epsilon\,]^2}\;\frac{(-i)^4}{[k_1^2 - M_1^2 + i\epsilon\,]\,[k_2^2 - M_2^2 + i\epsilon\,]\,[k_3^2 - M_3^2 + i\epsilon\,]}\right). \qquad (4.120)
\end{aligned}
$$

As usual we have neglected the fermion-mass m_f in the numerator.
The integration kernel can be simplified by making use of the fact that the following generic contributions will *not* lead to $(\log)^4$ corrections:

- terms with only one gauge boson propagator
- terms with no fermion propagator
- terms with one fermion propagator and only two gauge boson propagators
- terms with two fermion propagators and two gauge-boson propagators but only one $1/\vec{k}^2$
- terms $\sim (1/k_i)^l$ with $l < 8$ in the soft k_i limit; four of those powers will be compensated by the loop integrals, hence four more are required to obtain four logarithms

Moreover we can make use of effective identities like

$$\frac{(p-k_1)^2}{[(p-k_2)^2 - m_f^2 + i\epsilon]^2 \prod_{i=1}^{3} [k_i^2 - M_i^2 + i\epsilon]} \rightarrow \frac{k_{10}k_{20}}{\vec{k}_2^{\,2}} \frac{1}{[(p-k_2)^2 - m_f^2 + i\epsilon] \prod_{i=1}^{3} [k_i^2 - M_i^2 + i\epsilon]} \tag{4.121}$$

because the part of $(p-k_1)^2$ that is proportional to the $\vec{k}_1$ component perpendicular to $\vec{k}_2$ will not survive the $\vec{k}_1$ integration.

All this leads to

$$IK(d) \approx$$

$$\approx \frac{2\,k_{1\,0}\,p_0}{\vec{k_1}^{\,2}} \frac{1}{[(p-k_1)^2-m_f^2+i\epsilon]\,[k_1^2-M_1^2+i\epsilon]} \frac{2\,k_{2\,0}\,p_0}{\vec{k_2}^{\,2}} \frac{1}{[(p-k_2)^2-m_f^2+i\epsilon]\,[k_2^2-M_2^2+i\epsilon]} \tag{4.122a}$$

$$+ \frac{2\,k_{2\,0}\,p_0}{\vec{k_2}^{\,2}} \frac{1}{[(p-k_2)^2-m_f^2+i\epsilon]\,[k_2^2-M_2^2+i\epsilon]} \frac{2\,k_{3\,0}\,p_0}{\vec{k_3}^{\,2}} \frac{1}{[(p-k_1)^2-m_f^2+i\epsilon]\,[k_3^2-M_3^2+i\epsilon]} \tag{4.122b}$$

$$- \frac{2\,k_{1\,0}\,p_0}{\vec{k_1}^{\,2}} \frac{1}{[(p-k_1)^2-m_f^2+i\epsilon]\,[k_1^2-M_1^2+i\epsilon]} \frac{2\,k_{3\,0}\,p_0}{\vec{k_3}^{\,2}} \frac{1}{[(p-k_2)^2-m_f^2+i\epsilon]\,[k_3^2-M_3^2+i\epsilon]} \tag{4.122c}$$

$$+ \frac{4\,k_{1\,0}\,p_0}{\vec{k_1}^{\,2}} \frac{1}{[(p-k_2)^2-m_f^2+i\epsilon]\,[k_1^2-M_1^2+i\epsilon]\,[k_2^2-M_2^2+i\epsilon]\,[k_3^2-M_3^2+i\epsilon]} \tag{4.122d}$$

$$+ \frac{4\,k_{2\,0}\,p_0}{\vec{k_2}^{\,2}} \frac{1}{[(p-k_1)^2-m_f^2+i\epsilon]\,[k_1^2-M_1^2+i\epsilon]\,[k_2^2-M_2^2+i\epsilon]\,[k_3^2-M_3^2+i\epsilon]} \tag{4.122e}$$

$$- \frac{8\,k_{3\,0}\,p_0}{\vec{k_3}^{\,2}} \frac{1}{[(p-k_2)^2-m_f^2+i\epsilon]\,[k_1^2-M_1^2+i\epsilon]\,[k_2^2-M_2^2+i\epsilon]\,[k_3^2-M_3^2+i\epsilon]} \tag{4.122f}$$

$$+ \frac{8\,k_{3\,0}\,p_0}{\vec{k_3}^{\,2}} \frac{1}{[(p-k_1)^2-m_f^2+i\epsilon]\,[k_1^2-M_1^2+i\epsilon]\,[k_2^2-M_2^2+i\epsilon]\,[k_3^2-M_3^2+i\epsilon]} \tag{4.122g}$$

$$+ \frac{2\,k_{1\,0}\,p_0}{\vec{k_1}^{\,2}} \frac{1}{[(p-k_2)^2-m_f^2+i\epsilon]\,[k_2^2-M_2^2+i\epsilon]} \times \frac{2\,k_{3\,0}\,p_0}{\vec{k_3}^{\,2}} \frac{1}{[(p-(k_2+k_3))^2-m_f^2+i\epsilon]\,[k_3^2-M_3^2+i\epsilon]} \tag{4.122h}$$

$$- \frac{2\,k_{2\,0}\,p_0}{\vec{k_2}^{\,2}} \frac{1}{[(p-k_1)^2-m_f^2+i\epsilon]\,[k_1^2-M_1^2+i\epsilon]} \times \frac{2\,k_{3\,0}\,p_0}{\vec{k_3}^{\,2}} \frac{1}{[(p-(k_1-k_3))^2-m_f^2+i\epsilon]\,[k_3^2-M_3^2+i\epsilon]} \tag{4.122i}$$

$$- \frac{4\,k_{1\,0}\,p_0}{\vec{k_1}^{\,2}} \frac{1}{[(p-k_1)^2-m_f^2+i\epsilon]\,[k_1^2-M_1^2+i\epsilon]} \times \frac{2\,(k_{1\,0}-k_{2\,0})\,p_0}{(\vec{k_1}-\vec{k_2})^2} \frac{1}{[(p-k_2)^2-m_f^2+i\epsilon]\,[k_2^2-M_2^2+i\epsilon]} \tag{4.122j}$$

$$+ \frac{4\,k_{2\,0}\,p_0}{\vec{k_2}^{\,2}} \frac{1}{[(p-k_2)^2-m_f^2+i\epsilon]\,[k_2^2-M_2^2+i\epsilon]} \times \frac{2\,(k_{1\,0}-k_{2\,0})\,p_0}{(\vec{k_1}-\vec{k_2})^2} \frac{1}{[(p-k_1)^2-m_f^2+i\epsilon]\,[k_1^2-M_1^2+i\epsilon]} \tag{4.122k}$$

Note here that the same result is obtained for the full gauge boson propagator $P_{\mu\nu}$ as well

as for the purely transverse part $\sim Q_{\mu\nu}$, as expected in the collinear regime.
Apart from the coupling factor $\Gamma_{f f_1 V_1}\,\Gamma_{f_1 f_2 V_3}\,\Gamma_{f f_2 V_2}\,G_{132}$ the integrals in (4.116) have been normalized in the usual way. Therefore the first term (4.122a) is easily identified as the product of two one-loop contributions (4.61) with momenta k_1 and k_2, *i. e.*

$$(4.122a) \to \frac{1}{4}\,\mathcal{K}^{(1)}(s, m_f^2, M_1, y_1, z_1)\,\mathcal{K}^{(1)}(s, m_f^2, M_2, y_2, z_2)\,. \tag{4.123}$$

In the second term (4.122b) the momentum k_1 has to be expressed through the momenta k_2 and k_3, *i. e.* $k_1 = k_2 + k_3$, in the fermion propagator as well as in the integration variable. This is convenient since those are the momenta appearing in the boson propagators of (4.122b). (Remember that we have chosen to take the residue in the lower hemisphere in the pole of the gauge-boson propagators.) In doing this the 'rainbow'-like structure can be immediately recognized and upon integrating first the u_3 variable belonging to the Sudakov parametrisation of k_3 we obtain instantly

$$(4.122b) \to \frac{1}{4}\,\mathcal{K}^{(1)}(s, m_f^2, M_2, y_2, z_2)\,\mathcal{K}^{(1)}(s, m_f^2, M_3, y_3, z_3)\,\Theta(y_3 - y_2)\,. \tag{4.124}$$

Similarly replacing $k_2 = k_1 - k_3$ and subsequently reversing the sign of the k_3 integration variable in (4.122c) leads again to a 'rainbow'-like structure and

$$(4.122c) \to \frac{1}{4}\,\mathcal{K}^{(1)}(s, m_f^2, M_1, y_1, z_1)\,\mathcal{K}^{(1)}(s, m_f^2, M_3, y_3, z_3)\,\Theta(y_3 - y_1)\,. \tag{4.125}$$

The following four terms are unique in the sense that they only contain one fermion propagator and three gauge-boson propagators. As we will see later those can be identified as so-called 'frog' contributions. Now having three propagators serving as potential poles we have to sum over all three possibilities of taking either two of them on-shell. Let us do this step by step at the example of (4.122d). Starting by taking k_1 and k_2 as the integration variables, *i. e.* taking the corresponding propagators on-shell, the third gauge boson propagator becomes

$$\begin{aligned}
\frac{1}{[\,k_3^2 - M_3^2 + i\epsilon\,]} &= \frac{1}{[\,k_1^2 - 2\,k_1\cdot k_2 + k_2^2 - M_3^2 + i\epsilon]} \\
&\approx \frac{1}{-2\,k_1\cdot k_2} \\
&\to \frac{1}{-s(z_1\,y_2 + z_2\,y_1)}\,.
\end{aligned} \tag{4.126}$$

We need a $1/(y_1\, z_2)$ contribution, since from $k_{10}/\vec{k}_1^{\,2}$ and from $1/(p-k_2)^2$ we obtained $1/(z_1\, y_2)$ already. This leads to the Θ-function $\Theta(z_2\, y_1 - z_1\, y_2)$. Furthermore, performing the u_1 integration first, the third gauge boson propagator restricts the v_1 integration range to $0 \le v_1 \le v_2$. Hence we find for the first summand of kernel (4.122d)

$$\frac{1}{4}\,\mathcal{K}^{(1)}(s, m_f^2, M_1, y_1, z_1)\,\mathcal{K}^{(1)}(s, m_f^2, M_2, y_2, z_2)\,\Theta(z_2 - z_1)\,\Theta(z_2\, y_1 - z_1\, y_2). \tag{4.127}$$

Taking k_1 and $-k_3$ as the next two integration variables and performing the u_3 integration first we obtain

$$-\ \frac{1}{4}\,\mathcal{K}^{(1)}(s, m_f^2, M_1, y_1, z_1)\,\mathcal{K}^{(1)}(s, m_f^2, M_3, y_3, z_3)\,\Theta(y_3 - y_1)\,\Theta(z_3 - z_1)\,\Theta(z_3\, y_1 - z_1\, y_3)\,. \tag{4.128}$$

Finally for k_2 and k_3 being the on-shell gauge-boson momenta

$$-\frac{1}{4}\,\mathcal{K}^{(1)}(s, m_f^2, M_2, y_2, z_2)\,\mathcal{K}^{(1)}(s, m_f^2, M_3, y_3, z_3)\,\Theta(z_3 - z_2)\,\Theta(z_2 - z_3) \equiv 0\,,$$

since the two Θ-functions cannot be simultaneously fulfilled. Note that the first Θ-function originates from the $k_{1\,0} = k_{3\,0} + k_{2\,0} \approx k_{3\,0}$ constraint and the second Θ-function arises due to the restricted v_3 integration range.

In order to combine (4.127) and (4.128) we first relabel the integration variables of (4.128)

$$-\ \frac{1}{4}\,\mathcal{K}^{(1)}(s, m_f^2, M_1, y_1, z_1)\,\mathcal{K}^{(1)}(s, m_f^2, M_3, y_2, z_2)\,\Theta(y_2 - y_1)\,\Theta(z_2 - z_1)\,\Theta(z_2\, y_1 - z_1\, y_2)\,. \tag{4.129}$$

Adding to this the 'one-way' double ordered part of (4.127) leads to

$$\begin{aligned}
&\frac{1}{4}\,\mathcal{K}^{(1)}(s, m_f^2, M_1, y_1, z_1)\,\Theta(z_2\, y_1 - z_1\, y_2)\,\Theta(z_2 - z_1)\,\Theta(y_2 - y_1) \\
&\qquad \times \left[\mathcal{K}^{(1)}(s, m_f^2, M_2, y_2, z_2) - \mathcal{K}^{(1)}(s, m_f^2, M_3, y_2, z_2)\right] \\
&= \frac{1}{4}\,\mathcal{K}^{(1)}(s, m_f^2, M_1, y_1, z_1)\,\Theta(z_2\, y_1 - z_1\, y_2)\,\Theta(z_2 - z_1)\,\Theta(y_2 - y_1) \\
&\qquad \times \Theta\left(y_2 - \frac{m_f^2}{s}\, z_2\right)\left[\Theta\left(y_2\, z_2 - \frac{M_2^2}{s}\right) - \Theta\left(y_2\, z_2 - \frac{M_3^2}{s}\right)\right]
\end{aligned} \tag{4.130}$$

which vanishes for all possible combinations of M_i being the photon mass or the generic mass M. This is trivial for $M_2 = M_3$. For $M_2 = \lambda$ and $M_1 = M_3 = M$ the two Θ-functions

$\Theta(z_2-z_1)\,\Theta(y_2-y_1)$ restrict the y_2, z_2 integrations such that at least $y_2 z_2 \geq M^2/s$ and hence $\Theta\left(y_2\, z_2 - \frac{M_2^2}{s}\right) - \Theta\left(y_2\, z_2 - \frac{M_3^2}{s}\right)$ vanishes.. The same holds for $M_3 = \lambda$ and $M_1 = M_2 = M$. Hence we find for (4.122d)

$$\frac{1}{4}\,\mathcal{K}^{(1)}(s, m_f^2, M_1, y_1, z_1)\,\mathcal{K}^{(1)}(s, m_f^2, M_2, y_2, z_2)\,\Theta(z_2 - z_1)\,\Theta(y_1 - y_2)\,, \tag{4.131}$$

with $\Theta(z_2\, y_1 - z_1\, y_2)$ being obsolete for this combination of Θ-functions, for (4.122e) we find

$$\frac{1}{4}\,\mathcal{K}^{(1)}(s, m_f^2, M_1, y_1, z_1)\,\mathcal{K}^{(1)}(s, m_f^2, M_2, y_2, z_2)\,\Theta(z_1 - z_2)\,\Theta(y_2 - y_1)\,, \tag{4.132}$$

for (4.122f)

$$\frac{1}{2}\,\mathcal{K}^{(1)}(s, m_f^2, M_2, y_2, z_2)\,\mathcal{K}^{(1)}(s, m_f^2, M_3, y_3, z_3)\,\Theta(z_2 - z_3)\,\Theta(y_3 - y_2)\,, \tag{4.133}$$

and eventually for (4.122g)

$$\frac{1}{2}\,\mathcal{K}^{(1)}(s, m_f^2, M_1, y_1, z_1)\,\mathcal{K}^{(1)}(s, m_f^2, M_3, y_3, z_3)\,\Theta(z_1 - z_3)\,\Theta(y_3 - y_1)\,. \tag{4.134}$$

Next (4.122h) can be identified as the following double ordered contribution

$$(4.122h) \to \frac{1}{4}\,\mathcal{K}^{(1)}(s, m_f^2, M_2, y_2, z_2)\,\mathcal{K}^{(1)}(s, m_f^2, M_3, y_3, z_3)\,\Theta(y_3 - y_2)\,\Theta(z_2 - z_3)\,. \tag{4.135}$$

Similarly (4.122i) becomes

$$(4.122i) \to \frac{1}{4}\,\mathcal{K}^{(1)}(s, m_f^2, M_1, y_1, z_1)\,\mathcal{K}^{(1)}(s, m_f^2, M_3, y_3, z_3)\,\Theta(y_3 - y_1)\,\Theta(z_1 - z_3)\,. \tag{4.136}$$

The remaining two contributions are

$$(4.122j) \to \frac{1}{2}\,\mathcal{K}^{(1)}(s, m_f^2, M_1, y_1, z_1)\,\mathcal{K}^{(1)}(s, m_f^2, M_2, y_2, z_2)\,\Theta(z_2 - z_1)\,, \tag{4.137}$$

and

$$(4.122k) \to \frac{1}{2}\,\mathcal{K}^{(1)}(s, m_f^2, M_1, y_1, z_1)\,\mathcal{K}^{(1)}(s, m_f^2, M_2, y_2, z_2)\,\Theta(z_1 - z_2)\,, \tag{4.138}$$

and can be combined to

$$(4.122j) + (4.122k) \to \frac{1}{2}\,\mathcal{K}^{(1)}(s, m_f^2, M_1, y_1, z_1)\,\mathcal{K}^{(1)}(s, m_f^2, M_2, y_2, z_2)\,. \tag{4.139}$$

After some relabeling the two-loop correction factors originating from set (d) can be summarized as follows

$$\delta Z_f^{(2)}(d) = \frac{1}{4}\,\Gamma_{f f_1 V_1}\,\Gamma_{f_1 f_2 V_3}\,\Gamma_{f f_2 V_2}\,G_{132}\,\left(-\frac{\alpha}{\pi}\right)^2 \int_0^1 \frac{\mathrm{d}y_1}{y_1} \int_{y_1}^1 \frac{\mathrm{d}z_1}{z_1} \int_0^1 \frac{\mathrm{d}y_2}{y_2} \int_{y_2}^1 \frac{\mathrm{d}z_2}{z_2}$$
$$\left\{ \left[\mathcal{K}^{(1)}(s, m_f^2, M_1, y_1, z_1) + \mathcal{K}^{(1)}(s, m_f^2, M_2, y_1, z_1) \right] \times \right.$$
$$\times\ \mathcal{K}^{(1)}(s, m_f^2, M_3, y_2, z_2)\,\Theta(y_2 - y_1)\left[1 + 3\,\Theta(z_1 - z_2)\right]$$
$$+ \mathcal{K}^{(1)}(s, m_f^2, M_1, y_1, z_1)\,\mathcal{K}^{(1)}(s, m_f^2, M_2, y_2, z_2) \times$$
$$\left. \times\ \left[3 + \Theta(y_1 - y_2)\,\Theta(z_2 - z_1) + \Theta(y_2 - y_1)\,\Theta(z_1 - z_2)\right] \right\}. \tag{4.140}$$

Eventually we calculate the 'frog' diagrams of set (e). Labeling the loop momenta according to our specification in (4.3.2) we find

$$\delta Z_f^{(2)}(e) = -\,e^2\,\Gamma_{f f_1 V_1}\,\Gamma_{f f_1 V_2} \int \frac{\mathrm{d}^4 k_1}{(2\,\pi)^4}\, \frac{4\,p_{\mu'}\,p_{\nu'}\,P^{\mu'\mu}(k_1)\left(i\Sigma^{(1),V_4}_{V_1 V_2\,,\mathrm{g}}(V_3)\;\mathrm{g}_{\mu\nu}\right)\mathrm{P}^{\nu\nu'}(\mathrm{k}_1)}{[(p - k_1)^2 - m_f^2 + i\epsilon\,]^2}$$

where $\Sigma^{(1),V_4}_{V_1 V_2\,,\mathrm{g}}(V_3)$ is given by (4.80), (4.81), (4.89), (4.90) or (4.102). Whenever the soft particle $V_3 = W$, the sum of the contributions from the gauge boson and the two mixed propagators is implicitly understood. After the usual simplifications we obtain the following

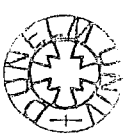

generic result

$$\delta Z_f^{(2)}(e) = -e^4 \frac{1}{2} \Gamma_{f f_1 V_1} \Gamma_{f f_1 V_2} G_{134} G_{243} \int \frac{\mathrm{d}^4 k_1}{(2\pi)^4} \int \frac{\mathrm{d}^4 k_2}{(2\pi)^4} \frac{16\, k_{20}\, p_0}{\vec{k}_2^{\,2}} \frac{1}{[(p-k_1)^2 - m_f^2 + i\epsilon]} \times \frac{[k_1^2 - M_1^2] + [k_1^2 - M_2^2]}{[k_1^2 - M_1^2 + i\epsilon]\,[k_1^2 - M_2^2 + i\epsilon]\,[k_2^2 - M_3^2 + i\epsilon]\,[(k_1-k_2)^2 - M_4^2 + i\epsilon]} \tag{4.141}$$

$$= (i\,e^2)^2 \frac{1}{2} \Gamma_{f f_1 V_1} \Gamma_{f f_1 V_2} G_{134} G_{243} \int \frac{\mathrm{d}^4 k_1}{(2\pi)^4} \int \frac{\mathrm{d}^4 k_2}{(2\pi)^4} \frac{16\, k_{20}\, p_0}{\vec{k}_2^{\,2}} \frac{1}{[(p-k_1)^2 - m_f^2 + i\epsilon]} \times \left[\frac{1}{[k_1^2 - M_2^2 + i\epsilon]\,[k_2^2 - M_3^2 + i\epsilon]\,[(k_1-k_2)^2 - M_4^2 + i\epsilon]} + \frac{1}{[k_1^2 - M_1^2 + i\epsilon]\,[k_2^2 - M_3^2 + i\epsilon]\,[(k_1-k_2)^2 - M_4^2 + i\epsilon]} \right], \tag{4.142}$$

yielding with the help of the result from (4.122e)

$$\delta Z_f^{(2)}(e) = +\frac{1}{2} \Gamma_{f f_1 V_1} \Gamma_{f f_1 V_2} G_{134} G_{243} \left(-\frac{\alpha}{\pi}\right)^2 \int_0^1 \frac{\mathrm{d}y_1}{y_1} \int_{y_1}^1 \frac{\mathrm{d}z_1}{z_1} \int_0^1 \frac{\mathrm{d}y_2}{y_2} \int_{y_2}^1 \frac{\mathrm{d}z_2}{z_2} \times \left[\mathcal{K}^{(1)}(s, m_f^2, M_1, y_1, z_1) + \mathcal{K}^{(1)}(s, m_f^2, M_2, y_1, z_1) \right] \mathcal{K}^{(1)}(s, m_f^2, M_3, y_2, z_2) \times \Theta(y_2 - y_1)\, \Theta(z_1 - z_2)\ . \tag{4.143}$$

Throughout this calculation we have assumed that the particle V_3 is the soft one (rather than V_4). With the purpose of making the bookkeeping as simple as possible for later summation of all possible combinations of particles in the various diagrams, we remove the explicit orientation in the inner loop and add the case that V_4 is soft:

$$\delta Z_f^{(2)}(e) = \frac{1}{2} \Gamma_{f f_1 V_1} \Gamma_{f f_1 V_2} G_{134} G_{243} \left(-\frac{\alpha}{\pi}\right)^2 \int_0^1 \frac{\mathrm{d}y_1}{y_1} \int_{y_1}^1 \frac{\mathrm{d}z_1}{z_1} \int_0^1 \frac{\mathrm{d}y_2}{y_2} \int_{y_2}^1 \frac{\mathrm{d}z_2}{z_2} \times \left[\mathcal{K}^{(1)}(s, m_f^2, M_1, y_1, z_1) + \mathcal{K}^{(1)}(s, m_f^2, M_2, y_1, z_1) \right] \times \left[\mathcal{K}^{(1)}(s, m_f^2, M_3, y_2, z_2) + \mathcal{K}^{(1)}(s, m_f^2, M_4, y_2, z_2) \right] \times \Theta(y_2 - y_1)\, \Theta(z_1 - z_2)\ . \tag{4.144}$$

To summarize the whole last section we write the generic two-loop contribution of Sudakov

logarithms to $\delta Z_f^{(2)}$ as:

$$\delta Z_f^{(2)} \approx \left(-\frac{\alpha}{\pi}\right)^2 \Gamma_f^{(2)} \int_0^1 \frac{\mathrm{d}y_1}{y_1} \int_{y_1}^1 \frac{\mathrm{d}z_1}{z_1} \int_0^1 \frac{\mathrm{d}y_2}{y_2} \int_{y_2}^1 \frac{\mathrm{d}z_2}{z_2}\, \mathcal{K}^{(2)}(y_1, z_1, y_2, z_2) \,. \quad (4.145)$$

For the five different topologies the various products $\Gamma_f^{(2)} \times \mathcal{K}^{(2)}$ of coupling factors and integration kernels are given by

$$\begin{aligned}
\text{set (a):}\quad & \left[\Gamma^2_{ff_1V_1}\, \mathcal{K}^{(1)}(s, m_f^2, M_1, y_1, z_1)\right] \left[\Gamma^2_{f_1f_2V_2}\, \mathcal{K}^{(1)}(s, m_f^2, M_2, y_2, z_2)\right] \Theta(y_2 - y_1) \,, \\
\text{set (b):}\quad & -\,\Gamma_{ff_1V_1}\, \Gamma_{f_1f_2V_2}\, \Gamma_{f_2f_3V_1}\, \Gamma_{ff_3V_2}\, \mathcal{K}^{(1)}(s, m_f^2, M_1, y_1, z_1)\, \mathcal{K}^{(1)}(s, m_f^2, M_2, y_2, z_2) \,, \\
\text{set (c):}\quad & \left[\Gamma^2_{ff_1V_1}\, \mathcal{K}^{(1)}(s, m_f^2, M_1, y_1, z_1)\right] \left[\Gamma^2_{ff_2V_2}\, \mathcal{K}^{(1)}(s, m_f^2, M_2, y_2, z_2)\right] \,, \\
\text{set (d):}\quad & \frac{1}{4}\, \Gamma_{ff_1V_1}\, \Gamma_{f_1f_2V_3}\, \Gamma_{ff_2V_2}\, G_{132} \Big\{ \left[\mathcal{K}^{(1)}(s, m_f^2, M_1, y_1, z_1) + \mathcal{K}^{(1)}(s, m_f^2, M_2, y_1, z_1)\right] \times \\
& \qquad \times\ \mathcal{K}^{(1)}(s, m_f^2, M_3, y_2, z_2)\, \Theta(y_2 - y_1) \left[1 + 3\,\Theta(z_1 - z_2)\right] \\
& \qquad\qquad + \mathcal{K}^{(1)}(s, m_f^2, M_1, y_1, z_1)\, \mathcal{K}^{(1)}(s, m_f^2, M_2, y_2, z_2) \ \times \\
& \qquad \times\ \left[3 + \Theta(y_1 - y_2)\, \Theta(z_2 - z_1) + \Theta(y_2 - y_1)\, \Theta(z_1 - z_2)\right] \Big\} \,, \\
\text{set (e):}\quad & \frac{1}{2}\, \Gamma_{ff_1V_1}\, \Gamma_{ff_1V_2}\, G_{134}\, G_{243} \left[\mathcal{K}^{(1)}(s, m_f^2, M_3, y_2, z_2) + \mathcal{K}^{(1)}(s, m_f^2, M_4, y_2, z_2)\right] \times \\
& \times \left[\mathcal{K}^{(1)}(s, m_f^2, M_1, y_1, z_1) + \mathcal{K}^{(1)}(s, m_f^2, M_2, y_1, z_1)\right] \Theta(y_2 - y_1)\, \Theta(z_1 - z_2) \quad (4.146)
\end{aligned}$$

In Appendix D we have derived all relevant one- and two-loop integrals. Here we give the results, using the generic notation

$$I^{(i)} = \left(-\frac{\alpha}{\pi}\right)^i \int_0^1 \frac{\mathrm{d}y_1}{y_1} \int_{y_1}^1 \frac{\mathrm{d}z_1}{z_1} \cdots \int_0^1 \frac{\mathrm{d}y_i}{y_i} \int_{y_i}^1 \frac{\mathrm{d}z_i}{z_i}\, \mathcal{K}^{(i)}(y_1, z_1, \ldots, y_i, z_i) \,. \quad (4.147)$$

At one-loop level we found

$$\mathcal{K}^{(1)}(s, m_f^2, M, y_1, z_1) : I^{(1)} = \mathrm{L}(M, M) \,, \quad (4.148)$$

$$\mathcal{K}^{(1)}(s, m_f^2, \lambda, y_1, z_1) : I^{(1)} = \mathrm{L}_\gamma(\lambda, m_f) \,. \quad (4.149)$$

The functions $\mathrm{L}(M_1, M_2)$ and $\mathrm{L}_\gamma(\lambda, M_1)$ are the ones defined in (4.68) and (4.69). At two-loop level we found for the angular ordered integrals:

$$\begin{aligned}
\mathcal{K}^{(1)}(s, m_f^2, M, y_1, z_1)\, \mathcal{K}^{(1)}(s, m_f^2, M, y_2, z_2)\, \Theta(y_2 - y_1) : I^{(2)} &= \frac{1}{2}\, \mathrm{L}^2(M, M) \;, \\
\mathcal{K}^{(1)}(s, m_f^2, \lambda, y_1, z_1)\, \mathcal{K}^{(1)}(s, m_f^2, \lambda, y_2, z_2)\, \Theta(y_2 - y_1) : I^{(2)} &= \frac{1}{2}\, \mathrm{L}_\gamma^2(\lambda, m_f) \;, \\
\mathcal{K}^{(1)}(s, m_f^2, M, y_1, z_1)\, \mathcal{K}^{(1)}(s, m_f^2, \lambda, y_2, z_2)\, \Theta(y_2 - y_1) : I^{(2)} &= \frac{7}{12}\, \mathrm{L}^2(M, M) \;, \\
\mathcal{K}^{(1)}(s, m_f^2, \lambda, y_1, z_1)\, \mathcal{K}^{(1)}(s, m_f^2, M, y_2, z_2)\, \Theta(y_2 - y_1) : I^{(2)} &= \mathrm{L}(M, M)\, \mathrm{L}_\gamma(\lambda, m_f) \\
&\quad - \frac{7}{12}\, \mathrm{L}^2(M, M) \;,
\end{aligned} \tag{4.150}$$

and for the double ordered integrals:

$$\begin{aligned}
\mathcal{K}^{(1)}(s, m_f^2, M, y_1, z_1)\, \mathcal{K}^{(1)}(s, m_f^2, M, y_2, z_2)\, \Theta(y_2 - y_1)\, \Theta(z_1 - z_2) : I^{(2)} &= \frac{1}{4}\, \mathrm{L}^2(M, M) \;, \\
\mathcal{K}^{(1)}(s, m_f^2, M, y_1, z_1)\, \mathcal{K}^{(1)}(s, m_f^2, \lambda, y_2, z_2)\, \Theta(y_2 - y_1)\, \Theta(z_1 - z_2) : I^{(2)} &= \frac{1}{3}\, \mathrm{L}^2(M, M) \;, \\
\mathcal{K}^{(1)}(s, m_f^2, \lambda, y_1, z_1)\, \mathcal{K}^{(1)}(s, m_f^2, M, y_2, z_2)\, \Theta(y_2 - y_1)\, \Theta(z_1 - z_2) : I^{(2)} &= \frac{2}{3}\, \mathrm{L}(M, M)\, \mathrm{L}(M, m_f) \\
&\quad - \frac{1}{4}\, \mathrm{L}^2(M, M) \;.
\end{aligned} \tag{4.151}$$

Note that in the case of double ordering the collinear cut-off m_f^2 of the y_2 integral is in fact redundant.

Now the task at hand is to sum all possible contributions to obtain the full two-loop correction to the external wave-function factor.

'rainbow' contributions:

$$
\begin{aligned}
V_1 = \gamma, V_2 = \gamma \quad &: \quad \frac{1}{2}\left(\delta Z^{(1)}_{f_{L/R}}(\gamma)\,\delta Z^{(1)}_{f_{L/R}}(\gamma)\right) \\
V_1 = Z, V_2 = Z \quad &: \quad \frac{1}{2}\left(\delta Z^{(1)}_{f_{L/R}}(Z)\,\delta Z^{(1)}_{f_{L/R}}(Z)\right) \\
V_1 = W, V_2 = W \quad &: \quad \frac{1}{2}\left(\delta Z^{(1)}_{f_L}(W)\,\delta Z^{(1)}_{f_L}(W)\right) \\
(V_1 = \gamma, V_2 = Z) + (V_1 = Z, V_2 = \gamma) \quad &: \quad \left(\delta Z^{(1)}_{f_{L/R}}(\gamma)\,\delta Z^{(1)}_{f_{L/R}}(Z)\right) \\
(V_1 = \gamma, V_2 = W) + (V_1 = W, V_2 = \gamma) \quad &: \quad \delta Z^{(1)}_{f_L}(W)\,\delta Z^{(1)}_{f_L}(\gamma) - \frac{7}{12}\frac{1}{\sin^2\theta_{\rm w}} I_f^3 Y_f^L \mathrm{L}^2 \\
(V_1 = Z, V_2 = W) + (V_1 = W, V_2 = Z) \quad &: \quad \delta Z^{(1)}_{f_L}(W)\,\delta Z^{(1)}_{f_L}(Z) + \frac{1}{2\sin^2\theta_{\rm w}} I_f^3 Y_f^L \mathrm{L}^2
\end{aligned}
$$

where we have used the abbreviations $\mathrm{L} \equiv \mathrm{L}(M, M)$ and $\mathrm{L}_\gamma \equiv \mathrm{L}_\gamma(\lambda, m_f)$ and $\delta Z^{(1)}_{f_{L/R}}(V)$ are the one-loop wave-function factors given in (4.67). And hence for the sum we obtain

$$
\sum(\text{rainbow}) = \begin{cases} \frac{1}{2}\left(\delta Z^{(1)}_{f_L}(W) + \delta Z^{(1)}_{f_L}(Z) + \delta Z^{(1)}_{f_L}(\gamma)\right)^2 - \frac{1}{6}\frac{I_f^3 Y_f^L}{2\sin^2\theta_{\rm w}}\mathrm{L}^2 \\ \frac{1}{2}\left(\delta Z^{(1)}_{f_R}(Z) + \delta Z^{(1)}_{f_R}(\gamma)\right)^2 \end{cases} \tag{4.153}
$$

'crossed rainbow' contributions:

$$
\begin{aligned}
V_1 = \gamma\,, V_2 = \gamma \;&: \; -\left(\delta Z^{(1)}_{f_{L/R}}(\gamma)\,\delta Z^{(1)}_{f_{L/R}}(\gamma)\right) \\
V_1 = Z\,, V_2 = Z \;&: \; -\left(\delta Z^{(1)}_{f_{L/R}}(Z)\,\delta Z^{(1)}_{f_{L/R}}(Z)\right) \\
V_1 = Z\,, V_2 = \gamma \;&: \; -\left(\delta Z^{(1)}_{f_{L/R}}(\gamma)\,\delta Z^{(1)}_{f_{L/R}}(Z)\right) \\
V_1 = \gamma\,, V_2 = Z \;&: \; -\left(\delta Z^{(1)}_{f_{L/R}}(\gamma)\,\delta Z^{(1)}_{f_{L/R}}(Z)\right)
\end{aligned}
$$

$$
(V_1 = W, V_2 = Z) + (V_1 = Z, V_2 = W) : -2\,\delta Z^{(1)}_{f_L}(W)\,\delta Z^{(1)}_{f_L}(Z) + \left(\frac{\cos^2\theta_{\rm w}}{2\sin^4\theta_{\rm w}} - \frac{I_f^3 Y_f^L}{\sin^2\theta_{\rm w}}\right)\mathrm{L}^2
$$

$$
(V_1 = W, V_2 = \gamma) + (V_1 = \gamma, V_2 = W) := -2\,\delta Z^{(1)}_{f_L}(W)\,\delta Z^{(1)}_{f_L}(\gamma) + \left(\frac{1}{2\sin^2\theta_{\rm w}} + \frac{I_f^3 Y_f^L}{\sin^2\theta_{\rm w}}\right)\mathrm{L}\,\mathrm{L}_\gamma
$$

leading to the sum

$$\sum(\text{crossed rainbow}) = \begin{cases} -\left(\delta Z_{f_L}^{(1)}(W) + \delta Z_{f_L}^{(1)}(Z) + \delta Z_{f_L}^{(1)}(\gamma)\right)^2 \\ +3\,\delta Z_{f_L}^{(1)}(W)\delta Z_{f_L}^{(1)}(W) + \delta Z_{f_L}^{(1)}(W)\,\left(1 + 2\,I_f^3 Y_f^L\right)\,[\mathrm{L}_\gamma - \mathrm{L}]\,, \\ -\left(\delta Z_{f_R}^{(1)}(Z) + \delta Z_{f_R}^{(1)}(\gamma)\right)^2 \end{cases} \tag{4.155}$$

'reducible' contributions:

$$\sum(\text{reducible}) = \begin{cases} \left(\delta Z_{f_L}^{(1)}(W) + \delta Z_{f_L}^{(1)}(Z) + \delta Z_{f_L}^{(1)}(\gamma)\right)^2 \\ \left(\delta Z_{f_R}^{(1)}(Z) + \delta Z_{f_R}^{(1)}(\gamma)\right)^2 \end{cases} \tag{4.156}$$

'TGB' contributions:

This topolgoy has contributions only for left-handed fermions, due to the $(V-A)$ structure of the W coupling (see Appendix B). In order to account for the fact that the sign of the triple gauge boson vertex depends on the charge of the incoming fermion, a factor $2\,I_f^3$ emerges in the overall coupling [*e. g.* $G_{132} = G_{\gamma W^+ W^-} = 1$ if $Q_f > 0$ and $I_f^3 = +1/2$;

$G_{132} = G_{\gamma W^- W^+} = -1$ if $Q_f < 0$ and $I_f^3 = -1/2$]. The individual contributions are given by

$$(V_1 = \gamma, V_2 = V_3 = W) + (V_1 = V_3 = W, V_2 = \gamma) \; : 2\,\frac{1}{4}\,\frac{2\,I_f^3(1)(-Q_f)}{2\,\sin^2\theta_{\rm w}} \times$$
$$\times \left[\left(\mathrm{L}\,\mathrm{L}_\gamma - \frac{7}{12}\,\mathrm{L}^2 + \frac{1}{2}\,\mathrm{L}^2 \right) + 3\,\frac{2}{3}\,\mathrm{L}\,\mathrm{L}_{m_f} - \frac{3}{4}\,\mathrm{L}^2 + \frac{3}{4}\,\mathrm{L}^2 + 3\,\mathrm{L}\,\mathrm{L}_\gamma + \frac{1}{3}\mathrm{L}^2 + \frac{2}{3}\,\mathrm{L}\,\mathrm{L}_{m_f} - \frac{1}{4}\,\mathrm{L}^2 \right]$$
$$= -\frac{1}{2}\,\frac{I_f^3\,Q_f}{\sin^2\theta_{\rm w}} \left[4\,\mathrm{L}\,\mathrm{L}_\gamma + \frac{8}{3}\,\mathrm{L}\,\mathrm{L}_{m_f} \right]$$

$$V_1 = V_2 = W, V_3 = \gamma \; : \frac{1}{4}\,\frac{I_f^3\,Q_{f'}}{\sin^2\theta_{\rm w}} \left[2\left(\frac{7}{12}\,\mathrm{L}^2 + 3\,\frac{1}{3}\mathrm{L}^2 \right) + \left(3\,\mathrm{L}^2 + 2\,\frac{1}{4}\,\mathrm{L}^2 \right) \right]$$
$$= \frac{1}{4}\,\frac{I_f^3\,Q_{f'}}{\sin^2\theta_{\rm w}} \left(6 + \frac{2}{3} \right) \mathrm{L}^2$$

$$(V_1 = Z, V_2 = V_3 = W) + (V_1 = V_3 = W, V_2 = Z) \; :$$
$$2\,\frac{1}{4}\,\frac{2\,I_f^3\,(-\cos\theta_{\rm w}/\sin\theta_{\rm w})\,(v_f + a_f)}{2\,\sin^2\theta_{\rm w}} \left[2\,\frac{1}{2}\,\mathrm{L}^2 + 2\,\frac{3}{4}\,\mathrm{L}^2 + 3\,\mathrm{L}^2 + 2\,\frac{1}{4}\mathrm{L}^2 \right]$$
$$= -\frac{1}{2}\,\frac{I_f^3\,(I_f^3 - Q_f\,\sin^2\theta_{\rm w})}{\sin^4\theta_{\rm w}} \left[6\,\mathrm{L}^2 \right]$$

$$V_1 = V_2 = W, V_3 = Z \; : \frac{1}{4}\,\frac{2\,I_f^3\,(\cos\theta_{\rm w}/\sin\theta_{\rm w})\,(v_{f'} + a_{f'})}{2\,\sin^2\theta_{\rm w}} \left[6\,\mathrm{L}^2 \right]$$
$$= \frac{1}{4}\,\frac{I_f^3\,(-I_f^3 - Q_{f'}\,\sin^2\theta_{\rm w})}{\sin^4\theta_{\rm w}} \left[6\,\mathrm{L}^2 \right]$$

with the abbreviation $\mathrm{L}_{m_f} \equiv \mathrm{L}(M, m_f)$. The change of sign between the first and the second as well as third and fourth contributions originates from the antisymmetricity of G_{132}. The sum of those contributions is given by

$$\sum (\mathrm{TGB})_L = -2\,\frac{I_f^3\,Q_f}{\sin^2\theta_{\rm w}} \left[\mathrm{L}\,\mathrm{L}_\gamma + \frac{2}{3}\,\mathrm{L}\,\mathrm{L}_{m_f} \right] - \frac{9}{8\,\sin^4\theta_{\rm w}}\,\mathrm{L}^2 + \frac{2}{3}\,\frac{I_f^3\,Q_{f'}}{4\,\sin^2\theta_{\rm w}}\,\mathrm{L}^2 + 3\,\frac{I_f^3\,Q_f}{\sin^2\theta_{\rm w}}\,\mathrm{L}^2$$
$$= -2\,\frac{I_f^3\,Q_f}{\sin^2\theta_{\rm w}} \left[\mathrm{L}\,\mathrm{L}_\gamma + \frac{2}{3}\,\mathrm{L}\,\mathrm{L}_{m_f} \right] - \frac{9}{8\,\sin^4\theta_{\rm w}}\,\mathrm{L}^2$$
$$+ \left[3 - \frac{1}{6} \right] \frac{1}{4\,\sin^2\theta_{\rm w}}\,\mathrm{L}^2 + \left[3 + \frac{1}{6} \right] \frac{I_f^3\,Y_f^L}{2\,\sin^2\theta_{\rm w}}\,\mathrm{L}^2 \qquad (4.158)$$

'frog' contributions:

If V_1 and V_2 are neutral gauge bosons, the 'frog' diagram will contribute for both left- and right-handed fermions. This is reflected in the $(v_f + a_f)$ and $(v_f - a_f)$ couplings of the fermions to the Z boson. For charged gauge bosons V_1 and V_2 only left-handed fermions contribute.

$$V_1 = V_2 = \gamma, V_3 = V_4 = W \; : \; \frac{Q_f^2}{2} 2 \cdot 2 \left[\frac{2}{3} \mathrm{L} \, \mathrm{L}_{m_f} - \frac{1}{4} \mathrm{L}^2 \right] \tag{4.159a}$$

$$V_1 = V_2 = Z, V_3 = V_4 = W \; : \; \frac{1}{2} \frac{\cos^2 \theta_\mathrm{w}}{\sin^2 \theta_\mathrm{w}} (v_f \pm a_f)^2 \, 2 \cdot 2 \left[\frac{1}{4} \mathrm{L}^2 \right] \tag{4.159b}$$

$$(V_1 = \gamma \, , V_2 = Z \, , V_3 = V_4 = W) + (V_1 = Z \, , V_2 = \gamma \, , V_3 = V_4 = W) :$$
$$2 \frac{1}{2} \frac{-\cos \theta_\mathrm{w}}{\sin \theta_\mathrm{w}} (v_f \pm a_f) (-Q_f) \, 2 \left[\frac{2}{3} \mathrm{L} \mathrm{L}_{m_f} - \frac{1}{4} \mathrm{L}^2 + \frac{1}{4} \mathrm{L}^2 \right] \tag{4.159c}$$

$$V_1 = V_2 = V_3 = W \, , V_4 = \gamma : \quad \frac{1}{2} \frac{1}{2 \sin^2 \theta_\mathrm{w}} 2 \left[\frac{1}{3} \mathrm{L}^2 + \frac{1}{4} \mathrm{L}^2 \right] \tag{4.159d}$$

$$V_1 = V_2 = V_3 = W \, , V_4 = Z : \quad \frac{1}{2} \frac{\cos^2 \theta_\mathrm{w}}{2 \sin^4 \theta_\mathrm{w}} 2 \cdot 2 \left[\frac{1}{4} \mathrm{L}^2 \right] \tag{4.159e}$$

Note that for the last two contributions we do *not* add a similar frog diagram with $V_3 = \gamma, Z$ being the soft gauge boson and $V_4 = W$, since this is implicitly done in our notation (4.144). For the sum of right-handed contributions we find

$$\sum (\mathrm{frog})_R = \frac{4}{3} Q_f^2 \mathrm{L} \, \mathrm{L}_{m_f} - \frac{1}{2} Q_f^2 \, \mathrm{L}^2 + \frac{1}{2} \frac{1}{4 \sin^4 \theta_\mathrm{w}} \left[-2 \sin^2 \theta_\mathrm{w} \, Q_f \right]^2 \mathrm{L}^2$$
$$+ \frac{1}{2 \sin^2 \theta_\mathrm{w}} \left[-2 \sin^2 \theta_\mathrm{w} Q_f \right] Q_f \frac{4}{3} \mathrm{L} \, \mathrm{L}_{m_f} = 0 \tag{4.160}$$

and similarly

$$\sum (\mathrm{frog})_L = \frac{7}{24 \sin^2 \theta_\mathrm{w}} \mathrm{L}^2 + \frac{1}{8 \sin^4 \theta_\mathrm{w}} \mathrm{L}^2 + \frac{\cos^2 \theta_\mathrm{w}}{4 \sin^4 \theta_\mathrm{w}} \mathrm{L}^2 + \frac{4}{3} \frac{I_f^3 Q_f}{\sin^2 \theta_\mathrm{w}} \mathrm{L} \, \mathrm{L}_{m_f} - \frac{I_f^3 Q_f}{\sin^2 \theta_\mathrm{w}} \mathrm{L}^2 \tag{4.161}$$

Adding up all contributions yields for right-handed fermions immediately

$$\delta Z_{f_R}^{(2)} = \frac{1}{2} \left(\delta Z_{f_R}^{(1)}(Z) + \delta Z_{f_R}^{(1)}(\gamma) \right)^2 \tag{4.162}$$

and with a bit of algebra we find for the left-handed fermions

$$\begin{aligned}
\delta Z_{f_L}^{(2)} &= \frac{1}{2}\left(\delta Z_{f_L}^{(1)}(W)+\delta Z_{f_L}^{(1)}(Z)+\delta Z_{f_L}^{(1)}(\gamma)\right)^2 - \frac{1}{12}\frac{I_f^3 Y_f^L}{\sin^2\theta_{\rm w}}\,{\rm L}^2 + \frac{3}{4\sin^4\theta_{\rm w}}\,{\rm L}^2 \\
&+ \frac{1}{2\sin^2\theta_{\rm w}}\left[1+2\,I_f^3\,Y_f^L\right]\left({\rm L}\,{\rm L}_\gamma-{\rm L}^2\right) - 2\,\frac{I_f^3\,Q_f}{\sin^2\theta_{\rm w}}\left[{\rm L}\,{\rm L}_\gamma+\frac{2}{3}\,{\rm L}\,{\rm L}_{m_f}\right] - \frac{9}{8\sin^4\theta_{\rm w}}\,{\rm L}^2 \\
&+ \left[3-\frac{1}{6}\right]\frac{1}{4\sin^2\theta_{\rm w}}\,{\rm L}^2 + \left[3+\frac{1}{6}\right]\frac{I_f^3\,Y_f^L}{2\sin^2\theta_{\rm w}}\,{\rm L}^2 \\
&+ \frac{7}{24\sin^2\theta_{\rm w}}\,{\rm L}^2 + \frac{1}{8\sin^4\theta_{\rm w}}\,{\rm L}^2 + \frac{\cos^2\theta_{\rm w}}{4\sin^4\theta_{\rm w}}\,{\rm L}^2 + \frac{4}{3}\,\frac{I_f^3\,Q_f}{\sin^2\theta_{\rm w}}\,{\rm L}\,{\rm L}_{m_f} - \frac{I_f^3\,Q_f}{\sin^2\theta_{\rm w}}\,{\rm L}^2 \\
&= \frac{1}{2}\left(\delta Z_{f_L}^{(1)}(W)+\delta Z_{f_L}^{(1)}(Z)+\delta Z_{f_L}^{(1)}(\gamma)\right)^2 + \left[-\frac{1}{12}-1+\frac{3}{2}+\frac{1}{12}-\frac{1}{2}\right]\frac{I_f^3\,Y_f^L}{\sin^2\theta_{\rm w}}\,{\rm L}^2 \\
&\left[-\frac{1}{2}+\frac{3}{4}-\frac{1}{24}+\frac{7}{24}-\frac{1}{4}-\frac{1}{4}\right]\frac{1}{\sin^2\theta_{\rm w}}\,{\rm L}^2 + \left[\frac{3}{4}-\frac{9}{8}+\frac{1}{8}+\frac{1}{4}\right]\frac{1}{\sin^4\theta_{\rm w}}\,{\rm L}^2 . \qquad (4.163)
\end{aligned}$$

And hence the full two-loop fermionic Sudakov correction factor reads

$$\boxed{\delta Z_f^{(2)} = \begin{cases} \frac{1}{2}\left(\delta Z_{f_L}^{(1)}(W)+\delta Z_{f_L}^{(1)}(Z)+\delta Z_{f_L}^{(1)}(\gamma)\right)^2 \\ \frac{1}{2}\left(\delta Z_{f_R}^{(1)}(Z)+\delta Z_{f_R}^{(1)}(\gamma)\right)^2 \end{cases}} \qquad (4.164)$$

From (4.164) we deduce our main statement, namely that the virtual electroweak two-loop Sudakov correction factor is obtained by a mere exponentiation of the one-loop Sudakov correction factor. This is in agreement with the corresponding results in Ref. [62] based on Gribov's theorem[13]. We also note that, in adding up all the contributions, we find that the 'rainbow' diagrams of set (a) yield the usual exponentiating terms plus an extra term for left-handed fermions similar to the one found in Ref. [61]. This extra term originates from the charged-current interactions and is only non-vanishing as a result of the mass gap between the massless photon and the massive Z boson. We therefore disagree with the

[13]This theorem was formally derived for QED. Up to now its applicability to multi-scale theories like the SM has not been proven yet.

statement in Ref. [62] that only rainbow diagrams contribute in physical gauges like the axial or the Coulomb gauge. Whereas in Ref. [61] the extra term was interpreted as a source of non-exponentiation, we observe that it in fact cancels against a specific term originating from the triple gauge-boson diagrams of set (d). Similar (gauge) cancellations take place between the 'crossed rainbow' diagrams of set (b), the reducible diagrams of set (c), and another part of the triple gauge-boson diagrams of set (d). Finally, the left-over terms of set (d) get cancelled by the contributions from the gauge-boson self-energy ('frog') diagrams of set (e). Hence, the cancellations that take place automatically in unbroken gauge theories also hold in the SM, in spite of it being a theory with more than one scale in the sense that the on-shell poles for photons and Z bosons do not coincide and therefore lead to different on-shell residues.

Comparing with the study in Ref. [60], we can make the following remark. A treatment of pure weak gauge-boson effects without reference to the photonic interactions obviously breaks gauge-invariance, since the photon has an explicit $SU(2)$ component. This holds even if the photon is treated fully inclusively as in Ref. [60]. Such a separation would require a very careful definition, for instance in terms of the typical energy regimes that govern the Sudakov effects of pure electromagnetic origin (ultrasoft energies: $\lambda/\sqrt{s} \leq z \leq M/\sqrt{s}$) and collective electroweak origin (soft energies: $M/\sqrt{s} \leq z \ll 1$).[14]

4.4.2 The bosonic self energy at two-loop level

As we already saw in the one-loop calculation, the mere difference between the different baseline particles is in the quantum numbers (*i. e.* couplings). Hence making use of (4.85) and (4.146) we collect all the relevant contributions for the two-loop Sudakov correction factor for transversely polarized W bosons:

[14] In a more recent paper [68] the authors of Ref. [60] agree on those points, which were also addressed in Refs. [61, 62].

'rainbow' contributions:

$$
\begin{aligned}
V_1 = \gamma\,, V_2 = \gamma\,: &\quad \frac{1}{2}\,\delta Z^{(1)}_{W_T}(\gamma)\;\delta Z^{(1)}_{W_T}(\gamma)\\
V_1 = Z\,, V_2 = Z\,: &\quad \frac{1}{2}\,\delta Z^{(1)}_{W_T}(Z)\;\delta Z^{(1)}_{W_T}(Z)\\
V_1 = Z\,, V_2 = \gamma\,: &\quad \frac{7}{12}\,\frac{\cos^2\theta_{\rm w}}{\sin^2\theta_{\rm w}}\,{\rm L}^2\\
V_1 = \gamma\,, V_2 = Z\,: &\quad -\frac{7}{12}\,\frac{\cos^2\theta_{\rm w}}{\sin^2\theta_{\rm w}}\,{\rm L}^2 + \frac{\cos^2\theta_{\rm w}}{\sin^2\theta_{\rm w}}\,{\rm L}\,{\rm L}_\gamma\\
V_1 = W\,, V_2 = W\,: &\quad 2\,\frac{1}{2}\,\delta Z^{(1)}_{W_T}(W)\;\delta Z^{(1)}_{W_T}(W)\\
V_1 = Z\,, V_2 = W\,: &\quad \frac{1}{2}\,\frac{\cos^2\theta_{\rm w}}{\sin^2\theta_{\rm w}}\left(1+\frac{\cos^2\theta_{\rm w}}{\sin^2\theta_{\rm w}}\right){\rm L}^2\\
V_1 = \gamma\,, V_2 = W\,: &\quad \left(1+\frac{\cos^2\theta_{\rm w}}{\sin^2\theta_{\rm w}}\right){\rm L}\,{\rm L}_\gamma - \left(1+\frac{\cos^2\theta_{\rm w}}{\sin^2\theta_{\rm w}}\right)\frac{7}{12}\,{\rm L}^2
\end{aligned}
$$

where we have used the abbreviations ${\rm L} \equiv {\rm L}(M,M)$ and ${\rm L}_\gamma = {\rm L}_\gamma(\lambda, M)$. The factors $\delta Z^{(1)}_{W_T}(V)$ are defined in (4.85) and are the corresponding one-loop correction factors. The factor 2 for $V_1 = V_2 = W$ originates from the fact that in the inner loop the charge is not fixed and we have to consider the two possibilities of W^+or W^-being V_2. Note that since the baseline particle is a W it is not possible to have a soft W in the outer loop ($V_1 = W$) and a neutral soft particle in the inner loop ($V_2 = N$). Adding up those 'rainbow' contributions we find

$$
\begin{aligned}
\sum(\text{rainbow}) = \frac{1}{2}\,&\left(\delta Z^{(1)}_{W_T}(W) + \delta Z^{(1)}_{W_T}(Z) + \delta Z^{(1)}_{W_T}(\gamma)\right)^2\\
&- \frac{1}{12}\,\delta Z^{(1)}_{W_T}(W)\,\left(\delta Z^{(1)}_{W_T}(W) - \delta Z^{(1)}_{W_T}(Z)\right)
\end{aligned}
\tag{4.165}
$$

'crossed rainbow' contributions:

$$
\begin{aligned}
V_1 = \gamma\,, V_2 = \gamma\,: &\quad -\delta Z^{(1)}_{W_T}(\gamma)\;\delta Z^{(1)}_{W_T}(\gamma)\\
V_1 = Z\,, V_2 = Z\,: &\quad -\delta Z^{(1)}_{W_T}(Z)\;\delta Z^{(1)}_{W_T}(Z)\\
V_1 = Z\,, V_2 = \gamma\,: &\quad -\delta Z^{(1)}_{W_T}(Z)\;\delta Z^{(1)}_{W_T}(\gamma)\\
V_1 = \gamma\,, V_2 = Z\,: &\quad -\delta Z^{(1)}_{W_T}(\gamma)\;\delta Z^{(1)}_{W_T}(Z)\,.\\
V_1 = W\,, V_2 = W\,: &\quad -\delta Z^{(1)}_{W_T}(W)\;\delta Z^{(1)}_{W_T}(W)\,,
\end{aligned}
$$

Hence the sum reads

$$\sum(\text{crossed rainbow}) = -\left(\delta Z^{(1)}_{W_T}(W) + \delta Z^{(1)}_{W_T}(Z) + \delta Z^{(1)}_{W_T}(\gamma)\right)^2 + 2\,\delta Z^{(1)}_{W_T}(W)\left(\delta Z^{(1)}_{W_T}(Z) + \delta Z^{(1)}_{W_T}(\gamma)\right). \tag{4.167}$$

Note here that contributions with one charged and one neutral gauge-boson are not possible.

'reducible' contributions:

$$\sum(\text{reducible}) = \left(\delta Z^{(1)}_{W_T}(W) + \delta Z^{(1)}_{W_T}(Z) + \delta Z^{(1)}_{W_T}(\gamma)\right)^2. \tag{4.168}$$

'TGB' contributions:

$$(V_1=\gamma, V_2=W, V_3=W) + (V_1=W, V_2=\gamma, V_3=W) \;:\quad -2\,\frac{1}{4}\left(1+\frac{\cos^2\theta_w}{\sin^2\theta_w}\right)\times$$
$$\times\left[\left(\mathrm{L}\,\mathrm{L}_\gamma - \frac{7}{12}\mathrm{L}^2 + \frac{1}{2}\mathrm{L}^2\right) + 3\,\frac{2}{3}\mathrm{L}^2 - \frac{3}{4}\mathrm{L}^2 + \frac{3}{4}\mathrm{L}^2 + 3\,\mathrm{L}\,\mathrm{L}_\gamma + \frac{1}{3}\mathrm{L}^2 + \frac{2}{3}\mathrm{L}^2 - \frac{1}{4}\mathrm{L}^2\right]$$
$$= -\frac{1}{2}\left(1+\frac{\cos^2\theta_w}{\sin^2\theta_w}\right)\left[4\,\mathrm{L}\,\mathrm{L}_\gamma + \frac{8}{3}\mathrm{L}^2\right]$$

$$(V_1=Z, V_2=W, V_3=W) + (V_1=W, V_2=Z, V_3=W) \;:$$
$$-2\,\frac{1}{4}\,\frac{\cos^2\theta_w}{\sin^2\theta_w}\left(1+\frac{\cos^2\theta_w}{\sin^2\theta_w}\right)\left[2\,\frac{1}{2}\mathrm{L}^2 + 2\,\frac{3}{4}\mathrm{L}^2 + 3\mathrm{L}^2 + 2\,\frac{1}{4}\mathrm{L}^2\right]$$
$$= -\frac{1}{2}\,\frac{\cos^2\theta_w}{\sin^2\theta_w}\left(1+\frac{\cos^2\theta_w}{\sin^2\theta_w}\right)\left[6\,\mathrm{L}^2\right],$$

where we have explicitly summed the photon and Z contributions for the appropriate neutral inner baseline particle. The result is

$$\sum(\text{TGB}) = -2\,\delta Z^{(1)}_{W_T}(W)\,\delta Z^{(1)}_{W_T}(\gamma) - \frac{4}{3}\,\delta Z^{(1)}_{W_T}(W)\left(\delta Z^{(1)}_{W_T}(W) - \delta Z^{(1)}_{W_T}(Z)\right) - 3\,\delta Z^{(1)}_{W_T}(W)\,\delta Z^{(1)}_{W_T}(Z) \tag{4.170}$$

'frog' contributions:

$$
\begin{aligned}
&V_1 = V_2 = \gamma\,, V_3 = V_4 = W: \quad \frac{1}{2}\Big(2\cdot 2\left[\frac{2}{3}\mathrm{L}^2 - \frac{1}{4}\mathrm{L}^2\right]\Big)\\
&V_1 = V_2 = Z\,, V_3 = V_4 = W: \quad \frac{1}{2}\left(\frac{\cos^2\theta_\mathrm{w}}{\sin^2\theta_\mathrm{w}}\right)^2\Big(2\cdot 2\left[\frac{1}{4}\mathrm{L}^2\right]\Big)\\
&(V_1 = \gamma\,, V_2 = Z\,, V_3 = V_4 = W) + (V_1 = Z\,, V_2 = \gamma\,, V_3 = V_4 = W):\\
&\qquad\qquad 2\,\frac{1}{2}\,\frac{\cos^2\theta_\mathrm{w}}{\sin^2\theta_\mathrm{w}}\Big(2\left[\frac{2}{3}\mathrm{L}^2 - \frac{1}{4}\mathrm{L}^2 + \frac{1}{4}\mathrm{L}^2\right]\Big)\\
&(V_1 = V_2 = V_3 = W\,, V_4 = \gamma):\\
&\qquad\qquad \frac{1}{2}\left(1 + \frac{\cos^2\theta_\mathrm{w}}{\sin^2\theta_\mathrm{w}}\right)\Big(2\left[\frac{1}{4}\mathrm{L}^2 + \frac{1}{3}\mathrm{L}^2\right]\Big)\\
&(V_1 = V_2 = V_3 = W\,, V_4 = Z):\\
&\qquad\qquad \frac{1}{2}\,\frac{\cos^2\theta_\mathrm{w}}{\sin^2\theta_\mathrm{w}}\left(1 + \frac{\cos^2\theta_\mathrm{w}}{\sin^2\theta_\mathrm{w}}\right)\Big(2\cdot 2\left[\frac{1}{4}\mathrm{L}^2\right]\Big)\,,
\end{aligned}
$$

and hence

$$
\sum(\text{frog}) = \delta Z^{(1)}_{W_T}(W)\,\delta Z^{(1)}_{W_T}(Z) + \frac{17}{12}\,\delta Z^{(1)}_{W_T}(W)\,\Big(\delta Z^{(1)}_{W_T}(W) - \delta Z^{(1)}_{W_T}(Z)\Big)\,. \tag{4.172}
$$

Finally upon adding all five topologies we are left with

$$
\boxed{\delta Z^{(2)}_{W_T} = \frac{1}{2}\,\Big(\,\delta Z^{(1)}_{W_T}(W) + \delta Z^{(1)}_{W_T}(Z) + \delta Z^{(1)}_{W_T}(\gamma)\,\Big)^2\,.} \tag{4.173}
$$

We conclude that also in the bosonic sector the two-loop Sudakov correction factor can be obtained from half of the square of the full one-loop result. Note here that the gauge cancellations conspire in a way very similar to what we already saw in the fermion case. Due to the mass gap between the massive Z boson and the massless photon, the 'rainbow' contributions from set (a) exhibit an extra term, which in the bosonic case is canceled in part by the contributions from the triple gauge boson diagrams of set (d) and in part by contributions from the 'frog' diagrams of set (e). The extra terms in the 'crossed rainbow' contribution of set (b), arising due to forbidden combinations of one charged and one neutral particle, are in the case of the photon compensated by contributions from the triple gauge

boson diagrams and in the case of the Z boson by contributions from both the triple gauge boson diagrams and the 'frog' diagrams. Eventually we are left with the very simple result $\delta Z_{W_T}^{(2)} = \frac{1}{2}\left(\delta Z_{W_T}^{(1)}\right)^2$ for the two-loop wave-function correction factor.

4.4.3 The scalar self energy at two-loop level

Well, as we have seen in the previous sections the mere difference between the various possible baseline particles is indeed manifest in the couplings. Again various gauge cancellations are going to take place between all five topologies and finally we find for the scalar two-loop correction factor

$$\boxed{\delta Z_\phi^{(2)} = \frac{1}{2}\left(\delta Z_\phi^{(1)}(W) + \delta Z_\phi^{(1)}(Z) + \delta Z_\phi^{(1)}(\gamma)\right)^2} \quad . \tag{4.174}$$

4.4.4 General two-loop Sudakov logarithms

We conclude this section with the general two-loop Sudakov correction factor $\delta Z = Z - 1$.

$$\boxed{\delta Z^{(2)} = \frac{1}{2}\left(\delta Z^{(1)}\right)^2} \quad . \tag{4.175}$$

In summary we would like to point out that to calculate the two-loop Sudakov correction factor for any species of charged[15] initial or final state particles, *i. e.* fermions, gauge bosons or would-be Goldstone bosons, the knowledge of the corresponding one-loop correction factor is sufficient. This is a well known fact in massless or one-mass-scale theories, such as QED, QCD or generally $SU(N)$, where in fact in covariant gauges the two-loop results are *effectively* obtained from so-called ladder diagrams, corresponding to our 'rainbow' diagrams. We like to stress again that for the SM, as a broken theory with two mass scales, the result $\delta Z^{(2)} = \frac{1}{2}\left(\delta Z^{(1)}\right)^2$ is identical, but at all intermediate stages extra terms arise due to the

[15] As mentioned a couple of times earlier on, the investigation of the neutral gauge boson and scalar sector is underway. Note that in the fermionic sector the self energy of the neutrino ν_ℓ is diagonal, so no dedicated investigation is required in that case.

mass gap. Therefore the calculation of only one topology, *i. e.* the 'rainbow' diagrams, does not lead (not even effectively) to the correct two-loop Sudakov correction factor.

4.5 Conclusions

We have calculated the electroweak Sudakov (double) logarithms at one- and two-loop level in the Coulomb gauge, applicable to any high energy scattering process involving fermions and/or W bosons. Especially the treatment of the longitudinal gauge bosons required some special attention. In this special gauge all the relevant contributions, involving the exchange of collinear-soft gauge bosons, are contained in the self-energies of the external on-shell particles.

Our one-loop results are in agreement with the calculations in the literature, including the distinctive terms originating from the mass gap between the photon and the weak gauge bosons. At two-loop level our findings are consistent with an exponentiation of the one-loop results. We conclude that as far as the balance between the one- and two-loop virtual Sudakov logarithms are concerned, the SM behaves like an unbroken theory at high energies. This conclusion can be extended to real-emission processes in a relatively straightforward way. After all, since the Sudakov logarithms originate from the exchange of soft, effectively on-shell gauge bosons, many of the features derived for the virtual corrections will be intimately related to properties of the corresponding real-emission processes.

Several of the derived features of the Coulomb gauge for massive gauge bosons are general and might find applications beyond this very special case of calculating Sudakov logarithms. In particular, any calculation involving collinear gauge bosons will be considerably simplified by means of this gauge. As a matter of fact, for a complete understanding of the perturbative structure of large logarithmic correction factors, single logarithms originating from soft, or collinear or ultraviolet singularities cannot be ignored [69, 70].

Appendix

A Conventions and Data

The four dimensional Dirac matrices γ^μ obey the Clifford algebra

$$\{\gamma^\mu, \gamma^\nu\} \equiv (\gamma^\mu \gamma^\nu + \gamma^\nu \gamma^\mu) = 2\, \mathrm{g}^{\mu\nu} \tag{A.176}$$

with

$$\mathrm{g}^{\mu\nu} = \begin{pmatrix} 1 & 0 & 0 & 0 \\ 0 & -1 & 0 & 0 \\ 0 & 0 & -1 & 0 \\ 0 & 0 & 0 & -1 \end{pmatrix} . \tag{A.177}$$

Working in the Pauli-Dirac representation the γ^μ matrices are defined

$$\gamma^0 = \begin{pmatrix} \mathbf{1} & 0 \\ 0 & -\mathbf{1} \end{pmatrix} , \; \gamma^k = \begin{pmatrix} 0 & \sigma^k \\ -\sigma^k & 0 \end{pmatrix} \tag{A.178}$$

with the two dimensional unit matrix $\mathbf{1}$ and the Pauli matrices σ^k, $k = 1, 2, 3$,

$$\begin{pmatrix} 0 & 1 \\ 1 & 0 \end{pmatrix} , \begin{pmatrix} 0 & -i \\ i & 0 \end{pmatrix} , \begin{pmatrix} 1 & 0 \\ 0 & -1 \end{pmatrix} . \tag{A.179}$$

With these definitions the following identities hold

$$\gamma^{\mu\dagger} = \gamma^0 \gamma^\mu \gamma^0 \tag{A.180}$$

$$\gamma^0 \gamma^0 = \mathbf{1} \tag{A.181}$$

$$\tag{A.182}$$

and with

$$\gamma^5 = i\, \gamma^0 \gamma^1 \gamma^2 \gamma^3 = \begin{pmatrix} 0 & \mathbf{1} \\ \mathbf{1} & 0 \end{pmatrix} , \tag{A.183}$$

it follows that

$$\{\gamma^\mu, \gamma^5\} = 0 \tag{A.184}$$

$$\gamma^5 \gamma^5 = \mathbf{1} \tag{A.185}$$

$$\gamma^{5\dagger} = \gamma^5 . \tag{A.186}$$

Converting the cross section from its natural units into its conventional units we make use of

$$[\sigma] = 1 \text{ GeV}^{-2} \mathrel{\widehat{=}} 0.389 \text{ mb} \tag{A.187}$$

and 1 barn $= 10^{-28} m^2$, 1 pb $= 10^{-12}$ barn and 1 fb $= 10^{-15}$ barn.
For the numerical calculations we have made use of the following data [53][16]

$$\begin{aligned} M_W &= 80.41 \text{ GeV}, & M_Z &= 91.18 \text{ GeV}, \\ \sin^2\theta_w &= 0.232, & \alpha &= \tfrac{e^2}{4\pi} = 1/137.035\,989 . \end{aligned} \tag{A.188}$$

A final reminder

$$\begin{aligned} (1 \pm x)^{1/2} &\approx 1 \pm \frac{1}{2}x - \frac{1\cdot 1}{2\cdot 4}x^2 \pm \frac{1\cdot 1\cdot 3}{2\cdot 4\cdot 6}x^3 - \frac{1\cdot 1\cdot 3\cdot 5}{2\cdot 4\cdot 6\cdot 8}x^4 \pm \ldots \quad \text{for } |x| \le 1 \\ (1 \pm x)^{-1/2} &\approx 1 \mp \frac{1}{2}x + \frac{1\cdot 3}{2\cdot 4}x^2 \mp \frac{1\cdot 3\cdot 5}{2\cdot 4\cdot 6}x^3 + \frac{1\cdot 3\cdot 5\cdot 7}{2\cdot 4\cdot 6\cdot 8}x^4 \mp \ldots \quad \text{for } |x| < 1 . \end{aligned} \tag{A.189}$$

B Feynman Rules

In the following all boson momenta are defined to be incoming and momentum is conserved at each vertex.

Propagators

fermion : $\alpha \bullet\!\!\xrightarrow{p}\!\!\bullet \beta$ $\qquad \left(\frac{i}{(\not{p} - m_f)}\right)_{\beta\alpha}$ (B.190)

[16] The most recent publication of the Particle Data Group [71] was not available at the time of the calculations.

boson : 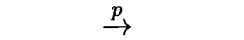 $\frac{-i}{p^2 - M_V^2 + i\epsilon}\left(g_{\mu\nu} - \frac{(1-\xi)\,p_\mu\,p_\nu}{p^2 - \xi\,M_V^2}\right)$ (B.191)

where $\xi = 1$ corresponds to the 't Hooft-Feynman gauge, $\xi = 0$ to the Landau gauge and $\xi = \infty$ to the unitary gauge.

Vertices

The coupling between a gauge boson and fermions ($Vf\bar{f}$) is

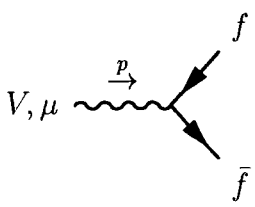

$$= i e\gamma^\mu (V - A\gamma_5) \quad \text{(B.192)}$$

$$= i e\gamma^\mu \left[\frac{1}{2}(\mathbf{1} - \gamma_5)(V + A) + \frac{1}{2}(\mathbf{1} + \gamma_5)(V - A)\right] \quad \text{(B.193)}$$

with

$$\begin{array}{lll} \gamma ff & : V = -Q_f\,, & A = 0 \\ Zff & : V = v_f\,, & A = a_f \\ Wff' & : V = 1/(2\sqrt{2}\sin\theta_w)\,, & A = 1/(2\sqrt{2}\sin\theta_w) \end{array} \quad \text{(B.194)}$$

and

$$v_f = \frac{I_f^3 - 2\,Q_f \sin^2\theta_w}{2\sin\theta_w\cos\theta_w}\,, \quad a_f = \frac{I_f^3}{2\sin\theta_w\cos\theta_w}. \quad \text{(B.195)}$$

The coupling between a gauge boson and scalars ($V\,S_1\,S_2$) is

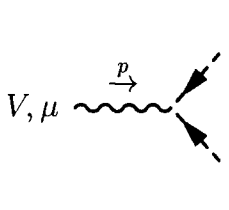

$$= i e G (p_1 - p_2)_\mu \quad \text{(B.196)}$$

with ($\lambda = \pm$)

$$\begin{array}{lll} \gamma\phi^\lambda\phi^{-\lambda} & : & G = -\lambda \\ Z\phi^\lambda\phi^{-\lambda} & : & G = \lambda\,\dfrac{\cos^2\theta_w - \sin^2\theta_w}{2\sin\theta_w\cos\theta_w} \\ Z\chi H & : & G = -\dfrac{i}{2\sin\theta_w\cos\theta_w} \\ W^\lambda\phi^{-\lambda}H & : & G = -\dfrac{\lambda}{2\sin\theta_w} \\ W^\lambda\phi^{-\lambda}\chi & : & G = -\dfrac{i}{2\sin\theta_w} \end{array} \quad \text{(B.197)}$$

Interchanging the two scalars S_1 and S_2 causes the coupling constant G to change sign. The coupling between a scalar and two gauge bosons ($S\,V_1\,V_2$) is

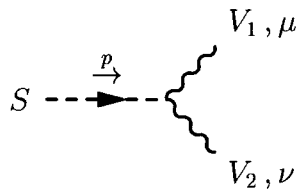

$$= i\,e\,\widetilde{G}\,g_{\mu\nu} \tag{B.198}$$

with

$$\begin{aligned} HZZ &: \widetilde{G} = \frac{M_W}{\sin\theta_w\,\cos^2\theta_w} \\ HWW &: \widetilde{G} = \frac{M_W}{\sin\theta_w} \\ \phi W\gamma &: \widetilde{G} = -M_W \\ \phi WZ &: \widetilde{G} = -\frac{M_W\,\sin\theta_w}{\cos\theta_w} \end{aligned} \tag{B.199}$$

Interchanging the two gauge bosons V_1 and V_2 has no influence on the coupling constant $\widetilde{G}$.

The trilinear and quartic gauge boson self interactions are derived from the kinetic part of the Lagrangian Eq. (1.1). To illustrate this we derive as an example the $W^+W^-\gamma$ vertex from the Lagrangian

$$\mathcal{L}_{kin} = -\frac{1}{4}\mathbf{W}_{\mu\nu}\mathbf{W}^{\mu\nu} \tag{B.200}$$

with

$$\mathbf{W}_{\mu\nu} = \partial_\mu\mathbf{W}_\nu - \partial_\nu\mathbf{W}_\mu + g\mathbf{W}_\mu\times\mathbf{W}_\nu \tag{B.201}$$

($g = e/\sin\theta_w$) and $\mathbf{W}_\mu$ being the SM vector

$$\mathbf{W}_\mu = \begin{pmatrix} W^1_\mu \\ W^2_\mu \\ W^3_\mu \end{pmatrix} = \begin{pmatrix} \frac{1}{\sqrt{2}}(W^+_\mu + W^-_\mu) \\ \frac{i}{\sqrt{2}}(W^+_\mu - W^-_\mu) \\ \cos\theta_w Z_\mu - \sin\theta_w A_\mu \end{pmatrix} . \tag{B.202}$$

The contribution to trilinear couplings is

$$\begin{aligned} &-\frac{1}{4}(\partial_\mu\mathbf{W}_\nu - \partial_\nu\mathbf{W}_\mu)(g\ \mathbf{W}^\mu\times\mathbf{W}^\nu) - \frac{1}{4}(\partial^\mu\mathbf{W}^\nu - \partial^\nu\mathbf{W}^\mu)(g\ \mathbf{W}_\mu\times\mathbf{W}_\nu) \\ &\quad = \frac{-g}{2}(\partial_\mu\mathbf{W}_\nu - \partial_\nu\mathbf{W}_\mu)(\ \mathbf{W}^\mu\times\mathbf{W}^\nu) \end{aligned} \tag{B.203}$$

For simplicity we study each component of this vector product separately. Selecting only the photon component of $W_{3\,\mu}$ to obtain the $W^+W^-\gamma$ vertex:

1. component

$$\frac{-g}{2}\left(\partial_\mu\frac{1}{\sqrt{2}}(W^+_\nu+W^-_\nu)-\partial_\nu\frac{1}{\sqrt{2}}(W^+_\mu+W^-_\mu)\right)(W^{\mu 2}W^{\nu 3}-W^{\mu 3}W^{\nu 2})$$

$$\xrightarrow[\text{rules}]{\text{Feynman}} i\,\frac{-ig}{2(\sqrt{2}\,)^2}\big((-ik_{+\mu})W^+_\nu+(-ik_{-\mu})W^-_\nu-(-ik_{+\nu})W^+_\mu-(-ik_{-\nu})W^-_\mu\big)$$

$$\times[(W^{\mu+}-W^{\mu-})(-\sin\theta_w A^\nu)+\sin\theta_w A^\mu(W^{\nu+}-W^{\nu-})]$$

$$= i\,\frac{\sin\theta_w g}{4}\Big((k_+\cdot W^+-k_+\cdot W^-)(A\cdot W^+)-(k_+\cdot A)(W^+\cdot W^+-W^+\cdot W^-)$$

$$+(k_-\cdot W^+-k_-\cdot W^-)(A\cdot W^-)-(k_-\cdot A)(W^-\cdot W^+-W^-\cdot W^-)$$

$$-(k_+\cdot A)(W^+\cdot W^+-W^+\cdot W^-)+(k_+\cdot W^+-k_+\cdot W^-)(A\cdot W^+)$$

$$-(k_-\cdot A)(W^+\cdot W^--W^-\cdot W^-)+(k_-\cdot W^+-k_-\cdot W^-)(A\cdot W^-)\Big)$$

$$= i\,\frac{\sin\theta_w g}{4}\Big(2\,(k_+\cdot W^+-k_+\cdot W^-)(A\cdot W^+)+2(k_-\cdot W^+-k_-\cdot W^-)(A\cdot W^-)$$

$$-2(k_+\cdot A)(W^+\cdot W^+-W^+\cdot W^-)-2(k_-\cdot A)(W^+\cdot W^--W^-\cdot W^-)\Big) \quad \text{(B.204)}$$

2. component

$$\frac{-g}{2}(\partial_\mu\frac{i}{\sqrt{2}}(W^+_\nu-W^-_\nu)-\partial_\nu\frac{i}{\sqrt{2}}(W^+_\mu-W^-_\mu))(W^{\mu 3}W^{\nu 1}-W^{\mu 1}W^{\nu 3})$$

$$\xrightarrow[\text{rules}]{\text{Feynman}} i\,\frac{\sin\theta_w g}{4}(k_{+\mu}W^+_\nu-k_{-\mu}W^-_\nu-k_{+\nu}W^+_\mu+k_{-\nu}W^-_\mu)$$

$$\times(A^\mu(W^{\nu+}+W^{\nu-})-(W^{\mu+}+W^{\mu-})A^\nu)$$

$$= i\,\frac{\sin\theta_w g}{4}\Big((k_+\cdot A)(W^+\cdot W^++W^+\cdot W^-)-(k_+\cdot W^++k_+\cdot W^-)(W^+\cdot A)$$

$$-(k_-\cdot A)(W^+\cdot W^-+W^-\cdot W^-)+(k_-\cdot W^++k_-\cdot W^-)(W^-\cdot A)$$

$$-(k_+\cdot W^++k_+\cdot W^-)(W^+\cdot A)+(k_+\cdot A)(W^+\cdot W^++W^+\cdot W^-)$$

$$+(k_-\cdot W^++k_-\cdot W^-)(W^-\cdot A)-(k_-\cdot A)(W^+\cdot W^-+W^-\cdot W^-)\Big) \quad \text{(B.205)}$$

3. component

$$\frac{\sin\theta_w g}{2}(\partial_\mu A_\nu-\partial_\nu A_\mu)(W^{\mu 1}W^{\nu 2}-W^{\nu 1}W^{\mu 2})$$

$$\xrightarrow[\text{rules}]{\text{Feynman}} i\,\frac{\sin\theta_w g}{2}(p_\mu A_\nu-p_\nu A_\mu)(W^{\mu-}W^{\nu+}-W^{\mu+}W^{\nu-})$$

$$= i\,\frac{\sin\theta_w g}{2}\Big((p\cdot W^-)(W^+\cdot A)-(p\cdot W^+)(W^-\cdot A)-(p\cdot W+)(A\cdot W^-)+(p\cdot W^-)(A\cdot W^+)\Big)$$

$$= i\,\sin\theta_w g\Big((p\cdot W^-)(W^+\cdot A)-(p\cdot W^+)(W^-\cdot A)\Big) \quad \text{(B.206)}$$

Summing up those three components results in

$$V_{\gamma W^+W^-} = ie\left(W^+\cdot W^-\,(k_+ - k_-)\cdot A + A\cdot W^+\,(p - k_+)\cdot W^- + W^-\cdot A\,(k_- - p)\cdot W^+\right)$$

from which we obtain the Feynman rules for the vertex

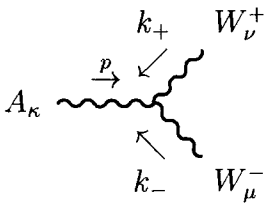

$$= ie\left(g_{\mu\nu}(k_+ - k_-)_\kappa + g_{\mu\kappa}(k_- - p)_\nu + g_{\nu\kappa}(p - k_+)_\mu\right), \qquad \text{(B.207)}$$

Interchanging the W bosons results in an overall minus sign

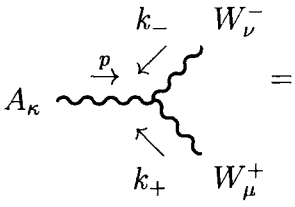

$$= -ie\left(g_{\mu\nu}(k_- - k_+)_\kappa + g_{\mu\kappa}(k_+ - p)_\nu + g_{\nu\kappa}(p - k_-)_\mu\right). \qquad \text{(B.208)}$$

Similarly the W^+W^-Z vertex is obtained by selecting the Z component of $W_{3\,\mu}$ and effectively can be obtained from the $W^+W^-\gamma$ vertex by substituting $-\sin\theta_w \to \cos\theta_w$. In summary the triple gauge boson couplings $(N\,V^\lambda\,V^{-\lambda})$ can be written

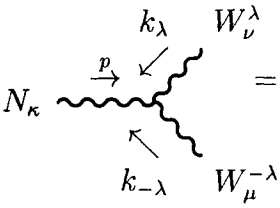

$$= -i\,e\,C\left(g_{\mu\nu}(k_\lambda - k_{-\lambda})_\kappa + g_{\mu\kappa}(k_{-\lambda} - p)_\nu + g_{\nu\kappa}(p - k_\lambda)_\mu\right) \qquad \text{(B.209)}$$

with

$$\begin{aligned} \gamma W^\lambda W^{-\lambda} &: \quad C = -\lambda \\ Z W^\lambda W^{-\lambda} &: \quad C = \lambda\cos\theta_w \,/\, \sin\theta_w\,. \end{aligned} \qquad \text{(B.210)}$$

Similarly the four boson vertex is obtained from the $g^2\,(\mathbf{W}_\mu \times \mathbf{W}_\nu)\,(\mathbf{W}_\mu \times \mathbf{W}_\nu)$ part of $\mathcal{L}_{kin}$

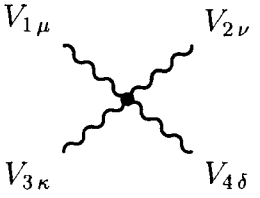

$$= -\,i\,e^2\,C\,\Big(2\,\mathrm{g}_{\mu\nu}\,\mathrm{g}_{\kappa\delta} - \mathrm{g}_{\mu\kappa}\,\mathrm{g}_{\nu\delta} - \mathrm{g}_{\mu\delta}\,\mathrm{g}_{\nu\kappa}\Big)\,. \tag{B.211}$$

where the coupling C for an explicit combination of $V_1V_2V_3V_4$ is given by

$$\begin{aligned} W^+W^-\gamma\gamma \quad &: \quad C = 1 \\ W^+W^-Z\gamma \quad &: \quad C = -\cos\theta_{\mathrm{w}} \,/\, \sin\theta_{\mathrm{w}} \\ W^+W^-ZZ \quad &: \quad C = \cos^2\theta_{\mathrm{w}} \,/\, \sin^2\theta_{\mathrm{w}} \\ W^+W^+W^-W^- \quad &: \quad C = -1 \,/\, \sin^2\theta_{\mathrm{w}}\,. \end{aligned} \tag{B.212}$$

The Feynman rules for the anomalous four boson vertex $W^+W^-\gamma\gamma$ are obtained from (2.8) and (2.9) and are given by

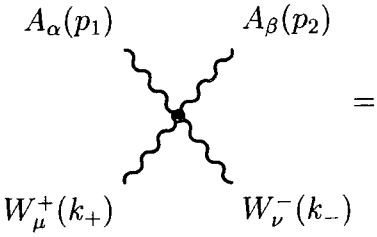

$$\begin{aligned} = \quad & i\,\frac{2e^2}{4\Lambda^2}\,a_0\big(\mathrm{g}_{\mu\nu}((p_1\cdot p_2)\mathrm{g}_{\alpha\beta} - (p_{1\beta}p_{2\alpha}))\big) \\ & + i\,\frac{e^2}{8\Lambda^2}\,a_c\big[(p_1\cdot p_2)(\mathrm{g}_{\nu\alpha}\mathrm{g}_{\mu\beta} + \mathrm{g}_{\mu\alpha}\mathrm{g}_{\nu\beta}) \\ & \qquad -p_{1\beta}(p_{2\mu}\mathrm{g}_{\nu\alpha} + \mathrm{p}_{2\nu}\mathrm{g}_{\mu\alpha}) \\ & \qquad -p_{2\alpha}(p_{1\nu}\mathrm{g}_{\mu\beta} + \mathrm{p}_{1\mu}\mathrm{g}_{\nu\beta}) \\ & \qquad + \mathrm{g}_{\alpha\beta}(\mathrm{p}_{1\nu}\mathrm{p}_{2\mu} + \mathrm{p}_{1\mu}\mathrm{p}_{2\nu})\big] \end{aligned} \tag{B.213}$$

and similarly for the $\gamma\,\gamma\,Z\,Z$ vertex for which an extra overall factor of $1/\cos^2\theta_{\mathrm{w}}$ has to be taken into account.

The Feynman rules for the anomalous four boson vertex $W^+W^-\gamma Z$ (obtained from (2.10)) are

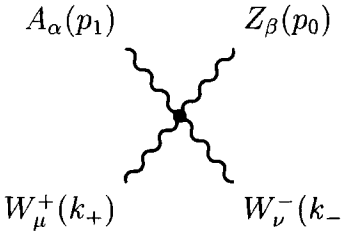

$$
\begin{aligned}
= i\frac{e^2\, a_n}{16\cos\theta_w\Lambda^2}\Big[&g_{\mu\nu}(g_{\alpha\beta}(p_1\cdot k_+) - k_{+\alpha}p_{1\beta} - g_{\alpha\beta}(p_1\cdot k_-) + p_{1\beta}k_{-\alpha})\\
&+g_{\mu\beta}(-g_{\nu\alpha}(p_1\cdot k_+) + p_{1\nu}k_{+\alpha} + g_{\nu\alpha}(p_0\cdot p_1) - p_{1\nu}p_{0\alpha})\\
&+g_{\nu\beta}(g_{\mu\alpha}(p_1\cdot k_-) - p_{1\mu}k_{-\alpha} - g_{\mu\alpha}(p_0\cdot p_1) + p_{1\mu}p_{0\alpha})\\
&+k_{+\beta}(p_{1\mu}g_{\alpha\nu} - p_{1\nu}g_{\alpha\mu}) - k_{+\nu}(p_{1\mu}g_{\alpha\beta} - p_{1\beta}g_{\alpha\mu})\\
&-k_{-\beta}(p_{1\nu}g_{\alpha\mu} - p_{1\mu}g_{\alpha\nu}) + k_{-\mu}(p_{1\nu}g_{\alpha\beta} - p_{1\beta}g_{\alpha\nu})\\
&-p_{0\mu}(p_{1\beta}g_{\alpha\nu} - p_{1\nu}g_{\alpha\beta}) + p_{0\nu}(p_{1\beta}g_{\alpha\mu} - p_{1\mu}g_{\alpha\beta})\Big]
\end{aligned}
\tag{B.214}
$$

C Matrix elements

In this appendix we are going to give a few illustrative examples of matrix-elements of $s-$ and $t-$channel diagrams. In the following all fermion momenta are taken to be in-coming, all boson momenta are taken to be out-coming; the flow of the charge of the fermions is assumed to be from the particle e^- to the anti-particle e^+. Here we only consider left-handed fermions, *i. e.* e^-_L and hence for the fermionic current *e. g.* $\bar{u}_-(p_2)\ (-i\,e\,\gamma^\mu)\ u_-(p_1)$. For right-handed fermions the spinors become $\bar{u}_+(p_2)$ and $u_+(p_1)$ and the coupling to the Z bosons changes from $v_e + a_e \to v_e - a_e$. We define $p = p_1 + p_2$. We are working in the unitary gauge.

C.1 For the process $e^+ e^- \to W^+ W^- \gamma$

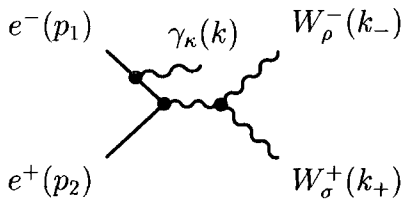

$$
\begin{aligned}
i\mathcal{M} = {} & \bar{u}_-(p_2)\,(-i\,e\,\gamma^\mu)\,\frac{i}{[\,(\not{p}_1 - \not{k}) - m + i\,\epsilon\,]}\,(-i\,e\,\gamma^\kappa)\,\epsilon^*_\kappa(k)\,u_-(p_1) \\
& \times \frac{(-i)\,g_{\mu\nu}}{[(p-k)^2 + i\epsilon\,]}\,(i\,e)\left[(-k_- + k_+)^\nu g^{\rho\sigma} - (k_+ + p)^\rho g^{\nu\sigma} + (p + k_-)^\sigma g^{\nu\rho}\right]\epsilon^*_\rho(k_-)\,\epsilon^*_\sigma(k_+) \\
& + \bar{u}_-(p_2)\,\left(i\,e\,(v_e + a_e)\,\gamma^\mu\right)\frac{i}{[\,(\not{p}_1 - \not{k}) - m + i\,\epsilon\,]}\,(-i\,e\,\gamma^\kappa)\,\epsilon^*_\kappa(k)\,u_-(p_1) \\
& \times (-i\,e)\,\frac{[\,g_{\mu\nu} - (p-k)_\mu\,(p-k)_\nu/{M_z}^2\,]}{[\,(p-k)^2 - {M_z}^2 + i\,\epsilon\,]} \\
& \times \left(\frac{-\,i\,e\,\cos\theta_w}{\sin\theta_w}\right)\left[(-k_- + k_+)^\nu g^{\rho\sigma} - (k_+ + p)^\rho g^{\nu\sigma} + (p + k_-)^\sigma g^{\nu\rho}\right]\epsilon^*_\rho(k_-)\,\epsilon^*_\sigma(k_+)
\end{aligned}
$$

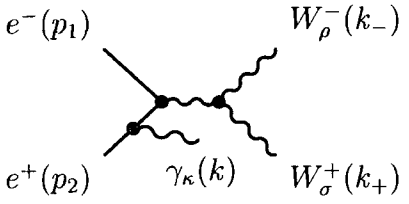

$$
\begin{aligned}
i\mathcal{M} = {} & \bar{u}_-(p_2)\,(-i\,e\,\gamma^\kappa)\,\epsilon^*_\kappa(k)\,\frac{i}{[\,-(\not{p}_2 - \not{k}) - m + i\,\epsilon\,]}\,(-i\,e\,\gamma^\mu)\,u_-(p_1) \\
& \times \frac{(-i)\,g_{\mu\nu}}{[(p-k)^2 + i\epsilon\,]}\,(i\,e)\left[(-k_- + k_+)^\nu g^{\rho\sigma} - (k_+ + p)^\rho g^{\nu\sigma} + (p + k_-)^\sigma g^{\nu\rho}\right]\epsilon^*_\rho(k_-)\,\epsilon^*_\sigma(k_+) \\
& + \bar{u}_-(p_2)\,(-i\,e\,\gamma^\kappa)\,\epsilon^*_\kappa(k)\,\frac{i}{[\,-(\not{p}_2 - \not{k}) - m + i\,\epsilon\,]}\,\left(i\,e\,(v_e + a_e)\,\gamma^\mu\right)\,u_-(p_1) \\
& \times (-i\,e)\,\frac{[\,g_{\mu\nu} - (p-k)_\mu\,(p-k)_\nu/{M_z}^2\,]}{[\,(p-k)^2 - {M_z}^2 + i\,\epsilon\,]} \\
& \times \left(\frac{-\,i\,e\,\cos\theta_w}{\sin\theta_w}\right)\left[(-k_- + k_+)^\nu g^{\rho\sigma} - (k_+ + p)^\rho g^{\nu\sigma} + (p + k_-)^\sigma g^{\nu\rho}\right]\epsilon^*_\rho(k_-)\,\epsilon^*_\sigma(k_+)
\end{aligned}
$$

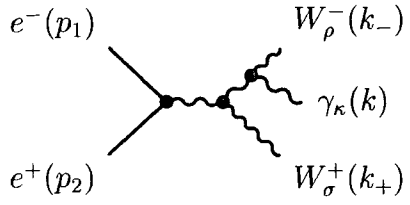

$$
\begin{aligned}
i\,\mathcal{M} = {} & \bar{u}_-(p_2)\ (-i\,e\,\gamma^\mu)\ u_-(p_1) \\
& \times \frac{(-i)\,g_{\mu\nu}}{[p^2 + i\epsilon\,]}\ (i\,e)\left[(-k_- + k_+)^\nu g^{\rho'\sigma} - (k_+ + p)^{\rho'}\,g^{\nu\sigma} + (p + k_-)^\sigma\,g^{\nu\rho'}\right]\ \epsilon^*_\rho(k_-)\ \epsilon^*_\sigma(k_+) \\
& \times (-i\,e)\,\frac{[\,g_{\rho'\eta} - (k_- + k)_{\rho'}\,(k_- + k)_\eta/M_W{}^2\,]}{[\,(k_- + k)^2 - M_W{}^2 + i\,\epsilon\,]}\ \epsilon^*_\kappa(k) \\
& (-i\,e)\left[(-(-(k + k_-)) + k_-)^\kappa g^{\eta\rho} - (k_- + (-k))^\eta\,g^{\kappa\rho} + ((-k) + (-(k + k_-)))^\rho\,g^{\kappa\eta}\right] \\
& + \bar{u}_-(p_2)\ \left(i\,e\,(v_e + a_e)\,\gamma^\mu\right)\ u_-(p_1)\ \ (-i\,e)\,\frac{[\,g_{\mu\nu} - p_\mu\,p_\nu/M_Z{}^2\,]}{[\,p^2 - M_Z{}^2 + i\,\epsilon\,]} \\
& \times \left(\frac{-\,i\,e\,\cos\theta_W}{\sin\theta_W}\right)\left[(-k_- + k_+)^\nu g^{\rho'\sigma} - (k_+ + p)^{\rho'}\,g^{\nu\sigma} + (p + k_-)^\sigma\,g^{\nu\rho'}\right]\ \epsilon^*_\rho(k_-)\ \epsilon^*_\sigma(k_+) \\
& \times (-i\,e)\,\frac{[\,g_{\rho'\eta} - (k_- + k)_{\rho'}\,(k_- + k)_\eta/M_W{}^2\,]}{[\,(k_- + k)^2 - M_W{}^2 + i\,\epsilon\,]}\ \epsilon^*_\kappa(k) \\
& (-i\,e)\left[(-(-(k + k_-)) + k_-)^\kappa g^{\eta\rho} - (k_- + (-k))^\eta\,g^{\kappa\rho} + ((-k) + (-(k + k_-)))^\rho\,g^{\kappa\eta}\right]
\end{aligned}
$$

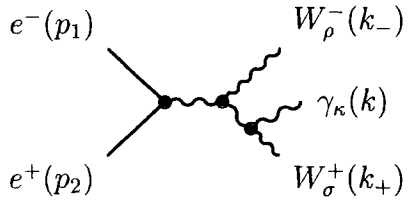

$$
\begin{aligned}
i\mathcal{M} = {} & \bar{u}_-(p_2)\ (-i\,e\,\gamma^\mu)\ u_-(p_1) \\
& \times \frac{(-i)\,g_{\mu\nu}}{[p^2 + i\epsilon]}\ (i\,e)\left[(-k_- + k_+)^\nu g^{\rho\sigma'} - (k_+ + p)^\rho\, g^{\nu\sigma'} + (p + k_-)^{\sigma'}\, g^{\nu\rho}\right]\ \epsilon_\rho^*(k_-)\ \epsilon_\sigma^*(k_+) \\
& \times (-i\,e)\,\frac{[g_{\sigma'\eta} - (k_+ + k)_{\sigma'}\,(k_+ + k)_\eta / M_W{}^2]}{[(k_+ + k)^2 - M_W{}^2 + i\epsilon]}\ \epsilon_\kappa^*(k) \\
& (-i\,e)\left[(-k_+ + (-k_+ - k))^\kappa g^{\sigma\eta} - ((-k_+ - k) + (-k))^\sigma\, g^{\kappa\eta} + ((-k) + k_+)^\eta\, g^{\kappa\sigma}\right] \\
& + \bar{u}_-(p_2)\ \left(i\,e\,(v_e + a_e)\,\gamma^\mu\right)\ u_-(p_1)\ \ (-i\,e)\,\frac{[g_{\mu\nu} - p_\mu\, p_\nu / M_Z{}^2]}{[p^2 - M_Z{}^2 + i\epsilon]} \\
& \times \left(\frac{-i\,e\,\cos\theta_W}{\sin\theta_W}\right)\left[(-k_- + k_+)^\nu g^{\rho\sigma'} - (k_+ + p)^\rho\, g^{\nu\sigma'} + (p + k_-)^{\sigma'}\, g^{\nu\rho}\right]\ \epsilon_\rho^*(k_-)\ \epsilon_\sigma^*(k_+) \\
& \times (-i\,e)\,\frac{[g_{\sigma'\eta} - (k_+ + k)_{\sigma'}\,(k_+ + k)_\eta / M_W{}^2]}{[(k_+ + k)^2 - M_W{}^2 + i\epsilon]}\ \epsilon_\kappa^*(k) \\
& (-i\,e)\left[(-k_+ + (-k_+ - k))^\kappa g^{\sigma\eta} - ((-k_+ - k) + (-k))^\sigma\, g^{\kappa\eta} + ((-k) + k_+)^\eta\, g^{\kappa\sigma}\right]
\end{aligned}
$$

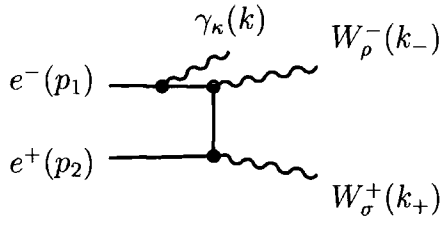

$$
\begin{aligned}
i\mathcal{M} = {} & \bar{u}_-(p_2)\ \left(\frac{i\,e}{\sqrt{2}\,\sin\theta_W}\,\gamma^\sigma\right)\ \epsilon_\sigma^*(k_+)\ \frac{i}{[(\not{p}_1 - \not{k} - \not{k}_-) - m + i\epsilon]}\ \left(\frac{i\,e}{\sqrt{2}\,\sin\theta_W}\,\gamma^\rho\right) \\
& \times \quad \epsilon_\rho^*(k_-)\ \frac{i}{[(\not{p}_1 - \not{k}) - m + i\epsilon]}\ (-i\,e\,\gamma^\kappa)\ \epsilon_\kappa^*(k)\ u_-(p_1)
\end{aligned}
$$

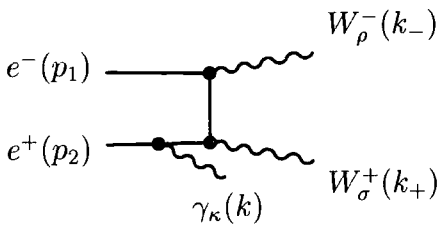

$$i\mathcal{M} = \bar{u}_-(p_2)\ (-i\,e\,\gamma^\kappa)\ \epsilon^*_\kappa(k)\ \frac{i}{[-(\not{p}_2 - \not{k}) - m + i\,\epsilon]}\ \left(\frac{i\,e}{\sqrt{2}\,\sin\theta_{\rm w}}\,\gamma^\sigma\right)\ \epsilon^*_\sigma(k_+)$$

$$\times\quad \frac{i}{[(\not{p}_1 - \not{k}_-) - m + i\,\epsilon]}\ \left(\frac{i\,e}{\sqrt{2}\,\sin\theta_{\rm w}}\,\gamma^\rho\right)\ \epsilon^*_\rho(k_-)$$

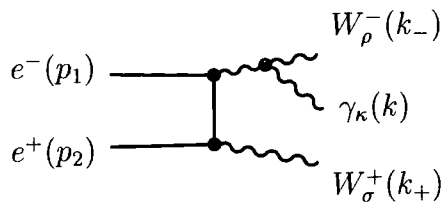

$$i\mathcal{M} = \bar{u}_-(p_2)\ \left(\frac{i\,e}{\sqrt{2}\,\sin\theta_{\rm w}}\,\gamma^\sigma\right)\ \epsilon^*_\sigma(k_+)\ \frac{i}{[(\not{p}_1 - \not{k}_- - \not{k}) - m + i\,\epsilon]}\ \left(\frac{i\,e}{\sqrt{2}\,\sin\theta_{\rm w}}\,\gamma^{\rho'}\right)\ u_-(p_1)$$

$$\times\quad (-i\,e)\,\frac{[\mathrm{g}_{\rho'\eta} - (\mathrm{k}_- + \mathrm{k})_{\rho'}\,(\mathrm{k}_- + \mathrm{k})_\eta/\mathrm{M_w}^2]}{[(k_- + k)^2 - M_W{}^2 + i\,\epsilon]}\ \epsilon^*_\rho(k_-)\ \epsilon^*_\kappa(k)\ u_-(p_1)$$

$$\times(-i\,e)\left[(-(-(k + k_-)) + k_-)^\kappa \mathrm{g}^{\eta\rho} - (\mathrm{k}_- + (-\mathrm{k}))^\eta\,\mathrm{g}^{\kappa\rho} + ((-\mathrm{k}) + (-(\mathrm{k} + \mathrm{k}_-)))^\rho\,\mathrm{g}^{\kappa\eta}\right]$$

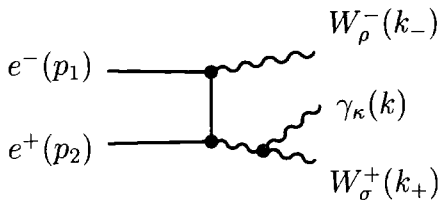

$$i\,\mathcal{M} = \bar{u}_-(p_2)\,\left(\frac{i\,e}{\sqrt{2}\,\sin\theta_{\rm w}}\,\gamma^{\sigma'}\right)\,\frac{i}{[\,(\not{p}_1 - \not{k}_-) - m + i\,\epsilon\,]}\,\left(\frac{i\,e}{\sqrt{2}\,\sin\theta_{\rm w}}\,\gamma^{\rho}\right)\,\epsilon^*_\rho(k_-)\;u_-(p_1)$$

$$\times\quad (-i\,e)\,\frac{[\,g_{\sigma'\eta} - (k_+ + k)_{\sigma'}\,(k_+ + k)_\eta/{M_W}^2\,]}{[\,(k_+ + k)^2 - {M_W}^2 + i\,\epsilon\,]}\,\epsilon^*_\kappa(k)\;\epsilon^*_\sigma(k_+)\;u_-(p_1)$$

$$\times(-i\,e)\,\Big[(-k_+ + (-k_+ - k))^\kappa g^{\sigma\eta} - ((-k_+ - k) + (-k))^\sigma\,g^{\kappa\eta} + ((-k) + k_+)^\eta\,g^{\kappa\sigma}\Big]$$

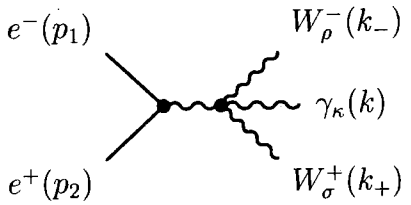

$$i\,\mathcal{M} = \bar{u}_-(p_2)\;(-i\,e\,\gamma^\mu)\;u_-(p_1)\,\frac{(-i)\,g_{\mu\nu}}{[p^2 + i\epsilon\,]}\,\epsilon^*_\kappa(k)\;\epsilon^*_\rho(k_-)\;\epsilon^*_\sigma(k_+)$$

$$\times\quad (-i\,e^2)\;[2\,g^{\nu\kappa}\,g^{\sigma\rho} - g^{\nu\sigma}\,g^{\kappa\rho} - g^{\nu\rho}\,g^{\kappa\sigma}]$$

$$+\,\bar{u}_-(p_2)\;\left(i\,e\,(v_e + a_e)\,\gamma^\mu\right)\;u_-(p_1)\;(-i\,e)\,\frac{[\,g_{\mu\nu} - p_\mu\,p_\nu/{M_z}^2\,]}{[\,p^2 - {M_z}^2 + i\,\epsilon\,]}\,\epsilon^*_\kappa(k)\;\epsilon^*_\rho(k_-)\;\epsilon^*_\sigma(k_+)$$

$$\times\quad \left(\frac{i\,e^2\,\cos\theta_{\rm w}}{\sin\theta_{\rm w}}\right)\;[2\,g^{\nu\kappa}\,g^{\sigma\rho} - g^{\nu\sigma}\,g^{\kappa\rho} - g^{\nu\rho}\,g^{\kappa\sigma}]$$

C.2 For the process $e^+e^- \to ZZ\gamma$

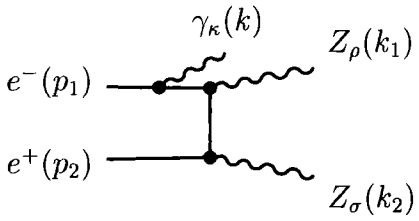

$$i\mathcal{M} = \bar{u}_-(p_2)\,\left(i\,e\,(v_e + a_e)\,\gamma^\sigma\right)\,\epsilon^*_\sigma(k_2)\,\frac{i}{\left[\,(\not{p}_1 - \not{k} - \not{k}_1) - m + i\,\epsilon\,\right]}\,\left(i\,e\,(v_e + a_e)\,\gamma^\rho\right)$$

$$\times \quad \epsilon^*_\rho(k_1)\,\frac{i}{\left[\,(\not{p}_1 - \not{k}) - m + i\,\epsilon\,\right]}\,(-i\,e\,\gamma^\kappa)\,\epsilon^*_\kappa(k)\,u_-(p_1)$$

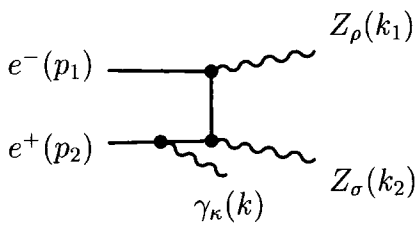

$$i\mathcal{M} = \bar{u}_-(p_2)\,(-i\,e\,\gamma^\kappa)\,\epsilon^*_\kappa(k)\,\frac{i}{\left[-(\not{p}_2 - \not{k}) - m + i\,\epsilon\,\right]}\,\left(i\,e\,(v_e + a_e)\,\gamma^\sigma\right)\,\epsilon^*_\sigma(k_2)$$

$$\times \quad \frac{i}{\left[\,(\not{p}_1 - \not{k}_1) - m + i\,\epsilon\,\right]}\,\left(i\,e\,(v_e + a_e)\,\gamma^\rho\right)\,\epsilon^*_\rho(k_1)$$

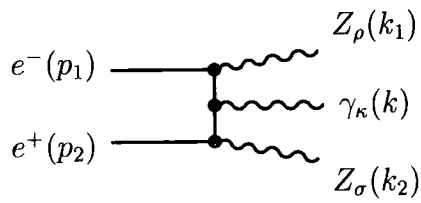

$$i\mathcal{M} = \bar{u}_-(p_2)\,\left(i\,e\,(v_e + a_e)\,\gamma^\sigma\right)\,\epsilon^*_\sigma(k_2)\,\frac{i}{\left[\,(\not{p}_1 - \not{k}_1 - \not{k}) - m + i\,\epsilon\,\right]}\,(-i\,e\,\gamma^\kappa)\,\epsilon^*_\kappa(k)$$

$$\times \quad \frac{i}{\left[\,(\not{p}_1 - \not{k}_1) - m + i\,\epsilon\,\right]}\,\left(i\,e\,(v_e + a_e)\,\gamma^\rho\right)\,\epsilon^*_\rho(k_1)$$

Plus the three u-channel diagrams, which can be obtained from these by $k_1 \leftrightarrow k_2$. Note that because of the two identical particles in the final states (ZZ) the square of the matrix element has to be divided by a symmetry factor of 2 to obtain the cross section.
Also the diagrams for the process $e^+e^- \to Z\gamma\gamma$ are easily obtained from those above by the exchange of $\left(i\,e\,(v_e + a_e)\,\gamma^\rho\right) \to \left(-i\,e\,\gamma^\rho\right)$.

D Some useful integrals

In this Appendix we give all relevant one- and two-loop integrals which have been used in Chapter 4.
At one-loop accuracy we have to distinguish between two different cases, *i. e.* the exchanged soft gauge-boson being a photon with the fictitious mass λ or a massive gauge-boson W or Z with the generic mass M. The exchanged gauge-boson being massive we extract from (4.66) with $M_1 = M$

$$J^{(1)}(M) = \int_0^1 \frac{\mathrm{d}y_1}{y_1} \int_{y_1}^1 \frac{\mathrm{d}z_1}{z_1}\, \Theta\Big(y_1 z_1 - \frac{M^2}{s}\Big)\, \Theta\Big(y_1 - \frac{m_f^2}{s}\, z_1\Big)\,. \tag{D.215}$$

From the first Θ-function we obtain the integration boundaries

$$J^{(1)}(M) = \int_{\frac{M}{\sqrt{s}}}^1 \frac{\mathrm{d}z_1}{z_1} \int_{\frac{M^2}{s\,z_1}}^{z_1} \frac{\mathrm{d}y_1}{y_1}\, \Theta\Big(y_1 - \frac{m_f^2}{s}\, z_1\Big)$$

making the second Θ-function redundant, since $m_f \leq \mathcal{O}(M)$. Therefore

$$J^{(1)}(M) = \int_{\frac{M}{\sqrt{s}}}^1 \frac{\mathrm{d}z_1}{z_1} \int_{\frac{M^2}{s\,z_1}}^{z_1} \frac{\mathrm{d}y_1}{y_1} = \int_{\frac{M}{\sqrt{s}}}^1 \frac{\mathrm{d}z_1}{z_1} \log\left(\frac{z_1}{M^2/(s\,z_1)}\right) = 2\int_{\frac{M}{\sqrt{s}}}^1 \frac{\mathrm{d}z_1}{z_1} \log\left(\frac{z_1\sqrt{s}}{M}\right)\,, \tag{D.216}$$

and with $t = \log\left(\frac{z_1\sqrt{s}}{M}\right)$

$$J^{(1)}(M) = 2\int_0^{\log\left(\frac{\sqrt{s}}{M}\right)} \mathrm{d}t\; t = \frac{1}{4}\log^2\left(\frac{M^2}{s}\right)\,. \tag{D.217}$$

And similarly for $M_1 = \lambda$

$$\begin{aligned} J^{(1)}(\lambda) &= \int_0^1 \frac{\mathrm{d}y_1}{y_1} \int_{y_1}^1 \frac{\mathrm{d}z_1}{z_1}\, \Theta\Big(y_1 z_1 - \frac{\lambda^2}{s}\Big)\, \Theta\Big(y_1 - \frac{m_f^2}{s}\, z_1\Big) \\ &= \int_{\frac{\lambda}{m_f}}^1 \frac{\mathrm{d}z_1}{z_1} \int_{\frac{m_f^2 z_1}{s}}^{z_1} \frac{\mathrm{d}y_1}{y_1} + \int_{\frac{\lambda}{\sqrt{s}}}^{\frac{\lambda}{m_f}} \frac{\mathrm{d}z_1}{z_1} \int_{\frac{\lambda^2}{s z_1}}^{z_1} \frac{\mathrm{d}y_1}{y_1} \\ &= \frac{1}{2} \log\left(\frac{m_f^2}{s}\right) \log\left(\frac{\lambda^2}{m_f^2}\right) + \frac{1}{4} \log^2\left(\frac{m_f^2}{s}\right) \\ &= \frac{1}{4} \log^2\left(\frac{\lambda^2}{s}\right) - \frac{1}{4} \log^2\left(\frac{\lambda^2}{m_f^2}\right) \end{aligned} \tag{D.218}$$

The two-loop integrals fall into two categories, namely the angular ordered and the simultaneously energy and angular ordered ones. For the angular ordered two-loop integrals (4.112) we find for $M_1 = M_2 = M$

$$J^{(2)}_{\text{angular}}(M, M) = \int_0^1 \frac{\mathrm{d}z_1}{z_1} \int_0^{z_1} \frac{\mathrm{d}y_1}{y_1} \int_0^1 \frac{\mathrm{d}z_2}{z_2} \int_0^{z_2} \frac{\mathrm{d}y_2}{y_2}\, \Theta\Big(y_1 z_1 - \frac{M^2}{s}\Big)\, \Theta\Big(y_2 z_2 - \frac{M^2}{s}\Big) \Theta(y_2 - y_1) \tag{D.219}$$

By means of symmetry arguments, *i. e.* $\Theta(y_2 - y_1) \to \frac{1}{2}\left[\Theta(y_2 - y_1) + \Theta(y_1 - y_2)\right] = \frac{1}{2}$, we find

$$J^{(2)}_{\text{angular}}(M, M) = \frac{1}{2} \left[\frac{1}{4} \log^2\left(\frac{M^2}{s}\right)\right]^2, \tag{D.220}$$

and similarly

$$J^{(2)}_{\text{angular}}(\lambda, \lambda) = \frac{1}{2} \left[\frac{1}{4} \log^2\left(\frac{\lambda^2}{s}\right) - \frac{1}{4} \log^2\left(\frac{\lambda^2}{m_f^2}\right)\right]^2. \tag{D.221}$$

Furthermore

$$J^{(2)}_{\text{angular}}(M,\lambda) = \int_0^1 \frac{\mathrm{d}z_1}{z_1} \int_0^{z_1} \frac{\mathrm{d}y_1}{y_1} \int_0^1 \frac{\mathrm{d}z_2}{z_2} \int_0^{z_2} \frac{\mathrm{d}y_2}{y_2}\, \Theta\Big(y_1 z_1 - \frac{M^2}{s}\Big)\, \Theta\Big(y_2 z_2 - \frac{\lambda^2}{s}\Big)$$

$$\times\, \Theta\Big(y_2 - \frac{m_f^2 z_2}{s}\Big)\, \Theta(y_2 - y_1)$$

$$= \int_{\frac{M}{\sqrt{s}}}^1 \frac{\mathrm{d}z_1}{z_1} \int_{\frac{M^2}{s\, z_1}}^{z_1} \frac{\mathrm{d}y_1}{y_1} \int_{y_1}^1 \frac{\mathrm{d}z_2}{z_2} \int_{y_1}^{z_2} \frac{\mathrm{d}y_2}{y_2}$$

$$= \int_{\frac{M}{\sqrt{s}}}^1 \frac{\mathrm{d}z_1}{z_1} \int_{\frac{M^2}{s\, z_1}}^{z_1} \frac{\mathrm{d}y_1}{y_1} \int_{y_1}^1 \frac{\mathrm{d}z_2}{z_2}\, (\log z_2 - \log y_1)$$

$$= \int_{\frac{M}{\sqrt{s}}}^1 \frac{\mathrm{d}z_1}{z_1} \int_{\frac{M^2}{s\, z_1}}^{z_1} \frac{\mathrm{d}y_1}{y_1}\, \frac{1}{2} \log^2 y_1$$

$$= \int_{\frac{M}{\sqrt{s}}}^1 \frac{\mathrm{d}z_1}{z_1}\, \frac{1}{2}\, \frac{1}{3} \Big[\log^3 z_1 + \log^3\Big(\frac{z_1\, s}{M^2}\Big)\Big]$$

$$\overset{t=\log\left(\frac{z_1 s}{M^2}\right)}{=\!=} \frac{1}{6} \left\{ -\frac{1}{4} \log^4\Big(\frac{M}{\sqrt{s}}\Big) + \int_{\log\left(\frac{\sqrt{s}}{M}\right)}^{\log\left(\frac{s}{M^2}\right)} \mathrm{d}t\; t^3 \right\}$$

$$= \frac{1}{6}\, \frac{1}{4} \log^4\Big(\frac{M}{\sqrt{s}}\Big)\, [-1 + 16 - 1] = \frac{7}{12} \log^4\Big(\frac{M}{\sqrt{s}}\Big)\,, \tag{D.222}$$

and hence by means of $\Theta(y_2 - y_1) = 1 - \Theta(y_1 - y_2)$ we find for $M_1 = \lambda$ and $M_2 = M$

$$J^{(2)}_{\text{angular}}(\lambda, M) = \Big[\frac{1}{4} \log^2\Big(\frac{M^2}{s}\Big)\Big] \times \Big[\frac{1}{4} \log^2\Big(\frac{\lambda^2}{s}\Big) - \frac{1}{4} \log^2\Big(\frac{\lambda^2}{m_f^2}\Big)\Big] - \frac{7}{12} \log^4\Big(\frac{M}{\sqrt{s}}\Big)\,. \tag{D.223}$$

For the double (energy and angular) ordered integrals (4.144) we find for the $M_1 = M_2 = M$ case again by means of symmetry arguments

$$J^{(2)}_{\text{double ordered}}(M, M) =$$

$$= \int_0^1 \frac{\mathrm{d}z_1}{z_1} \int_0^{z_1} \frac{\mathrm{d}y_1}{y_1} \int_0^1 \frac{\mathrm{d}z_2}{z_2} \int_0^{z_2} \frac{\mathrm{d}y_2}{y_2}\, \Theta\Big(y_1 z_1 - \frac{M^2}{s}\Big)\, \Theta\Big(y_2 z_2 - \frac{M^2}{s}\Big) \Theta(y_2 - y_1)\, \Theta(z_1 - z_2)$$

$$= \frac{1}{4} \Big[\frac{1}{4} \log^2\Big(\frac{M^2}{s}\Big)\Big]^2\,, \tag{D.224}$$

and for $M_1 = M$ and $M_2 = \lambda$ we obtain

$$
\begin{aligned}
&J^{(2)}_{\text{double ordered}}(M,\lambda) = \\
&= \int_0^1 \frac{\mathrm{d}z_1}{z_1} \int_0^{z_1} \frac{\mathrm{d}y_1}{y_1} \int_0^1 \frac{\mathrm{d}z_2}{z_2} \int_0^{z_2} \frac{\mathrm{d}y_2}{y_2}\, \Theta\Big(y_1 z_1 - \frac{M^2}{s}\Big)\, \Theta\Big(y_2 z_2 - \frac{\lambda^2}{s}\Big) \Theta(y_2 - y_1)\, \Theta(z_1 - z_2) \\
&= \int_{\frac{M}{\sqrt{s}}}^1 \frac{\mathrm{d}z_1}{z_1} \int_{\frac{M^2}{s\, z_1}}^{z_1} \frac{\mathrm{d}y_1}{y_1} \int_{y_1}^{z_1} \frac{\mathrm{d}z_2}{z_2} \int_{y_1}^{z_2} \frac{\mathrm{d}y_2}{y_2} \\
&= \int_{\frac{M}{\sqrt{s}}}^1 \frac{\mathrm{d}z_1}{z_1} \int_{\frac{M^2}{s\, z_1}}^{z_1} \frac{\mathrm{d}y_1}{y_1} \int_{y_1}^{z_1} \frac{\mathrm{d}z_2}{z_2} \left(\log z_2 - \log y_1\right) \\
&= \int_{\frac{M}{\sqrt{s}}}^1 \frac{\mathrm{d}z_1}{z_1} \int_{\frac{M^2}{s\, z_1}}^{z_1} \frac{\mathrm{d}y_1}{y_1} \left[\frac{1}{2}\log^2 z_1 - \frac{1}{2}\log^2 y_1 - \log y_1 \left(\log z_1 - \log y_1\right)\right] \\
&= \int_{\frac{M}{\sqrt{s}}}^1 \frac{\mathrm{d}z_1}{z_1} \left[\frac{1}{2}\log^2 z_1 \left(\log z_1 + \log\Big(\frac{s\, z_1}{M^2}\Big)\right) - \frac{1}{2}\log z_1 \left(\log^2 z_1 - \log^2\Big(\frac{s\, z_1}{M^2}\Big)\right)\right] \\
&\qquad + \frac{7}{12}\log^4\Big(\frac{M}{\sqrt{s}}\Big) \\
&= \int_{\frac{M}{\sqrt{s}}}^1 \frac{\mathrm{d}z_1}{z_1} \left[\log^3 z_1 + \frac{3}{2}\log^2 z_1 \log\Big(\frac{s}{M^2}\Big) + \frac{1}{2}\log z_1 \log^2\Big(\frac{s}{M^2}\Big)\right] + \frac{7}{12}\log^4\Big(\frac{M}{\sqrt{s}}\Big) \\
&= -\frac{1}{4}\log^4\Big(\frac{M}{\sqrt{s}}\Big) - \frac{1}{2}\log^3\Big(\frac{M}{\sqrt{s}}\Big)(-2)\log\Big(\frac{M}{\sqrt{s}}\Big) - \frac{1}{4}\log^2\Big(\frac{M}{\sqrt{s}}\Big) 4\log^2\Big(\frac{M}{\sqrt{s}}\Big) \\
&\qquad + \frac{7}{12}\log^4\Big(\frac{M}{\sqrt{s}}\Big) \\
&= \frac{1}{3}\log^4\Big(\frac{M}{\sqrt{s}}\Big)\,,
\end{aligned}
\tag{D.225}
$$

Finally for $M_1 = \lambda$ and $M_2 = M$ (note here that in the 'frog' configurations no two photons can appear in the integration kernel) the double-ordered integral reads

$$
\begin{aligned}
&J^{(2)}_{\text{double ordered}}(\lambda,M) = \\
&= \int_0^1 \frac{\mathrm{d}z_1}{z_1} \int_0^{z_1} \frac{\mathrm{d}y_1}{y_1} \int_0^1 \frac{\mathrm{d}z_2}{z_2} \int_0^{z_2} \frac{\mathrm{d}y_2}{y_2}\, \Theta\Big(y_1 z_1 - \frac{\lambda^2}{s}\Big)\, \Theta\Big(y_1 - \frac{m_f^2}{s} z_1\Big)\, \Theta\Big(y_2 z_2 - \frac{M^2}{s}\Big) \times \\
&\qquad \times \Theta(y_2 - y_1)\, \Theta(z_1 - z_2) \\
&= \int_0^1 \frac{\mathrm{d}z_1}{z_1} \int_0^{z_1} \frac{\mathrm{d}y_1}{y_1} \int_0^1 \frac{\mathrm{d}z_2}{z_2} \int_0^{z_2} \frac{\mathrm{d}y_2}{y_2}\, \Theta\Big(y_1 z_1 - \frac{M^2}{s}\Big)\, \Theta\Big(y_2 z_2 - \frac{\lambda^2}{s}\Big)\, \Theta\Big(y_2 - \frac{m_f^2}{s} z_2\Big) \times \\
&\qquad \times \Theta(y_1 - y_2)\, \Theta(z_2 - z_1)
\end{aligned}
\tag{D.226}
$$

where we can write

$$\begin{aligned}\Theta(y_1 - y_2)\,\Theta(z_2 - z_1) &= [1 - \Theta(y_2 - y_1)]\,\Theta(z_2 - z_1) \\ &= \Theta(z_2 - z_1) - \Theta(y_2 - y_1) + \Theta(y_2 - y_1)\,\Theta(z_1 - z_2) \qquad \text{(D.227)}\end{aligned}$$

and hence

$$\begin{aligned}J^{(2)}_{\text{double ordered}}(\lambda, M) &= -\frac{7}{12}\log^4\left(\frac{M}{\sqrt{s}}\right) + \frac{1}{3}\log^4\left(\frac{M}{\sqrt{s}}\right) \\ &+ \int_0^1 \frac{\mathrm{d}z_1}{z_1}\int_0^{z_1}\frac{\mathrm{d}y_1}{y_1}\int_0^1\frac{\mathrm{d}z_2}{z_2}\int_0^{z_2}\frac{\mathrm{d}y_2}{y_2}\,\Theta\left(y_1z_1 - \frac{M^2}{s}\right)\Theta\left(y_2z_2 - \frac{\lambda^2}{s}\right)\Theta\left(y_2 - \frac{m_f^2\,z_2}{s}\right)\Theta(z_2 - z_1) \\ &= -\frac{1}{4}\log^4\left(\frac{M}{\sqrt{s}}\right) + \int_{\frac{M}{\sqrt{s}}}^1\frac{\mathrm{d}z_1}{z_1}\int_{\frac{M^2}{s\,z_1}}^{z_1}\frac{\mathrm{d}y_1}{y_1}\left[\int_{z_1}^1\frac{\mathrm{d}z_2}{z_2}\int_{\frac{m_f^2\,z_2}{s}}^{z_2}\frac{\mathrm{d}y_2}{y_2}\right] \\ &= -\frac{1}{4}\log^4\left(\frac{M}{\sqrt{s}}\right) + \int_{\frac{M}{\sqrt{s}}}^1\frac{\mathrm{d}z_1}{z_1}\int_{\frac{M^2}{s\,z_1}}^{z_1}\frac{\mathrm{d}y_1}{y_1}\left[\log\left(\frac{m_f^2}{s}\right)\log z_1\right] \\ &= -\frac{1}{4}\log^4\left(\frac{M}{\sqrt{s}}\right) + \log\left(\frac{m_f^2}{s}\right)\int_{\frac{M}{\sqrt{s}}}^1\frac{\mathrm{d}z_1}{z_1}\log z_1\left[2\log z_1 - 2\log\left(\frac{M}{\sqrt{s}}\right)\right] \\ &= -\frac{1}{4}\log^4\left(\frac{M}{\sqrt{s}}\right) + \log\left(\frac{m_f^2}{s}\right)\left[-\frac{2}{3} + 1\right]\log^3\left(\frac{M}{\sqrt{s}}\right) \\ &= -\frac{1}{4}\log^4\left(\frac{M}{\sqrt{s}}\right) + \frac{2}{3}\log^3\left(\frac{M}{\sqrt{s}}\right)\log\left(\frac{m_f}{\sqrt{s}}\right). \qquad \text{(D.228)}\end{aligned}$$

Bibliography

[1] P. A. M. Dirac. The quantum theory of electron. *Proc. Roy. Soc. Lond.*, **A117**,610–624, 1928.

[2] M. Kaku. Quantum field theory: A modern introduction. New York, USA: Oxford Univ. Pr. (1993) 785 p.

[3] Julian Schwinger. Quantum electrodynamics two. vacuum polarization and selfenergy. *Phys. Rev.*, **75**,651, 1948.

R. P. Feynman. The theory of positrons. *Phys. Rev.*, **76**,749–759, 1949.

[4] S. L. Glashow. Partial symmetries of weak interactions. *Nucl. Phys.*, **22**,579–588, 1961.

A. Salam. Weak and electromagnetic interactions. Originally printed in *Svartholm: Elementary Particle Theory, Proceedings Of The Nobel Symposium Held 1968 At Lerum, Sweden*, Stockholm 1968, 367-377.

S. Weinberg. A model of leptons. *Phys. Rev. Lett.*, **19**,1264–1266, 1967.

[5] G. 't Hooft. Renormalizable lagrangians for massive Yang-Mills fields. *Nucl. Phys.*, **B35**,167–188, 1971.

G. 't Hooft and M. Veltman. Regularization and renormalization of gauge fields. *Nucl. Phys.*, **B44**,189–213, 1972.

[6] J. L. Hewett. The standard model and why we believe it. 1998, `hep-ph/9810316`.

[7] Y. Fukuda et al. Measurement of a small atmospheric $\nu\mu/\nu e$ ratio. *Phys. Lett.*, **B433**,9–18, 1998.

Y. Fukuda et al. Study of the atmospheric neutrino flux in the multi-GeV energy range. *Phys. Lett.*, **B436**,33, 1998.

Y. Fukuda et al. Evidence for oscillation of atmospheric neutrinos. *Phys. Rev. Lett.*, **81**,1562–1567, 1998.

[8] P. W. Higgs. Broken symmetries, massless particles and gauge fields. *Phys. Lett.*, **12**,132–133, 1964.

T. W. B. Kibble. Symmetry breaking in nonabelian gauge theories. *Phys. Rev.*, **155**,1554–1561, 1967.

G. S. Guralnik, C. R. Hagen, and T. W. B. Kibble. Global conservation laws and massless particles. *Phys. Rev. Lett.*, **13**,585, 1964.

[9] R. Kleiss and W. J. Stirling. Spinor techniques for calculating $p\bar{p} \to W^{+-}/Z^0$ + jets. *Nucl. Phys.*, **B262**,235–262, 1985.

[10] G. Arnison et al. Experimental observation of isolated large transverse energy electrons with associated missing energy at $\sqrt{s} = 540$ GeV. *Phys. Lett.*, **B122**,103–116, 1983.

M. Banner et al. Observation of single isolated electrons of high transverse momentum in events with missing transverse energy at the cern $\bar{p}p$ collider. *Phys. Lett.*, **B122**,476–485, 1983.

[11] K. Hagiwara, R. D. Peccei, D. Zeppenfeld, and K. Hikasa. Probing the weak boson sector in $e^+e^- \to W^+W^-$. *Nucl. Phys.*, **B282**,253, 1987.

[12] R. Barate et al. Measurement of W pair production in e^+e^- collisions at 189 GeV. *Phys. Lett.*, **B484**,205, 2000.

P. Abreu et al. W pair production cross-section and W branching fractions in e^+e^- interactions at 189 GeV. *Phys. Lett.*, **B479**,89, 2000.

[13] W. Beenakker, F. A. Berends, and A. P. Chapovsky. Radiative corrections to pair production of unstable particles: Results for $e^+e^- \to 4$ fermions. *Nucl. Phys.*, **B548**,3, 1999.

[14] A. Denner, S. Dittmaier, M. Roth, and D. Wackeroth. Electroweak radiative corrections to $e^+e^- \to WW \to$ 4fermions in double-pole approximation: The RACOONWW approach. 2000.

[15] S. Jadach, W. Placzek, M. Skrzypek, B. F. L. Ward, and Z. Was. Monte Carlo program KoralW 1.42 for all four-fermion final states in e^+e^- collisions. *Comput. Phys. Commun.*, **119**,272–311, 1999.

[16] Thorsten Ohl. Drawing feynman diagrams with latex and metafont. *Comput. Phys. Commun.*, **90**,340, 1995.

[17] R. Kleiss, W. J. Stirling, and S. D. Ellis. A new monte carlo treatment of multiparticle phase space at high-energies. *Comput. Phys. Commun.*, **40**,359, 1986.

[18] W. James Stirling and Anja Werthenbach. Anomalous quartic couplings in $W^+W^-\gamma, Z^0Z^0\gamma$ and $Z^0\gamma\gamma$ production at present and future e+ e- colliders. *Eur. Phys. J.*, **C14**,103, 2000.

[19] W. James Stirling and Anja Werthenbach. Anomalous quartic couplings in $\nu\bar{\nu}\gamma\gamma$ production via W W fusion at LEP2. *Phys. Lett.*, **B466**,369, 1999.

[20] W. James Stirling and Anja Werthenbach. Radiation zeros in $W^+W^-\gamma$ production at high energy colliders. *Eur. Phys. J.*, **C12**,441, 2000.

[21] W. Beenakker and A. Werthenbach. New insights into the perturbative structure of electroweak Sudakov logarithms. *Phys. Lett.*, **B489**,148–156, 2000.

[22] W. Beenakker and A. Werthenbach. Electroweak Sudakov logarithms in the Coulomb gauge. *Nucl. Phys. Proc. Suppl.*, **89**,88, 2000.

[23] W. Beenakker and A. Werthenbach. Electroweak two-loop Sudakov logarithms in the Coulomb gauge. in preparation.

[24] G. Gounaris et al. Triple gauge boson couplings. 1996, `hep-ph/9601233`.

[25] R. Barate et al. Measurement of triple gauge $WW\gamma$ couplings at LEP2 using photonic events. 1998, `hep-ex/9901030`.

[26] G. Abbiendi et al. W^+W^- production and triple gauge boson couplings at LEP energies up to 183-GeV. *Eur. Phys. J.*, **C8**,191, 1999.

[27] Stephen Godfrey. Quartic gauge boson couplings. 1995, `hep-ph/9505252`.

[28] G. Belanger and F. Boudjema. $\gamma\gamma \to W^+W^-$ and $\gamma\gamma \to ZZ$ as tests of novel quartic couplings. *Phys. Lett.*, **B288**,210–220, 1992.

[29] Ghadir Abu Leil and W. J. Stirling. Anomalous quartic couplings in $W^+W^-\gamma$ production at e^+e^- colliders. *J. Phys.*, **G21**,517–524, 1995.

[30] O. J. P. Eboli, M. C. Gonzalez-Garcia, and S. F. Novaes. Quartic anomalous couplings in $e\gamma$ colliders. *Nucl. Phys.*, **B411**,381–396, 1994.

[31] G. Belanger, F. Boudjema, Y. Kurihara, D. Perret-Gallix, and A. Semenov. Bosonic quartic couplings at LEP2. *Eur. Phys. J.*, **C13**,283, 2000.

[32] V. Barger, T. Han, and R. J. N. Phillips. WWZ, ZZZ and $WW\gamma$ production at e^+e^- colliders. *Phys. Rev.*, **D39**,146, 1989.

[33] T. Stelzer and W. F. Long. Automatic generation of tree level helicity amplitudes. *Comput. Phys. Commun.*, **81**,357–371, 1994.

[34] E. Accomando et al. Physics with e^+e^- linear colliders. *Phys. Rept.*, **299**,1, 1998.

[35] G. Abbiendi et al. Measurement of the $W^+W^-\gamma$ cross-section and first direct limits on anomalous electroweak quartic gauge couplings. *Phys. Lett.*, **B471**,293, 1999.

[36] M. Acciarri et al. Measurement of the $e^+e^- \to Z\gamma\gamma$ cross section and determination of quartic gauge boson couplings at LEP. *Phys. Lett.*, **B478**,39, 2000.

[37] M. Acciarri et al. Measurement of the $W^+W^-\gamma$ cross section and direct limits on anomalous quartic gauge boson couplings at LEP. 2000, `hep-ex/0008022`.

[38] K. O. Mikaelian, M. A. Samuel, and D. Sahdev. The magnetic moment of weak bosons produced in pp and $p\bar{p}$ collisions. *Phys. Rev. Lett.*, **43**,746, 1979.

[39] Robert W. Brown. Understanding something about nothing: Radiation zeros. 1995, `hep-th/9506018`.

[40] Robert W. Brown, K. L. Kowalski, and Stanley J. Brodsky. Classical radiation zeros in gauge theory amplitudes. *Phys. Rev.*, **D28**,624, 1983.

[41] R. W. Brown, D. Sahdev, and K. O. Mikaelian. $W^{+-}Z^0$ and $W^{+-}\gamma$ pair production in $\nu e, pp$, and $\bar{p}p$ collisions. *Phys. Rev.*, **D20**,1164, 1979.

[42] U. Baur, T. Han, N. Kauer, R. Sobey, and D. Zeppenfeld. $W\gamma\gamma$ production at the fermilab tevatron collider: Gauge invariance and radiation amplitude zero. *Phys. Rev.*, **D56**,140–150, 1997.

[43] U. Baur, T. Han, and J. Ohnemus. Amplitude zeros in $W^{+-}Z$ production. *Phys. Rev. Lett.*, **72**,3941–3944, 1994.

[44] Stanley J. Brodsky and Robert W. Brown. Zeros in amplitudes: Gauge theory and radiation interference. *Phys. Rev. Lett.*, **49**,966, 1982.

[45] C. J. Goebel, F. Halzen, and J. P. Leveille. Angular zeros of Brown, Mikaelian, Sahdev, and Samuel and the factorization of tree amplitudes in gauge theories. *Phys. Rev.*, **D23**,2682, 1981.

[46] Robert W. Brown and Kenneth L. Kowalski. Szeros. *Phys. Lett.*, **B144**,235, 1984.

[47] David DeLaney, Evalyn Gates, and Ola Tornkvist. Xeros. *Phys. Lett.*, **B186**,91, 1987.

[48] M. Heyssler and W. J. Stirling. Radiation zeros at hera: More about nothing. *Eur. Phys. J.*, **C4**,289, 1998.

[49] Doug Benjamin. $W\gamma$ and $Z\gamma$ production at the tevatron. Presented at 10th Topical Workshop on Proton-Antiproton Collider Physics, Batavia, IL, 9-13 May 1995.

[50] F. A. Berends and R. Kleiss. Hard photon effects in W^{+-} and Z^0 decay. *Z. Phys.*, **C27**,365, 1985.

[51] V. A. Khoze, W. J. Stirling, and Lynne H. Orr. Soft gluon radiation in $e^+e^- \to t\bar{t}$. *Nucl. Phys.*, **B378**,413–442, 1992.

[52] Yu. L. Dokshitzer, V. A. Khoze, Lynne H. Orr, and W. J. Stirling. Soft photons in W^+W^- production at LEP200. *Phys. Lett.*, **B313**,171–179, 1993.

[53] C. Caso et al. Review of particle physics. *Eur. Phys. J.*, **C3**,1–794, 1998.

[54] Mark A Samuel and Tesfaye Abraha. Finding the radiation amplitude zero in $W\gamma$ production. Is it unique to the standard model? 1997.,hep-ph/9706336.

[55] H. T. Diehl. Boson pair production and triple gauge couplings. *Nucl. Phys. Proc. Suppl.*, **65**,103, 1998.

[56] J. Smith, D. Thomas, and W. L. van Neerven. QCD corrections to the reaction $p\bar{p} \to W\gamma X$. *Z. Phys.*, **C44**,267, 1989.

[57] P. Ciafaloni and D. Comelli. Sudakov enhancement of electroweak corrections. *Phys. Lett.*, **B446**,278, 1999.

M. Beccaria, P. Ciafaloni, D. Comelli, F. M. Renard, and C. Verzegnassi. Logarithmic expansion of electroweak corrections to four- fermion processes in the TeV region. *Phys. Rev.*, **D61**,073005, 2000.

[58] W. Beenakker, A. Denner, S. Dittmaier, R. Mertig, and T. Sack. High-energy approximation for on-shell W pair production. *Nucl. Phys.*, **B410**,245–279, 1993.

W. Beenakker, A. Denner, S. Dittmaier, and R. Mertig. On shell W pair production in the tev range. *Phys. Lett.*, **B317**,622–630, 1993.

[59] V. V. Sudakov. Vertex parts at very high-energies in quantum electrodynamics. *Sov. Phys. JETP*, **3**,65–71, 1956.

[60] J. H. Kuhn and A. A. Penin. Sudakov logarithms in electroweak processes. 1999, hep-ph/9906545.

[61] P. Ciafaloni and D. Comelli. Electroweak sudakov form factors and nonfactorizable soft QED effects at NLC energies. *Phys. Lett.*, **B476**,49, 2000.

[62] V. S. Fadin, L. N. Lipatov, A. D. Martin, and M. Melles. Resummation of double logarithms in electroweak high energy processes. *Phys. Rev.*, **D61**,094002, 2000.

[63] M. Hori, H. Kawamura, and J. Kodaira. Electroweak Sudakov at two loop level. 2000, hep-ph/0007329.

[64] V. G. Gorshkov, V. N. Gribov, L. N. Lipatov, and G. V. Frolov. Double logarithmic asymptotics of quantum electrodynamics. *Phys. Lett.*, **22**,671–673, 1966.

John M. Cornwall and George Tiktopoulos. Infrared behavior of nonabelian gauge theories. 2. *Phys. Rev.*, **D15**,2937, 1977.

John M. Cornwall and George Tiktopoulos. Infrared behavior of nonabelian gauge theories. *Phys. Rev.*, **D13**,3370, 1976.

[65] J. Frenkel and J. C. Taylor. Exponentiation of leading infrared divergences in massless Yang-Mills theories. *Nucl. Phys.*, **B116**,185, 1976.

[66] J. Frenkel and R. Meuldermans. Infrared behavior of selfenergy functions in the axial gauge. *Phys. Lett.*, **B65**,64, 1976.

J. Frenkel. Behavior of leading infrared divergences of QCD in the axial gauge. *Phys. Lett.*, **B65**,383, 1976.

[67] K. I. Aoki, Z. Hioki, M. Konuma, R. Kawabe, and T. Muta. Electroweak theory. framework of on-shell renormalization and study of higher order effects. *Prog. Theor. Phys. Suppl.*, **73**,1–225, 1982.

[68] J. H. Kuhn, A. A. Penin, and V. A. Smirnov. Summing up subleading Sudakov logarithms. 1999, hep-ph/9912503.

[69] J. H. Kuhn, A. A. Penin, and V. A. Smirnov. Subleading Sudakov logarithms in electroweak processes. *Nucl. Phys. Proc. Suppl.*, **89**,94, 2000.

[70] W. Beenakker and A. Werthenbach. Large electroweak logarithms in the Coulomb gauge. in preparation.

[71] D. E. Groom et al. Review of particle physics. *Eur. Phys. J.*, **C15**,1, 2000.